Energy-Efficient Collaborative Communications for Wireless Sensor Networks

Syed Husnain Abbas Naqvi

A thesis submitted in partial fulfilment of the requirements for the degree of

Doctoral of Philosophy in Electrical and Electronic Engineering

The University of Auckland, New Zealand

2012

Abstract

In this thesis an energy efficient collaborative communication system for wireless sensor networks is presented in order to reduce the energy consumption of wireless sensor networks in the presence of AWGN and Rayleigh fading without decreasing the quality of service of data transmission. Due to the reduction of energy consumption of wireless sensor networks, the life time of sensor networks is extended. In collaborative communications, a set of transmitter nodes transmits the same data at the same time towards a common receiver, denoted as the base station, where the received signals are combined coherently. A coherently combined signal at the receiver indicates that a large amount of transmitted power is combined; this is referred to as constructive interference. As a result of this constructive interference, collaborative communications produce a substantial power gain, as well as a considerable reduction in bit error rate and a significant gain in capacity.

The main focus in this thesis is on theoretical aspects of the development of a collaborative communication system. The key factors that degrade the performance of collaborative communication systems i.e., phase, frequency and time synchronization errors, are identified. A synchronization process is designed to reduce the phase and frequency synchronization errors among the collaborative nodes and the base station. The theoretical model of the collaborative communication system with imperfect phase and frequency synchronization in the presence of AWGN and Rayleigh fading is proposed, modelled, theoretically analyzed and simulated. The performance of collaborative communication system is evaluated by investigating several figures of merit. The considered figures of merit are received power, bit error rate, energy efficiency and channel capacity. The theoretical findings of the collaborative communication system are verified using Monte Carlo simulation by considering the parameters of off-the-shelf products i.e., CC2420 and AT86RF212.

Closed form expressions are derived for the received power as a function of number of collaborative nodes, bit error rate (BER) as a function of SNR (E_b/N_0) and channel capacity as a function of signal to noise ratio and the number of collaborative nodes. To analyze the energy efficiency of the proposed collaborative communication system, the energy consumption of the collaborative communication system is modelled, simulated and analyzed.

The analytical and simulation results showed that the proposed collaborative communication system produces significant power gain, a reduction in BER and significant capacity gain in the presence of phase errors, frequency errors, AWGN and Rayleigh fading. A detailed theoretical analysis and Monte Carlo simulation revealed that the proposed collaborative communication system is an energy efficient communication system that can be implemented in sensor networks, as approximately N (number of collaborative nodes) times less the total transmitted power is required than for the single input single output (SISO) communication for a specifies transmission range.

Acknowledgement

My deepest gratitude goes to my supervisors, Dr. Stevan Mirko Berber and Professor Zoran Salcic. Their superb guidance, insightful comments, valuable advice and continuing encouragement have made my entire doctoral study a treasured experience.

Dr. Berber has been accessible in his office at all times; there we spent a countless number of hours discussing my research, critiquing research outcomes and reviewing my writing. He showed great enthusiasm for my proposals that, sometimes, were clearly naive. Dr. Berber gave me the maximum freedom to attempt whatever I desired in the research. His teachings still echo in my ears and, in the future, will guide me throughout my career.

I am grateful for the great effort that Professor Zoran Salcic put into discussing my research; he critiqued the research outcomes, proofread my manuscripts and checked every sentence with maximum care. From Professor Salcic I learnt how to write technical articles in a manner that makes the most use of the research results.

There are many excellent scholars inside and out of the Electrical and Computer Engineering Department at the University of Auckland. I am lucky to have Professor Allan Williamson, Dr. Morteza Biglari-Abhari, Dr. Michael Neve and Dr. Chris Smaill serve on the committee to appraise my thesis. I would also like to give thanks for their unreserved support to the excellent departmental technicians, Peter Wigan, Edmond Lo, Wai Leung Yeung, and the IT manager, Gerry Smith whose devotion greatly eased my task in the handling of numerous computer-related problems. The Librarian, Susan Brookes, has offered me her professional service throughout the course of my research, for which I thank her.

I would like to thank Professor Khalid Rashid, Professor I.M Qureshi and Professor Muhammad Sher at International Islamic University, Islamabad, Pakistan, where I spent several memorable years of study. They shepherded me onto the road of scientific research.

I deeply appreciate the actions of the Higher Education Commission of Pakistan (HEC) and the International Islamic University Islamabad (IIUI), Pakistan in awarding me a PhD scholarship and study leave in 2007. Without this scholarship, I could not have envisaged being able to study overseas in New Zealand. I also would like to thank the Higher Education Commission of Pakistan for generously granting me a six-month scholarship extension.

No words can express my gratitude to my mother, Irshad Fatima, who died during my PhD research in February 2011. Although we have been oceans apart, our hearts were never disconnected even a second while she was alive. My mother had the magic power of magnifying my tiniest joy, to remove my growing depression and return my sense of reason. My thanks go to my brother, Syed Mohsan Abbas Naqvi, sisters Shoukat Fatima, Shafqat Fatima, Fazilat Naqvi and Saeda Sadaf for taking care of my mother and encouraging me whenever I needed it. I would like to thank my wife Tayyab Naoreen for take care of my family and my daughters for last four years. My wife has always supported me and scarified her desires over my studies. My thanks also go to Sherry who has taken care of all my affairs in Pakistan over past four years. He has always been just a phone call away and has done whatever was required, immediately.

I am very grateful to Muhammad Sulayman and his wife Mehwish Riaz, whom I regard as family here in Auckland, I thank the Lord for placing you in my path when I was achingly coping with my settlement in the early days. My thanks must also go to Fahim Khan and his family who supported and encouraged me during my PhD studies, especially when I was in trouble. Also to all my friends in Pakistan who have encouraged and helped me during last four years, especially, Shehzad Ashraf Ch, Syed Muhammad Saqlain, Rana Imran Khan, Qaisar Javed, Zahid Mahmood, Tahir Mahmood, Hassan Arif, Muhammad Ahsan, Atif Jaffery, Muhammad Waseem, Majid Jaffery, Azhar Manaias and Zafar Manais.

A chapter would be needed to list all the names of the many intelligent, loyal, talented and warm-hearted people, with whom I have been privileged to make my life-long friendships. Here I name but a few: Dr. Shudong Fang, Ramin Vali, Bashir Ahmad, Amanullah, Arif Khan, Shafique Alam Barki, Amir Quereshi, Shahzad Akhatar, Shakeel Ahmad, Sher Khan, Saddam Abbasi, Faiz Rasool, Majid Ali, Danial Qadir, Ch. Umer etc. From you I learnt to respect and embrace the diversity of culture that transcends nations and races. You have made my life colourful outside the laboratory.

If I could fly higher than an eagle, thank you Lord for you are the wind beneath my wings.

Table of Contents

List of Acronyms

ADV_CH	Advertising message broadcasted from the base station
AP	Acknowledgement Period
AWGN	Additive White Gaussian Noise
BER	Bit Error Rate
BPSK	Binary Phase Shift Keying
BS	Base Station
CDF	Cumulative Density Function
CDMA	Code Division Multiple Access
CH	Cluster Head
CLT	Central Limit Theorem
CSMA	Carrier Sensing Multiple Access
CSMS	Carrier Sensing Mini-Slot Access
DCS	Digital Communication System
DPSK	Differential Phase Shift Keying
DS-CDMA	Direct Sequence Code Division Multiple Access
DSSS	Direct Sequence Spread Spectrum
FDMA	Frequency Division Multiple Access
FFD	Full-Function Device
FND	Network lifetime at the round when the First Node Dies
GSM	Global System for Mobile communications
HND	Network lifetime at the round when Half (50%) of the Nodes Die
I-branch	In-phase branch of the optimal quadrature demodulator
ID	Node identification number
IEEE	Institute of Electrical and Electronics Engineers
i.i.d.	Independent and identically distributed
IP	Initial Period
ISI	Inter-Symbol Interference
Join_REQ	Membership application message from non-CH node to CH node
kbps	kilo-bit-per-second
LPF	Low Pass Filter

LOS	Line-of-Sight
MAC	Medium Access Control
MAI	Multiple Access Interference
MF	Mapping Function
MIMO	Multi-Input-Multi-Output
MRC	Maximum Ratio Combining
NARE	Neighborhood Area Residual Energy
NRE	Network Residual Energy
OQPSK	Offset Quadrature Phase Shift Keying
OEM	Original Equipment Manufacturer
pdf	Probability density function
PHY	Physical Layer
PLL	Phase-Locked Loop
PN	Pseudo-Noise
Q-branch	Quadrature-phase branch of the optimal quadrature demodulator
QPSK	Quadrature Phase Shift Keying
RFD	Reduced-Function Device
RV	Random Variable
SEP	Symbol Error Probability
SINR	Signal-to-Interference-Noise Ratio
SNR	Signal-to-Noise Ratio
TDMA	Time Division Multiple Access
TD-SCDMA	Time Division Synchronous Code Division Multiple Access
TP	Transmission Period
WiMAX	Worldwide Interoperability for Microwave Access
WPAN	Wireless Personal Area Network
WSN	Wireless Sensor Network

Chapter 1 Thesis Introduction

This dissertation presents the design and analysis of an energy efficient collaborative communication system for wireless sensor networks. In collaborative communications, a set of transmitter nodes transmits the same data at a same time towards a common receiver, denoted as the base station, where the received signals are combined coherently. A coherently combined signal at the receiver indicates that a large amount of transmitted power is combined; this is referred to as constructive interference. As a result of this constructive interference, collaborative communications produce a substantial power gain, as well as a considerable reduction in bit error rate and a significant capacity gain.

1.1 Wireless Digital Communication Systems to Wireless Sensor Networks

1.1.1 Wireless digital communication systems

Currently, wireless communication systems are the most popular form of communication systems due to their massive applications such as, AM and FM radio, television, cellular phones, WiMAX, Wi-Fi and wireless internet [1]. The invention of a wireless telegraph system almost a century ago can be regarded as the beginning of wireless communication systems. The recent past has witnessed progress in the methods of wireless communication as a result of improvement in the size and processing speed of wireless radio devices. A high rate of competition combined with a decrease in the price of wireless devices is considered to be another reason for the rapid growth of wireless communication systems. The WiMAX (Worldwide Interoperability for Microwave Access), mobile broadband and cellular mobile services i.e., GSM (Global System for Mobile communications), CDMA (Code Division Multiple Access) and TD-SCDMA (Time Division Synchronous Code Division Multiple Access) have provided a way for fast wireless communication to develop. The International Telecommunication Union reported that by the end of 2001, every other person in the US and Europe, every third person in Asia and every fourth person in Africa would have a mobile phone. [2]. According to a recently published report from Global Analyst House, CCS Insight, Mobile Broadband was expected to grow in Europe at a high rate by the end of 2011, doubling the, then current number of subscribers and the amount of revenue [3].

A phenomenal development in communication technology in terms of its size and processing speed has been possible due to the introduction of microelectronics in the 1990s. During the 1990s, a number of factors, such as the invention of microelectronic circuits, an improvement in sensing materials, and the development of high speed wireless and networking equipment made possible the invention of the Wireless Sensor Network (WSN) [4]. The Wireless Sensor Network is ubiquitous computing system enabling efficient communication [5-7].

1.1.2 The wireless sensor network (WSN)

The wireless sensor network is composed of a large number of low cost, small, battery powered sensor nodes that are linked using wireless communication [8-10]. Sensor network applications include; military applications, such as battlefield surveillance and enemy tracking; civil applications include; habitat monitoring, environmental observation and forecast system, health and other commercial applications. A sensor node reads the physical data using onboard sensing devices, and transfers this data to the network users through the intermediate sensor nodes [10, 11].

Due to the small size, low cost and high processing power, wireless sensor networks are growing rapidly. Their rapid growth has meant that in the 1990s wireless sensor networks gained well-deserved attention in industrial standardization, academic research and the global business market. Wireless sensor networks were successfully commercialized by several companies in Europe and America in 1995 [12, 13]. Business In September 1999, Week Magazine ranked the wireless sensor network as one of the 21 most important technologies of the 21st century [12]. In July 2002, the Commission of the European Community recommended and sponsored the setup of sensor networks across Europe [14]. Due to the significant increase in the popularity of wireless networks, different communication standards have been introduced for the wireless network. The first standard, introduced in 2003 by IEEE (Institute of Electrical and Electronics Engineers) for Wireless Personal Area Networks (WPANs), is IEEE 802.15.4 [15]. IEEE 802.15.4 is a standard made with low-data-rate, low-power, and low-complexity short-range radio frequency devices [15]. Later, the IEEE 802.15.4 was recognized and adopted by a renowned industrial group, Original Equipment Manufacturers (OEM) for wireless sensor network transceivers [16]. Application driven methodologies to address real world problems using sensor networks were introduced and sponsored by the Chinese

Government in 2006 [17]. The market value of the wireless sensor network was expected to reach USD $5.9 billion in North America by 2010 [18].

New Zealand has a major share of the world's agriculture, horticulture, fishing, forestry and tourism industries. It is reported in [19] that approximately half of New Zealand's export revenue is generated through these industries. The advancement in wireless sensor network technology and its applications has great potential in the areas stated above. Wireless sensor network applications for precise, intelligent, farming and environment monitoring may assist in providing an environmentally sustainable New Zealand and enhancing the competitiveness of New Zealand's products in the international market.

1.1.3 General challenges and requirements

Despite the potential applications for wireless sensor networks, there are several constraints, challenges and requirements. The main challenge is the design of the wireless sensor network and particularly the development of energy efficient wireless communication protocol. The other challenges are hardware constraints, the dense node deployment and the infrastructural-free network. It is very difficult to design a wireless sensor network that meets all the requirements of several applications [8].

As the wireless sensor networks are composed of a large amount of finite energy and non-rechargeable battery powered sensor nodes, the key requirement for design is to increase the life time of sensor networks. The life time of sensor networks can be increased by achieving the energy efficient data transmission. Furthermore, due to the limited processing capability of processors embedded in sensor nodes, a wireless sensor network communication protocols must be of low-complexity and easy-to-implement. Moreover, in several cases, it is not possible for infrastructure be set up beforehand; for this reason, wireless sensor networks communication protocols need to allow for the organizing of sensor nodes to meet scalability requirements free of infrastructure or human interventions.

1.2 Thesis Motivation, Objectives, Methodology and Significance

Due to the limited power of sensor nodes, this thesis is motivated to reduce the energy consumption of sensor nodes in wireless communication using collaborative

communication to extend the lifetime of wireless sensor network while providing satisfactory services of data sensing and transmission. One of the key focuses of this thesis is to determine the key factors that reduce the energy efficiency of collaborative communication in sensor networks in additive white Gaussian noise (AWGN) and Rayleigh fading channels. The other key focus is to develop a communication system in relevant protocol layers to reduce the energy expenditure of sensor nodes.

The main objectives of this thesis are as follows:

1. To understand the energy consumption requirements of the wireless sensor networks required for wireless communications.
2. To develop energy-efficient communication algorithms for wireless sensor networks in the presence of AWGN and Rayleigh fading.
3. To identify the key factors that reduces the efficiency of the proposed communication algorithms for wireless sensor networks.
4. To evaluate the performance of the proposed communication algorithms for wireless sensor networks in terms of received power, Bit Error Rate (BER) and channel capacity.

To achieve the above objectives, the methodology taken in this thesis is to develop algorithms in theory, and then to verify the theoretical algorithms via numerical analysis and simulation using the parameters of off-the-shelf products i.e., CC2420 [20] and AT86RF212 [21].

For the first objectives, we studied and theoretically analyzed different wireless sensor networks topologies. The main topologies are mesh, tree or cluster topologies and are arrived at by using the protocols surveyed in [22-25]. From surveyed paper [22-25] it is analyzed that tree and cluster topologies are highly saleable. Moreover, star topology has substantial impact on the wireless sensor networks in light of IEEE 802.15.4 standard [14].

For the second objective, we studied the various existing techniques i.e., cluster based algorithms [26-28], dynamic modulation scaling [30], multi-frequency assignment [31], cooperative communications [32-34], chip interleaving technique [35-37] and Multi-Input-Multi-Output (MIMO) signal processing [38-40]. The theory of centralized array to achieve space diversity is widely used in cellular networks [41-42]. The feasibility of the virtual array of independent transmitters to achieve the benefits of centralized antenna array has been well reported in recent literature [43-46]. The feasibility of the virtual array of independent transmitters, design requirements, constraints and a fundamental

model for the wireless sensor network are studied and presented in [44]. The authors in [44] have claimed that this is the first work done in this area i.e., the feasibility of the virtual array of independent transmitters, entitled distributed beamforming.

We have exploited the space diversity concept to develop an energy efficient collaborative communication system for wireless sensor networks. Collaborative communication aims to produce substantial power gain, significant reduction in Bit Error Rate (BER) and significant capacity gain. To the author's best knowledge, this is the first study that introduces the bit error rate (BER), energy consumption, energy efficiency and the capacity of collaborative communication for wireless sensor networks. In collaborative communication, a network of transmitter nodes, denoted as collaborative nodes, are established to transmit the same data at same time towards a common receiver in such a way that received signals are combined coherently at the receiver denoted as the base station. To receive the data coherently at the receiver synchronization process is developed between the collaborative nodes and the base station. The combined signal at the receiver is a strong signal due to the fact that large amounts of transmitted power are combined to form a constructive interference that leads towards substantial power gain, significant reduction in Bit Error Rate (BER), and significant capacity gain.

In order to have a clear understanding of effective collaborative communication technique, we have developed theoretical expressions for received power Bit Error Rate (BER), energy consumption, energy efficiency, and channel capacity, in the presence of Rayleigh fading and Additive White Gaussian Noise (AWGN). These expressions for received power, Bit Error Rate (BER), energy consumptions, energy efficiency and channel capacity are very useful theoretical tools for analyzing the energy savings of the sensor network. Collaborative communication transceivers are considered in compliance with the IEEE 802.15.4 standard, using the parameters of the off-the-shelf products [20-21].

In this fixed antenna array system there is a common network node (controller) that is used to achieve the frequency, phase and time synchronization. The distances between transmitter antennas are fixed and known accurately by the controller [47-50]. However in a distributed sensor network, the accurate position of sensor nodes is not generally known and each transmitter has its own local oscillator; the theory of fixed antenna array cannot be applied directly. Specifically, the two related assumptions of frequency synchronization, and phase synchronization among the transmitters are much more challenging for a distributed wireless sensor networks than for a fixed antenna array. The

key factors i.e., phase, time and frequency synchronization, that reduce the efficiency of the proposed collaborative communication for wireless sensor networks are identified in order to achieve the third research objective of the thesis.

From the literature review it is analyzed that a significant part of node energy is used to overcome the channel fading in wireless data transmission. Therefore, alternative fading-mitigating techniques are investigated. In literature a variety of diversity techniques i.e., dynamic modulation scaling [30], multi-frequency assignment [31], cooperative communications [32-34], chip interleaving technique [35-37] and Multi-Input-Multi-Output (MIMO) signal processing [38-40] are proposed to mitigate channel fading. In this thesis, the collaborative communication technique, considered as space diversity, is investigated and employed to mitigate the channel fading for wireless sensor networks. To the author's best knowledge, this is the first study to introduce the fading mitigation capability of collaborative communication for wireless sensor networks.

To achieve the fourth research objective, randomly deployed sensor nodes are considered for collaborative communication. Several SIMULINK and MATLAB® based wireless sensor network simulators are developed for collaborative communication in the presence of AWGN and Rayleigh fading using parameters of off-the-shelf products, i.e. CC2420 [20] and AT86RF212 [21]. The wireless communication environment used in simulation is established using SIMULINK's AWGN and Rayleigh channel blocks. The attainable energy efficiencies for collaborative communication based wireless sensor networks are evaluated by theoretical analyses and Monte Carlo simulations.

Collaborative communication is found to significantly improve the energy efficiency of wireless sensor networks. Hence, the significance of this thesis resides in its contribution to the theoretical development of WSN communication algorithms that can lead to the development of new WSNs of higher energy efficiency. Although the studies in this thesis are presented from the algorithmic perspective, the thesis outcomes are likely to guide WSN designers by providing a firm theoretical ground that may impact upon standardization approaches.

1.3 Contributions and Thesis Structure

The primary contributions of this thesis are summarized as follows:

1. An ideal collaborative communication model is developed to investigate the power gain for wireless sensor networks. The key factors that degrade the performance of

collaborative communication are identified. A synchronization process to synchronize the phase and frequency among collaborative nodes and the base station is developed. Mathematical expressions for received power for several collaborative communication models are developed. Specifically mathematical expressions for the received power of a collaborative communication system with imperfect phase and frequency synchronization in the presence of AWGN and Rayleigh fading are derived and expressed as the function of the number of collaborative nodes.

2. Simulation-based investigations are carried out to confirm the theoretical findings of received power for several collaborative communication systems. Also, via simulation, the power gain of several collaborative communication systems, in the presence of AWCN and Rayleigh fading, are evaluated for wireless sensor networks.
3. In order to explore energy-saving means in the lower protocol layers, a collaborative communication technique to mitigate channel fading is investigated for wireless sensor networks. The BER expressions of several collaborative communication systems are developed in the presence of Rayleigh fading, AWGN. Specifically closed form expressions for BER for a collaborative communication system with imperfect phase and frequency synchronization are derived.
4. Simulation-based investigations are carried out to verify the derived BER expressions of several collaborative communication systems. The BER curves of the collaborative communication systems are compared to those of SISO systems, showing that the collaborative communication systems outperform the SISO systems in attaining significant signal-to-noise ratio gains in the fading channel.
5. As the number of collaborative nodes increases, the circuit power consumption of nodes becomes considerable and reduces the overall power efficiency of the network. Therefore, energy consumption and energy efficiency models for SISO and collaborative systems are developed in order to investigate the energy savings of collaborative communication.
6. The energy efficiency of several collaborative communication systems, over the SISO system, in the presence of flat Rayleigh fading are analyzed in compliance with the IEEE 802.15.4 standard i.e., using the parameters of off-the-shelf products i.e. CC2420 [20] and AT86RF212 [21].

7. Simulation-based investigations are conducted to verify the theoretical energy savings, over those of the SISO system, of several collaborative communication systems and, in particular the collaborative communication system with imperfect phase and frequency synchronization.
8. To explore the channel capacity of a collaborative communication system, closed form expressions are developed to measure the channel capacity of several collaborative communication systems for wireless sensor networks. Specifically closed form expressions for the channel capacity are derived for a collaborative communication system with imperfect phase and frequency synchronization.
9. Simulation-based investigations are carried out to verify the derived channel capacity expressions of several collaborative communication systems. In particular, analytical and simulation results are obtained and analyzed for a collaborative communication system with imperfect phase and frequency synchronization in presence of AWGN and Rayleigh fading using parameters of CC2420 [20] and AT86RF212 [21].

There are eight chapters in this thesis. Figure 1.1 shows the route map which presents the interconnections among these chapters in structuring this thesis as follows.

Chapter 1 introduces the motivation, objectives, methodology, and the primary and significant contributions of this thesis.

Chapter 2 presents the study of some basics and presents a detailed literature review of wireless digital communications. The study mainly focuses on the signal power loss in the fading channel and the channel access among multiple users, determining their fundamental importance to the development of node energy consumption models. These models are used in analysing the energy-efficiency of wireless sensor networks communication algorithms.

Chapter 3 provides a comprehensive introduction to wireless sensor networks, putting WSNs in a broader perspective that covers; the applications and hardware of a sensor node, the WSN communication protocol stack, the core challenges of designing WSN communication algorithms, state-of-the-art research and industrial standardization.

Chapter 4 begins with the study of ideal collaborative communication algorithms. The key factors that can degrade the performance of collaborative communication i.e., phase, frequency and time synchronization, are identified. A synchronization process is presented in order to reduce the phase and frequency errors. The figure of merit considered in this chapter is received power. Several collaborative communication

algorithms are proposed, modelled, and theoretically analyzed. The algorithms presented in this chapter are:

1. Collaborative communication algorithm with imperfect phase synchronization and assuming perfect time and frequency synchronization.
2. Collaborative communication algorithm with imperfect frequency synchronization and assuming perfect time and phase synchronization.
3. Collaborative communication algorithm with imperfect phase and frequency synchronization in the presence of AWGN and Rayleigh fading.

The SIMULINK and MATLAB® simulation results, in terms of the received power of the various collaborative communication models, are also presented in this chapter.

Chapter 5 presents the procedures for developing the closed-form BER expressions for several collaborative communication systems for the AWGN channel with Rayleigh fading. The fading mitigation capability of collaborative communication is also analyzed. MATLAB® based analytical and simulation results are also presented and demonstrated.

Chapter 6 introduces the development of the energy consumption of single input, single output, (SISO) systems and the collaborative communication system using the parameters of off-the-shelf products i.e. CC2420 [20] and AT86RF212 [21]. The energy efficiency model of the collaborative communication system over the SISO system is also presented. The numerical results of the node energy savings of collaborative communication obtained from the theoretical analyses and simulations are illustrated and discussed.

Chapter 7 presents the procedures for developing the closed-form expressions for channel capacity for several collaborative communication systems for AWGN channel with Rayleigh fading. The MATLAB® based analytical and simulation results are also presented, demonstrated and analyzed.

Chapter 8 concludes this thesis, summarizes the key research findings, and makes suggestions for potential further work.

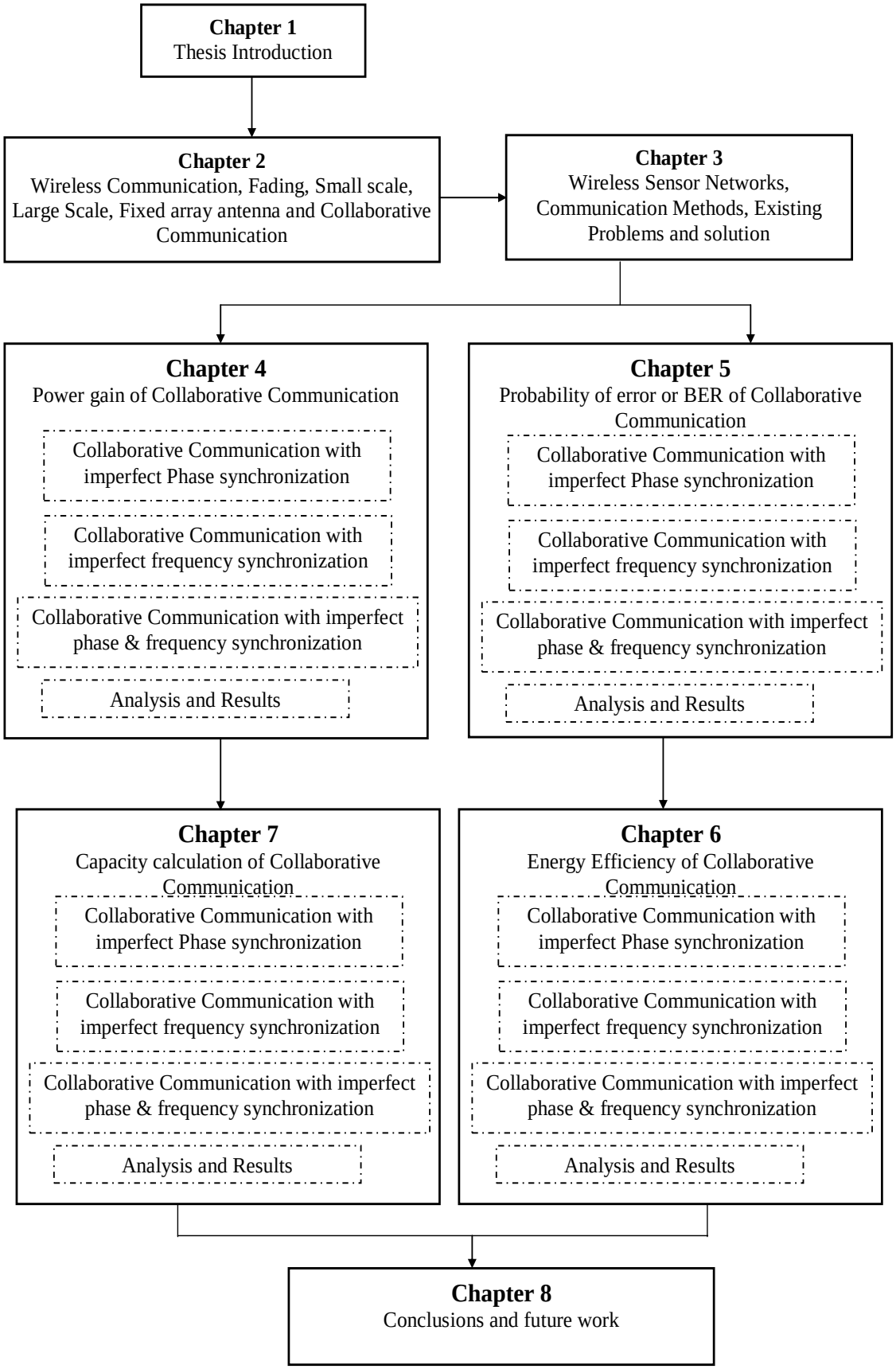

Figure 1.1 Thesis route map

1.4 Publications

Relevant to the research carried out to date, the list of publications is given blow:

Journal papers:

[1] H. Naqvi, S. M. Berber and Z. Salcic, "Energy Efficient Collaborative Communication with imperfect Phase Synchronization and Rayleigh Fading in Wireless Sensor Networks", Elsevier Physical Communication journal, Volume 3, Issue 2, pp. 119-128, June 2010.

[2] H. Naqvi, S. M. Berber and Z. Salcic, "Energy Efficiency of Collaborative Communication with imperfect Frequency Synchronization in Wireless Sensor Networks", International Journal of Multimedia and Ubiquitous Engineering, Vol. 5, No. 4, pp. 19-30, October, 2010.

[3] H. Naqvi, S. M. Berber and Z. Salcic, "Collaborative Communication with imperfect Phase and Frequency Synchronization in AWGN Channel for ad-hoc Sensor Networks", accepted for publication in International Journal of Multimedia and Ubiquitous Engineering.

[4] H. Naqvi, S. M. Berber and Z. Salcic, "Energy Efficient Collaborative Communications in AWGN and Rayleigh Fading Channel in Wireless Sensor Networks" accepted for publication in Wireless Communications and Mobile Computing.

Book Chapters:

[5] H. Naqvi, S. M. Berber and Z. Salcic, "Performance Analysis of Collaborative Communication with imperfect Frequency Synchronization and AWGN in Wireless Sensor Networks," Communications in Computer and Information Science, Volume 56, pp. 114-121, December 2009.

[6] H. Naqvi, M. Sulayman and M. Riaz "Adaptive Beamforming in Wireless Sensor Network in the Presence of Interference Sources," Communications in Computer and Information Science, Volume 56, pp. 105-113, December 2009.

Conference Papers:

[7] H. Naqvi, S. M. Berber and Z. Salcic, "Performance Analysis of Collaborative Communication in the Presence of Phase Errors and AWGN in Wireless Sensor Networks," International Conference on Wireless Comm. and Mobile Computing, Leipzig, Germany, pp. 394-398, June 2009.

[8] H. Naqvi, S. M. Berber, Z. Salcic and S. Fang, "Energy Efficiency of Collaborative Communication with Imperfect Phase Synchronization and Rayleigh Fading in Wireless Sensor Networks," The 2009 International Conference on Wireless

Communications and Signal Processing (WCSP 2009), Nanjing, China, pp. 1–5, November 2009.

[9] H. Naqvi, S. M. Berber and Z. Salcic, “Collaborative Communication with imperfect Phase and Frequency Synchronization in AWGN Channel in Wireless Sensor Networks”, IEEE Sensors Applications Symposium, Limerick, Ireland, pp. 241 – 244, 2010.

[10] H. Naqvi, S. M. Berber and Z. Salcic, “Energy Efficient MISO Collaborative Communication System in AWGN and Rayleigh Fading Channel”, IEEE GLOBCOM, Miami, USA, pp. 1-5, December 2010.

[11] H. Naqvi, S. Berber, Z. Salcic, "Capacity Calculation for Collaborative Communication with Imperfect Phase Synchronization, AWGN and Fading in Sensor Networks", 15th WSEAS Int. Conf. on Communications, Corfu, Greece, pp. 277-282,July 15-17, 2011.

[12] S. Berber, H. Naqvi, M. Temerinac, V. Kovacevic, Capacity Calculation for Multi-Relay Channel in the Presence of Noise and Fading, 15th WSEAS Int. Conf. on Communications, Corfu, Greece, pp. 271-276, July 15-17, 2011.

Technical report:

[13] H. Naqvi, S. M. Berber, Z. Salcic, “Collaborative Communications in Sensor Networks,” Technical report for School of Engineering, No. 672, 2009.

Due to time constraints, some research results are still being prepared for submission to publications or to be patented. Planned publications are the following:

[14] H. Naqvi, S. M. Berber, Z. Salcic, “Energy Efficient Collaborative Communication system with Imperfect frequency Synchronization and Rayleigh Fading in Wireless Sensor Networks,” in preparation for submission to Wireless Communications and Mobile Computing.

[15] H. Naqvi, S. M. Berber, Z. Salcic, “Capacity calculation of Collaborative Communication system with Imperfect phase and frequency Synchronization in presence of AWGN and Rayleigh Fading in Wireless Sensor Networks,” in preparation for submission to IEEE Transactions on Wireless Communication.

References

[1] P. J. Nahin, The science of radio. AIP, 2001.

[2] “Global ICT Developments” by International Telecommunication Union. [Online]. Available: http://www.itu.int/ITU-D/ict/statistics/ict/index.html [Access: January 10, 2012].

[3] “Analysts at CCS Insight”, by Global Analyst House, CCS Insight. [Online]. Available: at http://www.contextworld.com/c/document_library/get_file?p_l_id= 47472&folderId=52910&name=DLFE-2968.pdf [Access: January 10, 2012].

[4] J. G. Proakis et al., Shallow water acoustic networks, IEEE Commun. Mag., v. 39, n. 11, 2001, pp. 114–119.

[5] A. Swami, et al., Wireless sensor networks : signal processing and communications perspectives, NJ : J. Wiley, 2007, pp.1-2.

[6] H. Saito, O. Kagami, M. Umehira, Y. Kado, "Wide area ubiquitous network: the network operator’s view of a sensor network," IEEE Commun. Mag., 2008, pp.112-120.

[7] "Ubiquitous Sensor Networks,"International Telecommunciation Union Watch Report, 2008.

[8] C. C. Kumar, and S. P. Kumar, "Sensor networks: evolution, opportunities, and challenges," Proceedings of the IEEE, vol. 91, no.8, 2003, pp. 1247-1256.

[9] I.F. Akyildiz, W. Su, Y. Sankarasubramaniam, and E. Cayirci., "A survey on sensor networks," IEEE Commun. Mag., vol. 40, no. 8, 2002, pp. 102-114.

[10] M. Tubaishat and S. Madria., "Sensor Networks: an Overview," IEEE Potentials, vol.22, no.2, 2003, pp.20-23.

[11] "21 ideas for the 21st century," Business Week, 1999, pp. 78.-167.

[12] CrossBow Technology, [Online]. Available: www.xbow.com. [Access: Aug 5, 2009].

[13] Arch Rock Technology, [Online]. Available: http://www.archrock.com/. [Access: Aug 5, 2009].

[14] European CSIRT network, [Online]. Available: http://www.ecsirt.net/. [Access: Aug 5, 2009].

[15] IEEE 802.15.4 version 2006, IEEE Standards Association. [Online]. Available: http://standards.ieee.org/getieee802/download/802.15.4-2003.pdf. [Access: Aug 5, 2009].

[16] Zigbee Alliance, [Online]. Available: http://www.zigbee.org/.[Access: Aug 5, 2009].

[17] L. M. Ni, "China's National Research Project on Wireless Sensor Networks," in Proc. IEEE CSNUTC’08, 2008, pp. 19.

[18] M. Horton, Crossbow wireless sensing solutions conference, Chicago, 2004.

[19] "The World Factbook - New Zealand," [Online]. Available: https://www.cia.gov/library/ publications/the-world-factbook/geos/nz.html.[Access: Aug 5, 2009].

[20] CC2420, Texas Instruments Chipcon Products, http://focus.ti.com/analog/docs/ enggresdetail.tsp ?familyId=367&genContentId=3573.

[21] AT86RF212, ATMEL Products, http://www.atmel.com/dyn/products/product_ card.asp ?PN=AT86RF212.

[22] I. Demirkol, C. Ersoy, and F. Alagoz, "MAC Protocols for Wireless sensor Networks: A Survey," IEEE Commun. Mag., vol. 44, no. 4, 2006, pp. 115 – 121.

[23] J.N. Al-Karaki, and A.E. Kamal, "Routing techniques in wireless sensor networks: a survey," IEEE Wireless Commun., vol. 11, no. 6, 2004, pp.6 – 28.

[24] C. Wang; K. Sohraby, B. Li, M. Daneshmand, and Y. Hu, "A survey of transport protocols for wireless sensor networks," IEEE Network, vol. 20, no. 3, 2006, pp. 34-40.

[25] S. Ozdemir, and X. Yang, "Secure data aggregation in wireless sensor networks: A comprehensive overview," Comput. Netw., vol. 53, no.12, 2009, pp. 2022-2037.

[26] P. Gupta, and P.R., Kumar, "The capacity of wireless networks," IEEE Trans.on Inf. Theory, vol 46, no. 2, 2000, pp. 388 – 404.

[27] W. B. Heinzelman, A. P. Chandrakasan, and H. Balakrishnan "An application-specific protocol architecture for wireless microsensor networks," IEEE Trans. on Wireless Commun., vol. 1, 2000, pp. 660-670.

[28] O. Younis and S. Fahmy, "HEED: a hybrid, energy-efficient, distributed clustering approach for ad hoc sensor networks," IEEE Trans. on Mob. Comput., vol. 3, 2004, pp. 366-379.

[29] M. J. McGlynn, and S. A. Borbash, "Birthday protocols for low energy deployment and flexible neighbor discovery in ad hoc wireless networks", in Proc. MOBIHOC'01, 2001, pp. 137-45

[30] Z. Yang, Y. Yuan, J. He, and W. Chen, "Adaptive modulation scaling scheme for wireless sensor networks," IEICE Trans. on Commun., vol. E88-B, no. 3, 2005, pp.882-889.

[31] S. Waharte, and R. Boutaba, "A Comparative Study of Distributed Frequency Assignment Algorithms for Wireless Sensor Networks", in Annals of Telecommun. (special issue on Sensor Networks), vol. 60, no. 7-8, 2005, pp. 858-871.

[32] Z. Zhou, S. Zhou, S.Cui, and J. Cui , "Energy-efficient cooperative communication in a clustered wireless sensor network," IEEE Trans. Veh. Technol., vol.57, no.6, 2008, pp. 3618-3628.

[33] S. Cui and A. J. Goldsmith, "Cross-layer design in energy-constrained networks using cooperative MIMO Techniques," EURASIP Signal Processing Journal, vol. 86, no. 8, 2006, pp. 1804-1814.

[34] L. Simic, S. M. Berber, K. W. Sowerby, "Partner choice and power allocation for energy efficient cooperation in wireless sensor networks. in Proc. IEEE ICC'08, 2008, pp. 4255-4260.

[35] Y. Kimura, K. Shibata, and T. Sakai, "Precoder for chip-interleaved CDMA using space-time block-coding," IEICE Trans. Fundam. Electron. Commun. Comput. Sci., vol.E91-A, no.10, 2008, pp.2885-2888.

[36] Y. Lin and D. W. Lin, "Multicode chip-interleaved DS-CDMA to effect synchronous correlation of spreading codes in quasi-synchronous transmission over multipath channels," IEEE Transactions on Wireless Commun, vol. 5, no.10, 2006, pp. 2638-2642.

[37] S. Fang; S.M. Berber, A.K.Swain, "Closed-form average BER expression for chip-interleaved DS-CDMA system conducting M-ary communication and noncoherent demodulation in flat Rayleigh fading channel," 15th Asia-Pacific Conference on Communications, 2009, pp. 144 – 147.

[38] L. Xiao and M. Xiao, "A new energy-efficient MIMO-sensor network architecture M-SENMA," in Proc. VTC'04, vol. 4, Sept. 2004, pp. 2941- 2945.

[39] G. J. Miao, "Multiple-input multiple-output wireless sensor networks communications," US Patent, No. US7091854, August 15, 2006.

[40] S. Cui, A. J. Goldsmith, and A. Bahai, "Energy-efficiency of MIMO and cooperative MIMO techniques in sensor networks," IEEE J. Sel. Areas Commun., vol.22, no.6, 2004, pp.1089-1098.

[41] K. Raith and J. Uddenfeldt, "Capacity of digital cellular TDMA systems," IEEE Transactions of Vehicular Technolology, vol. 40, 1991, pp. 323–332.

[42] [12] W. C. Y. Lee, "Overview of cellular CDMA," IEEE Transactions of Vehicular Technolology, vol. 40, 1991, pp. 291–302.

[43] R. Mudumbai, D.R. Brown, U. Madhow and H.V. Poor, “Distributed transmit beamforming: challenges and recent progress ,” IEEE Communications Magazine, Vol. 47, Issue 2, 2009, pp. 102 - 110.

[44] R. Mudumbai, G. Barriac, and U. Madhow, “On the feasibility of distributed beamforming in wireless networks," IEEE Trans. Wireless Commun., vol. 6, no. 5, May 2007, pp. 1754-1763.

[45] K. Zarifi, S. Affes, and A. Ghrayeb, “Distributed beamforming for wireless sensor networks with random node location,” IEEE International Conference on Acoustics, Speech and Signal Processing, 2009, pp. 2261– 2264.

[46] Z. Han and H. V. Poor, "Lifetime improvement in wireless sensor networks via collaborative beamforming and cooperative transmission," Microwaves, Antennas & Propagation, IET, vol. 1, 2007, pp. 1103-1110.

[47] J. D. Kraus, Antennas, Second Edition. Mc-Graw Hill, 1988.

[48] S. Uda and Y. Mushiake, Yagi-Uda Antennas, 1954.

[49] K. Yao, R. Hudson, C. Reed, D. Chen, and F. Lorenzelli, “Blind beamforming on a randomly distributed sensor array system,” IEEE Journal of selected Areas in Communication, vol. 16, no. 8, 1998, pp. 1555–1567.

[50] J. Winters, “Smart antennas for wireless systems,” IEEE Personal Communications, vol. 5, no. 1, 1998, pp. 23–27.

Chapter 2 Wireless Communication System

2.1 Introduction

This chapter presents some basics about the wireless digital communications, antenna array, channel fading and multiple access techniques for wireless communication. The intellectual ability of these basics is required to be known, because few communication algorithms in the superior cover protocols of Wireless Sensor Networks (WSN) are impassive by the physical layer [1]. The main focus in this chapter is on signal power loss during transmission and channel fading and the determining of their fundamental importance to the development of node energy consumption models in the energy efficiency analysis of wireless sensor networks communication systems.

The study begins with the major components of a wireless communication system. The function of the each component is explained in Section 2.2. The Terminology of the wireless digital communication scheme introduced in this part of the research will be adhered to in the following chapters.

In Section 2.3, the theory of antenna and antenna arrays are presented; this is one of the most important components of wireless communication. The advantages of an antenna array over single antenna systems are also explained. In Section 2.4 one of the important applications of an antenna array i.e., multiple input multiple output (MIMO) systems, is presented. The advantages of MIMO systems and antenna array i.e., space diversity form the basic motivation in the development of the proposed collaborative communication systems that are presented in Chapter 4 and 5.

Signal path loss models for wireless communication systems are presented in Section 2.5. The key factors that contribute to signal power loss in transmission are identified and presented. The mathematical expressions of these path loss models are also investigated and presented. In wireless communication, it is observed that a signal loses its power significantly due to the channel's path loss, shadow fading and small-scale fading [2]. These signal path loss models are utilized to calculate the energy consumption and energy efficiency of collaborative communication systems, as presented in Chapter 6.

In Section 2.6 channel fading is investigated and presented. The phenomenon of multipath is elaborated and effects of multipath on signal power are presented. The concept of fading and the physical factors that influence fading are analyzed and

presented. Different types of fading, their characteristics and key factors are also investigated and presented. Signal power path loss and shadow fading are together referred to as large-scale fading [2]. Small-scale fading is also known as Rayleigh fading. Field-test measurements have confirmed that shadow fading and the Rayleigh fading affect signal propagations between sensor nodes deployed in indoor and outdoor environments [3, 4].

From the practices of many realistic wireless communication systems, it has been found that Rayleigh fading significantly reduces the power of the received signal [2, 5]. Power required to compensate for the fading effect, known as fade margin, is investigated and presented. Fade margins for different fading types are identified. It is found that many existing wireless sensor networks communication algorithms consider fade margins as the most conventional engineering means of compensating for signal power loss due to channel fading [6, 7]. This motivates us to consider reducing node energy consumption by means of fading mitigation using a collaborative communication system, as studied in Chapter 5.

In Section 2.7, the study expands to multi-user communication systems where the wireless path is shared, to broadcast data, by several users. Numerous multiple access methods are presented, including Frequency division multiple access (FDMA), Time division multiple access (TDMA), Frequency time division multiple access (F/TDMA), Code division multiple access (CDMA) and Space division multiple access (SDMA).

2.2 Wireless Communication Systems

The Encyclopedia Britannica dictionary [8] defines “communication” as “interchange of thoughts or opinions through shared symbols” and “system” as “an organized integrated whole made up of diverse but interrelated and interdependent parts”. Therefore, “communication system” may be defined as the exchange of data/symbols among separate sources using interrelated and independent components. “Wireless” is defined as “medium without any physical connection”. Hence, wireless communication systems may be defined as the interchange of information among difference sources using unguided media or medium without any physical connection, i.e. air.

This section presents the major components of a wireless digital communication system (DCS). Figure 2.1 presents the major components of a wireless digital communication system to transfer data between a transmitter and a receiver using a

wireless channel [9]. Grey boxes represent the necessary components and optional components are represented by simple white boxes. The description and functions of each of the components shown in Figure 2.1 are explained below.

Format: A format is the basic component of the wireless digital communication system [9]. Data to be transferred is formatted into binary bits; then a set of bits may be grouped. The grouped bits are called message symbols.

Source encoder/decoder: Source encoder/decoder is an optional component of a wireless digital communication system. This component is used in instances where the transmitted data is in analog form. Analog data is converted to digital data by the transmitter using the encoder. On the receiver the received digital data is converted to analog form by the decoder.

Channel encode/decode: Channel encode/decode is an optional component of the wireless digital communication system. Transmitted message symbols are converted into channel symbols, known as channel codes, by the channel encoder. Channel coding is useful in minimizing the effect of noise and other channel impairments. On the receiver side, channel codes are converted into message symbols by the channel decoder.

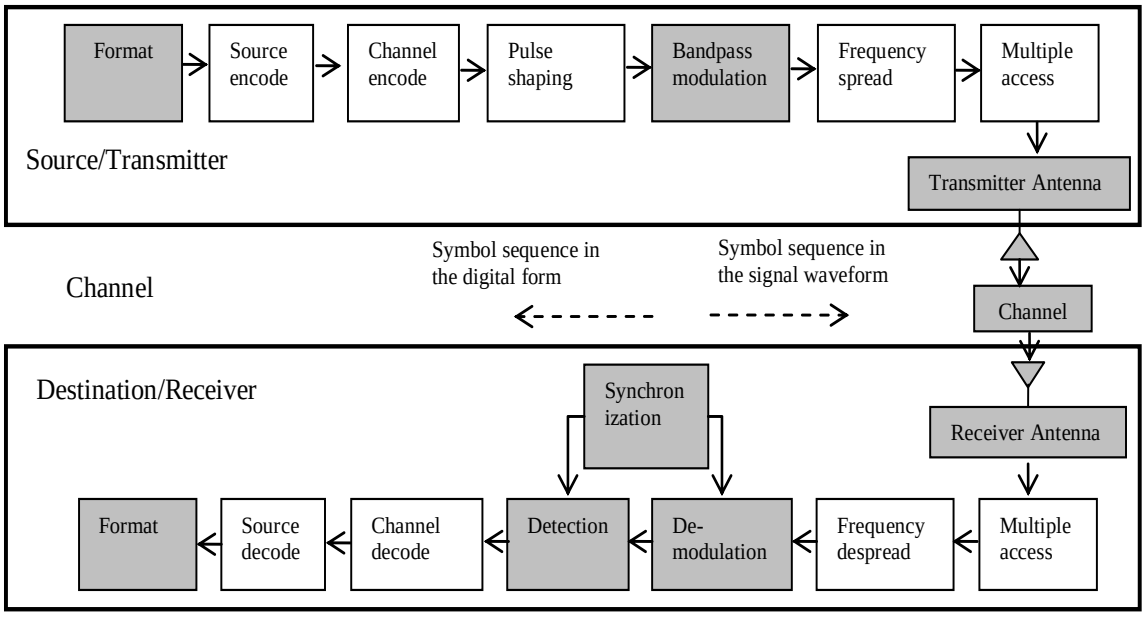

Figure 2.1 Major components of wireless digital communication system [9]

Pulse shaping: Pulse shaping is an optional component of the wireless digital communication system. The pulse shaping filter adjusts the bandwidth of the transmitting message symbols within the required channel bandwidth.

Bandpass modulation/demodulation: Bandpass modulation/demodulation is a necessary component of the wireless digital communication system. The band pass modulates the information data into a high frequency waveform called a modulated signal; this is done by using a carrier signal which is appropriate for broadcasting via the wireless channel. A modulated signal can travel a long distance. Hence the intonation scheme in use needs to be able to make the modulated signal compatible with the needs of the wireless path. At the destination the modulated signal is demodulated using the same carrier to covert the waveform into the digital data.

Frequency spread/de-spread: Frequency spread/de-spread is an optional component of wireless digital communication system. Higher frequency signals normally can accommodate higher bandwidth. Using frequency spread bandwidth of a signal is significantly extended to several times wider. The frequency-spread signal is relatively immune to the noise and interruption induced in the wireless channel. At the destination the frequency de-spread converts the frequency-spread wideband signal to a narrowband signal.

Multiple access: Multiple access is an optional component of a wireless digital communication system. Using the multiple access method, the same channel can be utilized by several users. The various multiple access techniques used for wireless communication channels and their characteristics are explained in Section 2.5.

Transmitter Antenna: The transmitter antenna is a necessary component of a wireless digital communication system. The transmitter antenna is the last component on the transmitter side. The modulated signal is sent to air using the transmitter antenna.

Receiver Antenna: The receiver antenna is a necessary component of wireless digital communication system. The receiver antenna is the first component at the destination. The modulated signal transmitted by the source is captured by the receiver antenna.

Detection: Detection is a necessary component of a wireless digital communication system. In detection the decision is made on demodulated signal in accordance to certain conclusion rules. The demodulated signal is converted to binary bits after detection.

Synchronization: Synchronization is a necessary component of a wireless digital communication system. For efficient communication, most digital communication

systems require synchronization between the source and the destination in terms of time and frequency.

Wireless channel: A wireless channel is a necessary component of a wireless digital communication system. Unguided media, i.e., the air space that is used for wireless channels; when the signal is transmitted to air, signals undertake different forms of corruption due to reflection, diffraction and scattering.

2.3 Antennas and Antenna-Arrays

In wireless communication, antennas are used to radiate electromagnetic waves. The design for an efficient antenna structure is very challenging and important for wireless communication. Although constantly varying currents generate radiation, any metal device can be used as an antenna by using the appropriate current or voltage [10]. One of the major problems in antenna design is reducing the amount of energy loss due to the internal resistance of the antenna. Secondly antennas may have large reactive impedance. Due to large reactive impedance, high voltages are required to generate any appreciable amount of radiation. Moreover, for single input, single output (SISO) systems, high directivity is required so that the major part of transmitted power is received by the receiver. In addition, for point-to-point (as opposed to broadcast) applications, it is usually desirable to have high directivity, so that the transmitted power is focused in the direction of the receiver. One of the viable solutions to the above mentioned problems is antenna arrays [11].

In an antenna array, a set of independent, identical, antennas with regularly spaced elements are combined in such a way that the currents running through them have different amplitudes and phases. Antenna arrays can produce high directivity and less energy loss resulting in a high power gain at the receiver when compared to a single antenna [11]. In this research, the concept of an antenna array is exploited for the development of collaborative communication systems, as presented in Chapter 4. As an antenna array consists of identical antenna, the current distribution can be specified by a discrete number of currents. Therefore, electromagnetic (EM) field equations of the antenna array can be represented by set of linear equations [12], which can be solved using digital calculators/computers.

One of the main applications of antenna arrays is radar application. The other applications are for; radio-astronomy [13], Direction of Arrival estimation (DoA), localization using acoustic signals [14] and Multiple input multiple output (MIMO) systems. Antenna arrays are also referred to as “smart antennas” or “adaptive antenna arrays” [15].

2.4 Multiple input multiple output (MIMO) Systems

One of the major applications of the antenna array is in multiple input multiple output (MIMO) systems. In MIMO systems an array of antennas is deployed on both the transmitter and the receiver sides. Both the transmitter and the receiver can transfer multiple streams of data at the same time using the same frequency band. This will result in the transmission of a large amount of data using the same bandwidth in comparison with single input single output (SISO) systems [16]. Moreover, this results in the concept of space diversity [16], which is very useful in the mitigation of fading effects. For MIMO systems, the diversity gains of MIMO systems are analyzed according to the design of their space-time orthogonal codes.

In order to analyze the performance of MIMO systems in terms of fading mitigation, For all the antenna elements, the commonly used channel model is Rayleigh fading. This was employed in [17-21], where novel signal processing schemes for MIMO systems were introduced. The simplicity of this channel model made the performance analysis of these schemes less complicated, allowing the authors to place more emphasis on introducing transmit and receive signal processing algorithms. The Fundamental information and theoretical results for the capacity of MIMO channels and transmission diversity techniques are presented in [22-23].Using space-time coding techniques; the concept of space diversity can also be achieved by the combination of several transmitters and having only one antenna. This results in a concept of virtual MIMO systems. Using virtual MIMO multiple nodes cooperatively transmits the same data [24-25] towards the receiver. The analysis performed in [24-25] is based upon baseband models of multi-user information theory. Hence, synchronization among the multiple transmitters and receivers is not considered. However, recent literature reports that the synchronization errors significantly degrade the performance of virtual MIMO systems [26]. A synchronization method that reduces the phase and frequency errors is developed and presented in Chapter 4.

2.5 Signal Power Loss in Wireless Channels

When the signal is transmitted through a channel that is either wired or wireless, the signal power degrades due to noise, impairment, cross talk, path loss, fading and etc. In this section we will present different path loss models and their characteristics for wireless channels. The total power loss between transmitted and received signal is explained in sections 2.5.1 to 2.5.4. Let signal S be transmitted towards receiver at distance d. The received signal power at the receiver is denoted as P_r and may be generally expressed as

$$P_r(d) = P_t / g(d), \tag{2.1}$$

where $P_r(d)$ is the received power at the receiver residing at distance d from the transmitter, P_t is the transmitted power and $g(d)$ is power loss as a function of the transmission distance d.

To characterize the communication systems, signal to noise ratio (SNR) or signal to interference ration (SINR) are widely used. For communication links SNR and SNIR should be above a certain threshold value [27]. The threshold values of SNR and SNIR vary for different wireless channels [27] and depend upon acceptable receiver error probability. The SNR is defined as the ratio of power of received signal P_r and the power of noise.

Power loss $g(d)$ depends upon channel effects. The most influential channel effect that degrades the power of a received signal is fading [2]. Several mathematical models and their characteristics for signal power loss $g(d)$ are well studied in [1, 2, 9, 28].

In this section, several signal power loss models are presented and analyzed. These models are very important and are the perquisites for the calculation of the energy consumption and energy efficiency of a wireless network. These models are utilized to calculate the energy consumption of SISO and collaborative communication systems, presented in Chapter 6.

2.5.1 Free space signal path loss model

The free space signal path loss model is an ideal and basic path loss model for wireless communication and is widely adopted in fiction for the minimalism of its form. This model is applicable where transmitter and receiver have a clear line-of-sight (LOS).

It is assumed that there is no obstacle between the transmitter and receiver. In this case received power may be represented [1, 2, 28] as

$$P_r(d) = \frac{P_t G_t G_r \lambda_w^2}{(4\pi)^2 d^2 L}, \tag{2.2}$$

where G_r is receiver antenna gain, G_t is transmitter respectively, λ_w is the wavelength i.e., c/f_c, c is the speed of light, f_c is the carrier frequency, L is the miscellaneous system loss due to transmission loss attenuation, filter loss and antenna loss, and d is distance between transmitter and receiver.

2.5.2 Two-ray ground signal path loss model

The two-ray ground signal path loss model is an extension of the free space signal path loss model [28]. In this model, the LOS path and a ground-reflection path are considered. The two-ray ground signal path loss model is widely used as a path loss model and has high accuracy [1]. For the two-ray-ground signal path loss model, the received power may be calculated [1, 2, 28] as

$$P_r(d) = \frac{P_t G_t G_r h_t^2 h_r^2}{d^4 L}, \tag{2.3}$$

where h_t is the height of transmitter antenna and h_r is the height of receiver antenna.

2.5.3 Log-normal shadowing signal power loss model

The log-normal shadowing signal power loss model is used when a channel has shadow fading. The shadow fading is due to ground effects, such as; absorption, reflection, scattering and diffraction [1]. This model is derived on the basis of analytical and experimental methods. It is analyzed that the mean value of the received power decreases logarithmically with the transmission distance d. It is analyzed that the path loss follows the log-normal distribution. The received power of the log-normal shadowing signal power loss model may be calculated [1,2,28] as

$$P_r(d) = P_t + 10\log_{10}\left(\frac{\lambda_w}{4\pi d_o}\right)^2 - 10k\log_{10}\left(\frac{d}{d_o}\right)^2 + X_\sigma, \tag{2.4}$$

where d_o is the reference distance for the antenna far-field region, k is the path loss exponent, shadow fading is represented as X_σ i.e., a zero-mean Gaussian random variable in dB with standard deviation σ is also in dB. Path loss exponent k depends upon the wireless environment i.e., for indoor environment, the value of k may be set to 5 or even greater, whereas in the outdoor environment, k may take low values, such as 2 or even lower. Normally the values taken by σ are between 6dB and 10dB, if not greater [2].

2.5.4 Simplified signal path loss model

The simplified signal path loss model is widely used to calculate the path loss. It combines the properties of the free space path loss model and the two-ray-ground model; moreover, it does not include the effect of fading in path loss. It is the approximation of analytical results of the free space path loss model and two-ray-ground model [1]. It is claimed that simplified path loss has high signal power loss estimation accuracy [1]. Using this model, the power of the received signal is given in [1] and may be represented as

$$P_r(d) = P_t\left(\frac{\lambda_w}{4\pi d_0}\right)^2\left(\frac{d_0}{d}\right)^{\chi}, \qquad (2.5)$$

where the value of χ depends on the signal propagation environment and ranges from 2 to 8. The simplified path loss model presented in equation (2.5) is the general form of signal path loss defined in equations (2.2) and (2.3). Fading effects are not considered in signal path loss. In this regard, this simplified signal path loss model allows us to evaluate the effect of the Rayleigh fading on node energy consumption and the node energy saving arising from the fading mitigation technique i.e., collaborative communication, as studied in Chapter 5.

2.6 Multipath and Small-scale Fading

"Fading" is defined as rapid fluctuations of the amplitudes, phases, due to the multipath transmission of signal over a short period of time, or over short transmission distance [2]. Generally, in real time enjoinments there are a lot of objects, e.g., hills, trees, buildings, etc., which reside in a transmission path. Due to the presence of these objects, transmitter waves are reflected and scattered. This results in multiple

transmission paths between transmitter and receiver. The transmitted signal arrives at the receiver via different paths and this produces multipath interference known as multipath fading. If the transmitters and receivers are not stationary, multipath effects enhance changes in the amplitude and the phase of the received signal. Therefore, signal power is also degraded. Multipath fading effects are summarized below:

- The signal loses its power rapidly over a small time interval and short transmission distance.
- Due to multipath propagation delay, echoes and time dispersion are produced.
- Mobility produces the Doppler shift that results into random frequency modulation.

2.6.1 Physical factors influencing Fading

There are several physical factors that may influence fading in radio propagation channels. In this subsection, the important factors that influence the fading are elaborated.

2.6.1.1 Multipath effect

Due to reflection and scattering, transmitted signals arrive at the receiver from multiple paths. The multipath phenomenon produces constructive and destructive interference. It may also result in phase changes for the received signal.

2.6.1.2 Mobility of transmitter and receiver

The mobility of both the transmitter and the receiver produces Doppler shift in the propagated signals on multiple paths. Doppler shift results in random frequency modulation.

2.6.1.3 Mobility of surrounding objects

The mobility of objects residing within the transmission channel produces time varying Doppler shift for multipath components. If the mobility of surrounding objects is greater than the mobility of transmitter and receiver, it also produces fading; this is the most dominant factor in fading.

2.6.1.4 Transmission Bandwidth of the signal

If the transmitted radio signal bandwidth is greater than the “bandwidth” of the multipath channel, also known as coherence bandwidth, the received signal significantly losses its power.

2.6.2 Types of Small Scale fading

Fading depends upon the relationship between transmitted signal parameters and the channel parameters. The signal parameters are time period and bandwidth, while the channel parameters are Doppler shift and delay spread. Different types of fading are discussed in this section.

2.6.2.1 Flat Fading

When the bandwidth of a transmitted signal is less than the coherence bandwidth of the channel, or when the time period of the transmitted signal is more than the root mean square (rms) value of the delay spread of the channel, this results in fading. This type of fading is known as flat fading or Rayleigh fading [2]. Rayleigh fading is dependent on the movement of transmitters and receivers and channel coherence bandwidth. When the transmitter and receiver are moving slowly Rayleigh fading is considered to be flat. In wireless sensor networks, transmitters and receivers are not fast moving therefore, the channels between stationary sensor nodes may be characterized as flat Rayleigh fading channel. Therefore, for a collaborative communication system, the Rayleigh fading channels have been considered; these are presented in Chapters 4 and 5. Although it can be seen from the literature, many advanced indication dispensation techniques have been proposed to moderate Rayleigh fading, adding sufficient fade edge is taken to be one of the most conservative engineering methods, as explained in section 2.6.3.

2.6.2.2 Frequency selective fading

When the bandwidth of the transmitted signal is wider than the coherence bandwidth of the channel, or the time period of the transmitted signal is less than the root mean square (rms) value of the delay spread, ,fading occurs. This type of fading is called frequency selective fading [2].

2.6.2.3 Fast Fading

The mobility of transmitters, receivers or surrounding objects produces Doppler shift. Due to Doppler shift, random frequency modulation is produced, resulting in fading. This type of fading is called fast fading. Due to fast fading, the channel very rapidly fades within the time period of transmitted signal [2].

2.6.2.4 Slow Fading

When a channel does not change the impulse response within the time period of the transmitted signal, but changes its state after the time period has elapsed, this type of fading is called slow fading [2].

2.6.3 Fade Margin

Fade margin is defined as the power required to compensate for the power loss due to channel fading. It is found in [2, 29] that, for many wireless applications, a substantial amount of fade margin is required to compensate for the power loss due to channel fading. Fade margins for the cellular system are shown in Figure 2.2. In Figure 2.2, path loss may be calculated using equations (2.2), (2.3), (2.4) or (2.5), depending on the signal power loss model. The typical value of the fade margin for shadow fading is often set to at 6-10 dB [2] and the typical value of the fade boundary for Rayleigh fading is often set at 20 dB to 30 dB [2].

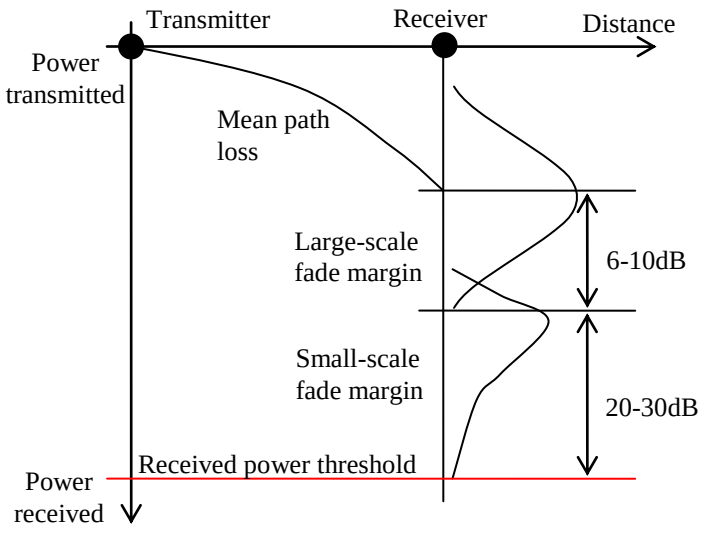

Figure 2.2 Fade margins in the cellular application [2]

From Figure 2.2 it is observed that small-scale fading has a higher fade margin than shadow fading. The large amount of necessary fade margin suggests that a significant amount of transmitted power has to be received at the receiver in order to achieve required SNR. Energy efficient communication is the primary requirement in wireless sensor networks and energy saving is the one of the primary design requirements in wireless sensor networks [6, 7]. Therefore, there is a need for an appropriate signal processing technique, or other method, to mitigate the channel fading, effectively

A variety of fading mitigation techniques i.e., channel equalization, Rake receiver, maximum ratio combining, and transmitter and receiver assortment in space, time and frequency [1] are proposed to mitigate the channel fading. These fading mitigation techniques require high signal processing and also require a large amount of additional hardware. Although it is often assumed that the amount of energy required for signal processing is small, the results in [30-32] argue that the energy expenditure for complex signal processing is significant.

This research proposes a collaborative communication system to mitigate the channel fading. The proposed collaborative communication system exploits the concept of space diversity to compensate for fading effects. Collaborative communication systems are presented in Chapter 4 and the fading mitigation capability is studied in chapter 5. From Chapter 5 it can be observed that fading can be significantly mitigated by the utilization of collaborative communication, at the expense of circuit power. Therefore, as described in chapter 6, a trade-off analysis is performed between the circuit power required and the power gain achieved using collaborative communication.

2.7 Multiple Access Methods for Multi-user Communication Systems

In the multi-user system, high-capacity communication services are required. As the wireless channel is shared by a large number of users who may be accessing the channel concurrently, there is a demand for methods that allow for the sharing of the available channel between many users, thus reducing the interference. Hence the nature of the multi-user system becomes more complicated than that of the transmitter-to-receiver system studied in the previous section. In multi-user systems, the received signal is the sum of transmitted signals by source and unwanted signals from other transmitters. The interference signals are regarded as noise to the intended signal. This result in a

considerable decrease in the signal-to-interference-noise (SINR) ratio and therefore the receiver error performance become significantly degrade.

To use the public wireless channel effectively, several multiple access methods that are widely used in wireless communication systems are proposed. The most commonly used multiple access methods are given below:

- Frequency division multiple access (FDMA)
- Time division multiple access (TDMA)
- Frequency time division multiple access (F/TDMA).
- Code division multiple access (CDMA)
- Space division multiple access (SDMA).

2.7.1 Frequency Division Multiple Access (FDMA)

In frequency division multiple access (FDMA), multiple users access the available frequency bandwidth at the same time. The frequency bandwidth is split into a number of narrow bandwidth channels. Each user is assigned a particular narrowband channel which is not shared by other users, as shown in Figure 2.3 (a). In FDMA multiple users can transmit and receive data continuously at the same time.

2.7.2 Time Division Multiple Access (TDMA)

In time division multiple access (TDMA) multiple users can access the total available bandwidth for certain period of time. In TDMA, the time for system users to transmit data is divided into slots, as shown in Figure 2.3 (b). At any given time, a pair of users may access the entire available frequency bandwidth of the system. Thus data transmission for any users in a TDMA multi-user system is not continuous, but occurs in bursts. Because the time is slotted in TDMA, time-synchronization needs to be established between the transmitter and the receiver in order for the data transmission to proceed.

2.7.3 Frequency Time Division Multiple Access (F/TDMA).

In FDMA a specific part of the channel bandwidth is assigned to a specific user. If the user does not have to transmit the data at a particular time, this part of the bandwidth is not used by other users, resulting in poor capacity. In TDMA, also, specific time slots

are assigned to a specific user. If the user does not have to transmit the data at a particular time, the time slot is not used by other users, resulting in poor capacity. Therefore, a hybrid F/TDMA system is proposed that is a combination of both FDMA and TDMA. This F/TDMA method is used in various practical wireless applications such as GSM, amongst others

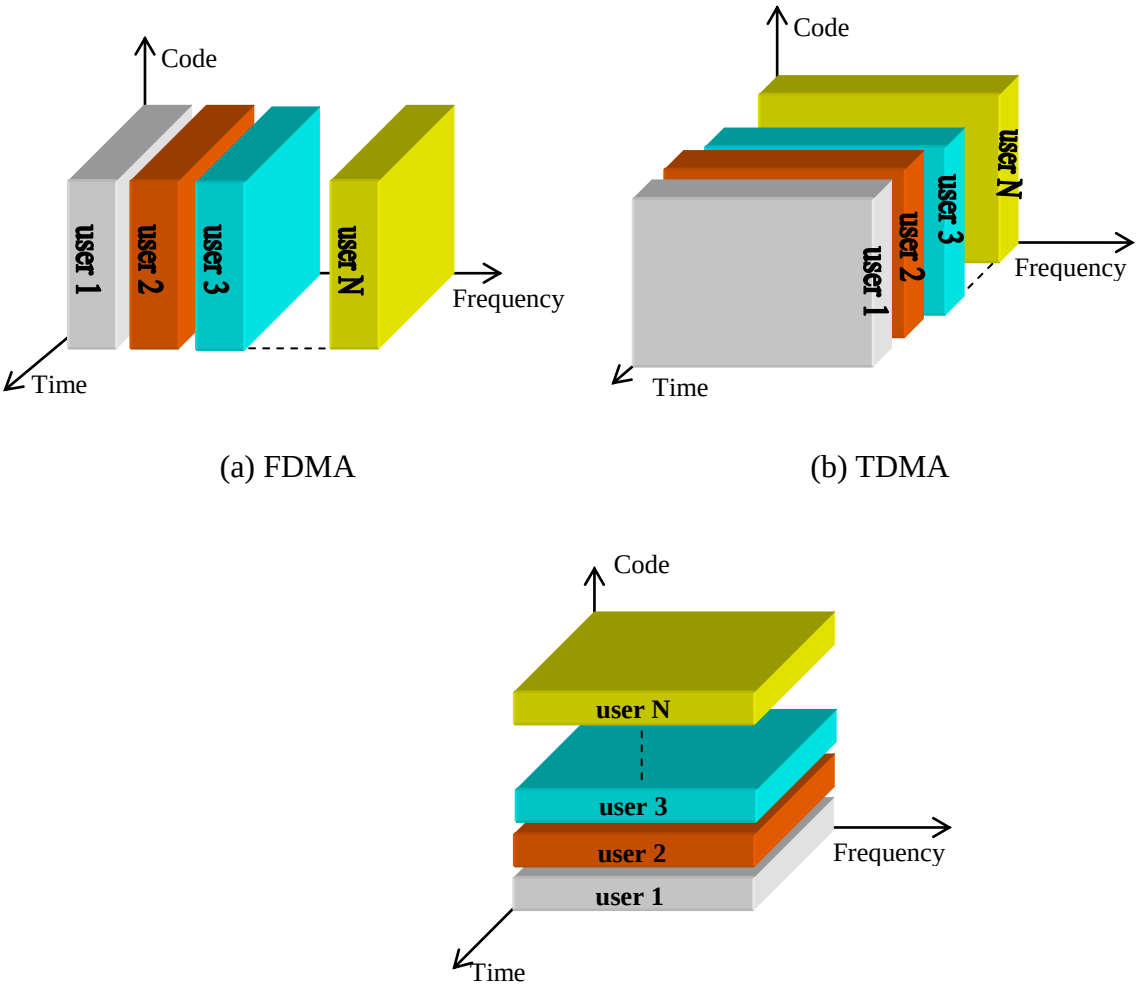

(a) FDMA

(b) TDMA

(c) CDMA

Figure 2.3 FDMA, TDMA, and CDMA in time and frequency domains.

2.7.4 Code Division Multiple Access (CDMA)

In CDMA multiple users access the entire bandwidth at the same time. Users are distinguished from each other using a pseudo random sequence known as spreading

codes. These spread codes are orthogonal to each other. Therefore, multiple users can transmit and receive data using the entire bandwidth at the same time, at the expense of the multi-user interference induced in the receiver, as shown in Figure 2.3 (c). CDMA systems can be divided into two categories i.e., frequency hopping CDMA (FH-CDMA) and direct sequence CDMA (DS-CDMA). In frequency hopping CDMA, rapid frequency changes are achieved using spread codes. While in direct sequence CDMA, transmitted data bits are multiplied with a spreading code i.e., a pseudo noise sequence also known as the PN sequence; the receiver de-spreads the received signal using the same code. As the PN sequences are orthogonal, the receiver may de-spread signals from the intended user by conducting a time-domain correlation of the received signals.

2.7.5 Space Division Multiple Access (SDMA)

Space Division Multiple Access (SDMA) is based on the concept of sectors [33]. This is widely used in cellular networks. In SDMA a wireless channel is divided among the different users in accordance with the direction of motion of radio waves. At the receiver, the direction of the motion of radio waves is the direction of arrival. For transmitter motion, the direction of radio waves is the direction of departure. SDMA can be implemented by sectorised antennas or antenna arrays with beamforming [33].

2.8 Chapter Conclusions

This chapter presents the study of some of the fundamentals of physical layer and wireless digital communication. As few of the upper layer algorithms are unaffected, the physical layer is important in the design and analysis of wireless sensor network communication algorithms. Several signal power loss models are presented to estimate the power loss. Mathematical expressions of signal power loss models are also presented. These models will be used to develop the energy efficient collaborative communication system for sensor networks, as presented in Chapters 4, 5 and 6. It is observed that a large fade margin is required to compensate for signal power loss due to channel fading. This has motivated us to investigate fading-mitigating techniques, presented in Chapter 5. Appropriate channel multiple access methods are needed to reduce data collision and to support the energy-efficient operation of communication algorithms in the higher layers of the network protocol stack.

References

[1] A. Goldsmith, Wireless communications, Cambridge University Press, 2005, pp. 453-454, 553-554, 27-52.

[2] B. Sklar, "Rayleigh fading channels in mobile digital communication systems part I: characterization," IEEE Commun. Mag., 1997, pp.90-100.

[3] A. Fanimokun, J. Frolik, "Effects of natural propagation environments on wireless sensor network coverage area," in Proc. the 35th Southeastern Symposium on System Theory, 2003, pp. 16 - 20.

[4] S. Hara, D. Zhao, K. Yanagihara, J. Taketsugu, K.Fukui, S. Fukunaga, and K. Kitayama, "Propagation characteristics of IEEE 802.15.4 radio signal and their application for location estimation," in Proc. IEEE VTC'05, vol. 1, 2005. pp. 97 - 101.

[5] K. Iniewski, Wireless technologies: circuits, systems, and devices, CRC Press , 2008, pp.110-111.

[6] W. B. Heinzelman, A. P. Chandrakasan, and H. Balakrishnan "An application-specific protocol architecture for wireless microsensor networks," IEEE Trans. on Wireless Commun., vol. 1, 2000, pp. 660-670.

[7] O. Younis and S. Fahmy, "HEED: a hybrid, energy-efficient, distributed clustering approach for ad hoc sensor networks," IEEE Trans. on Mob. Comput., vol. 3, 2004, pp. 366-379.

[8] M. El-Sayed, J. Jaffe, "A View of Telecommunications Network Evolution", IEEE Communications Magazine, vol. 40, no. 12, 2002, pp. 74-81.

[9] B. Sklar, Digital communications: fundamentals and applications, N.J.: Prentice-Hall, 2001, pp.5.

[10] J. D. Kraus, Antennas, Second Edition. Mc-Graw Hill, 1988.

[11] V.V. Swarte, Electromagnetic fields and waves. New Dehli: New Age International Limited. 1993, Reprint-2006, pp. 396, 397.

[12] S. Uda and Y. Mushiake, Yagi-Uda Antennas, 1954.

[13] A. R. Thompson, B. G. Clark, C. M. Wade, and P. J. Napier, "The Very Large Array," Astrophysical Journal Supplement Series, vol. 44, October 1980, pp. 151–167.

[14] K. Yao, R. Hudson, C. Reed, D. Chen, and F. Lorenzelli, "Blind beamforming on a randomly distributed sensor array system," IEEE J. Sel. Areas Communication, vol. 16, no. 8, 1998, pp. 1555–1567.

[15] J. Winters, "Smart antennas for wireless systems," IEEE Personal Communications, vol. 5, no. 1, 1998, pp. 23–27.

[16] A. R. Thompson, B. G. Clark, C. M. Wade, and P. J. Napier, "The Very Large Array," Astrophysical Journal Supplement Series, vol. 44, October 1980, pp. 151–167.

[17] V. Tarokh, N. Seshadri, and A.R. Calderbank, "Space-time codes for high data rate wireless communications: performance criterion and code construction," IEEE Trans. Inform. Theory, vol. 44, March 1998, pp.744-765.

[18] G.J. Foschini, "Layered Space-Time Architecture for wireless communication in a fading environment when using multiple antennas," Bell laboratories technical journal, vol.1, No.2, 1996, pp.41-59.

[19] V. Tarokh, H. Jafarkhani, and A. R. Calderbank, "Space-time block coding for wireless communications: performance results," IEEE J. Select Areas in Communication, vol.17, March 1999, pp.451-460.

[20] V. Tarokh, A. Naguib, N. Seshadri, and A.R. Calderbank,"Combining array processing and space-time coding ,"IEEE Trans. on Inform. Theory, vol.45, no.4, May, 1999, pp.1121-1128.

[21] S. M. Alamouti, "A simple transmit diversity technique for wireless communications," IEEE J. Select. Areas in Commun., vol.16, Oct, 1998, pp. 1451-1458.

[22] G.J. Foschini and M.J. Gans, “On limits of wireless communication in a fading environment when using multiple antennas,” Wireless Personal Commun., vol.6, No.3, 1989, pp.311-366.
[23] A. Narula, M. D. Trott, and G. W. Wornell, “Performance limits of coded diversity methods for transmitter antenna arrays,” IEEE Trans. on Inform. Theory, vol.45, no.7, Nov, 1999, pp.2418-2433.
[24] A. Sendonaris, E. Erkip, and B. Aazhang, “User cooperation diversity. Part I. System description,” IEEE Trans. on Commun., vol. 51, no. 11, Nov 2003, pp. 1927–1938.
[25] S. Alamouti, “A simple transmit diversity technique for wireless communications,” IEEE Selected Areas in Communications, vol. 16, no. 8, October 1998, pp. 1451–1458.
[26] J. Laneman and G. Wornell, “Distributed space-time-coded protocols for exploiting cooperative diversity in wireless networks,” IEEE Trans. on Inform. Theory, vol. 49, no. 10, Oct 2003, pp. 2415–2425.
[27] X. Li, Wireless ad hoc and sensor networks : theory and applications, Cambridge University Press, 2008, pp.17-20.
[28] T. S. Rappaport, Wireless communications: principles and practice, N.J. : Prentice Hall, 1996, pp.69-90.
[29] S. Cui, A. Goldsmith, A. Bahai, "Energy-efficiency of MIMO and cooperative MIMO techniques in sensor networks," IEEE J. Sel. Areas Commun., vol. 22, no. 6, 2004, pp. 1089-1098.
[30] R. Olexa, Implementing 802.11, 802.16 and 802.20 wireless networks, Boston : Newnes, 2004, pp. 124-126. P. Agrawal, "Energy efficienct protocols for wireless systems," in Proc. Internat. Sympos. Pers., Indoor, Mobile Radio Commun., 1998, pp. 564-569.
[31] W.R. Heinzelman, A. Sinha, and A.P. Chandrakasan, "Energy-scalable algorithms and prototocls for wireless micro-sensor networks," in Proc. IEEE Internat. Conf. Acous., Speech, Signal Proc., 2000, pp. 3722-3725.
[32] H. Karl and A. Willig, Protocols and architectures for wireless sensor networks, NJ: Wiley, 2005, pp. 129-131, 113-114.
[33] C.-Y. Huang, R. Yates, “Rate of Convergence for Minimum Power Assignment Algorithms in Cellular Radio Systems”, ACM/Baltzer Wireless Networks Journal, vol. 4, no. 3, 1998, pp. 223-231.

Chapter 3 Introduction of Wireless Sensor Networks

3.1 Introduction

This chapter presents a comprehensive introduction, hardware framework and communication protocols for Wireless Sensor Networks (WSNs). The main focus of this chapter is on the applications of the wireless sensor network, the sensor node hardware structure, the communication protocol stack and the core challenges to the design of wireless sensor network communication protocols. The standards for industry and the latest research related to wireless sensor networks are also presented in this chapter.

The study begins with the major applications of wireless sensor networks. The constraints of wireless sensor networks and the requirements for different applications are presented in Section 3.2. In Section 3.3, the hardware framework of a sensor node is presented; the major components of hardware framework are also identified and the function of each component is explained.

In section 3.4, the layered architecture wireless sensor networks communication protocol is presented; the functions of each layer and their requirements are also elaborated on. The planes of wireless sensor networks communication protocol are identified and explained. The challenges to the designing of wireless sensor network communication algorithms are presented in section 3.5; the key challenges are identified and possible solutions are proposed. A comprehensive review of the literature relating to recent work in the designing of wireless sensor network communication protocols is presented in Section 3.6. The design challenges and solutions for each layer of sensor network communication protocol are elaborated. From the reviewed literature, it is revealed that there is a need for energy efficient communication system for wireless sensor networks. In this regard, a collaborative communication system is designed, analyzed and simulated, and presented in Chapters 4 and 5.

The industrial standardization of the wireless sensor network is explained in section 3.6. The parameters of off-the-shelf products that follow the industry standards are identified and presented. The parameters of these off-the-shelf products are used to investigate the performance of proposed collaborative communication systems, presented in Chapters 4, 5, 6 and 7.

3.2 Wireless Sensor Networks Applications

A sensor network is composed of a large number of low cost, small size, battery powered sensor nodes that communicate with a receiver denoted as the base station. Wireless sensor networks are becoming very popular due to their large number of applications. Some of the wireless sensor networks applications are: military applications, such as battlefield surveillance, enemy tracking and battle damage assessment; civil applications, such as environment-friendly buildings and logistics, disaster detection and rescue, environment observation and forecast system; health applications such as biodiversity and habitat monitoring; these are all in addition to other commercial applications [1-5]. Due to numerous applications stated above, The Wireless Sensor Network is recognized as one of 21 most important technologies of the 21st century, Week [6].

With all these applications, there are constraints on wireless sensor networks i.e., the limited battery power of sensor nodes. Therefore, energy efficient communication is the primary requirement in wireless sensor networks. In view of the application diversity of wireless sensor networks, it is difficult to set up a, one-for-all, node hardware framework and a standard communication protocol stack in order to achieve energy efficient communication and satisfy the specific requirements of each application. However, to satisfy the basic requirements of different sensor networks applications, a generalized node hardware framework and communication protocol stack are presented in the literature review [1, 2, 7].

3.3 Hardware Framework of a Sensor Node

The basic requirement of wireless sensor networks is to create node hardware using simple and cheap electronic components in order to decrease the size and cost of a sensor node. There are five basic components of a wireless sensor node [1, 2, 7]. These components are:

1. Power supply
2. Wireless communication device
3. Computation device
4. Memory
5. Sensor

The architecture of a sensor node and the interconnection between the components are presented in [1, 2, 7] and shown in Figure 3.1.

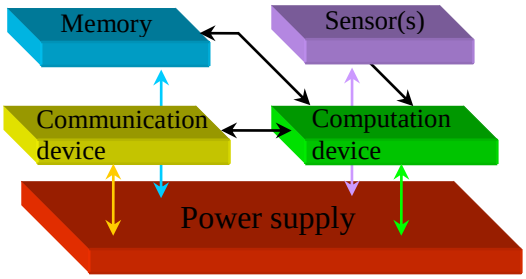

Figure 3.1 Sensor node hardware framework [1, 2, 7].

The sensor component of the sensor node framework captures the data from the physical environment, then converts it in the form of signals and passes it on to the computation device. The computation device performs the basic computing for the received signal and passes it to the communication device and/or, to memory. The wireless communication device enables the node to establish wireless connections with other nodes in the network, or with the base station, to exchange the information. A memory component is used for data storage. The power supply component provides the driving force for the other four electronic components.

The performance of the electronic components can be increased using high performance computing devices. But, high performance devices such as the processors in modern personal computers, and the transceivers in cell-phones, are very costly and consume a lot of power. Moreover, in wireless sensor networks, a battery is the only power supply for other onboard electronic components of a sensor node. As sensor networks consist of a large number of nodes, and nodes are randomly deployed in a vast area, it is very difficult to recharge or replace the battery of a node. Therefore, there is a tradeoff between energy consumption of the node and the computational complexity of the sensor node. Hence, in the design of computing components and wireless communication components, a balance is required between node energy consumption and the performance requirement of the application [8].

Due to limitations in cost and power, microcontrollers are used as the computing device in wireless sensor networks. The main advantage of microcontrollers is their low power consumption and flexible programmable/reprogrammable capability at a

reasonable expenditure [1]. A wide range of low-cost wireless transceivers are available in the market and one of these can be utilized as the sensor node's wireless communication device. These transceivers support data transmission rates ranging from tens to hundreds of kilo-bits-per-second (kbps) and have a relatively short transmission distance; this varies from tens to hundreds of meters at acceptable error rates and with reasonable energy consumption.

3.4 Wireless Sensor Network Communication Protocol Stack

"Communication Protocol" is defined as a set of rules and regulations for the interchange of information between different devices [1]. Communication protocol design has a substantial impact on the performance of any communication system. A wireless sensor network communication protocol for node to node data communication is proposed in [1, 7], as shown in Figure 3.2. This protocol allows the design of each layer to optimize the use of the node energy resource.

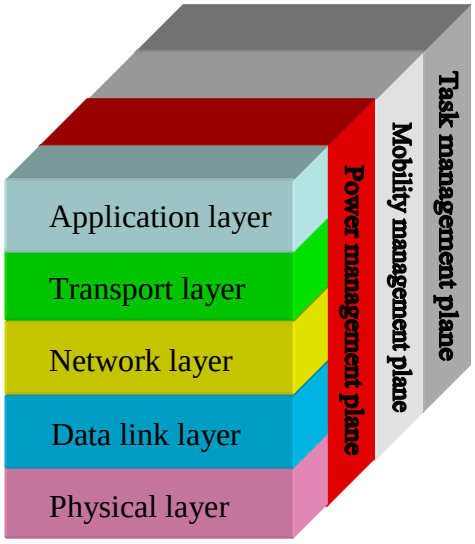

Figure 3.2 A compelling communication protocol stack of Wireless sensor network [1,7].

There are five layers and three planes of communication protocol for wireless sensor networks [1].

These layers of communication protocol are given below:

- Physical layer

- Data link layer
- Network layer
- Transport layer
- Application layer

The planes of communication protocol for wireless sensor networks are:

- Power management plane
- Mobility management plane (optional)
- Task management plane (optional)

3.4.1 Physical layer

The physical layer is the first layer of the wireless sensor network communication protocol stack. The physical layer consists of the basic networking hardware transmission technologies of a network. It is directly attached to the wireless channel. It defines the physical specifications for the wireless transceiver to access wireless channels, such as; the operating frequency band, modulation scheme, signal transmission power, etc. The physical layer is intended to provide reliable signal transmission and reception for the data link layer.

3.4.2 Data link layer

The data link layer is responsible for packet flow control and medium access control. For example, in a case such as where the received packet is found to have erroneous bits, the data link layer drops the faulty packet and makes decisions on whether, how and when to request packet re-transmission from the sender.

3.4.3 Network layer

The network layer has a decisive role in shaping the topology of wireless sensor network and its network traffic flow. The internet layer has three basic functions: For outgoing packets, the next-hop host (gateway) is selected and the packet is transmitted the to the host by passing it to the appropriate link layer implementation; for incoming packets, if appropriate, the packets are captured and passed, payload up, to the

appropriate transport-layer protocol. In addition the network layer provides error detection and diagnostic capability.

3.4.4 Transport layer

The transport layer provides reliable packet transmission and reception for the application layer on the top. The transport layer provides convenient services, such as; connection-oriented data stream support, reliability, flow control, and multiplexing.

3.4.5 Application layer

Various wireless sensor network applications are embodied in the application layer. The application layer contains all the protocols and methods that fall into the area of process-to-process communications across the network. Application layer methods use the underlying transport layer protocols to establish host-to-host connections.

3.4.6 Power management plane

The power management plane provides node power information to all layers in the wireless sensor network communication protocol stack. This information is very useful for the performing of power optimization.

3.4.7 Mobility management plane

The mobility management plane provides node mobility information to all layers in wireless sensor network communication protocol stack. This information is very useful for perform position or mobility optimization.

3.4.8 Task management plane

The task management plane provides the task fulfillment information to all layers in the wireless sensor network communication protocol stack. This information is very useful in performing performance optimization.

The wireless sensor network protocols have a significant impact on the performances of node-to-node communication, as well as on network-wide data transmission. Understanding the challenges that confront the design of WSN communication algorithms and protocols is the first step towards yielding effective solutions. From the WSN application requirements and the sensor node hardware constraints, several core challenges are drawn and explained in the next section.

3.5 Challenges in Designing Wireless Sensor Network Communication Algorithms

From the existing literature it is found that there are many challenges to the design of efficient wireless sensor network communication systems. Several of the core challenges revealed from literature [1-3, 8] are summarized in the followings:

- **Energy efficiency.** The life time of the sensor network is dependent on the limited availability of battery power. The energy depletion of a few nodes may cause serious connectivity issues and result in a network breakdown [9]. Hence, energy efficiency is the key requirement and the primary goal of the design of wireless sensor network communication protocols.
- **Simplicity.** In wireless sensor networks, sensor nodes have limited computational capability. Therefore, communication systems need to be simple so that less computation is needed from the computing device and thus, the efficiency of communication protocol can be enhanced.
- **Time synchronization.** The sensor network consists of a large number of nodes with each node being dependent on the time clock independently generated by the oscillator onboard. As each node has an independent oscillator, there may be time-drift among the various nodes [10]. This introduces time synchronization errors, which creates fundamental challenges to the performance of communication protocols.
- **Decentralized operation.** Wireless sensor networks are infrastructure free networks. Also wireless sensor nodes are randomly deployed in vast rear. Therefore, there is no infrastructure and human intervention once the sensor nodes have been deployed. Hence, wireless sensor network communication protocols must be decentralized and

the network must be able to perform its communication without being dependent upon either infrastructure or, human assistance.

- **Scalability.** As a sensor network consists of large number of sensor nodes and is deployed in vast area, communication protocol should produce a high performance for a large number of nodes [1]. This concept is also known as scalability. The communication protocols that produce high performance levels for nodes should not, at the same time degrade their performance for the dense node deployment scenario.
- **Fault resistance.** As the sensor nodes are of low cost and cheap hardware is used for communication and storage, there is a requirement of communication protocols that they should be designed to stabilize hardware outages. In the case of node failure, communication protocols need to support the network re-organization.

3.6 Related Work in Designing Wireless Sensor Network Communication Protocols

Due to the vast applications of wireless sensor networks, there is intense interest in the design of wireless sensor network communication protocols both in academia and in industry. Several solutions are proposed to tackle the challenges of design in wireless sensor networks. In this section some of the more influential solutions are presented. The solutions for every challenge to each layer of wireless sensor network communication protocols are developed and are summarized in this section. For practical application, for the design of wireless sensor networks, the Zigbee protocol [13] is adopted, in addition to the IEEE 802.15.4 standard [13].

3.6.1 Solutions for the physical layer

The physical layer is directly attached to the wireless channel and consists of the basic networking hardware transmission technologies of a network. Therefore, the solutions to the design challenges related to physical layer are implemented using advanced signal dispensation techniques in the transceiver. Node energy efficiency may be achieved using; dynamic modulation scaling [14], adaptive channel coding [15], multi-input-multi-out-put signal meting out [16, 17], the spread spectrum (direct spreading or frequency hopping) [18-21], etc. Node energy can also be saved using dynamic voltage

scaling [22], which exploits the electronic nature of the transceiver that does not consume so much energy at low voltage.

3.6.2 Solutions for the data link layer

The data link layer is responsible for packet flow control and medium access control. Several Medium Access Control (MAC) algorithms are designed to overcome the challenges of the data link layer for wireless sensor networks. Multiple users can effectively and efficiently share the same wireless channel using these Medium Access Control (MAC) algorithms. Several MAC algorithms that are designed to reduce data loss due to channel collision are presented in [1]. The reduction in data loss results in a saving in node energy.

To control the sensor node's status i.e., transmitting or sleeping, several node scheduling algorithms [23-25] are designed. In the scheduling algorithms, the sensor node turns on its transceiver to transmit data. The decision as to when, and for how long, the node turns on its transceiver to transmit the data is made. These scheduling algorithms are known as the wireless sensor networks data link layer algorithm. Because of the fact that nodes consume much less power in a sleeping state than they do in a transmitting state, significant energy can be saved using the scheduling algorithms [23].

3.6.3 Solutions for the network layer

The network layer is responsible for packet forwarding through intermediate nodes to the receiver. In sensor networks, data is transmitted from the source node to the receiver using intermediate nodes, also known as multi-hops. Significant energy can be saved using Multi-hop routing algorithms [1, 26]. The routing algorithm shapes wireless sensor network topologies on the basis that data flows from the source node to the receiver. There are three important network topologies for wireless sensor networks, as shown in Figure 3.3. These topologies are:

- Tree topology
- Cluster topology
- Mesh topology

In the tree topology, the receiver resides in the centre and other nodes are around the receiver node. Data from sensor nodes are transmitted to the receiver via intermediate

nodes. Therefore data traffic converges towards the receiver and forms a tree-like network topology.

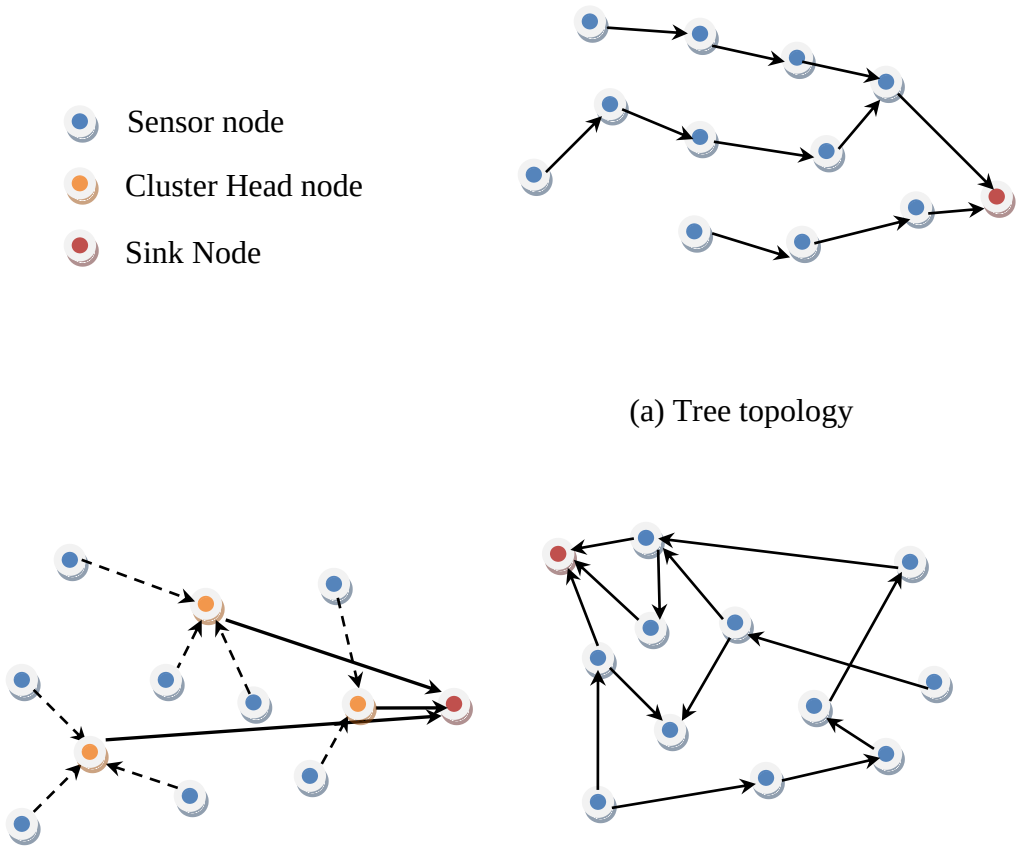

(a) Tree topology

(b) Cluster (star) topology

(d) Mesh topology

Figure 3.3 Primary topologies of wireless sensor networks [1].

Cluster nodes are also known as star topology. In the cluster topology, a set of sensor nodes gather themselves to transmit data. This group of sensor nodes is called a cluster. In the cluster, the topology set of sensor nodes transmit data to one node within the cluster; this is named the Cluster Head (CH) node. The CH node then forwards the data to the receiver. Mainly CH nodes reside in the centre of the cluster. All nodes within the cluster send the data to the CH and then the Ch transmits the data towards the receiver. The cluster based topology is widely used in several wireless sensor networks, such as environment monitoring and intelligent agriculture. In cluster based topology, the network data flow pattern is characterized as being “many-to-one” [1, 26, 27].

In mesh topology, wireless links can be established between any two sensor nodes. Mesh topology is very useful for achieving high data transmission reliability. In mesh topology, a few redundant links for sensor nodes are established to transmit the data towards the receiver. These redundant links ensure data transmission reliability when there is path failure or congestion in the network.

3.6.4 Solutions for the transport layer

The key responsibility of the transport layer is to provide reliable packet transmission and reception for the application layer on the top. For the design of the transport layer algorithms for wireless sensor networks, the key challenge is to achieve reliability. To ensure reliable packet transmission several transport layer algorithms are proposed and developed in [1, 28]. Using these algorithms, packet transmission between the nodes is quickly retransmitted in cases where a transmitted packet is lost due to congestion or other reasons.

3.6.5 Solutions for the application layer

User applications reside on the application layer. Different applications may have different requirements, therefore different solutions are proposed for each application layer. Although applications are different from each other, data aggregation is performed before transmitting [23, 27]. Significant energy can be saved using data aggregation; the node energy consumption for wireless data transmission is very much larger than the energy consumption for local data processing [29].

3.7 Industrial standardizations of the wireless sensor network

In 2003, the IEEE defined the standard for low power, low cost and low rate wireless communication devices for the Wireless Personal Area Network (WPAN). The protocols and interconnection for such wireless communication devices are defined in the standard known as the IEEE 802.15.4 [13]. In this standard, the functionality of the physical layer and the data link layer of the communication stack are specified. Later on the Zigbee standard was advocated by the Zigbee alliance [12] as the de-facto industrial standard for wireless sensor networks; this was adopted in IEEE 802.15.4. The network layer and the

upper layer of the communication stack for wireless sensor networks are defined in the Zigbee standard. In compliance with IEEE 802.15.4 and Zigbee standard, a large number of transceivers have recently become commercially available on the market i.e., CC2420 [30] and AT86RF21 [31].

In order to analyze the performance of a collaborative communication system, in this research, circuit parameters from off-the-shelf RF products i.e., CC2420 and AT86RF21, have been considered. The product data and the relevant parameters are shown in Table 3.1.

Two types of device i.e., Full-Function Device (FFD) Reduced-function device (RFD) are defined in IEEE 802.15.4. The constituting of a WPAN is considered for the analysis of the performance of the collaborative communication system and for the physical layer specifications of the suggested devices and their topology. As for the WPAN topology, IEEE 802.15.4 defines the star (cluster) or the mesh topology, which is shown in Figure 3.3 (b) and (c). In the cluster-based WPAN, the FFD takes the role of the CH node, whereas the RFDs are affiliated to the FFD in the same cluster.

Table 3.1 Product data and parameters [30-31]

Symbol	**Description**	**AT86RF212 [31]**	**CC2420 [30]**
-	modulation	BPSK	BPSK
w_0	operating frequency	915 MHz	2.45 GHz
Δw	Maximum Frequency error	55 KHz	200 KHz
R_s	transmission data rate (BPSK)	40Kbps	250Kbps
U	operating voltage (typical)	3 V	3 V
I_{rx}	currency for receiving states	9 mA	17.4 mA
P_{rx}	Receiving power, $P_{rx}= UI_{rx}$	27 mW	52.2 mW
I_{idle}	currency for idle states	0.4 mA	0.4 mA
P_{cir}	electronic circuitry power, $P_{cir} =UI_{idle}$	1.2 mW	1.2 mW
Psen	receiver sensitivity	- 110 dBm	- 95 dBm

3.8 Motivation for this Work

From the study presented in this Chapter, it is revealed that energy efficiency is the key design requirement for the design of wireless sensor networks. From the literature review presented in Chapters 3 and 4 it is observed that different factors i.e., path loss and fading, contribute to the energy expenditure in wireless sensor networks. The influential factor that degrades the energy efficiency of a wireless sensor network is fading. Therefore, for energy efficient communication, there is the need for a method that significantly mitigates the fading effects. There are several methods for fading mitigation available in the literature. One of the methods is use of the diversity technique. This has motivated us to design a system that exploits the concept of space diversity to mitigate the fading. Therefore in this thesis, a collaborative communication system that exploits the concept of space diversity is modelled, theoretically analyzed, and simulated.

3.9 Chapter Conclusions

This chapter presents study of the fundamentals of the wireless sensor networks. The importance of wireless sensor networks and there real time application is presented. The sensor node hardware framework and wireless sensor network protocols are also presented. Wireless sensor network protocol layers and protocol planes are elaborated on; the challenges of the requirements for the design of efficient protocols are identified and presented. The literature review relates to the state-of-the-art research on wireless sensor networks communication protocol; the design requirements and constraints are conducted and elaborated.

It is observed, that due to the limited battery power of sensor node, energy efficiency is the primary requirement in wireless sensor networks. Therefore, there is requirement for the design of an energy efficient wireless sensor networks communication system. From a study of the existing literature it is revealed that energy efficient and low-complexity communication protocols remain an open issue and, in particular, in the thick node deployment where protocol scalability becomes hard to attain. Therefore, in this thesis, we propose an energy efficient collaborative communication system for wireless sensor networks. In Chapter 4, a collaborative communication system is developed and its power gain is calculated. The fading mitigation capability of the collaborative communication system and the expressions for probability of error are derived and

simulated in Chapter 5. In Chapter 6, energy consumption models of single input single output (SISO) systems and collaborative communication systems are derived and compared. It is observed that a collaborative communication system outperforms the SISO system. The channel capacity of a collaborative communication system is studied in Chapter 7.

References

[1] H. Karl and A. Willig, Protocols and architectures for wireless sensor networks, NJ: Wiley, 2005, pp. 3-8, 18-36, 114-145, 289-357, 393-398.

[2] C.S. Raghavendra, K. M. Sivalingam, and T. Znatil, Wireless sensor networks, Boston : Kluwer Academic Publishers, 2004, pp.5-7, 53-55.

[3] C. Chong and S.P. Kumar, "Sensor networks: evolution, opportunities, and challenges," Proceedings of the IEEE, vol. 91, no. 8, 2003, pp.1247-1256.

[4] J. Burrell, T. Brooke, and R.Beckwith, "Vineyard computing: sensor networks in agricultural production," IEEE Pervasive Computing, vol. 3, no. 1, 2004, pp. 38 - 45.

[5] T. Wark, P. Corke, P. Sikka, L. Klingbeil, Y. Guo, C. Crossman, P. Valencia, D. Swain, and G. Bishop-Hurley, "Transforming Agriculture through Pervasive Wireless Sensor Networks," IEEE Pervasive Computing, vol. 6, no.2, 2007, pp. 50-57.

[6] "21 ideas for the 21st century," Business Week, Vol. 39, August, 1999, pp. 78-167.

[7] A. Boukerche, Handbook of algorithms for wireless networking and mobile computing, FL : Chapman & Hall, 2006, pp. 868-870.

[8] A. Goldsmith, Wireless communications, Cambridge University Press, 2005, pp. 540-542, 553-554, 27-52, 562-563.

[9] A. S. Tanenbaum, Computer networks, N.J. : Prentice Hall, 2003.

[10] Y. Zou and K. Chakrabarty, "A distributed coverage- and connectivity-centric technique for selecting active nodes in wireless sensor networks," IEEE Trans. Comput., vol 54, no. 8, 2005, pp. 978 - 991.

[11] Ivan Stojmenović (editor), Handbook of Sensor Networks: Algorithms and Architectures, Wiley, 2005, pp.112-114.

[12] Zigbee Alliance, [Online]. Available: http://www.zigbee.org/.[Access: Aug 5, 2009].

[13] IEEE 802.15.4 version 2006, IEEE Standards Association. [Online]. Available: http://standards.ieee.org/getieee802/download/802.15.4-2003.pdf. [Access: Aug 5, 2009].

[14] Z. Yang, Y. Yuan, J. He, and W. Chen, "Adaptive modulation scaling scheme for wireless sensor networks," IEICE Trans. on Commun., vol. E88-B, no. 3, 2005, pp.882-889.

[15] R. Min and A. Chandrakasan, "A framework for energy-scalable communication in high-density wireless networks," in Proc. ISLPED '02, 2002, pp. 36- 41.

[16] S. Cui, A. Goldsmith, and A. Bahai, "Energy-efficiency of MIMO and cooperative MIMO techniques in sensor networks," IEEE J. Sel. Areas Commun., vol. 22, no. 6, 2004, pp. 1089-1098.

[17] G. J. Miao, Multiple-input multiple-output wireless sensor networks communications, US Patent 7091854.

[18] M. Elmusrati, N. Tarhuni, and R. Jäntti, "Performance Analysis of Wireless Deaf CDMA Sensor Networks in Fading Channels," in Proc. IEEE VTC'07, 2007, pp. 189-192.

[19] S. De, C. Qiao, D.A. Pados, M. Chatterjee, and S.J. Philip, "An integrated cross-layer study of wireless CDMA sensor networks," IEEE J. Sel. Areas Commun**.,** vol. 22, no.7, 2004, pp. 1271- 1285.

[20] H. Kang, H. Hong, S. Sung, and K. Kim, "Interference and sink capacity of wireless CDMA sensor networks with layered architecture," ETRI journal, vol. 30, no.1, 2008, pp. 13-20.

[21] M. Gandetto, A. F. Cattoni, and C.S. Regazzoni, "A Distributed Wireless Sensor Network for Radio Scene Analysis," International Journal of Distributed Sensor Networks, vol.2, no. 3 ,2006 , pp. 201 – 223.

[22] R. Min, T. Furrer, and A. Chandrakasan, "Dynamic Voltage Scaling Techniques for Distributed Microsensor Networks," in Proc.WVLSI'00, 2000, pp.43-46.

[23] Jing Deng, S. Han, W. B. Heinzelman, and P. K. Varshney, "Balanced-energy sleep scheduling scheme for high-density cluster-based sensor networks," Computer Communications, vol. 28, no.14, 2005, pp. 1631-1642.
[24] G. Shi and M. Liao, "Stochastic sleeping with sink-oriented connectivity and coverage in large-scale sensor networks," Internat. Journal of Commun. Systems, vol. 20, no. 7, 2007, pp. 809 – 828.
[25] Z. Hu, J. Zhang, and L. Tong, "Adaptive Sensor Activity Control in Many-to-One Sensor Networks," IEEE J. Sel. Areas Commun., vol.24, no.8, 2006, pp.1525-1534.
[26] J.N. Al-Karaki and A.E. Kamal, "Routing techniques in wireless sensor networks: a survey," IEEE Wireless Commun., vol. 11, no. 6 , 2004, pp. 6-28
[27] W. B. Heinzelman, A. P. Chandrakasan, and H. Balakrishnan, "An application-specific protocol architecture for wireless microsensor networks," IEEE Trans. on Wireless Commun., vol. 1, 2000, pp. 660-670.
[28] Md. A. Rahman, A. El. Saddik, and W. Gueaieb, "Wireless Sensor Network Transport Layer: State of the Art," Springer Lecture Notes in Electrical Engineering, vol.21, pp. 221-245
[29] R. Rajagopalan and P.K. Varshney, "Data-aggregation techniques in sensor networks: a survey," IEEE Communications Surveys & Tutorials, vol. 8, no. 4, 2006, pp. 48-63.
[30] CC2420, Texas Instruments, [Online]. Available: http://focus.ti.com/analog/docs/enggresdetail.tsp?familyId=367&genContentId=3573. [Access: Jan 5, 2009].
[31] AT86RF212, ATMEL Products, [Online]. Available: http://www.atmel.com/dyn/products/ product_card.asp?PN=AT86RF212. [Access: Jan 5, 2009].

Chapter 4 Power Gain using Collaborative Communication

4.1 Introduction

From the literature review presented in chapters 2 and 3, it is revealed that wireless sensor networks (WSNs) inherit many properties of wireless digital communication systems. Due to the limited power of sensor nodes, an energy efficient transmission is the key requirement in wireless sensor networks. In the cases where the receiver, denoted as the base station, resides far away from the transmitter, multi-hop transmission is often taken as one of the viable solutions [1-3]. However, when the transmission distance increases, more hops are needed to accomplish the multi-hop transmission. This results in significant increase of overheads to implement the multi-hop routing. In addition, if transmission errors occur, data have to be retransmitted from the source node along the multi-hop path. This may result in significant increases in the energy consumption of all the nodes along the path. To overcome these problems, collaborative communication can be a viable solution. In collaborative communication, multiple transmitters transmit the same data towards the same receiver at the same time.

In a sensor network, the sensor nodes are randomly distributed; the above mentioned techniques require that some factors need to be addressed. These factors are; time synchronization, frequency synchronization and phase synchronization between the sensor nodes and the base station. The gains of collaborative communication depend upon the time synchronization, frequency synchronization and phase synchronization among the transmitters and the receiver. The recent literature reports [4-22] showed that, with perfect time, frequency and phase synchronization, a large power gain can be achieved. This has been confirmed by a detailed analysis presented in section 4.2.

The theory of a fixed array to achieve space diversity is widely used in cellular networks [7]. The idea of collaborative communication is based on the idea of using a fixed array in a communication system. In this research, the space diversity concept is exploited to develop an energy efficient collaborative communication system for wireless sensor networks. In a fixed antenna array system there are a set of antennas that collaboratively transmit the same signal to the base station, as shown in Figure 4.1. The base station receives the cumulative signal (sum of all the signals). Therefore, a large power gain and reduction in BER can be achieved in this kind of system. In this fixed

antenna array system there is a common network node that is used to achieve frequency, phase and time synchronization. The distances between transmitter antennas are fixed and are accurately known to the controller. As the accurate positions of the antennas are known, there are no distance estimation errors or phase errors in this system [23-26].

However in a distributed sensor network, the accurate position of the sensor nodes is generally not known and the theory of the fixed antenna array cannot be applied directly. Namely, there is no network node that performs phase, time and frequency synchronization. This results in a position estimation error (called the displacement error), that is translated into the phase error of the transmitted signal. To achieve a high power gain and to reduce the BER using collaborative transmission, the synchronization of frequency, time and phase needs to be achieved.

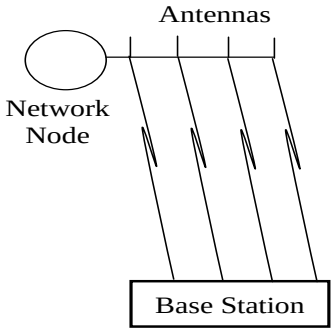

Figure 4.1 Fixed Antenna Array

In regard to the advantages stated above, the study in this chapter is dedicated to the design of a collaborative communication system that can provide significant power gain with imperfect phase and frequency synchronization in the presence of AWGN and Rayleigh fading.

Of particular interest to this study is the achievement of the following:

- To understand the development of collaborative communication model;
- To investigate the effect of phase and frequency errors on power gain achieved using collaborative communication in wireless sensor networks;
- To design an energy efficient collaborative communication system;
- To establish a WSN simulator to assess power gain using collaborative communication with imperfect phase and frequency synchronization in the presence of AWGN and Rayleigh fading using the parameters of off-the-shelf products i.e. CC2420 [27] and AT86RF212 [28].

The studied models will be utilized in the investigation of energy consumption, energy efficiency and channel capacity of collaborative communication systems and this is presented in Chapter 6 and Chapter 7.

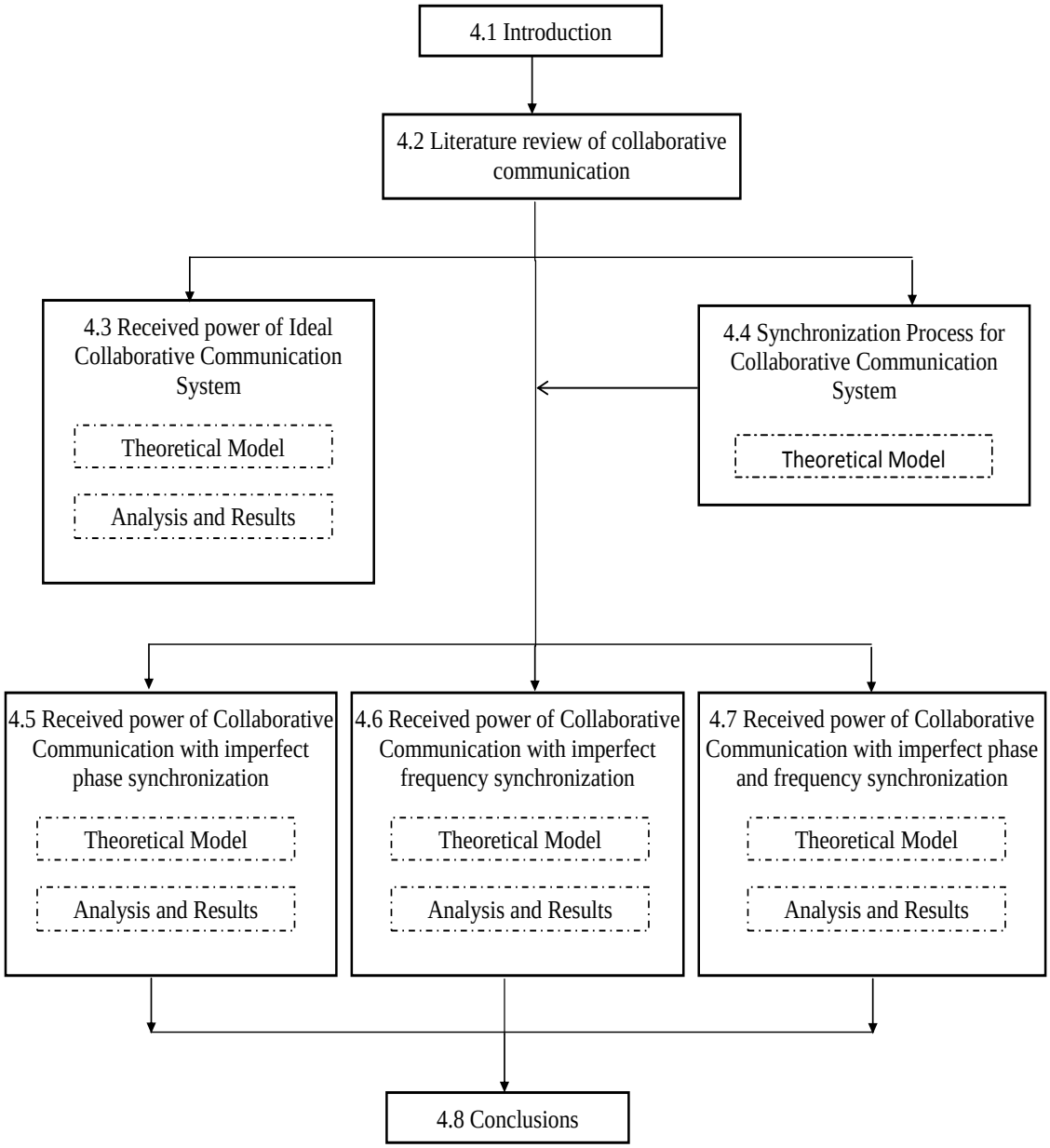

Figure 4.2 Route map of study in Chapter 4

Figure 4.2 demonstrates the route map of this chapter. The study in this chapter unfolds in the following sequence.

In Chapters 2 and 3, a review of the literature pertaining to wireless communication and wireless sensor networks has been presented. In Section 4.2, an extensive analysis of

the related research achievements of collaborative communication is presented. The literature reveals that collaborative communication is a relatively new area but that there has much potential in this area. From the existing literature [4]-[22], it is observed that phase, frequency and time synchronization errors degrade the performance of collaborative communication.

Section 4.3 presents the development of an ideal collaborative communication system i.e., by assuming perfect phase, frequency and time synchronization. For this system a mathematical model is developed and simulated. Theoretical and simulation results reveal that high power gain can be achieved using collaborative communication. As it is very difficult to achieve perfect phase and frequency synchronization in sensor networks, a synchronization process is presented to reduce the phase and frequency error in section 4.4.

In section 4.5, a collaborative communication system with imperfect phase synchronization with the assumption of perfect frequency synchronization, including the influence of noise and Rayleigh fading, is presented in section 4.5. The theoretical model of the system is presented; theoretical analysis and Monte Carlo simulation are conducted to validate the performances of the collaborative communication algorithm.

In Section 4.6 the collaborative communication system with imperfect frequency synchronization with the assumption of perfect frequency synchronization, including the influence of noise and Rayleigh fading, is modelled, theoretically analyzed and simulated. The models presented in sections 4.5 and 4.6 are further extended without any assumption concerning phase and frequency errors. In Section 4.7 a more realistic collaborative communication system with imperfect phase and frequency synchronization, including the influence of noise and Rayleigh fading, is modelled, theoretically analyzed, and simulated.

In summary, the contribution of this chapter is three-fold:

1. The development of mathematical model for collaborative communication system that includes the influence of the phase error, frequency error, AWGN and Rayleigh fading in the channel;
2. The derivation of theoretical expressions for the received power as a function of the number of collaborative nodes;
3. Simulation-based investigations to confirm that the proposed collaborative communication system produces high power gain with imperfect phase and frequency synchronization in the presence of AWGN and Fading;

4.2 Related Work

The feasibility of collaborative communication, design requirements, constraints and fundamental model of collaborative communication in sensor network is presented in [4-11]. It is observed in [4-6] that, for collaborative communication, the synchronization (frequency, time and phase) between nodes is considered as very important in achieving a high SNR. The benefits of collaborative communication, in terms of security and interference reduction, are also presented and analyzed in [4-6]. A decode and forward collaborative communication model is presented to analyze the performance of collaborative communication in terms of achievable rate, power gain, and the reduction of resource requirements [9]. The prototype for the phase synchronization method and its convergence rate, using an iterative one bit feedback control mechanism for collaborative communication, is presented and analyzed in [12]. In the synchronization method presented in [12], the sensor nodes correct the phase error using a 1 bit signal received from the base station. The convergence rate of the proposed synchronization algorithm in static and time-varying channels is also analyzed in [12]. The method presented in [12] is further improved using positive and negative feedback in [13]. The feedback from the base station is used by phase offset correction [13] and results in a significant reduction in phase error. A quantized feedback protocol to achieve synchronization and high power gain for Wireless Relay Networks is proposed and analyzed in [14]. The effectiveness of collaborative and cooperative communication to improve the lifetime of the network is presented in [15]. The feasibility of blind or zero-feedback collaborative communication for wireless sensor networks is analyzed in [16]. It is shown in [16] that, without communication, with base station collaborative communication can be performed and results in good power gain.

The impact on power gain of the power allocation of collaborative nodes in collaborative communication systems is analyzed in [17]. It is shown in [17] that by using proper power allocation, substantial power gain can be achieved in collaborative communication. An algorithm to find the weight of relay (collaborative) nodes using minimum mean square error (MMSE) criterion with a dual decomposition method, are proposed and analyzed in [18]. It is shown in [18], that the proposed MMSE-based distributed beamforming produce high power gain using very few collaborative nodes.

The beam pattern analysis of collaborative beamforming is performed using the theory of random arrays in [19]. The distribution function and mean value of the beam-

pattern generated by randomly phased arrays are derived for wireless ad hoc sensor networks. In [19] every sensor node has a single isotropic antenna and the sensor nodes in the cluster collaboratively transmit the signal. The transmitted signals from all nodes are coherently added at the receiver on the assumption that, when sensor nodes are uniformly distributed over a disk with enough space between them, high directivity can be achieved. The effects of phase error and localization errors on an average beam pattern are also analyzed. The impact of the selection of collaborative nodes for collaborative communication on the beam-pattern main-lobe [19] is analyzed in [19]. The impact of collaborative node distribution on power gain is analyzed in [20]. It is shown that if collaborative nodes are distributed using Gaussian distribution, high power gain, and low side-lobes can be achieved. In [20] a node selection algorithm with low-rate feedback is developed to search over different node combinations. It is shown that the proposed algorithm is scalable, simple and produces substantial power gain.

In [5]-[20] collaborative communication, analysis has been performed under the assumption of perfect timing and frequency offset synchronization. The frequency synchronization method for collaborative communication is presented and analyzed in [21]. The estimation bounds and the associated maximum a posteriori estimators for frequency offset estimation for collaborative communication are derived and analyzed in [21]. An adoptive method is proposed to reduce the frequency estimation errors based on the correlation sequence of the data; this has a mean squared error close to the Cramér-Rao Bound (CRB) [21].

The time synchronization algorithm for collaborative communication is presented and numerically analyzed in [22]. The time synchronization algorithm presented in [22] is based on time-slotted round-trip carrier synchronization. The impact of the mobility of sensor nodes on the performance of the round-trip carrier synchronization protocol is also analyzed in [22].

4.3 Ideal Collaborative Communication Model

In this section, we present an ideal collaborative communication model with the assumption that there is perfect time, frequency and phase synchronization between the collaborative nodes and the base station. A collaborative node has to transfer data to the base station. Using collaborative communication let the N collaborative nodes make a network to transfer the information to the base station. The geometry for the sensor

network used for collaborative communication is shown in Figure 4.3. It is composed of *N* collaborative nodes. In the first step, the collaborative node that has the data to be transferred to base station sends the data to all the *N*-1 collaborative nodes in the network. In the second step, all the collaborative nodes transfer the data at the same time towards the base station.

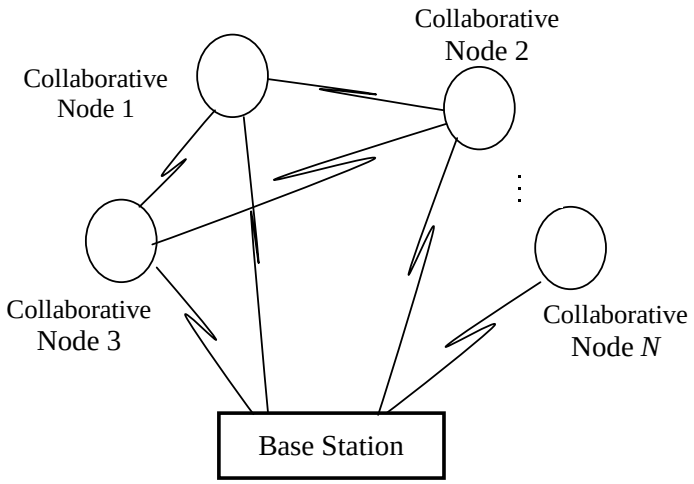

Figure 4.3 Geometry of a Sensor Network

4.3.1 Theoretical Model of Ideal Collaborative Communication

The collaborative communication network shown in Figure 4.3 can be presented by the scheme shown in Figure 4.4. It is composed of *N* collaborative node transmitters represented as Source (Node). Each collaborative node has a transceiver to receive signals from other collaborative nodes within the network and also to transmit the signal to the base station. Each collaborative node also has a phase lock loop (PLL) for offset correction and a modulator to modulate the signal. The channel is considered as an AWGN channel. On the receiver side denoted as the base station, there is a demodulator to demodulate the received signal. The demodulator multiplies the received signal with a cosine signal; passes it through a low pass filter (LPF) and then integrates it. Then the power of demodulated signal is calculated.

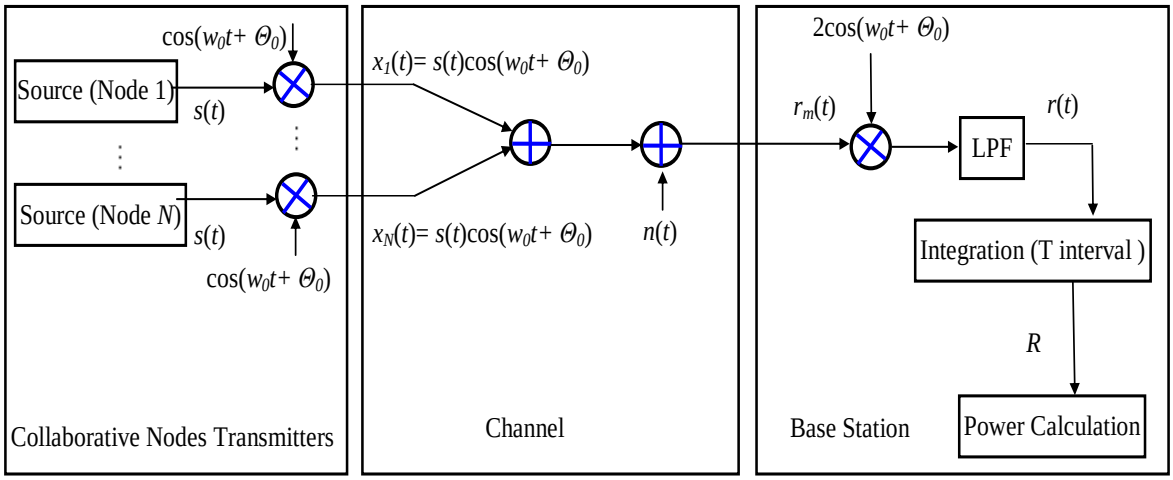

Figure 4.4 System Model

Let $s(t)$ be the information data transmitted to the base station by the collaborative nodes. With the assumption that there is perfect time, frequency and time synchronization between all the collaborative nodes and the base station, the signal transmitted of i^{th} collaborative node received at the base station is given by

$$x_i(t) = s(t)\cos(w_0 t + \Theta_0)\,. \tag{4.1}$$

The cumulative received signal at the Base station is given by

$$r_m(t) = \Re\left(\sum_{i=1}^{N} s(t)e^{j(w_0 t+\Theta_0)}\right) + n(t), \tag{4.2}$$

where $n(t)$ is AWGN.

At the base station the demodulated signal is integrated and its output is given by

$$R = \sum_{i=1}^{N} S + n, \tag{4.3}$$

where $S = \pm\sqrt{E_b}$ is the signal amplitude and n is the noise amplitude at sampling time T.

Power of R is given by

$$P_R = \left[\sum_{i=1}^{N} S + n\right]^2. \tag{4.4}$$

As n are the independent random variables and n is zero-mean, we have to calculate the mean value of received power as

$$E[P_R] = E\left[\left[\sum_{i=1}^{N} S\right]^2\right] + \sigma_n^2, \tag{4.5}$$

where σ^2_n is the variance of noise. Equation (4.5) can also be developed as follows

$$E[P_R] = N^2 S^2 + \frac{N_0}{2}. \tag{4.6}$$

The analytical results obtained from equations (4.6) and Monte Carlo simulation are discussed in section 4.3.2.

4.3.2 Analysis and Results of the Ideal Collaborative Communication Model

A Monte Carlo simulation is performed using SIMULINK and MATLAB® to analyze the ideal collaborative communication model. The wireless communication environment used in the simulation is established using SIMULINK's AWGN channel blocks. The simulation model of the ideal collaborative communication system is shown in Figure 4.5. For each value of *N* i.e., the number of collaborative nodes 1200 Monte Carlo simulations is run.

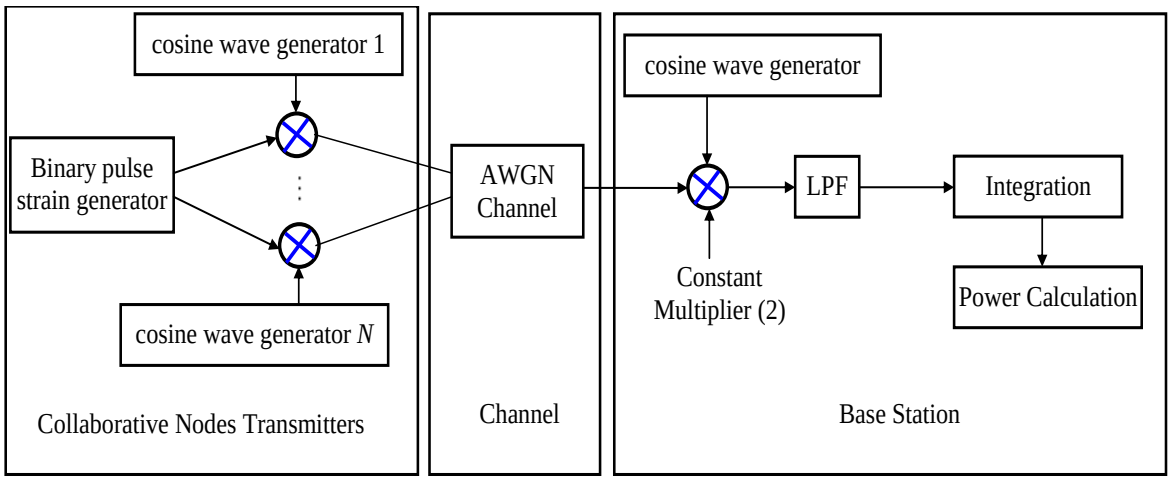

Figure 4.5 Simulation Model of the Ideal Collaborative Communication System

Each collaborative node transmits the same binary pulse strain. To avoid the inter symbol interference; the considered signal rate is 15% of the carrier frequency. For simulation the parameters of the off-the-shelf products i.e., CC2420 [27] and AT86RF212 [28] are considered. Each collaborative node modulates the data and transmits it to the base station. The receiver demodulates the received signal and calculates the power of demodulated signal. The analytical results are compared with the simulation results. Figure 4.6 shows the analytical and simulation results for average total received power at

the base station of the ideal collaborative communication model. Results show that the analytical results match with the results of the simulation and that the total received power increases as the number of collaborative nodes increases. It is revealed that under ideal conditions N^2 power gain can be achieved using collaborative communication.

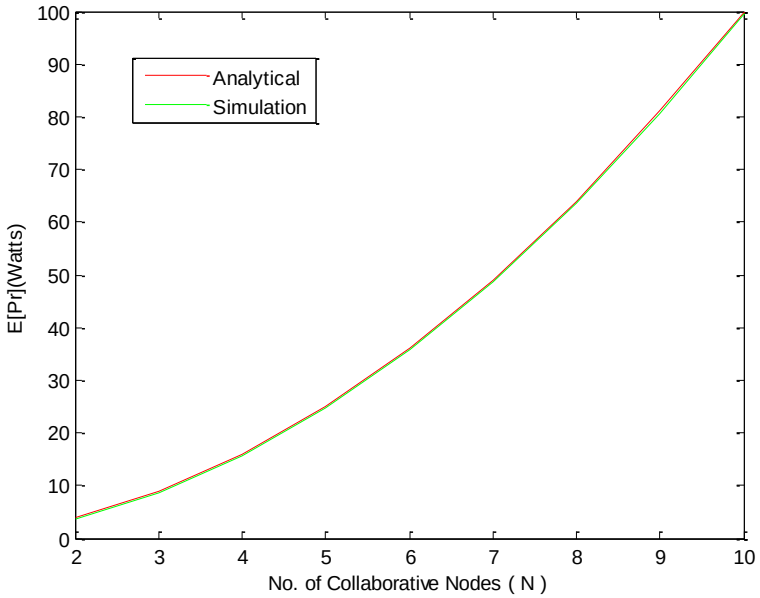

Figure 4.6 Average total received power Vs No of collaborative nodes

4.4 Synchronization Process

In the previous section it has been analyzed that high power gain can be achieved using collaborative communication. However power gain depends upon phase, frequency and time synchronization. As each sensor node has its own oscillator, there may be a frequency offset among the transmitted signals. As the sensor nodes are randomly deployed, the exact position of the sensor nodes cannot be estimated with 100% accuracy. This results in a distance estimation error that is translated into phase error. For high carrier frequency, a small displacement error can produce a high phase error. The phase error can be calculated as $\Theta_f = 2\pi f_0 d_f/c$, where Θ_f is phase error, f_0 is the carrier frequency, d_f is the displacement error and c is speed of light. For example if f_0 =915 MHz, c = $3*10^8$, the displacement error of 5cm will produce a phase error of 60^0. If the phase error is 180^0, the received signal will be inverted which results in destructive interference. Thus it is very important that phase and frequency errors are corrected. In this section the frequency and phase synchronization process is presented in order to enable a reduction

in frequency and phase errors. Phase synchronization is multi-step and the periodic process and its architecture are shown in Figure 4.7. For the synchronization process, the base station sends a known signal to all collaborative nodes. The received signal from the base station is passed through a Low noise amplifier (LNA). The phase lock loop (PLL) locks itself on to the incoming signal frequency and performs the phase offset. This process is repeated after a time interval depending upon the nature of the channel. If the channel is fast variant, the time interval to repeat the synchronization process is small.

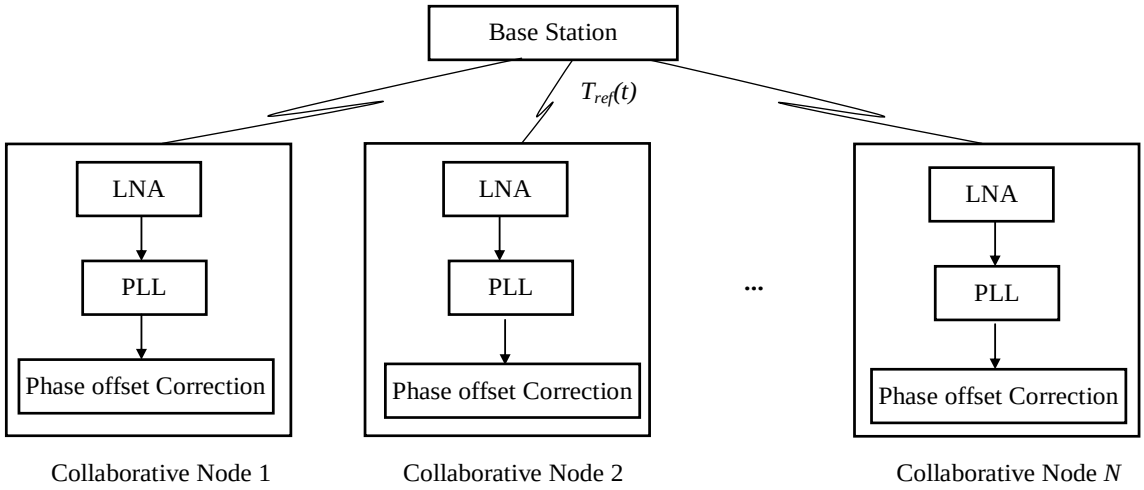

Figure 4.7 Synchronization Model

The base station transmits a known signal to all sensor nodes in the network; this is used as reference signal for the network and is given by

$$T_{ref}(t) = \Re\left(A_0 e^{j(2\pi f_0 t+\Theta_0)}\right) = A_0 \cos(2\pi f_0 t+\Theta_0) \tag{4.7}$$

Sensor nodes receive the signal; it then locks itself with the carrier frequency [29] after achieving its steady state. The signal at the i^{th} sensor node can be written as

$$T_i(t) = A_0 \cos(2\pi f_0 t+\Theta_0+\Theta_i) \tag{4.8}$$

where Θ_i is the phase error between the transmitted and received signal and is due to the displacement error and PLL error. But at steady state PLL error is approximately zero and the Θ_i is due to a displacement error. The output of the PLL is passed through phase offset correction to minimize phase error. Base station feedback is presented in order to reduce phase error. The base station sends feedback to the sensor nodes. The feedback from the base station is used for phase offset correction [13] and results in a significant reduction in phase error.

4.5 Collaborative communication model with imperfect phase synchronization

In this section we present a collaborative communication model with imperfect phase synchronization and with the assumption that there is perfect time and frequency synchronization between the collaborative nodes and the base station in the presence of AWGN and Rayleigh fading. Let N collaborative nodes make a network to transfer the information to the base station. As the distance between the collaborative nodes and the base station cannot be estimated accurately, there is, therefore, a certain amount of error in distance estimation. This error in distance estimation is translated into phase errors.

Let d_0 be the nominal distance between collaborative and the base station. Let w_0 be the carrier frequency, and assuming a line of sight propagation, the phase produced due to distance d_0 can be written as $\Theta_0 = w_0\, d_0/c$, where c is the speed of light. Let $d_f(i)$ be the distance estimation error between base station and the i^{th} collaborative node, then the phase error due to distance estimation error is given by $\Theta_f(i) = w_0\, d_f(i)/c$.

Let $\cos(w_0 t + \Theta_0)$ be the carrier/reference signal used by all collaborative nodes. On the assumption that the signal delay is very small with respect to the signal bit interval T, there is a significant guard interval and thus, inter symbol interference (ISI) can be ignored. The system model of the collaborative communication model with imperfect phase synchronization in the presence of AWGN and Rayleigh fading is shown in Figure 4.8. It is composed of N collaborative node transmitters represented as Source (Node). Each collaborative node has a transceiver to receive signals from other collaborative nodes within the network and to transmit signals to the base station. Each collaborative node also has a phase lock loop (PLL) for offset correction, and a modulator to modulate the signal. As there is no perfect phase synchronization between the collaborative nodes and the base station, there is a random phase offset among all transmitted signals. The channel is considered as the AWGN and the Rayleigh fading channel. The Rayleigh fading channel for each transmitted signal has an independent effect. On the receiver side denoted as the base station, there is a demodulator to demodulate the received signal. The demodulator multiplies the received signal with a cosine signal; passes it through a low pass filter (LPF) and then integrates it. Following this, the power of demodulated signal is calculated.

4.5.1 Theoretical Model of Collaborative communication with imperfect phase synchronization

Let $s(t)$ be the information data transmitted to the base station by the collaborative nodes. As the distance between the collaborative nodes and base station cannot be estimated accurately and thus produces displacement error that is converted into phase error.

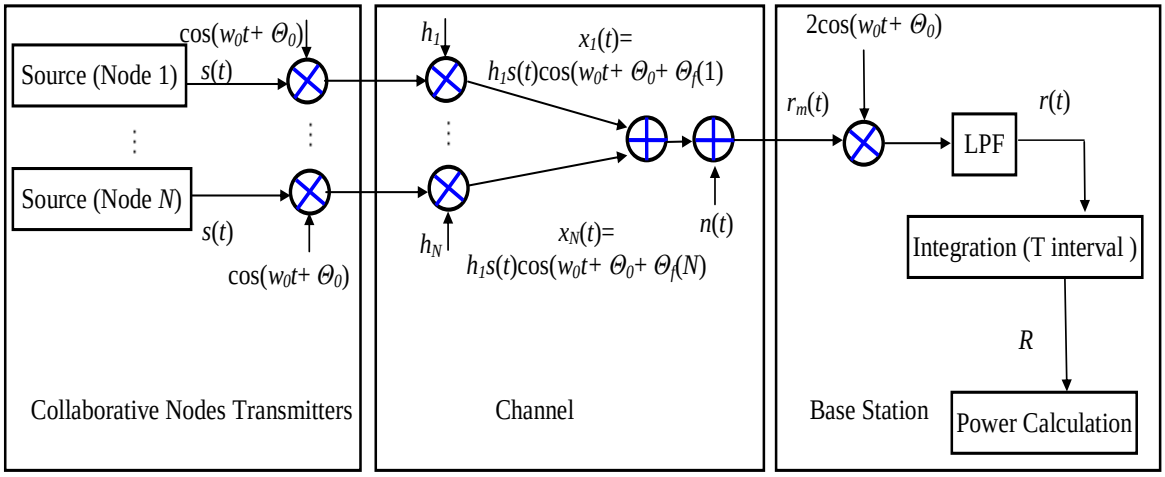

Figure 4.8 System Model

The signal transmitted from the i^{th} collaborative node received at the base station is given by

$$x_i(t) = s(t)\cos(w_0 t + \Theta_0 + \Theta_f(i)). \tag{4.9}$$

The cumulative received signal at the base station is given by:

$$r_m(t) = \Re\left(\sum_{i=1}^{N} h_i s(t) e^{j(w_0 t + \Theta_0 + \Theta_f(i))}\right) + n(t), \tag{4.10}$$

where $n(t)$ is AWGN and h_i is the Rayleigh fading.
At the base station the demodulated signal is given by

$$R = \sum_{i=1}^{N} h_i S\cos(\Theta_f(i)) + n, \tag{4.11}$$

where S is the signal amplitude and n is the noise amplitude at sampling time T.
Power of R is given by

$$P_R = \left[\sum_{i=1}^{N} h_i S \cos(\Theta_f(i)) + n \right]^2 . \quad (4.12)$$

As $\Theta_f(i)$, h_i and n are the independent random variables and n is zero-mean, the mean value of received power is calculated as

$$E[P_R] = E\left[\left[\sum_{i=1}^{N} h_i S \cos(\Theta_f(i)) \right]^2 \right] + \sigma_n^2 , \quad (4.13)$$

where σ^2_n is the variance of noise. Equation (4.11) can also be developed as follows

$$E[P_R] = \sum_{i=1}^{N} S^2 E\left[\cos^2(\Theta_f(i))\right] E\left[h_i^2\right] + \sum_{\substack{i=1 \\ i \neq j}}^{N} \sum_{j=1}^{N} S^2 E\left[\cos(\Theta_f(i))\cos(\Theta_f(j))\right] E\left[h_i h_j\right] + \sigma_n^2 . \quad (4.14)$$

As all $\Theta_f(i)$ are independent for each collaborative node and can be recognised as i.i.d. random variables, therefore $E[\Theta_f(i)] \approx E[\Theta_f]$. As all channels are independently affected by fading, therefore, all h_i are i.i.d. random variables, hence $E[h_i] \approx E[h]$. The equation (4.14) can be written as

$$E[P_R] = NS^2 E[\cos^2(\Theta_f)] E[h_i^2] + N(N-1) S^2 E\left[\cos(\Theta_f)\right] E\left[\cos(\Theta_f)\right] E[h] E[h] + \sigma_n^2 . \quad (4.15)$$

The mean value of $\cos(\Theta_f)$ and $\cos^2(\Theta_f)$ are calculated in appendix A.1 and A.2, respectively. Using the values of equations (A.1), (A.2), mean value of h and $E[h^2]=1$ equation (4.15) becomes

$$E[P_R] = NS^2 \left[\frac{1}{2} + \frac{\sin(2\varphi)}{4\varphi} \right] + \frac{N(N-1) b^2 S^2 \pi}{2} \left[\frac{\sin(\varphi)}{\varphi} \right]^2 + \frac{N_0}{2} , \quad (4.16)$$

where φ is distribution limit of phase error and b is the mode of Rayleigh random variable h. The results obtained from equations (4.16) and Monte Carlo simulation are discussed in section 4.2.2.

4.5.2 Analysis and Results

The Monte Carlo simulation is performed in order to analyze the collaborative communication system with imperfect phase synchronization in the presence of AWGN and Rayleigh fading using SIMULINK and MATLAB®. The wireless communication environment used in simulation is established using SIMULINK's AWGN and Rayleigh

channel blocks. The simulation model of collaborative communication system with imperfect phase synchronization is shown in Figure 4.9. For each value of N i.e., the number of collaborative nodes and the distribution of phase error i.e., {-0.1π~0.1π}, {-0.2π~0.2π}, {-0.3π~0.3π} and {-0.4π~0.4π}, 1200 Monte Carlo simulations are run. Each collaborative node transmits the same binary pulse strain. To avoid the inter symbol interference; the considered signal rate is 15% of carrier frequency. For the simulation the parameters of the off-the-shelf products i.e., CC2420 [27] and AT86RF212 [28] are considered. Each collaborative node modulates the data using the carrier wave (obtained from the VCO output of the PLL). A random phase error distributed over different distributions i.e., {-0.1π~0.1π}, {-0.2π~0.2π}, {-0.3π~0.3π} and {-0.4π~0.4π} is added to the carrier wave. The modulated signal is transmitted to the base station. The receiver demodulates the received signal and calculates the power of demodulated signal.

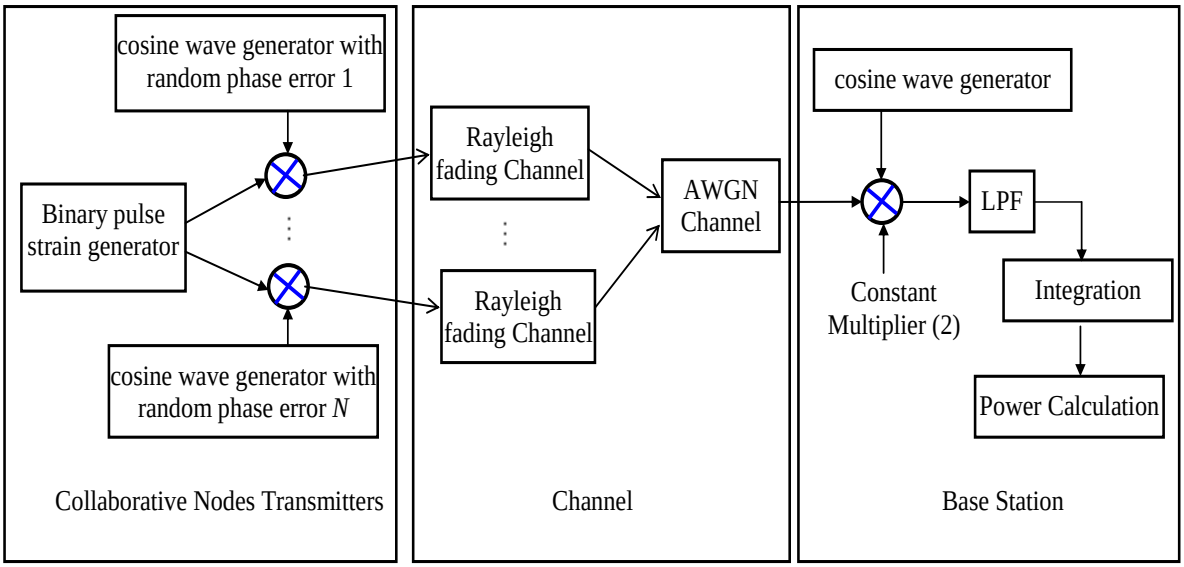

Figure 4.9 Simulation Model of Collaborative Communication with imperfect phase synchronization

The analytical results are compared with the results of the simulation. For analysis, the phase error is considered to be uniformly distributed over interval {-φ~φ}. In the analysis, four phase error distributions are considered i.e. {-0.1π~0.1π}, {-0.2π~0.2π}, {-0.3π~0.3π} and {-0.4π~0.4π}.

Figure 4.10 shows the analytical and simulation results of the collaborative communication system with imperfect phase synchronization in the presence of AWGN

and Rayleigh fading for total received power/N at the base station. Results show that the analytical results match up with the simulation results. It is observed that received power decreases by; approximately 11% for phase error distributed over {-0.1π~0.1π}, by 20% for phase error distributed over {-0.2π~0.2π}, by 35% for phase error distributed over {-0.3π~0.3π} and by 50% for phase error distributed over {-0.4π~0.4π} than the received power without phase errors i.e. N^2, as shown in Figure 4.6. The total received, power/N, increases as the number of collaborative nodes increases and the total received power decreases as phase error increases. It is observed that high power gain can be achieved using collaborative communication even in the presence of phase error and fading. The power gain of 0.62N^2 can be achieved if phase error is distributed over {-0.3π~0.3π} and 0.48 N^2 can be achieved if phase error is distributed over {-0.4π~0.4π}.

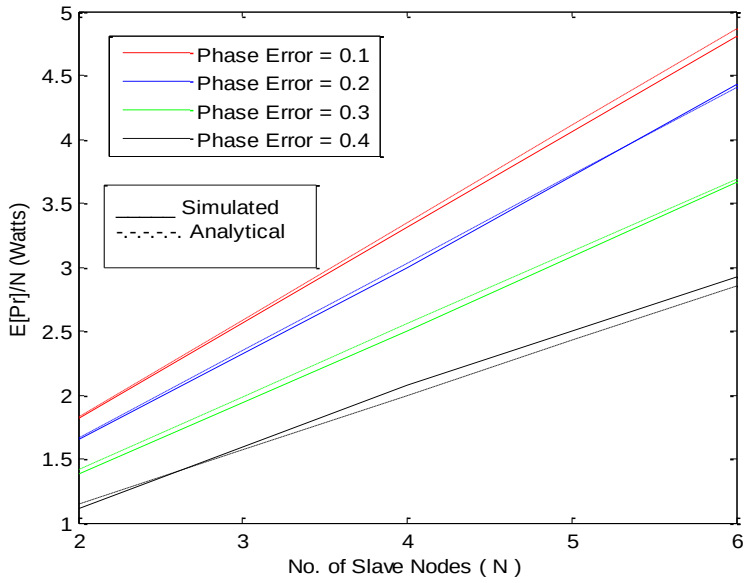

Figure 4.10 Average total received power Versus Number of collaborative nodes with Rayleigh fading

4.6 Collaborative communication model with imperfect frequency synchronization

In this section we present a collaborative communication model with imperfect frequency synchronization and with the assumption that there is perfect time and phase synchronization between the collaborative nodes and the base station in the presence of AWGN and Rayleigh fading. Let the N collaborative nodes make a network to transfer

the information to the base station. As each collaborative node has its own oscillator, there may be a frequency mismatch between the collaborative nodes and the base station. The system model for the collaborative communication model with imperfect frequency synchronization in the presence of AWGN and Rayleigh fading is shown in Figure 4.11. It is composed of *N* collaborative node transmitters represented as Source (Node). Each collaborative node has a transceiver to receive signals from other collaborative nodes within the network and to transmit signals to the base station. Each collaborative node also has a phase lock loop (PLL) for offset correction and a modulator to modulate the signal. The channel is considered as the AWGN and the Rayleigh fading channel. As there is no perfect frequency synchronization between the collaborative nodes and the base station, there is a random frequency that is offset between all the transmitted signals. The Rayleigh fading channel for each transmitted signal has an independent effect. On the receiver side, denoted as the base station, there is a demodulator to demodulate the received signal. The demodulator multiplies the received signal with a cosine signal; passes it through a low pass filter (LPF) and then integrates it. Following this, the power of demodulated signal is calculated.

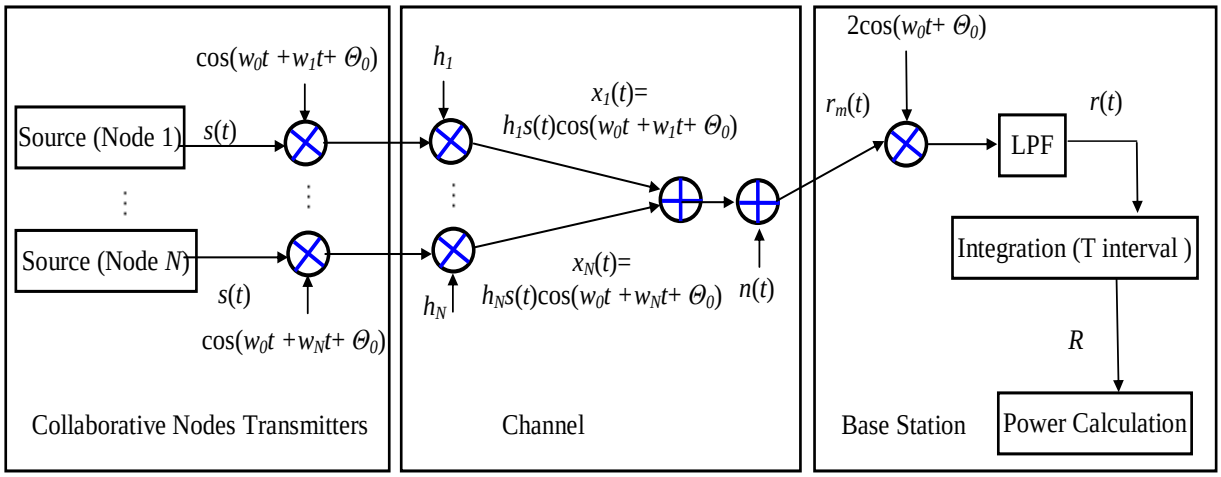

Figure 4.11 System Model

4.6.1 Theoretical Model

Let *s*(*t*) represents the data signal to be transmitted to the base station. As each collaborative node has its own oscillator there will be a frequency mismatch between the

collaborative nodes and the base station. The signal transmitted from the i^{th} collaborative node received at the base station is given by

$$x_i(t) = s(t)\cos(w_0 t + w_i t + \Theta_0). \tag{4.17}$$

The received signal at the base station ($r_m(t)$) is the sum of all the signals transmitted by sensor nodes and the noise and is given by

$$r_m(t) = \sum_{i=1}^{N} h_i s(t)\cos(w_i t) + n(t), \tag{4.18}$$

where $n(t)$ is zero-mean AWGN and h_i is the fading coefficient and $w_i = w_0 + \Delta w_i$, w_0 is the carrier frequency and Δw_i is the frequency offset.

$$r(t) = \sum_{i=1}^{N} h_i s(t)\cos(\Delta w_i t) + n(t), \tag{4.19}$$

where $n(t)$ is low pass noise. The demodulated signal at the base station may be written as

$$R = \sum_{i=1}^{N} h_i S \frac{\sin(\Delta w_i T)}{\Delta w_i T} + n, \tag{4.20}$$

where S is the signal amplitude and n is the noise amplitude at time T.

Power of received signal R is given by

$$P_R = \left| \sum_{i=1}^{N} h_i S \frac{\sin(\Delta w_i T)}{\Delta w_i T} + n \right|^2. \tag{4.21}$$

As h_i, Δw_i and n are the random variables, so we have to calculate the mean value of received power.

$$E[P_R] = E\left[\left| \sum_{i=1}^{N} h_i S \frac{\sin(\Delta w_i T)}{\Delta w_i T} + n \right|^2 \right]. \tag{4.22}$$

As h_i, Δw_i and n are the independent random variables and n is zero-mean random variable, the above equation can be written as

$$E[P_R] = \sum_{i=1}^{N} S^2 E[h_i^2] E\left[\left(\frac{\sin(\Delta w_i T)}{\Delta w_i T} \right)^2 \right] + \sum_{i=1}^{N} \sum_{\substack{j=1 \\ i \neq j}}^{N} S^2 E[h_i] E[h_j] E\left[\frac{\sin(\Delta w_i T)}{\Delta w_i T} \frac{\sin(\Delta w_j T)}{\Delta w_j T} \right] + \sigma_n^2, \tag{4.23}$$

where σ^2_n is the variance of noise.

As all Δw_i are independent for each of the collaborative nodes and can be recognized as i.i.d random variables having uniform distribution from $\{-w_e$ to $w_e\}$ for all i, therefore $E[\Delta w_i] = E[\Delta w]$ and all the channels are independently affected by fading therefore, h_i are i.i.d random variables for all i, hence $E[h_i] = E[h]$. The equation (4.23) can now be written as

$$E[P_R] = NS^2E[h^2]E\left[\left(\frac{\sin(\Delta wT)}{\Delta wT}\right)^2\right] + N(N-1)S^2E[h]E[h]E\left[\frac{\sin(\Delta wT)}{\Delta wT}\right]E\left[\frac{\sin(\Delta wT)}{\Delta wT}\right] + \sigma_n^2 . \quad (4.24)$$

Mean value of $\frac{\sin(\Delta wT)}{\Delta wT}$ and $\left[\frac{\sin(\Delta wT)}{\Delta wT}\right]^2$ are calculated in appendix A.3 and A.4 respectively.

Using the values of equation (A.3), (A.4) and mean value of h, equation (4.24) becomes

$$E[P_R] = NS^2\left[1 + \frac{(w_eT)^4}{180} - \frac{(w_eT)^2}{9}\right] + \frac{N(N-1)\pi b^2S^2}{2}\left[1 - \frac{(w_eT)^2}{18}\right]^2 + \frac{N_0}{2}. \quad (4.25)$$

where w_e is distribution limit of frequency error and b is the mode of Rayleigh random variable h.

The results obtained from equation (4.25) and Monte Carlo simulation of the same system are discussed and compared in section 4.5.2.

4.6.2 Analysis and Results

A Monte Carlo simulation is performed to analyze the collaborative communication system with imperfect frequency synchronization in the presence of AWGN and Rayleigh fading using SIMULINK and MATLAB®. The wireless communication environment used in simulation is established using SIMULINK's AWGN and Rayleigh channel blocks. The simulation model for the collaborative communication system with imperfect frequency synchronization is shown in Figure 4.9. For the simulation, the parameters of the off-the-shelf products i.e., CC2420 [27] and AT86RF212 [28] are considered. For each value of N i.e., the number of collaborative nodes and distribution of frequency error i.e., {-150 KHz~150 KHz}, {-250 KHz~250 KHz}, {-350 KHz~350 KHz}, {-35 KHz~35 KHz}, {-55 KHz~55 KHz} and {-65 KHz~65 KHz}, 1200 Monte Carlo simulations are run. Each collaborative node transmits the same binary pulse strain. To avoid the inter

symbol interference; the considered signal rate is 15% of the carrier frequency. Each collaborative node modulates the data using the carrier wave (obtained from the VCO output of the PLL). A random frequency error distributed over different distributions i.e., frequency error i.e., {-150 KHz~150 KHz}, {-250 KHz~250 KHz}, {-350 KHz~350 KHz}, {-35 KHz~35 KHz}, {-55 KHz~55 KHz} and {-65 KHz~65 KHz} is added to the carrier wave. The modulated signal is transmitted to the base station. The receiver demodulates the received signal and calculates the power of demodulated signal.

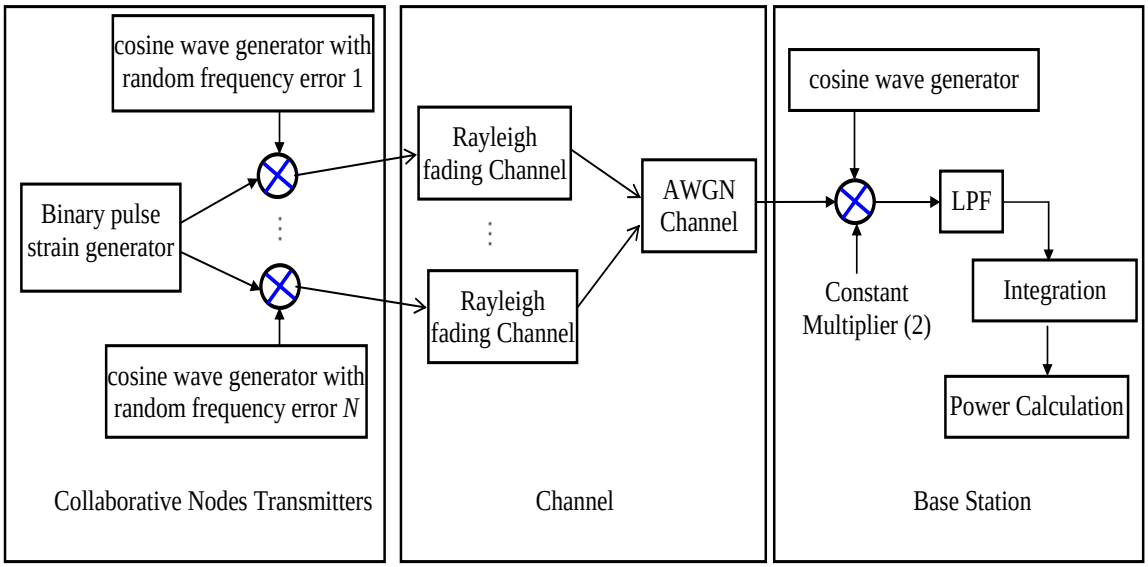

Figure 4.12 Simulation Model of Collaborative Communication with imperfect frequency synchronization

The analytical results are compared with the simulation results. For analysis, the frequency error is considered to be uniformly distributed over interval $\{- w_e \sim w_e\}$. In the analysis the parameters of two off-the-shelf products i.e. CC2420 [27] and AT86RF212 [28] are considered. Figures 4.13 and 4.14 show the analytical and simulation results for the collaborative communication model with imperfect frequency synchronization in the presence of Rayleigh fading for average total received power at the base station for CC2420 and AT86RF212, respectively. Results show that the analytical results match very well with the simulation results. Results in Figure 4.13 show that, by considering the parameters of CC2420, a power gain of 78 N^2, 0.70 N^2 and 0.62 N^2 can be achieved for frequency errors distributed over {-150 KHz~150 KHz}, {-250 KHz~250 KHz} and {-350 KHz~350 KHz}, respectively.

The results in Figure 4.14 show that, by considering the parameters of AT86RF212, the power gain of 0.72 N^2, 0.65 N^2 and 0.55 N^2 can be achieved for frequency errors distributed over {-35 KHz~35 KHz}, {-55 KHz~55 KHz} and {-65 KHz~65 KHz}, respectively. Therefore, by using the proposed model, approximately N times less transmission power is required for this collaborative communication than for a direct communication between the transmitter and the base station. It is also confirmed that the received power with frequency errors decreases with respect to the received power without frequency errors, as follows: for product CC2420 received power decreases by approximately 22% for frequency errors distributed over {-150 KHz~150 KHz}, by 30% for frequency errors distributed over {-250 KHz~250 KHz} and by 38% for frequency errors distributed over {-350 KHz~350 KHz}.

For product AT86RF212, received power decreases by approximately 28% for frequency errors distributed over {-35 KHz~35 KHz}, by 35% for frequency errors distributed over {-55 KHz~55 KHz} and by 45% for frequency errors distributed over {-65 KHz~65 KHz}.

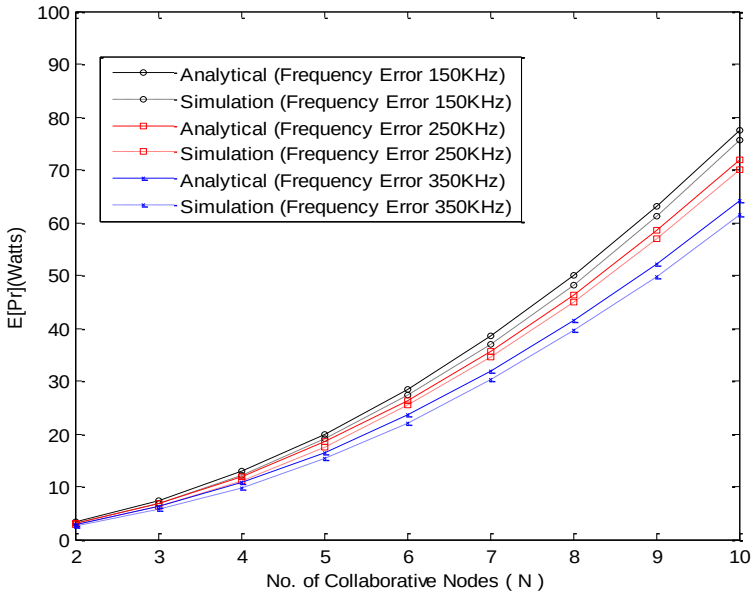

Figure 4.13 Received Power for CC2420 with data rate 250Kbps with fading

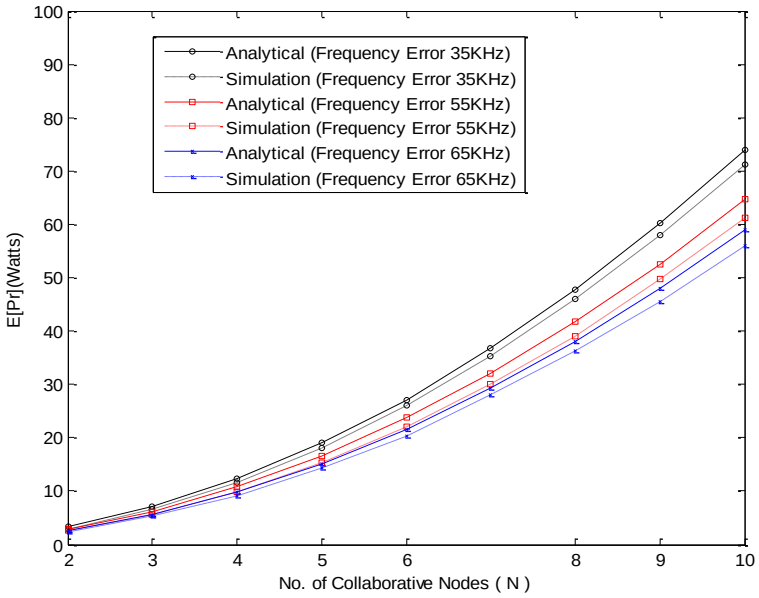

Figure 4.14 Received Power for AT86RF21 with data rate 40Kbps with fading

4.7 Collaborative communication model with imperfect phase and frequency synchronization

In sections 4.5 and 4.6 we have presented collaborative communication models with the assumption of imperfect frequency and perfect phase synchronization, respectively. In a sensor network collaborative nodes are randomly distributed and the distance between the collaborative nodes and the base station cannot be estimated accurately and results as distance estimation error. The distance estimation error is translated into the phase error. Moreover, each collaborative node has its own oscillator; there may be a frequency mismatch among the collaborative nodes and the base station and thus it is very difficult to achieve perfect phase and frequency between the collaborative nodes and the base station in real time environment. In this section, a realistic collaborative communication model with imperfect phase and frequency synchronization among the collaborative nodes and the base station in the presence of AWGN and Rayleigh fading is presented.

Let *N* collaborative nodes make a network to transfer information to the base station. The system model for the collaborative communication model with imperfect phase and frequency synchronization in the presence of AWGN and Rayleigh fading is shown in Figure 4.15. It is composed of *N* collaborative node transmitters represented as Source (Node). Each collaborative node has a transceiver to receive signals from other

collaborative nodes within the network and to transmit signals to the base station. Each collaborative node also has a phase lock loop (PLL) for offset correction and modulator to modulate the signal. As there is no perfect phase and frequency synchronization between the collaborative nodes and the base station, there is a random phase and frequency offset between all transmitted signals. The channel is considered as an AWGN and a Rayleigh fading channel. The Rayleigh fading channel for each transmitted signal has an independent effect. On the receiver side, denoted as the base station, there is a demodulator to demodulate the received signal. The demodulator multiplies the received signal with a cosine signal; passes it through a low pass filter (LPF) and then integrates it. Then the power of demodulated signal is calculated.

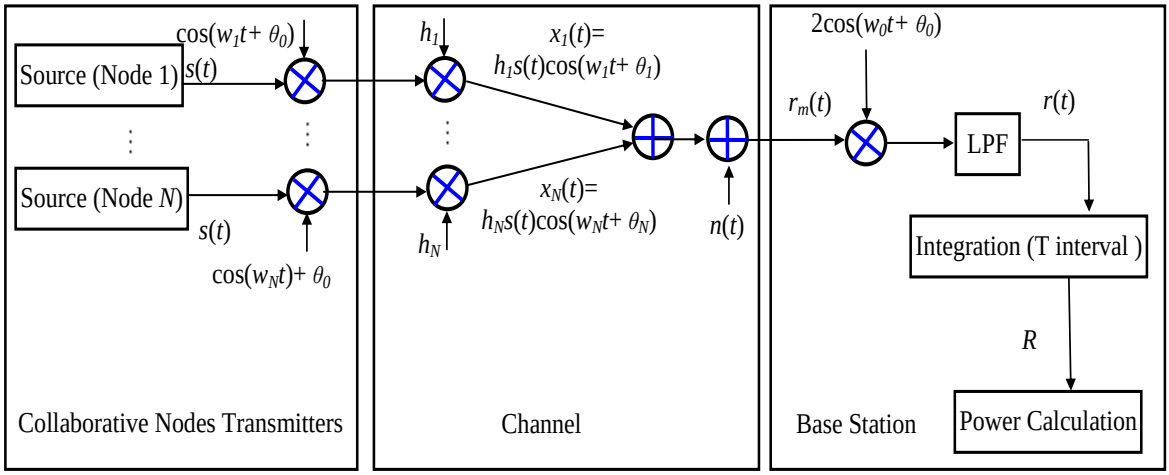

Figure 4.15 System Model

4.7.1 Theoretical Model

Let $s(t)$ be the information data transmitted to the base station by the collaborative nodes. As the distance between the collaborative nodes and base station cannot be estimated accurately and produces displacement error that is converted to phase error and as each collaborative node has its own oscillator, there will be a frequency mismatch between the collaborative nodes and the base station.

The signal transmitted by i^{th} collaborative node received at the base station is given by

$$x_i(t) = s(t)\cos(w_i t + \theta_i), \tag{4.26}$$

Where $w_i = w_0 + \Delta w_i$, where w_0 is the carrier frequency and Δw_i is the frequency offset and $\theta_i = \theta_0 + \Delta\theta_i$, where θ_0 is the nominal phase and $\Delta\theta_i$ is phase offset

The received signal at the base station is the sum of all the signals transmitted by collaborative nodes and the noise added in the channel. The composite received signal at the base station can be expressed as

$$r_m(t) = \sum_{i=1}^{N} h_i s(t) \cos(w_i t + \theta_i) + n(t), \tag{4.27}$$

where i=1 to N, the frequency is $w_i = w_0 + \Delta w_i$, where w_0 is the carrier frequency and Δw_i is the frequency offset and the phase is $\theta_i = \theta_0 + \Delta\theta_i$, where θ_0 is the nominal phase and $\Delta\theta_i$ is phase offset, h_i is the Rayleigh fading and $n(t)$ is zero-mean AWGN.
The demodulated signal at the decision circuit is given by

$$R = \sum_{i=1}^{N} h_i S\left(\frac{\sin(\Delta w_i T + \Delta\theta_i)}{\Delta w_i T} - \frac{\sin(\Delta\theta_i)}{\Delta w_i T}\right) + n, \tag{4.28}$$

where S is the signal amplitude and n is the noise amplitude at sampling time T. Power of R is given by

$$P_R = \left[\sum_{i=1}^{N} h_i S\left(\frac{\sin(\Delta w_i T + \Delta\theta_i)}{\Delta w_i T} - \frac{\sin(\Delta\theta_i)}{\Delta w_i T}\right) + n\right]^2. \tag{4.29}$$

As Δw_i, $\Delta\theta_i$, h_i and n are the random variables, so we have to calculate the mean value of received power as

$$E[P_R] = E\left[\sum_{i=1}^{N} h_i S\left(\frac{\sin(\Delta w_i T + \Delta\theta_i)}{\Delta w_i T} - \frac{\sin(\Delta\theta_i)}{\Delta w_i T}\right) + n\right]^2. \tag{4.30}$$

As Δw_i, $\Delta\theta_i$, h_i and n are the independent random variables and n is zero-mean random variable, the above equation can be written as

$$E[P_R] = E\left[\sum_{i=1}^{N} h_i S\left(\frac{\sin(\Delta w_i T + \Delta\theta_i)}{\Delta w_i T} - \frac{\sin(\Delta\theta_i)}{\Delta w_i T}\right)\right]^2 + \sigma_n^2, \tag{4.31}$$

where σ^2_n is the variance of noise. Equation (4.31) can also be developed as follows

$$E[P_R] = \sum_{i=1}^{N} S^2 E\left[h_i^2\right] E\left[\left(\frac{\sin(\Delta w_i T + \Delta\theta_i)}{\Delta w_i T} - \frac{\sin(\Delta\theta_i)}{\Delta w_i T}\right)^2\right] +$$
$$\sum_{\substack{i=1 \\ i\neq j}}^{N}\sum_{j=1}^{N} S^2 E\left[h_i h_j\right] E\left[\left(\frac{\sin(\Delta w_i T + \Delta\theta_i)}{\Delta w_i T} - \frac{\sin(\Delta\theta_i)}{\Delta w_i T}\right)\left(\frac{\sin(\Delta w_j T + \Delta\theta_i)}{\Delta w_j T} - \frac{\sin(\Delta\theta_j)}{\Delta w_j T}\right)\right] + \sigma_n^2 \quad (4.32)$$

As all h_i are i.i.d random variables then $E[h_i] \approx E[h]$, $E[h_i^2]=1$, the frequency offsets Δw_i are i.i.d random variables having uniform distribution from $\{-w_e$ to $w_e\}$ for all i and equal mean value i.e., $E[\Delta w_i] \approx E[\Delta w]$. Also $\Delta\theta_i$ are i.i.d random variables having uniform distribution from $\{-\psi$ to $\psi\}$ for all i and equal mean value i.e., $E[\Delta\theta_i] \approx E[\Delta\theta]$. Thus the equation (4.32) can now be written as

$$E[P_R] = NS^2 E\left[\left(\frac{\sin(\Delta wT + \Delta\theta)}{\Delta wT} - \frac{\sin(\Delta\theta)}{\Delta wT}\right)^2\right]$$
$$+ N(N-1)S^2\{E[h]\}^2\left\{E\left[\frac{\sin(\Delta wT + \Delta\theta)}{\Delta wT} - \frac{\sin(\Delta\theta)}{\Delta wT}\right]\right\}^2 + \sigma_n^2 \quad (4.33)$$

The mean value of $\frac{\sin(\Delta wT + \Delta\theta)}{\Delta wT} - \frac{\sin(\Delta\theta)}{\Delta wT}$ and $\left(\frac{\sin(\Delta wT + \Delta\theta)}{\Delta wT} - \frac{\sin(\Delta\theta)}{\Delta wT}\right)^2$ are calculated in Appendix A.5 and A.6. Using the values of equation (A.5), (A.6) and mean value of h in equation (4.33), we can have

$$E[P_R] = NS^2\left[1 + \frac{(w_e T)^4}{180} - \frac{(w_e T)^2}{9}\right]\left[\frac{1}{2} + \frac{\sin(2\psi)}{4\psi}\right] + \frac{N(N-1)S^2 b^2 \pi}{2}\left[\left(1 - \frac{(w_e T)^2}{18}\right)\left(\frac{\sin(\psi)}{\psi}\right)\right]^2 + \frac{N_0}{2} \quad (4.34)$$

where ψ is distribution limit of phase error, w_e is distribution limit of frequency error and b is the mode of Rayleigh random variable h.

In the absence of fading and phase error, i.e., when ψ=0, the equation (4.34) reduces to the equation (4.16) and in the absence of fading and frequency offset, i.e. when w_e =0, the equation (4.34) reduces to the equation (4.25). The results obtained from equation (4.34) and the related results obtained by Monte Carlo simulation are discussed in section 4.6.2.

4.7.2 Analysis and Results

A Monte Carlo simulation is performed to analyze the collaborative communication system with imperfect phase and frequency synchronization in the presence of AWGN and Rayleigh fading using SIMULINK and MATLAB®. The wireless communication environment used in the simulation is established using SIMULINK's AWGN and Rayleigh channel blocks. The simulation model for a collaborative communication system with imperfect phase and frequency synchronization is shown in Figure 4.16.

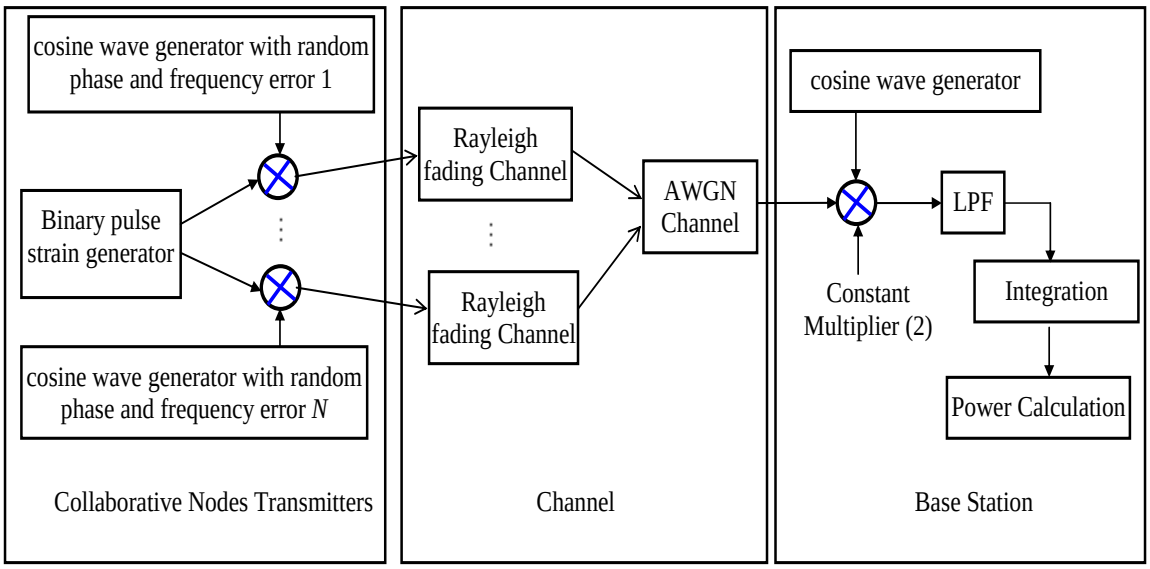

Figure 4.16 Simulation Model of Collaborative Communication with imperfect phase and frequency synchronization

For simulation, the parameters of the off-the-shelf products i.e., CC2420 [27] and AT86RF212 [28] are considered. For each value of N i.e., the number of collaborative nodes, distribution of phase error i.e., $\{-0.1\pi \sim 0.1\pi\}$, $\{-0.2\pi \sim 0.2\pi\}$, $\{-0.3\pi \sim 0.3\pi\}$ and $\{-0.4\pi \sim 0.4\pi\}$ and distribution of frequency error i.e., {-150 KHz~150 KHz}, {-250 KHz~250 KHz}, {-350 KHz~350 KHz}, {-35 KHz~35 KHz}, {-55 KHz~55 KHz} and {-65 KHz~65 KHz}, 1200 Monte Carlo simulations are run. Each collaborative node transmits the same binary pulse strain. To avoid inter symbol interference; the considered signal rate is 15% of the carrier frequency. Each collaborative node modulates the data using the carrier wave (obtained from the VCO output of the PLL). A random phase error distributed over different distributions i.e., $\{-0.1\pi \sim 0.1\pi\}$, $\{-0.2\pi \sim 0.2\pi\}$, $\{-0.3\pi \sim 0.3\pi\}$ and

{-0.4π~0.4π} is added to the carrier wave. A random frequency error distributed over different distributions i.e., frequency error i.e., {-150 KHz~150 KHz}, {-250 KHz~250 KHz}, {-350 KHz~350 KHz}, {-35 KHz~35 KHz}, {-55 KHz~55 KHz} and {-65 KHz~65 KHz} is also added to the carrier wave. The modulated signal is transmitted to the base station. The receiver demodulates the received signal and calculates the power of demodulated signal.

The analytical results are compared with the simulation results. For analysis, the phase error is considered to be uniformly distributed over interval {- ψ ~ ψ} and the frequency error is considered to be uniformly distributed over interval {- w_e ~ w_e}. In this analysis two phase error distributions, i.e. {-0.1π~0.1π} and {-0.3π~0.3π}, parameters of CC2420, i.e., frequency error distributed over {-200 KHz ~200 KHz}, data rate 250 Kbps and parameters of AT86RF21, i.e., frequency error distributed over {-55 KHz ~55 KHz}, data rate 40 Kbps are analyzed.

Figures 4.17 and 4.18 show the analytical and simulation results of the model in the presence of Rayleigh fading for average total received power at the base station for products CC2420 and AT86RF21, respectively. Results show that the analytical results match very well with the results of the simulation. The total received power increases as the number of collaborative nodes increases, and the total received power decreases as the phase error increases. It is observed that a high power gain can still be achieved using collaborative communication in the presence of phase errors, frequency errors and fading. A power gain of $0.57N^2$ can be achieved if the phase error is distributed over {-0.3π~0.3π}, frequency error distributed over {-200 KHz ~200 KHz} and a power gain of $0.50\ N^2$ can be achieved if the phase error is distributed over {-0.3π~0.3π}}, frequency error distributed over {-55 KHz ~55 KHz}. It is confirmed that the received power with phase errors decreases in respect to the received power without phase error for products CC2420 and AT86RF21 as follows:

by approximately 28% for phase errors distributed over {-0.1π~0.1π} and frequency error distributed over {-200 KHz ~200 KHz}, by 43% for phase errors distributed over {-0.3π~0.3π} and frequency error distributed over {-200 KHz ~200 KHz}, by 37% for phase errors distributed over {-0.1π~0.1π} and frequency error distributed over {-55 KHz ~55 KHz} and by 50% for phase errors distributed over {-0.3π~0.3π} and frequency error distributed over {-55 KHz ~55 KHz}.

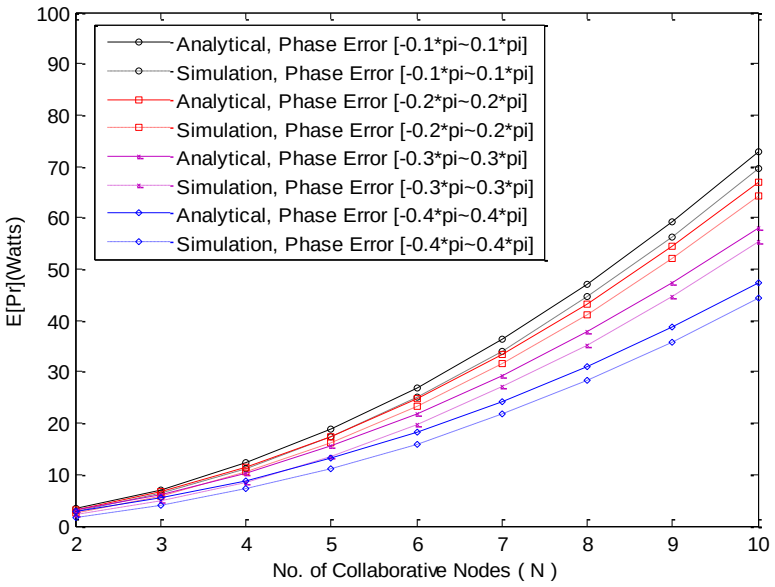

Figure 4.17 Average total received power Vs No of collaborative nodes with frequency error 200 KHz and data rate 250 Kbps

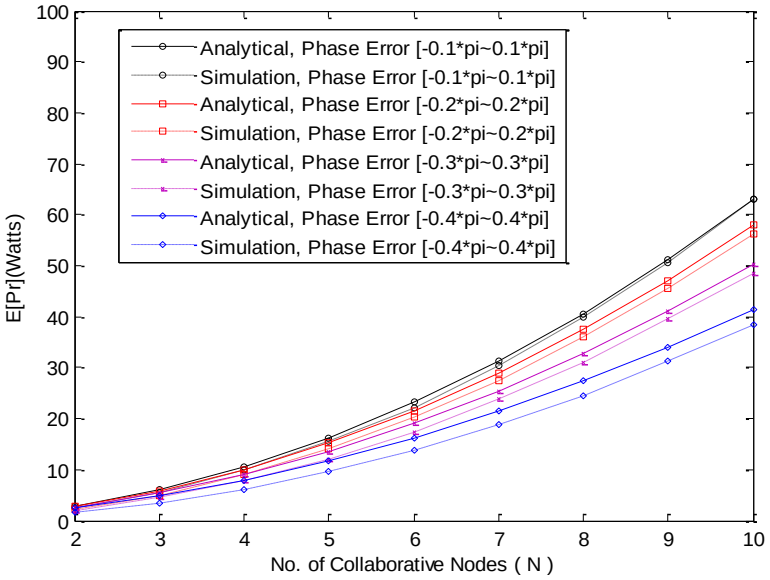

Figure 4.18 Average total received power versus number of collaborative nodes with frequency error 55 KHz and data rate 40 Kbps

4.8 Chapter Conclusions

The chapter focuses on the study of collaborative communication models for wireless sensor networks. The figure of merit considered in this chapter is received power at the base station. The theoretical analysis of the ideal collaborative communication models is

presented and the expressions for received power are derived and expressed as the function of the number of collaborative nodes. Key factors i.e., phase, frequency and time synchronization, which degrade the performance of collaborative communication, are identified. The mathematical model for the synchronization process to reduce the phase and frequency error is presented. Collaborative communication models for imperfect phase and frequency synchronization are developed and analyzed. The combined effect of phase and frequency on the performance of collaborative communication is also investigated. Collaborative communication models with imperfect phase synchronization only, frequency synchronization only, and for imperfect phase and frequency synchronization for sensor networks in the presence of AWGN and Rayleigh fading, are presented. The theoretical analysis of the collaborative communication models is presented and the expressions for received power are derived and expressed as the function of the number of collaborative nodes.

A MATLAB®-based WSN simulator is developed to confirm the results of these algorithms. For analysis, the parameters of two off-the-shelf products i.e. CC2420 and AT86RF212 are considered. It is concluded that a significant power gain can be achieved by increasing the number of collaborative nodes without increasing the total amount of transmitted power. This is the consequence of the collaborative communication and can be considered as a space diversity system. It is observed that the received power gain significantly increases as the number of collaborative nodes increases, and that power gain significantly decreases as phase error and frequency error increases.

In this chapter the considered figure of merit is received power only. In collaborative communication received signals are constructively added and produce high power gain. But if the phase error is π radian or 180^{o}, received data at the base station will have 100% error. Hence the constructive interference is converted into destructive interference, but it results in a high level of received power. Thus, only received power cannot be considered as figure of merit for the analysis of collaborative communication systems. In Chapter 5 a bit error rate (BER) analysis that is widely used to characterize communication systems to analyze the proposed collaborative communication system, is presented.

References

[1] D. Estrin, L. Girod, G. Pottie, and M. Srivastava, “Instrumenting the world with wireless sensor networks,” Proc. IEEE Intl. Conf. on Acoustics, Speech, and Signal Processing (ICASSP), vol. 4, 2001, pp. 2033–2036.

[2] M. Gastpar and M.Vetterli, “On the capacity of wireless networks: the relay case,” Twenty-First Annual Joint Conference of the IEEE Computer and Communications Societies (INFOCOM 2002), 2002, pp. 1577 – 1586.

[3] W.R. Heinzelmann, A. Chandrakasan and H. Balakrishnan, “Energy-efficient communication protocol for wireless microsensor networks,” 33rd Annual Hawaii International Conference on System Sciences, January 2000, pp. 1-10.

[4] R. Mudumbai, D.R. Brown, U. Madhow and H.V. Poor, “Distributed transmit beamforming: challenges and recent progress,” IEEE Communications Magazine, Vol. 47, Issue 2, 2009, pp. 102 - 110.

[5] G. Barriac, R. Mudumbai, and U. Madhow, “Distributed beamforming for information transfer in sensor networks,” in Proc. 3rd International Symposium on Information Processing in Sensor Networks (IPSN’04), Apr. 26–27, 2004, pp. 81–88.

[6] R. Mudumbai, G. Barriac, and U. Madhow, “On the feasibility of distributed beamforming in wireless networks," IEEE Trans. Wireless Commun., vol. 6, no. 5, May 2007, pp. 1754-1763.

[7] W. C. Y. Lee, “Overview of cellular CDMA,” IEEE Transactions of Vehicular Technolology, vol. 40, 1991, pp. 291–302.

[8] S. Savazzi and U. Spagnolini, “Cooperative Fading Regions for Decode and Forward Relaying,” IEEE Transactions on Information Theory, Vol. 54, Issue 11, Nov. 2008, pp. 4908 – 4924.

[9] S.A Astaneh and S. Gazor, “Collaborative communications: Joint relay and protocol selection,” 11th Canadian Workshop on Information Theory, 2009. CWIT 2009, May 2009, pp. 25-28.

[10] K. Zarifi, S. Affes, and A. Ghrayeb, “Distributed beamforming for wireless sensor networks with random node location,” IEEE International Conference on Acoustics, Speech and Signal Processing, 2009, pp. 2261– 2264.

[11] A. El-Keyi, A and B. Champagne, “Collaborative Uplink Transmit Beamforming With Robustness Against Channel Estimation Errors,” IEEE Transactions on Vehicular Technology, Vol. 58, Issue 1, Jan. 2009, pp. 126 – 139.

[12] R. Mudumbai, J. Hespanha, U. Madhow, and G. Barriac, “Distributed Transmit Beamforming Using Feedback Control,” IEEE Transactions on Information Theory, Vol. 56, Issue 1, 2010, pp. 411 – 426.

[13] J.A. Bucklew, W.A. Sethares, “Convergence of a Class of Decentralized Beamforming Algorithms,” IEEE Transactions on Signal Processing, Vol. 56, Issue 6, 2008, pp. 2280 – 2288.

[14] E. Koyuncu, Y. Jing, Y and H. Jafarkhani “Distributed beamforming in wireless relay networks with quantized feedback,” IEEE Journal on Selected Areas in Communications, Vol. 26, Issue 8, October 2008, pp. 1429 – 1439.

[15] Z. Han and H. V. Poor, "Lifetime improvement in wireless sensor networks via collaborative beamforming and cooperative transmission," Microwaves, Antennas & Propagation, IET, vol. 1, 2007, pp. 1103-1110.

[16] A. Bletsas, A. Lippman, J.N. Sahalos, “Simple, zero-feedback, distributed beamforming with unsynchronized carriers,” IEEE journal on selected areas in communications, Vol. 28, No. 7, September 2010, pp. 1046-1054.

[17] D. Zhiguo, H. C. Woon and K.K. Leung, “Distributed beamforming and power allocation for cooperative networks,” IEEE Transactions on Wireless Communications, Vol. 7, Issue 5, May 2008, pp. 1817 – 1822.

[18] M.F.A. Ahmed, S.A. Vorobyov, “Collaborative beamforming for wireless sensor networks with Gaussian distributed sensor nodes,” IEEE Transactions on Wireless Communications, Vol. 8, Issue 2, 2009, pp. 638 – 643.

[19] M.F.A. Ahmed, S.A. Vorobyov, "Side-lobe Control in Collaborative Beamforming via Node Selection," IEEE Transactions on Signal Processing, Vol. 58, Issue 12, November 2010, pp. 6168 – 6180.
[20] J. Choi, "Distributed Beamforming Using a Consensus Algorithm for Cooperative Relay Networks," IEEE Communications Letters, Vol. 15, Issue 4, April 2011, pp. 368 – 370.
[21] P.A. Parker, P. Mitran, D. Bliss and V. Tarokh, "On Bounds and Algorithms for Frequency Synchronization for Collaborative Communication Systems," IEEE Transactions on Signal Processing, Vol. 56, Issue 8, Aug. 2008, pp. 3742 – 3752.
[22] D. R. Brown and H.V Poor, "Time-Slotted Round-Trip Carrier Synchronization for Distributed Beamforming" IEEE Transactions on Signal Processing, Vol. 56, Issue 11, Nov. 2008, pp. 5630 – 5643.
[23] J. D. Kraus, Antennas, Second Edition. Mc-Graw Hill, 1988.
[24] S. Uda and Y. Mushiake, Yagi-Uda Antennas, 1954.
[25] K. Yao, R. Hudson, C. Reed, D. Chen, and F. Lorenzelli, "Blind beamforming on a randomly distributed sensor array system," IEEE Journal of selected Areas in Communication, vol. 16, no. 8, 1998, pp. 1555–1567.
[26] J. Winters, "Smart antennas for wireless systems," IEEE Personal Communications, vol. 5, no. 1, pp. 23–27, 1998.
[27] CC2420, Texas Instruments Chipcon Products, http://focus.ti.com/analog/docs/enggresdetail.tsp?familyId=367&genContentId=3573.
[28] AT86RF212, ATMEL Products, http://www.atmel.com/dyn/products/product_card.asp? PN =AT86RF212.
[29] H. Meyr and G. Ascheid, Synchronization in Digital Communications. Wiley and Sons, NY, 1990.

Chapter 5 Probability of Error or Bit Error Rate (BER) for Collaborative Communication Systems

5.1 Introduction

From the collaborative communication systems presented in Chapter 4, it is revealed that a high power gain can be achieved without perfect frequency and phase synchronization in the presence of AWGN and fading. But if the phase error is π radian or 180^{o}, received data at the base station will have 100% error. Therefore, bit error rate (BER) analysis that is widely used to characterize communication systems is required to analyze collaborative communication systems. Moreover, due to the power constraints of sensor network fading mitigation is also required for energy efficient communication in sensor networks. Chapter 2 shows that a large amount of fade margin is needed for wireless communication systems to achieve reliable data acceptance in a fading channel. The large amount of fade margin suggests significant node energy expenditure in data communication. Various fading-mitigating techniques have been explored to save node energy in data communication. In the literature many fading-mitigating signal processing techniques, which exploit the signal processing diversity in space, time, frequency, have been applied to WSNs, such as cooperative communication [1-5], Multi-Input-Multi-Output (MIMO) signal processing [6-9] and chip interleaving technique [10-13].

The aim of this chapter is to analyze the BER of a collaborative communication system, the capability of collaborative communication on mitigating flat Rayleigh fading and this technique's limitations. A route map showing the studied collaborative communication models and their properties is presented in Figure 5.1. The bit error performance of different collaborative communication models in the Additive White Gaussian Noise (AWGN) channel with flat Rayleigh fading is investigated. The First collaborative communication model performs binary data communication, Binary Phase Shift Keying (BPSK) modulation and coherent demodulation with perfect time, frequency and phase synchronization between the collaborative nodes and the base station. The second collaborative communication model performs binary data communication, Binary Phase Shift Keying (BPSK) modulation and coherent demodulation with imperfect phase synchronization and assuming perfect time and frequency synchronization between the collaborative nodes and the base station. The third collaborative communication model

performs binary data communication, Binary Phase Shift Keying (BPSK) modulation and coherent demodulation with imperfect frequency synchronization and assuming perfect time and phase synchronization between the collaborative nodes and the base station. As sensor nodes are randomly distributed, it is very difficult to achieve perfect phase and frequency synchronization between collaborative nodes and the base station in a real time environment. A realistic collaborative communication model to perform binary data communication, Binary Phase Shift Keying (BPSK) modulation and coherent demodulation with imperfect phase and frequency synchronization between the collaborative nodes and the base station, is presented. Of particular interest to this study is the achievement of the following:

- The development of a closed form expression for BER for collaborative communication models;
- An investigation of the effect of phase and frequency errors on BER for collaborative communication systems in wireless sensor networks;
- An investigation of the fading mitigation ability of collaborative communication models for wireless sensor networks;
- The establishment of a WSN simulator to assess BER using collaborative communication with imperfect phase and frequency synchronization in presence of AWGN and Rayleigh fading using the parameters of off-the-shelf products i.e. CC2420 [14] and AT86RF212 [15].

The studied BER analysis of collaborative communication models will be utilized in the investigation of energy-efficient physical layer communication algorithms, as presented in Chapter 6.

Figure 5.1 demonstrates the route map of the chapter. The study in this chapter unfolds in the following sequence.

In Section 5.2, an extensive literature review of BER and collaborative communication is presented. Section 5.3 presents the development of a closed form expression of BER for an ideal collaborative communication system i.e., by assuming perfect phase, frequency and time synchronization. A system model, which is a mathematical model for BER for an ideal collaborative communication system is developed. Theoretical and simulation results reveal that BER is significantly reduced using collaborative communication.

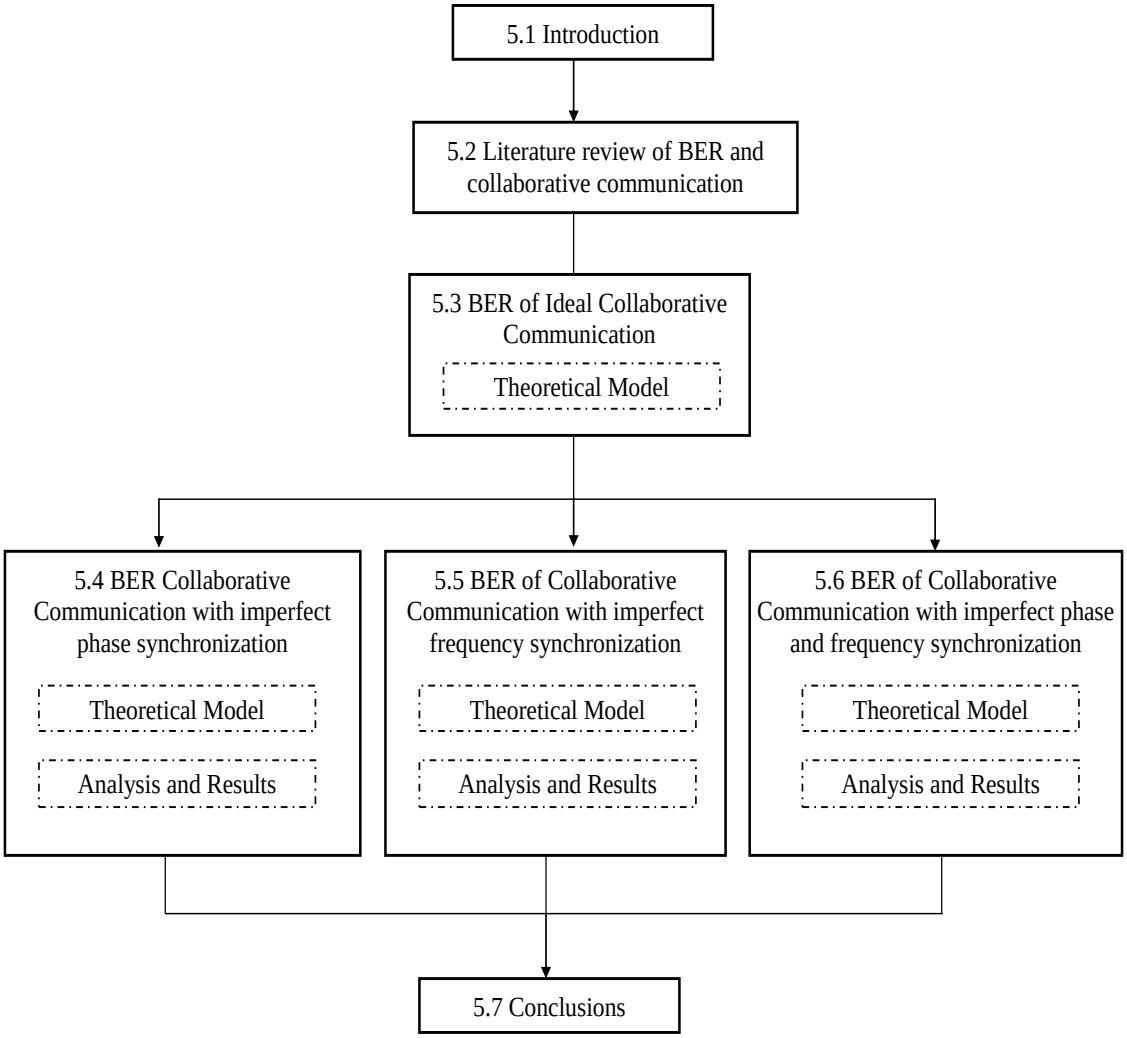

Figure 5.1 Route map of the study in Chapter 5

In section 5.4 a closed form expression of BER for collaborative communication system with imperfect phase synchronization with the assumption of perfect frequency synchronization that includes the influence of noise and Rayleigh fading is presented. The theoretical model of the system is presented and a theoretical analysis and Monte Carlo simulation are conducted to validate the performances of the collaborative communication algorithm in terms of the BER for various phase errors. In Section 5.5, a closed form expression of BER for a collaborative communication system with imperfect frequency synchronization, with the assumption of perfect phase synchronization that includes the influence of noise and Rayleigh fading, is modelled, theoretically analyzed and simulated using the parameters of off-the-shelf products i.e. CC2420 [14] and AT86RF212 [15]. In Section 5.6 closed form expressions of BER for more realistic

collaborative a communication system with imperfect phase and frequency synchronization, which includes the influence of noise and Rayleigh fading, is modelled, theoretically analyzed, and simulated.

In summary, the contribution of this chapter is three-fold:

4. The development of closed form expressions of BER, expressed as a function of signal to noise ratio for the number of collaborative nodes, as the parameter, for a collaborative communication system that includes the influence of the phase error, frequency error, AWGN and Rayleigh fading in the channel;
5. The verification of the fact that fading can be significantly mitigated using collaborative communication. This is the consequence of collaborative communication and can be considered as a space diversity system;
6. Simulation-based investigations to confirm that the proposed collaborative communication system significantly reduces BER with imperfect phase and frequency synchronization in the presence of AWGN and Fading;

5.2 Related Work

BER analysis is widely used to characterise and analyze the performance of communication systems. The expression of bit error rate (BER) for cooperative communication with multiple relays by exploiting the concepts of Alamouti space-time code is presented and analyzed in [16]. In [17] and [18], the symbol error rate (SER) performance for decode-and-forward (DF) cooperation is analyzed under Rayleigh fading channel. In [19] and [20], the authors analyzed the SER performance over Nakagami fading channels for both amplify-and-forward (AF) and decode-and-forward (DF) protocols, respectively. However, all the investigations considered the classical three node model. The BER analysis for low density parity checks (LDPC) coded transmission is presented and analyzed in [21]. The comparison between the ergodic and outage capacity over average SNRs for different Nakagami channel parameters is also performed in [21].

The effects of node density, correlation amongst interferers, and power control error on BER, packet error rate (PER), average amount of retransmission and energy consumption for the successful reception of a packet at sink in a single hop, are investigated for CDMA based sensor networks in [22]. The performance of a CDMA based static wireless sensor network (WSN), in terms of bit error rate (BER), considering

the correlation between signal and interferers in a large scale fading environment is presented and evaluated in [23]. The effects of node density, and the number of antennas used for spatial diversity on BER are also presented and investigated in [23].

In the block Chip-Interleaved DS-CDMA (CIDS-CDMA) system reported in [10], a block of uncoded bits is directly spread onto chips. Then the indexed chips of blocked bits are interleaved, modulated and transmitted in turn by the transmitter. In the receiver, the transmitted data bits are recovered, thus reversing the signal processing steps performed in the transmitter. In the presence of Rayleigh fading and AWGN, notable bit error gains are observed from the simulation results of single-user CIDS-CDMA systems [10]. It has been understood that the bit error rate improvement rises from the time diversity of chip interleaving, which effectively releases temporarily, heavily-correlated channel response caused by fading [10]. Closed-form average BER expression for a chip-interleaved DS-CDMA system for sensor network conducting M-ary communication and non-coherent demodulation in a flat Rayleigh fading channel is presented and analyzed in [24]. The influence of the noisy phase error on the system BER for CIDS-CDMA systems is studied in [24]. In [25-26] noisy phase error is found to be dependent on the nature of the practical demodulators and may follow various distributions that are taken into account in this study.

However, the procedure for developing closed-form average BER expressions of collaborative communication systems with imperfect phase and frequency synchronization stays as an open issue. Moreover, such expressions are absent in existing literature. These BER expressions may be used as the baseline for the study of collaborative communication systems enhanced by advanced signal processing techniques. The fading mitigation ability of collaborative communication can also be analyzed using BER analysis.

5.3 Probability of Error for an Ideal Collaborative communication model

In this section, a closed form of Probability of Error or BER for an ideal collaborative communication model with the assumption that there is perfect time, frequency, and phase synchronization, between the collaborative nodes and the base station, is presented. A collaborative node has to transfer the data to the base station. Using collaborative

communication let *N* collaborative nodes make a network to transfer information to the base station. The geometry of the sensor network used for collaborative communication is shown in Figure 4.3. It is composed of *N* collaborative nodes. For an ideal collaborative communication model, it is assumed that there is perfect phase, time and frequency synchronization between the collaborative odes and the base station. In the first step, collaborative nodes that have data to be transferred to the base station send the data to all *N*-1 collaborative nodes in the network. In the second step, all collaborative nodes transfer data at the same time towards the base station.

5.3.1 Theoretical Model

The collaborative communication network shown in Figure 4.3 can be presented by a scheme shown in Figure 5.2. It is composed of *N* collaborative node transmitters represented as Source (Node). Each collaborative node has a transceiver to receive signals from other collaborative nodes within the network and to transmit the signals to the base station. Each collaborative node also has a phase lock loop (PLL) for offset correction and a modulator to modulate the signal. The channel is considered as the AWGN channel. On the receiver side denoted as the base station, there is a demodulator to demodulate the received signal. The demodulator multiplies the received signal with a cosine signal; passes it through a low pass filter (LPF) and then integrates it. Then the BER of the system is calculated.

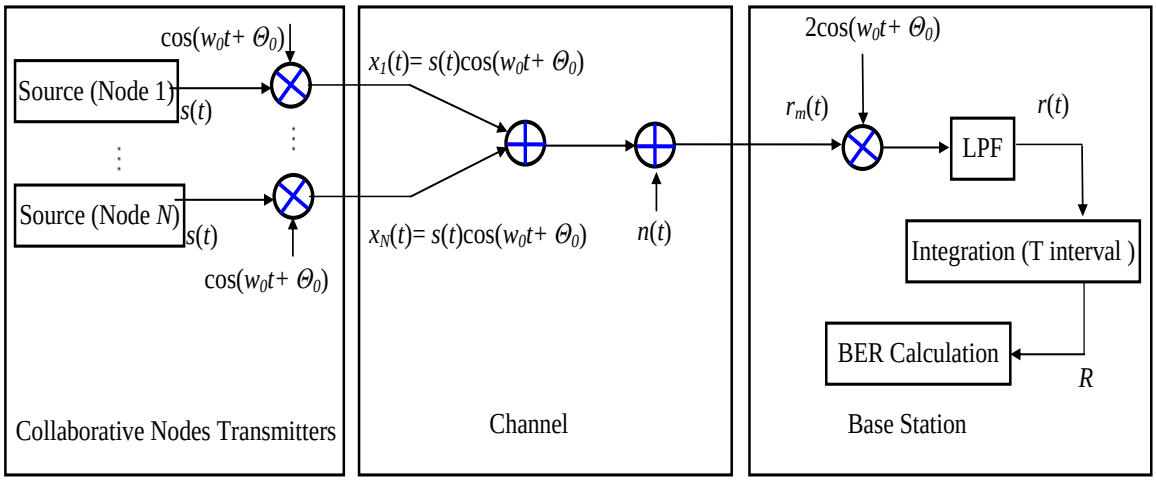

Figure 5.2 System Model

Let $s(t)$ be the information data transmitted to the base station by the collaborative nodes. The cumulative received signal at the Base station is given by

$$r_m(t) = \Re\left(\sum_{i=1}^{N} s(t)e^{j(w_0 t+\Theta_0)}\right) + n(t), \tag{5.1}$$

where $n(t)$ is AWGN.

The system model of the collaborative communication system is shown in Figure 4.4. At the base station the demodulated signal is integrated and its output is given by

$$R = \sum_{i=1}^{N} S + n = NS + n, \tag{5.2}$$

where $S = \pm\sqrt{E_b}$ is the signal amplitude [27] and n is the noise amplitude at sampling time T.

Suppose the data is sent using BPSK and the received signal R depends upon independent random variables n. The input of the decision circuit R is given by equation (5.2).

As n has Gaussian, R will also have Gaussian distribution and probability of error in the system is given by

$$P_e = 0.5erfc\left(\frac{\mu_R}{\sqrt{2\sigma_R^2}}\right). \tag{5.3}$$

Using mean value and variance of R from equation 5.2, equation 5.3 may be written as

$$P_e = 0.5erfc\left(\frac{NS}{\sqrt{2\frac{N_0}{2}}}\right). \tag{5.4}$$

As $S^2 = E_b$ the probability of error in (5.4) can be expressed as

$$P_e = 0.5erfc\left(\sqrt{\frac{N^2 E_b}{N_0}}\right). \tag{5.5}$$

Special Case:

If the amplitude of each bit for each collaborative node is $S = \pm(\sqrt{E_b})/N$, we have

$$P_e = 0.5 erfc\left(\sqrt{\frac{E_b}{N_0}}\right). \quad (5.6)$$

From equation (5.6), it is clear that if the transmitted power of each collaborative node is reduced by N^2 i.e., the total transmitted power of the network is N, the probability of error remains the same as for a single input single output case with the total transmitted power N.

5.4 Probability of Error for a Collaborative Communication System with imperfect phase synchronization

This section presents a closed form of Probability of Error or BER for a collaborative communication model with imperfect phase synchronization and with the assumption that there is perfect time and frequency synchronization between the collaborative nodes and the base station in the presence of AWGN and Rayleigh fading. The system model for a collaborative communication model with imperfect phase synchronization in the presence of AWGN and Rayleigh fading is shown in Figure 5.3.

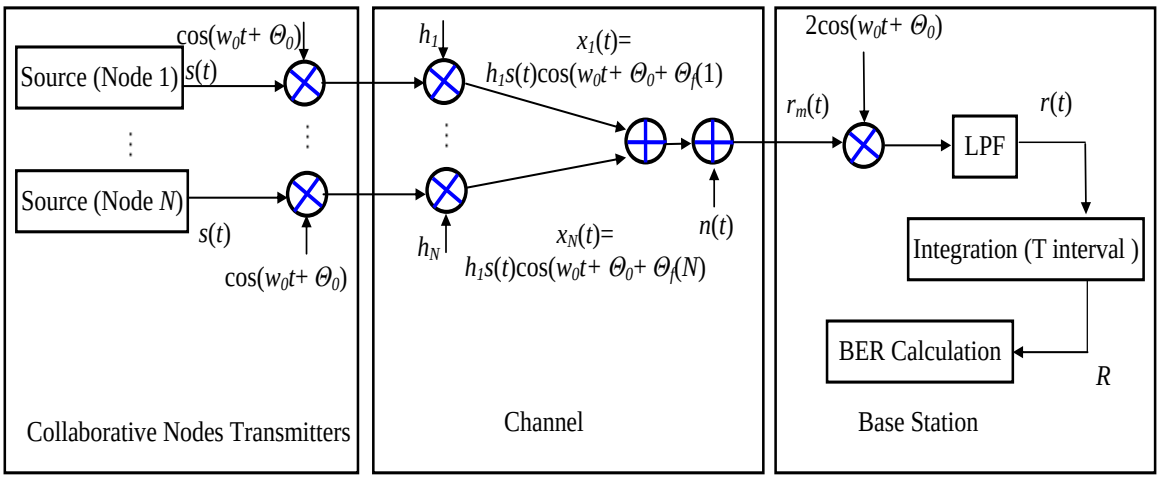

Figure 5.3 System Model

It is composed of N collaborative node transmitters represented as Source (Node). Each collaborative node has a transceiver to receive signal from other collaborative nodes within the network and to transmit the signal to the base station. Each collaborative node also has a phase lock loop (PLL) for offset correction and a modulator to modulate the signal. The channel is considered as the AWGN and Rayleigh fading channel. The

Rayleigh fading channel for each transmitted signal has an independent effect. On the receiver side, denoted as the base station, there is a demodulator to demodulate the received signal. The demodulator multiplies the received signal with a cosine signal; passes it through a low pass filter (LPF) and then integrates it. Then the BER of the system is calculated

5.4.1 Theoretical Model

Let $s(t)$ be the information data transmitted to the base station by the collaborative nodes. The distance between the nodes and the base station is estimated with certain errors in the estimation. These errors in distance estimation will be known as, displacement errors. In the mathematical model of the network, these displacement errors will be translated into phase errors. Let d_0 be the nominal distance between the collaborative and the base station. Let w_0 be the carrier frequency, and assuming a line of sight propagation, the phase produced due to distance d_0 can be written as $\Theta_0 = w_0 d_0 / c$, where c is the speed of light. Let $d_f(i)$ be the displacement error between the base station and the i^{th} collaborative node, then the phase error due to displacement error is given by $\Theta_f(i) = w_0 d_f(i) / c$.

Let $\cos(w_0 t)$ be the carrier/reference signal used by all collaborative nodes. Assuming that the signal delay is minimal with respect to the signal bit interval T, so that there is significant guard interval and thus, inter symbol interference (ISI) can be ignored.
The cumulative received signal at the Base station is given by:

$$r_m(t) = \Re\left(\sum_{i=1}^{N} h_i s(t) e^{j(w_0 t + \Theta_0 + \Theta_f(i))} \right) + n(t), \tag{5.7}$$

where $n(t)$ is AWGN and h_i is the Rayleigh fading. At the base station the demodulated signal is integrated and its output is given by

$$R = \sum_{i=1}^{N} h_i S \cos(\Theta_f(i)) + n, \tag{5.8}$$

where $S = \pm\sqrt{E_b}$ is the signal amplitude and n is the noise amplitude at sampling time T.

Suppose the data is sent using BPSK and the received signal R depends upon independent random variables h_i and $\Theta_f(i)$. The input of the decision circuit R is given by equation (5.8).

Let $R = x + n$, where $x = \sum_{i=1}^{N} h_i S\cos(\Theta_f(i))$. Because x is sum of i.i.d random variables, according to the central limit theorem, its distribution tends to be Gaussian when N tends to infinity. If N is sufficiently large, then the sum of x and n also tends to be Gaussian and the probability of error in the system is given by [27]

$$P_e = 0.5 erfc\left(\frac{\mu_R}{\sqrt{2\sigma_R^2}}\right). \tag{5.9}$$

As h_i and $\Theta_f(i)$ are independent random variables, we have

$$\mu_R = \mu_x + \mu_n . \tag{5.10}$$

$$\mu_R = E\left[\sum_{i=1}^{N} h_i S\cos(\Theta_f(i))\right] + E[n] = S\sum_{i=1}^{N} E[h_i]E\left[\cos(\Theta_f(i))\right]. \tag{5.11}$$

The mean value of $\cos(\Theta_f)$ is calculated in appendix A.1. Using equation (A.1) and value of $E[h_i]$, equation (5.11) becomes

$$\mu_R = \frac{\sqrt{\pi} bNS\sin(\varphi)}{\sqrt{2}\varphi}, \tag{5.12}$$

where φ distribution limit of phase error and b is the mode of Rayleigh random variable h. Variance of R, which is sum of two independent random variables, can be calculated as follows

$$\sigma_R^2 = \sigma_x^2 + \sigma_n^2 . \tag{5.13}$$

$$\sigma_R^2 = Var\left[\sum_{i=1}^{N} h_i S\cos(\Theta_f(i))\right] + Var[n] = \sum_{i=1}^{N} Var\left[h_i S\cos(\Theta_f(i))\right] + \frac{N_0}{2}, \tag{5.14}$$

Variance of $\cos(\Theta_f)$ and $Sh\cos(\Theta_f)$ are calculated in appendix A.3 and A.5, respectively. Using equations (A.3) and (A.5), equation (5.14) can be written as,

$$\sigma_R^2 = Nb^2S^2\left[1 - \frac{\pi}{2}\left(\frac{\sin(\varphi)}{\varphi}\right)^2 + \frac{\sin(2\varphi)}{2\varphi}\right] + \frac{N_0}{2}. \tag{5.15}$$

Using equations (5.9), (5.12) and (5.15), the probability of error is given by

$$P_e = 0.5 erfc\left(\frac{\frac{\sqrt{\pi} bNS \sin(\varphi)}{\sqrt{2}\varphi}}{\sqrt{2\left(Nb^2 S^2 \left[1 - \frac{\pi}{2}\left(\frac{\sin(\varphi)}{\varphi} \right)^2 + \frac{\sin(2\varphi)}{2\varphi} \right] + \frac{N_0}{2} \right)}} \right). \quad (5.16)$$

As $S^2 = E_b$ the probability of error in (5.16) can be expressed as

$$P_e = 0.5 erfc\left(\frac{\sqrt{\pi} b \sin(\varphi)}{\sqrt{2}\varphi} \sqrt{\frac{N^2 (E_b / N_0)}{\left(2Nb^2 \left[1 - \frac{\pi}{2}\left(\frac{\sin(\varphi)}{\varphi} \right)^2 + \frac{\sin(2\varphi)}{2\varphi} \right] (E_b / N_0) + 1 \right)}} \right). \quad (5.17)$$

Special Case:

If the amplitude of each bit for each collaborative node is $S = \pm(\sqrt{E_b})/N$, we have

$$P_e = 0.5 erfc\left(\frac{\sqrt{\pi} \sin(\varphi)}{2\varphi} \sqrt{\frac{(E_b / N_0)}{\left(\frac{2b^2}{N} \left[1 - \frac{\pi}{2}\left(\frac{\sin(\varphi)}{\varphi} \right)^2 + \frac{\sin(2\varphi)}{2\varphi} \right] (E_b / N_0) + 1 \right)}} \right). \quad (5.18)$$

This is a case where the signal amplitude of all collaborative nodes are reduced by factor N, i.e., the total transmitted energy is E_b/N.. This reduction is used to investigate the characteristics of a system with reduced power consumption for each collaborative node. This case can be used to investigate the effect of total transmitted power on BER.

5.4.2 Analysis and Results

A Monte Carlo simulation using SIMULINK and MATLAB® is performed to analyze the probability of error, or BER, of the collaborative communication system with imperfect phase synchronization in the presence of AWGN and Rayleigh fading. The wireless communication environment used in the simulation is established using SIMULINK's AWGN channel blocks.

The simulation model for a collaborative communication system with imperfect phase synchronization is shown in Figure 5.4. For each value of N i.e., the number of collaborative nodes and the distribution of phase error i.e., {-0.1π~0.1π}, {-0.2π~0.2π}, {-0.3π~0.3π} and {-0.4π~0.4π}, 1200 Monte Carlo simulations are run. Each collaborative node transmits the same binary pulse strain. To avoid the inter symbol interference; the considered signal rate is 15% of carrier frequency.

For simulation, the parameters of the off-the-shelf products i.e., CC2420 [14] and AT86RF212 [15] are considered. Each collaborative node modulates the data using the carrier wave (obtained from the VCO output of the PLL). A random phase error distributed over different distributions i.e., {-0.1π~0.1π}, {-0.2π~0.2π}, {-0.3π~0.3π} and {-0.4π~0.4π} is added to the carrier wave. The modulated signal is transmitted to the base station. The receiver demodulates the received signal and calculates the BER.

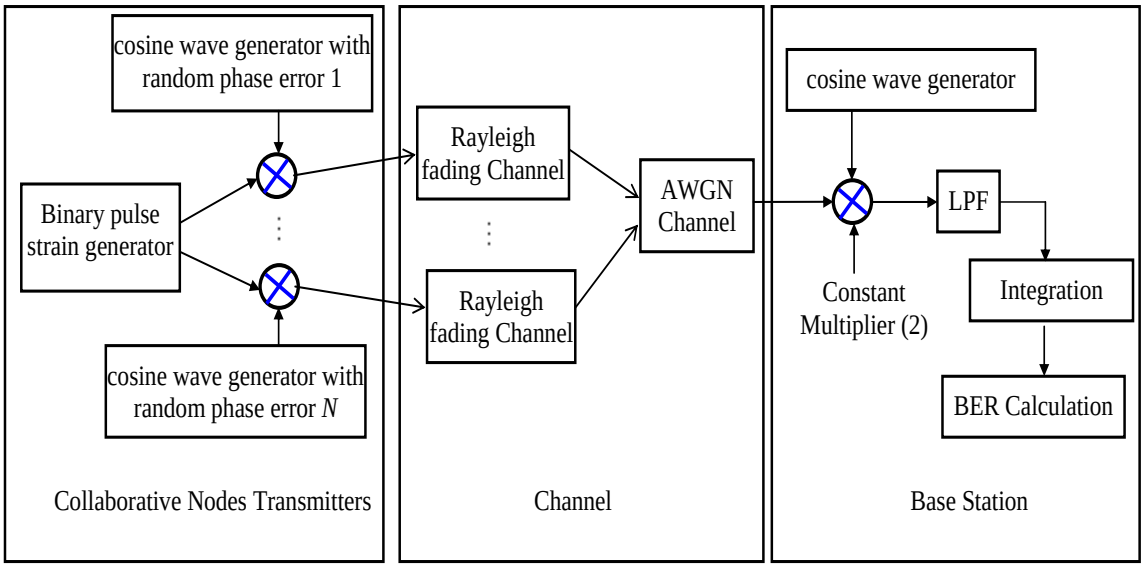

Figure 5.4 Simulation Model of Collaborative Communication with imperfect phase synchronization

To perform BER analysis, the energy per bit of each collaborative node is set to be E_b/N^2, so that the total energy used by all collaborative nodes is E_b/N. In this way the energy of each bit is reduced by N times. Figures 5.5, 5.6, 5.7 and 5.8 show analytical (calculated using equation (5.18)) and simulated results for BER with phase errors distributed over {-0.1π~0.1π}, {-0.2π~0.2π}, {-0.3π~0.3π} and {-0.4π~0.34}, respectively in the presence of AWGN and Rayleigh fading, for various number of

collaborative nodes. It is confirmed that the analytical and simulated BER curves are very close to each other for the various phase errors. The small difference between the analytical and the simulation results is due to the approximation used for calculating BER. It is observed that BER decreases as the number of collaborative nodes increases, which is confirmation of the fact that collaborative communication overcomes the fading effect. It is found that BER increases as the phase error increases. From the analytical and simulated results, it is shown that a single user case i.e., N=1, to achieve BER 10^{-3}, 7dB, SNR is required in an AWGN case without fading. For AWGN and Rayleigh fading channel 24 dB, SNR is required for a single user case i.e., N=1. Using collaborative communication, and for a number of collaborative nodes i.e., N=7, to achieve BER 10^{-3}, required SNR is 10dB for phase error, this is distributed over $\{-0.1\pi \sim 0.1\pi\}$, 11dB for phase error is distributed over $\{-0.2\pi \sim 0.2\pi\}$, 12dB for phase error is distributed over $\{-0.3\pi \sim 0.3\pi\}$ and 14dB for phase error is distributed over $\{-0.4\pi \sim 0.4\pi\}$. By increasing the number of collaborative nodes i.e., N=11, to achieve BER 10^{-3}, requires that SNR is 9dB for phase error is distributed over $\{-0.1\pi \sim 0.1\pi\}$, 9.75dB for phase error is distributed over $\{-0.2\pi \sim 0.2\pi\}$, 10.5dB for phase error is distributed over $\{-0.3\pi \sim 0.3\pi\}$ and 12.25dB for phase error is distributed over $\{-0.4\pi \sim 0.4\pi\}$.

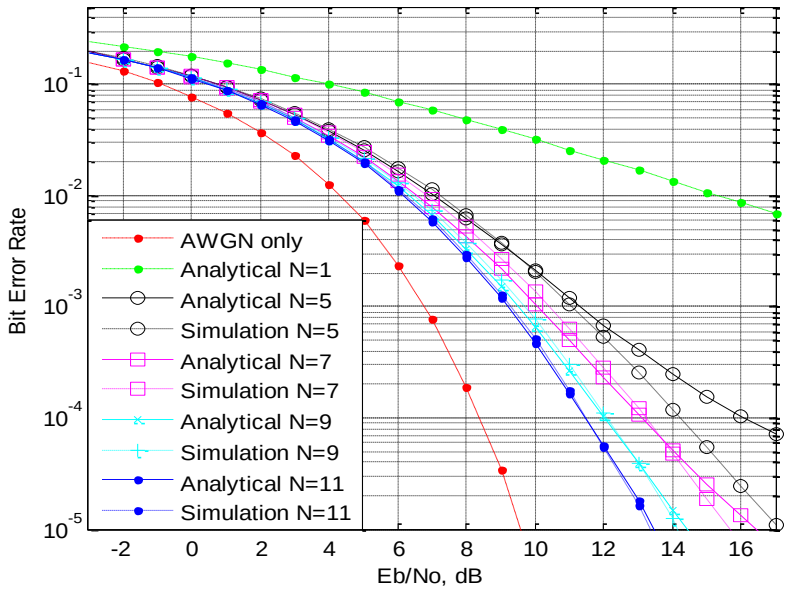

Figure 5.5 BER for phase error distributed over $\{-0.1\pi \sim 0.1\pi\}$ for different N with fading and total transmitted energy E_b/N

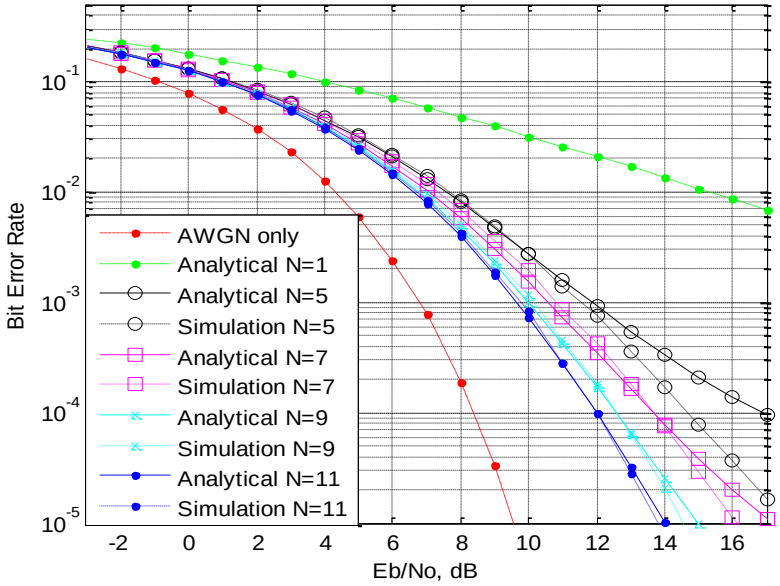

Figure 5.6 BER for phase error distributed over $\{-0.2\pi \sim 0.2\pi\}$ for different N with fading and total transmitted energy E_b/N

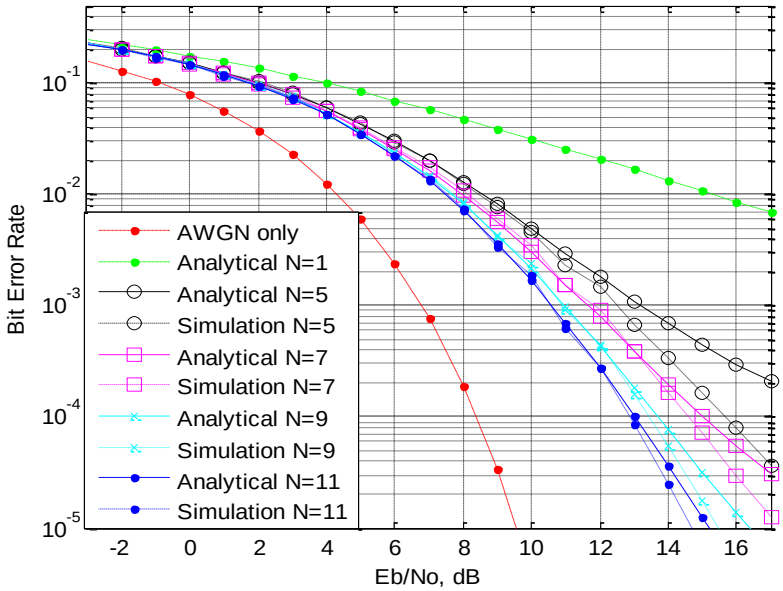

Figure 5.7 BER for phase error distributed over $\{-0.3\pi \sim 0.3\pi\}$ for different N with fading and total transmitted energy E_b/N

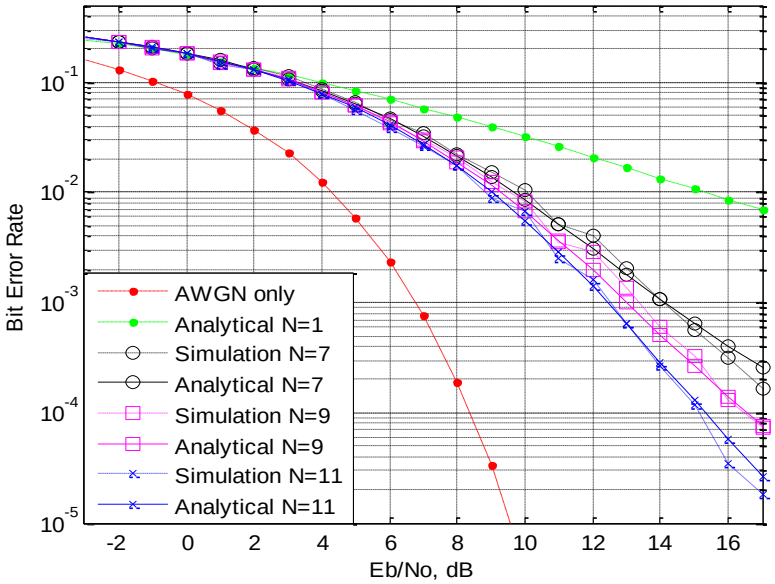

Figure 5.8 BER for phase error distributed over $\{-0.4\pi \sim 0.4\pi\}$ for different N with fading and total transmitted energy E_b/N

5.5 Collaborative communication model with imperfect frequency synchronization

In this section, a closed form of the Probability of Error or BER for a collaborative communication model with imperfect frequency synchronization and with the assumption that there is perfect time and phase synchronization between the collaborative nodes and the base station in the presence of AWGN and Rayleigh fading is presented. Let N collaborative nodes make a network to transfer the information to the base station. As each collaborative node has its own oscillator, there may be a frequency mismatch between the collaborative nodes and the base station. The system model for a collaborative communication model with imperfect frequency synchronization in the presence of AWGN and Rayleigh fading is shown in Figure 5.9.

The system model is composed of N collaborative node transmitters represented as Source (Node). Each collaborative node has a transceiver to receive signals from other collaborative nodes within the network and to transmit the signal to the base station. Each collaborative node also has a phase lock loop (PLL) for offset correction and a modulator to modulate the signal. The channel is considered as an AWGN and Rayleigh fading channel. The Rayleigh fading channel for each transmitted signal has an independent effect. On the receiver side, denoted as the base station, there is a demodulator to

demodulate the received signal. The demodulator multiplies the received signal with a cosine signal; passes it through a low pass filter (LPF) and then integrates it. Then the BER of the system is calculated.

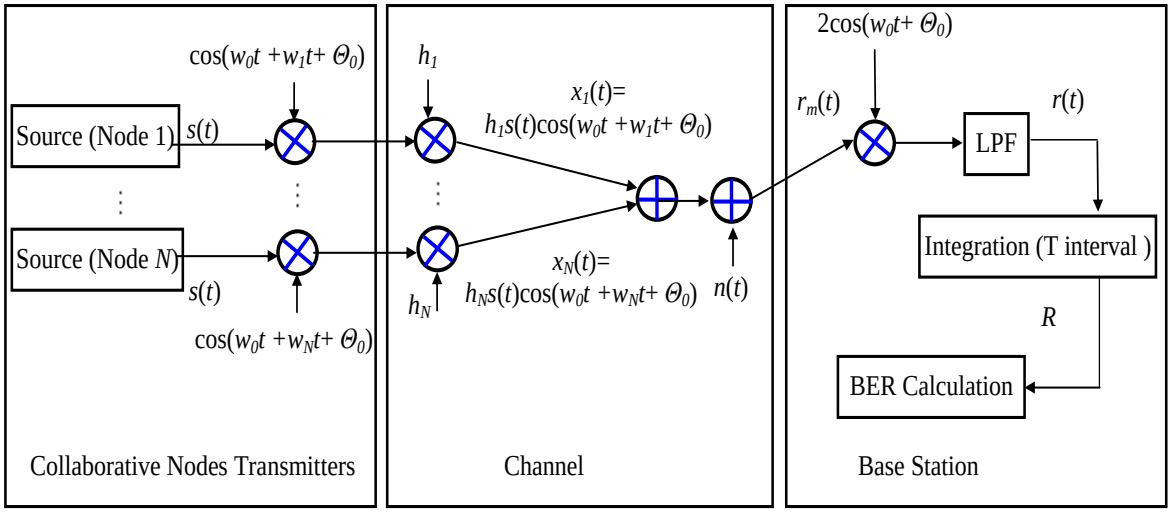

Figure 5.9 Theoretical Model of the System

5.5.1 Theoretical Model

Let $s(t)$ represent the data signal to be transmitted to the base station. The received signal at the base station ($r_m(t)$) is the sum of all the signals transmitted by sensor nodes and the noise and is given by

$$r_m(t) = \sum_{i=1}^{N} h_i s(t) \cos(w_0 + w_i t + \Theta) + n(t), \tag{5.19}$$

where $n(t)$ is zero-mean AWGN and h_i is the fading coefficient and w_i is the frequency offset. After demodulation we have

$$r(t) = \sum_{i=1}^{N} h_i s(t) \cos(w_i t) + n(t), \tag{5.20}$$

where $n(t)$ is low pass noise, then the result of the integrator is

$$R = \sum_{i=1}^{N} h_i S \frac{\sin(w_i T)}{w_i T} + n, \tag{5.21}$$

Suppose that the data is sent using BPSK. The received signal R depends upon the random variables h_i, w_i and n. The input of the decision circuit is given in equation (5.21). The probability of error in BPSK system [27] is given by

$$P_e = 0.5 erfc\left(\frac{\mu_R}{\sqrt{2\sigma_R^2}}\right). \tag{5.22}$$

We can represent R = g + n (sum of two random variables), where $g = \sum_{i=1}^{N} Sh_i \frac{\sin(w_i T)}{w_i T}$.

Due to statistical independence of the two random variables and using equation (A.1) and μ_n=0, we have

$$\mu_R = NSb\sqrt{\frac{\pi}{2}}\left[1 - \frac{(w_e T)^2}{18}\right], \tag{5.23}$$

where w_e is distribution limit of frequency error and b is the mode of Rayleigh random variable h. Using equation (A.4), the variance of R, i.e., a sum of two independent random variables, may be written as

$$\sigma_R^2 = NS^2 b^2 \left(0.429 - .048(w_e T)^2 + 0.0063(w_e T)^4\right) + \frac{N_0}{2}. \tag{5.24}$$

Let $u = 0.429 - .048(w_e T)^2 + 0.0063(w_e T)^4$. Because g is a sum of i.i.d random variables, according to the central limit theorem, its distribution tends to be Gaussian when N is sufficiently large. Then the sum of g and n is also Gaussian. If we insert (5.23) and (5.24) into (5.22), we may find the probability of error as

$$P_e = 0.5 erfc\left(\frac{NSb\sqrt{\frac{\pi}{2}}\left[1 - \frac{(w_e T)^2}{18}\right]}{\sqrt{2\left(NS^2 b^2 u + \frac{N_0}{2}\right)}}\right). \tag{5.25}$$

As S^2=E_b, Equation (5.25) can be written as

$$P_e = 0.5 erfc\left(b\sqrt{\frac{\pi}{2}}\left[1 - \frac{(w_e T)^2}{18}\right]\sqrt{\frac{N^2 (E_b / N_0)}{(2Nb^2 u(E_b / N_0) + 1)}}\right). \tag{5.26}$$

Special Case:

Now we will develop the basic idea of energy saving by using the collaborative communication. If the amplitude of each bit for each sensor node is $S = \pm(\sqrt{E_b})/N$, we have

$$P_e = 0.5erfc\left(b\sqrt{\frac{\pi}{2}}\left[1 - \frac{(w_e T)^2}{18}\right]\sqrt{\frac{E_b / N_0}{\left(\frac{2b^2 u(E_b / N_0)}{N} + 1\right)}}\right). \quad (5.27)$$

This is the case when we reduce the signal amplitude of all sensor nodes by factor N, i.e., the total transmitted energy is E_b/N. This reduction will be used to investigate the characteristics of the system with reduced power consumption for each sensor node. This case can be used to investigate the effect of total transmitted power on BER.

5.5.2 Analysis and Results

A Monte Carlo simulation using SIMULINK and MATLAB® is performed to analyze the BER of collaborative communication system with imperfect frequency synchronization in the presence of AWGN and Rayleigh fading. The wireless communication environment used in the simulation is established using SIMULINK's AWGN channel blocks.

The simulation model of a collaborative communication system with imperfect frequency synchronization is shown in Figure 5.10. For the simulation the parameters of the off-the-shelf products i.e., CC2420 [14] and AT86RF212 [15] are considered. For each value of N i.e., the number of collaborative nodes and the distribution of frequency error i.e., {-150 KHz~150 KHz}, {-250 KHz~250 KHz}, {-350 KHz~350 KHz}, {-35 KHz~35 KHz}, {-55 KHz~55 KHz} and {-65 KHz~65 KHz}, 1200 Monte Carlo simulations are run. Each collaborative node transmits the same binary pulse strain. To avoid the inter symbol interference; the considered signal rate is 15% of carrier frequency. Each collaborative node modulates the data using the carrier wave (obtained from the VCO output of the PLL). A random frequency error distributed over different distributions i.e., frequency error i.e., {-150 KHz~150 KHz}, {-250 KHz~250 KHz}, {-350 KHz~350 KHz}, {-35 KHz~35 KHz}, {-55 KHz~55 KHz} and {-65 KHz~65 KHz} is added to the carrier wave. The modulated signal is transmitted to the base station. The receiver demodulates the received signal and calculates the BER.

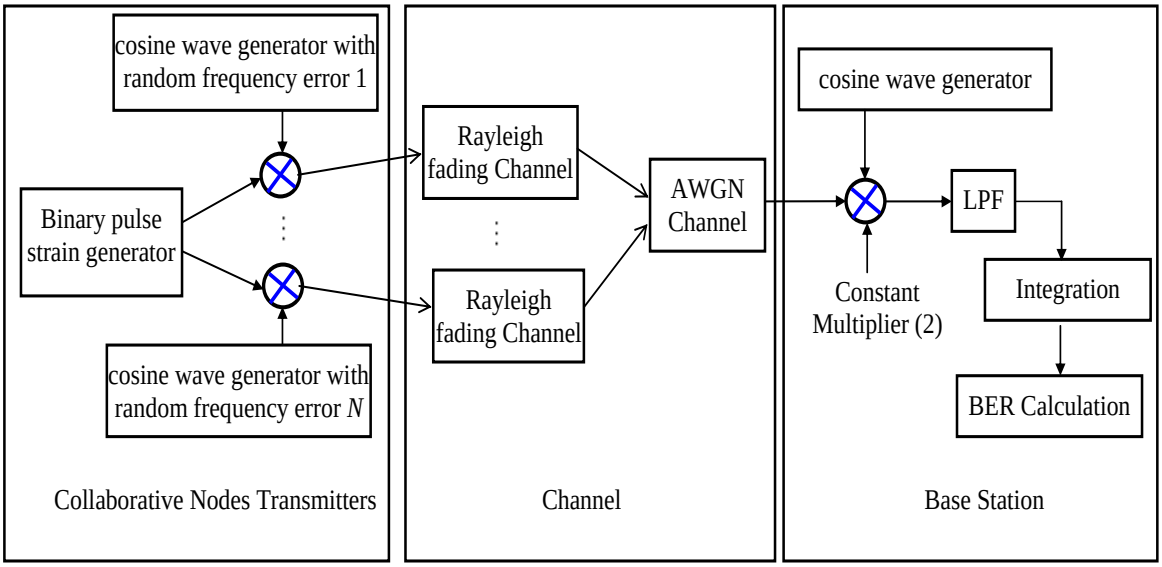

Figure 5.10 Simulation Model of Collaborative Communication with imperfect frequency synchronization

To perform BER analysis, the energy per bit of each sensor node is set to be E_b/N^2, so the total energy used by all sensor nodes is E_b/N. Figures 5.11, 5.12 and 5.13 show the analytical and simulated results for BER with frequency errors distributed over {−250 KHz ~ 250 KHz}, {−350 KHz ~ 350 KHz} and {−60 KHz ~ 60 KHz}, respectively, for CC2420 [14] and AT86RF212 [15], in the presence of AWGN and Rayleigh fading for different numbers of collaborative nodes N. It is confirmed that analytical and simulated BER curves are very close to each other for the various values of frequency error. The small differences between the analytical and the simulation results are due to the approximation used for calculating BER. It is shown that BER decreases as the number of collaborative nodes increase; this is confirmation of the fact that collaborative communication overcomes the fading effect.

From the analytical and simulation results, it is shown that in order to achieve a BER of 10^{-2} for one node (non-collaborative system) in an AWGN channel without fading, a signal to noise ratio of 4 dB is needed, while a 16 dB signal to noise ratio is required in for the fading channel. However, for N = 5 collaborative nodes, the required signal to noise ratio is 7 dB if the frequency errors are distributed over {−250 KHz ~ 250 KHz}, 8 dB if frequency errors are distributed over {−350 KHz ~ 350 KHz} for CC2420 and 8 dB if frequency errors are distributed over {−60 KHz ~ 60 KHz} for AT86RF212 in cases

where noise and fading are present in the channel. Therefore, a significant gain in signal to noise ratio can be achieved using the collaboration of nodes in the network.

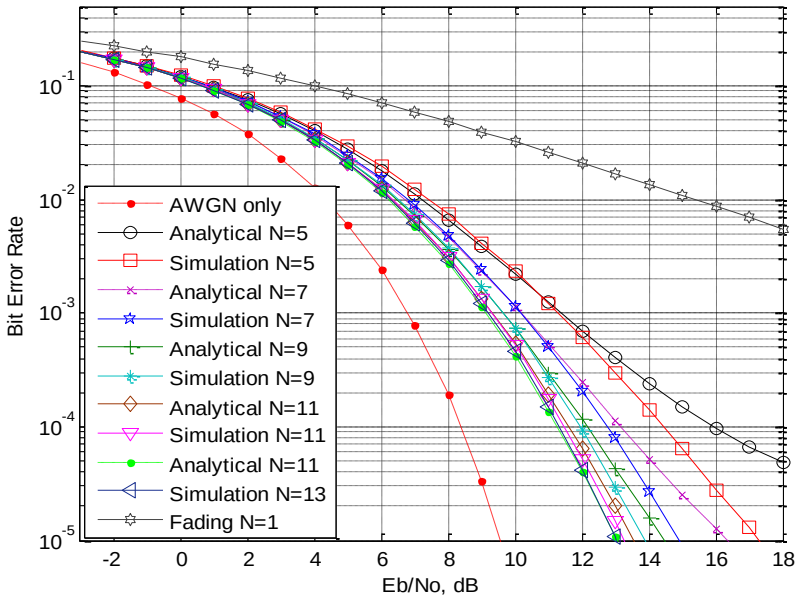

Figure 5.11 BER for CC2420 with transmitted total power E_b/N and data rate 250Kbps with fading.

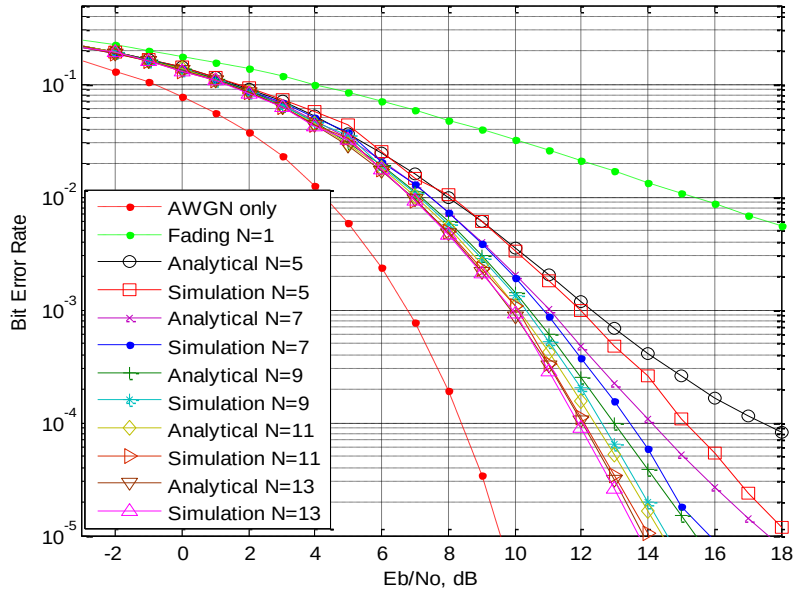

Figure 5.12 BER for CC2420 with transmitted total power E_b/N and data rate 350Kbps with fading

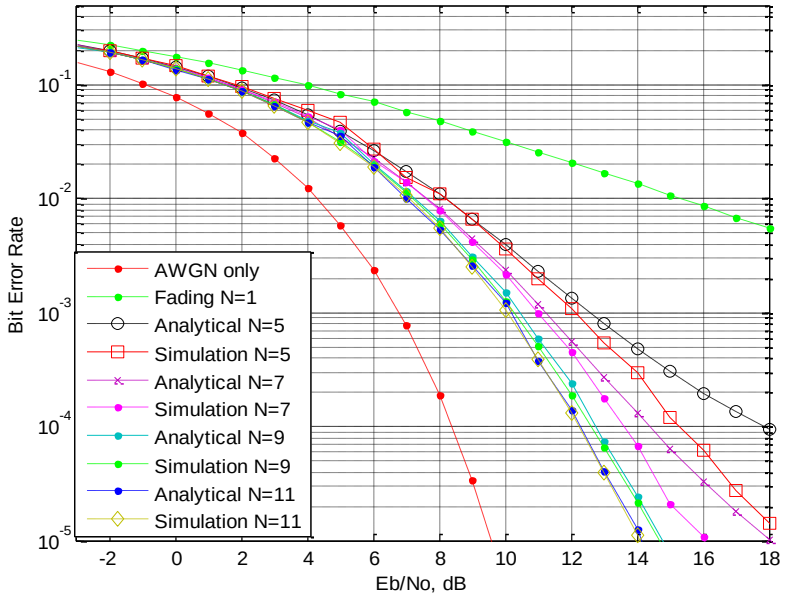

Figure 5.13 BER for AT86RF212 with total transmitted power E_b/N and data rate 40 Kbps with fading.

5.6 Collaborative communication model with imperfect phase and frequency synchronization

In sections 5.4 and 4.5 the closed form expressions of Probability of Error or BER for collaborative communication models with the assumption of imperfect frequency and perfect phase synchronization, respectively, have been presented. In a sensor network, collaborative nodes are randomly distributed and the distance between collaborative nodes and the base station cannot be estimated accurately and results in distance estimation error. The distance estimation error is translated into phase error. Moreover, each collaborative has his own oscillator; there may be frequency mismatch between the collaborative nodes and the base station, thus it is very difficult to achieve perfect phase and frequency between the collaborative nodes and the base station in a real time environment.

In this section, a closed form of probability of error or a BER for a realistic collaborative communication model with imperfect phase and frequency synchronization among the collaborative nodes and the base station, in the presence of AWGN and Rayleigh fading, is presented. Let N collaborative nodes make a network to transfer the information to the base station. The system model for the collaborative communication model with imperfect phase and frequency synchronization, in the presence of AWGN

and Rayleigh fading, is shown in Figure 5.14. It is composed of *N* collaborative node transmitters represented as Source (Node). Each collaborative node has a transceiver to receive signals from other collaborative nodes within the network and to transmit signals to the base station. Each collaborative node also has a phase lock loop (PLL) for offset correction and a modulator to modulate the signal. The channel is considered as an AWGN and a Rayleigh fading channel. The Rayleigh fading channel for each transmitted signal has an independent effect. On the receiver side, denoted as base station, there is a demodulator to demodulate the received signal. The demodulator multiplies the received signal with a cosine signal; passes it through a low pass filter (LPF) and then integrates it. Then the BER of the system is calculated.

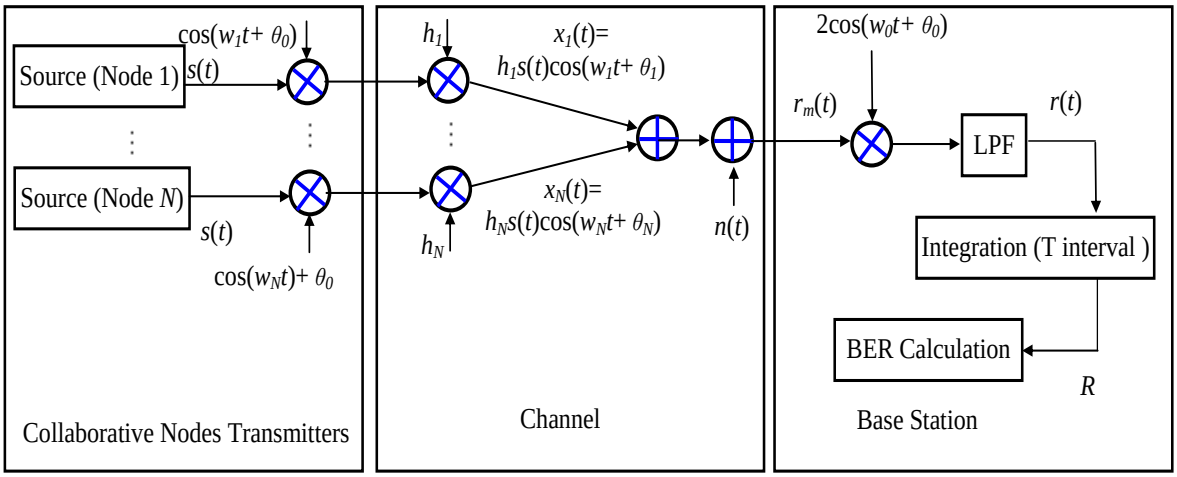

Figure 5.14 System Model

5.6.1 Theoretical Model

Let *s*(*t*) be the information data transmitted to the base station by the collaborative nodes. The distance between the nodes and the base station is estimated with certain error of estimation. Let these errors in distance estimation be called displacement errors. In this mathematical model of the network, these displacement errors will be translated into phase errors. All the collaborative nodes have their own oscillators; hence there is a carrier frequency mismatch between the signals transmitted from each collaborative node.

Let d_0 be the nominal distance between a collaborative node and the base station. Let w_0 be the node's carrier frequency. Assuming a line of sight propagation, the phase

produced due to distance d_0 can be written as $\theta_0 = w_0\, d_0/c$, where c is the speed of light. Let $d_e(i)$ is the displacement error between the i^{th} collaborative node and the base station then the phase error due to displacement error is given by $\theta_e(i) = w_0\, d_e(i)/c$.

Let $\cos(w_0 t)$ be the carrier/reference signal. We assume that the signal delay is minimal with respect to the signal bit interval T, so there is significant guard interval and thus, inter symbol interference (ISI) can be ignored. The received signal at the base station is the sum of all the signals transmitted by the collaborative nodes and the noise added in the channel. The composite received signal at the base station can be expressed as

$$r_m(t) = \sum_{i=1}^{N} h_i s(t) \cos(w_i t + \theta_i) + n(t), \tag{5.28}$$

where i=1 to N, $w_i = w_0 + \Delta w_i$, where w_0 is the carrier frequency and Δw_i is the frequency offset and $\theta_i = \theta_0 + \Delta\theta_i$, where θ_0 is the nominal phase and $\Delta\theta_i$ is phase offset, h_i is the Rayleigh fading and $n(t)$ is zero-mean AWGN.

The demodulated signal at the decision circuit is given by

$$R = \sum_{i=1}^{N} h_i S\left(\frac{\sin(\Delta w_i T + \Delta\theta_i)}{\Delta w_i T} - \frac{\sin(\Delta\theta_i)}{\Delta w_i T} \right) + n, \tag{5.29}$$

where $S = \pm\sqrt{E_b}$ is the signal amplitude and n is the noise amplitude at sampling time T. Suppose the data is sent using BPSK. Then, the demodulated signal value R depends upon independent random variables h_i, Δw_i $\Delta\theta_i$ and n as presented in equation (5.29). For BPSK the probability of error in the system is given by [27]

$$P_e = 0.5 erfc\left(\frac{\mu_R}{\sqrt{2\sigma_R^2}} \right), \tag{5.30}$$

$$\mu_R = E\left[\sum_{i=1}^{N} h_i S\left(\frac{\sin(\Delta w_i T + \Delta\theta_i)}{\Delta w_i T} - \frac{\sin(\Delta\theta_i)}{\Delta w_i T} \right) + n \right]. \tag{5.31}$$

As h_i, Δw_i, $\Delta\theta_i$ and n are independent random variables the above equation may be written as

$$\mu_R = NSE[h]E\left[\frac{\sin(\Delta wT + \Delta\theta)}{\Delta wT} - \frac{\sin(\Delta\theta)}{\Delta wT} \right] + E[n]. \tag{5.32}$$

As n is zero mean, using derived equation (A.1) and mean value of h, equation (5.32) becomes

$$\mu_R = NbS\sqrt{\frac{\pi}{2}}\left(1-\frac{(w_eT)^2}{18}\right)\left(\frac{\sin(\psi)}{\psi}\right). \tag{5.33}$$

Variance of R is calculated as

$$Var[R] = \mathrm{var}\left[\sum_{i=1}^{N} h_i S\left(\frac{\sin(\Delta w_i T+\Delta\theta_i)}{\Delta w_i T}-\frac{\sin(\Delta\theta_i)}{\Delta w_i T}\right)+n\right]. \tag{5.34}$$

$$Var[R] = NS^2\,\mathrm{var}\left[h\left(\frac{\sin(\Delta wT+\Delta\theta)}{\Delta wT}-\frac{\sin(\Delta\theta)}{\Delta wT}\right)\right]+\mathrm{var}[n]. \tag{5.35}$$

Using derived equation (A.5) and var[n]=N_0/2, the above equation becomes

$$Var[R] = NS^2b^2\left\{\left(2-\frac{\pi}{2}\right)\left(1-\frac{(w_eT)^2}{18}\right)\left(\frac{\sin(\psi)}{\psi}\right)+2X\right\}+\frac{N_0}{2}. \tag{5.36}$$

where $$X = \left[\begin{array}{l}\frac{1}{2}-\frac{(w_eT)^2}{18}+\frac{(w_eT)^4}{180}+\frac{\sin(2\psi)}{4\psi}-\frac{(w_eT)^2\sin(2\psi)}{36\psi}+\frac{(w_eT)^4\sin(2\psi)}{720\psi}- \\ \frac{\sin^2(\psi)}{\psi^2}-\frac{(w_eT)^4\sin^2(\psi)}{324\psi^2}+\frac{(w_eT)^2\sin^2(\psi)}{9\psi^2}\end{array}\right]. \tag{5.37}$$

Because R is a sum of i.i.d random variables, according to the central limit theorem, its distribution tends to be Gaussian when N is sufficiently large. Inserting equations (5.33) and (5.36) into equation (5.30), we may have

$$P_e = 0.5erfc\left(\frac{NbS\sqrt{\frac{\pi}{2}}\left[1-\frac{(w_eT)^2}{18}\right]\left[\frac{\sin(\psi)}{\psi}\right]}{\sqrt{2\left(NS^2b^2\left\{\left(2-\frac{\pi}{2}\right)\left(1-\frac{(w_eT)^2}{18}\right)\left(\frac{\sin(\psi)}{\psi}\right)+2X\right\}+\frac{N_0}{2}\right)}}\right). \tag{5.38}$$

As $S^2=E_b$, equation (5.38) can be written as

$$P_e = 0.5 erfc\left(b\sqrt{\frac{\pi}{2}}\left[1-\frac{(w_e T)^2}{18}\right]\left[\frac{\sin(\psi)}{\psi}\right]\sqrt{\frac{N^2(E_b/N_0)}{2Nb^2\left\{\left(2-\frac{\pi}{2}\right)\left(1-\frac{(w_e T)^2}{18}\right)\left(\frac{\sin(\psi)}{\psi}\right)+2X\right\}(E_b/N_0)+1}}\right) \quad (5.39)$$

5.6.2 Analysis and Results

The Monte Carlo simulation using SIMULINK and MATLAB® is performed to analyze the probability of error or the BER of the collaborative communication system with imperfect phase synchronization in the presence of AWGN and Rayleigh fading. The wireless communication environment used in the simulation is established using SIMULINK's AWGN channel blocks. The simulation model of the collaborative communication system with imperfect phase and frequency synchronization is shown in Figure 5.15.

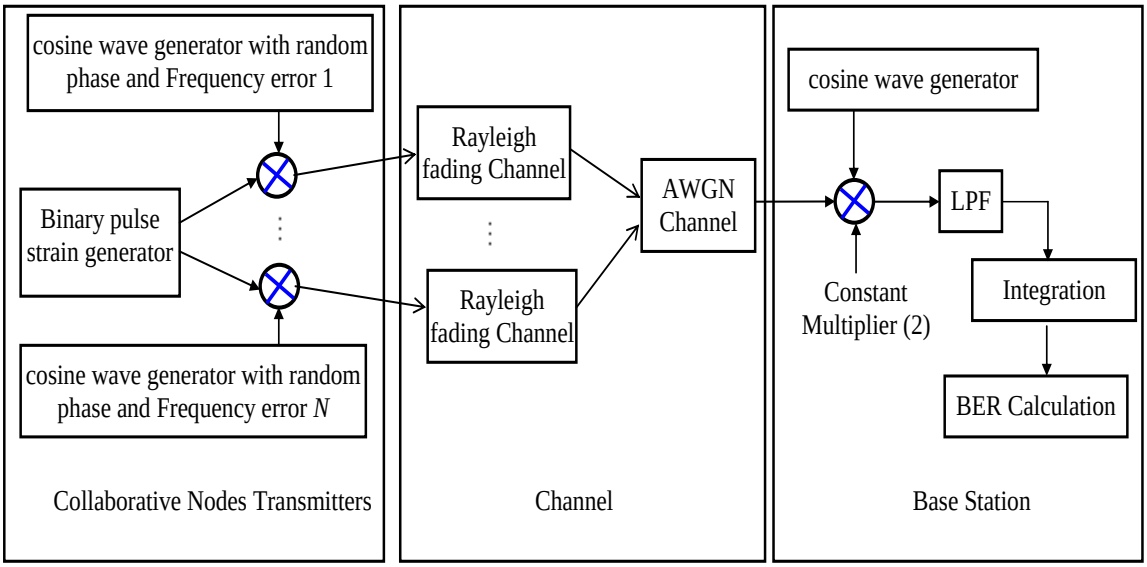

Figure 5.15 Simulation Model of the Collaborative Communication with imperfect phase and frequency synchronization

For simulation, the parameters of the off-the-shelf products i.e., CC2420 [14] and AT86RF212 [15] are considered. For each value of N i.e., the number of collaborative nodes, distribution of phase error i.e., {-0.1π~0.1π}, {-0.2π~0.2π}, {-0.3π~0.3π} and {-

0.4π~0.4π} and distribution of frequency error i.e., {-150 KHz~150 KHz}, {-250 KHz~250 KHz}, {-350 KHz~350 KHz}, {-35 KHz~35 KHz}, {-55 KHz~55 KHz} and {-65 KHz~65 KHz}, 1200 Monte Carlo simulations are run. Each collaborative node transmits the same binary pulse strain. To avoid inter symbol interference; the considered signal rate is 15% of carrier frequency. Each collaborative node modulates the data using the carrier wave (obtained from the VCO output of the PLL). A random phase error distributed over different distributions i.e., {-0.1π~0.1π}, {-0.2π~0.2π}, {-0.3π~0.3π} and {-0.4π~0.4π} is added to the carrier wave. A random frequency error distributed over different distributions i.e., frequency error i.e., {-150 KHz~150 KHz}, {-250 KHz~250 KHz}, {-350 KHz~350 KHz}, {-35 KHz~35 KHz}, {-55 KHz~55 KHz} and {-65 KHz~65 KHz} is also added to the carrier wave. The modulated signal is transmitted to the base station. The receiver demodulates the received signal and calculates the BER.

To perform BER analysis, the energy per bit of each collaborative node is set to be E_b/N^2, so that the total energy used by all collaborative nodes is E_b/N. Figures 5.16, 5.17 and 5.18 show analytical and simulated results for BER by considering the parameters of CC2420 i.e., frequency error distributed over {-200 KHz ~200 KHz} and with phase errors distributed over {-0.1π~0.1π}, {-0.2π~0.2π} and {-0.3π~0.3π}, respectively, in the presence of AWGN and Rayleigh fading for different number of collaborative nodes N. Figures 5.19, 5.20 and 5.21 show the analytical and simulated results for BER by considering the parameters of AT86RF21 i.e., frequency error distributed over {-55 KHz ~55 KHz} and with phase errors distributed over {-0.1π~0.1π}, {-0.2π~0.2π} and {-0.3π~0.3π}.

It is confirmed that the analytical and simulated BER curves are very close to each other for the various phase errors. The small difference between analytical and the simulated results is due to the Gaussian approximation used for calculating BER. It is shown that the BER decreases as the number of collaborative nodes increase; this is the confirmation of the fact that collaborative communication overcomes the fading effect.

From the analytical and simulated results, it is shown that, in order to achieve a BER of 10^{-3} for one sensor node (non-collaborative system) in an AWGN channel without fading, the required signal to noise ratio is 7dB, while a 24dB signal to noise ratio is required for the fading channel. However, by considering the parameters of CC2420 i.e., for frequency error distributed over {-200 KHz ~200 KHz} and N=7 (collaborative nodes), the required signal to noise ratio is 11dB if the phase errors are distributed over {-0.1π~0.1π}, 13dB if phase errors are distributed over {-0.2π~0.2π} and 14dB if phase

errors are distributed over {-0.3π~0.3π} for cases where noise and fading are present in the channel. Therefore, for product CC2420, a significant gain in the signal to noise ratio can be achieved using collaboration of nodes in the network.

By considering the parameters of AT86RF21 i.e., for frequency error distributed over {-55 KHz ~55 KHz} and N=7 (collaborative nodes), the required signal to noise ratio is 10.5dB if the phase errors are distributed over {-0.1π~0.1π}, 12dB if phase errors are distributed over {-0.2π~0.2π}, and 13dB if phase errors are distributed over {-0.3π~0.3π} for cases where noise and fading are present in the channel. Therefore, for product AT86RF21, a significant gain in signal to noise ratio can be achieved using the collaboration of nodes in the network.

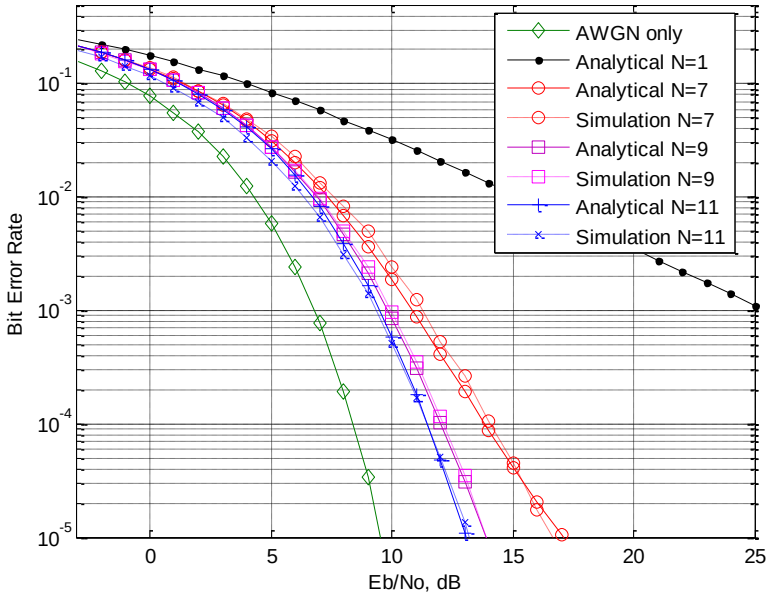

Figure 5.16 BER by considering the parameters of CC2420 i.e., frequency error distributed over {-200 KHz ~200 KHz} and data rate 250 Kbps, with phase error distributed over {-0.1π~0.1π} for different N with fading and total transmitted energy E_b/N

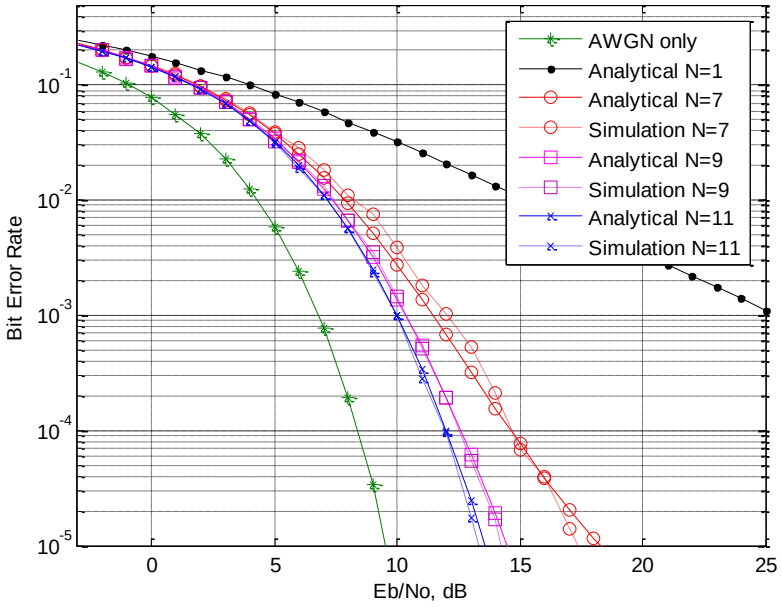

Figure 5.17 BER by considering the parameters of CC2420 i.e., frequency error distributed over {-200 KHz ~200 KHz} and data rate 250 Kbps, with phase error distributed over {-0.2π~0.2π} for different N with fading and total transmitted energy E_b/N

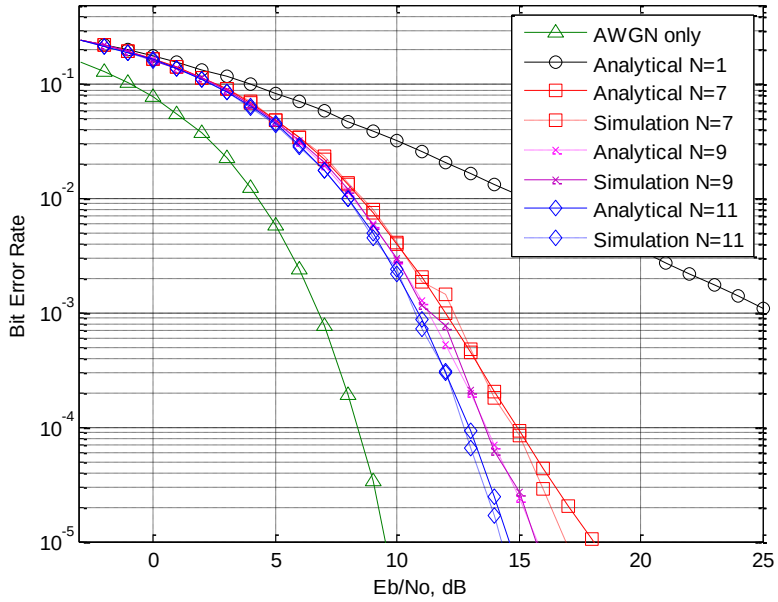

Figure 5.18 BER by considering the parameters of CC2420 i.e., frequency error distributed over {-200 KHz ~200 KHz} and data rate 250 Kbps, with phase error distributed over {-0.3π~0.3π} for different N with fading and total transmitted energy E_b/N

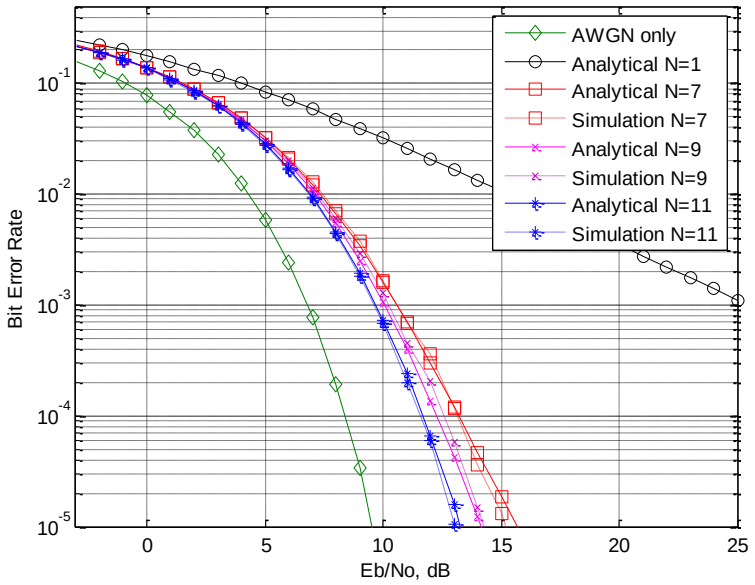

Figure 5.19 BER by considering the parameters of AT86RF21 i.e., frequency error distributed over {-55 KHz ~55 KHz} and data rate 40 Kbps, with phase error distributed over $\{-0.1\pi \sim 0.1\pi\}$ for different N with fading and total transmitted energy E_b/N

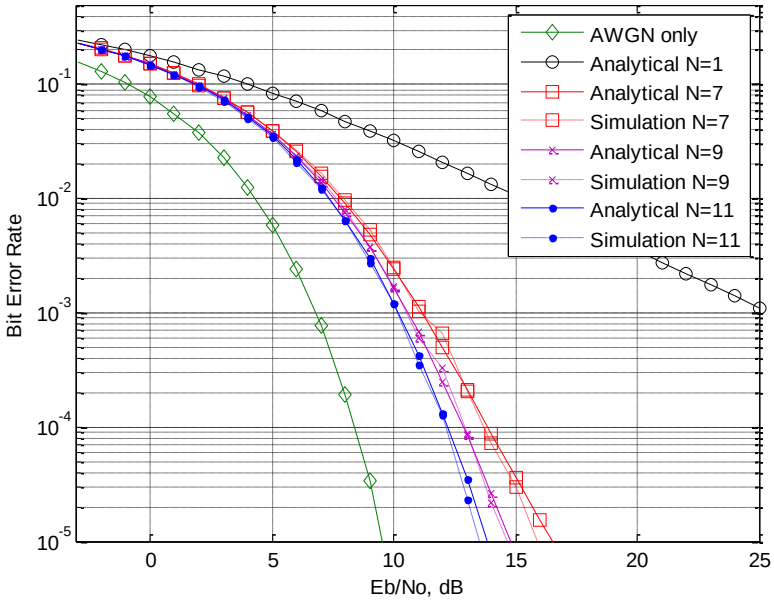

Figure 5.20 BER by considering the parameters of AT86RF21 i.e., frequency error distributed over {-55 KHz ~55 KHz} and data rate 40 Kbps, with phase error distributed over $\{-0.2\pi \sim 0.2\pi\}$ for different N with fading and total transmitted energy E_b/N

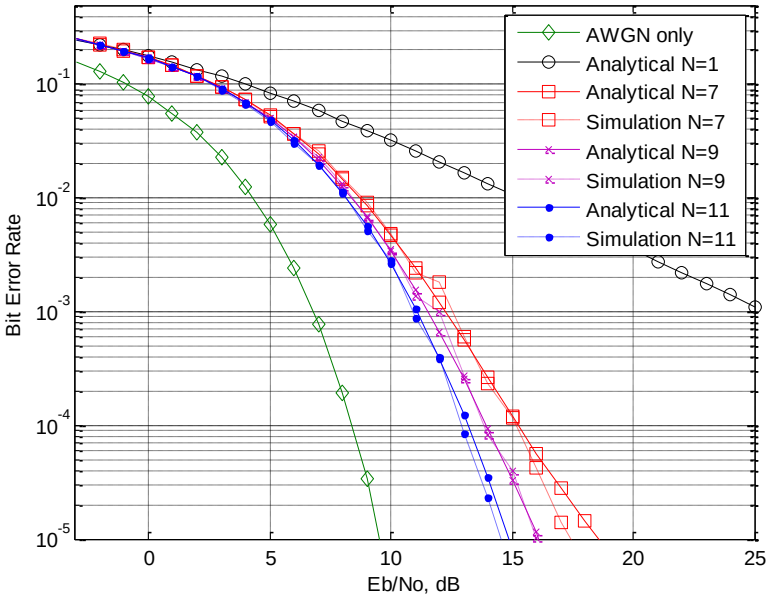

Figure 5.21 BER by considering the parameters of AT86RF21 i.e., frequency error distributed over {-55 KHz ~55 KHz} and data rate 40 Kbps, with phase error distributed over {-0.3π~0.3π} for different N with fading and total transmitted energy E_b/N

5.7 Chapter Conclusions

In this chapter the data acceptance performance of three collaborative communication systems are investigated i.e., collaborative communication with imperfect phase synchronization only, collaborative communication with imperfect frequency synchronization only and collaborative communication with imperfect phase and frequency synchronization, in the presence of flat Rayleigh fading and AWGN. This research contributes to the development of the average BER expressions for these three systems, expressed as a function of signal to noise ratio for the number of collaborative nodes as the parameter. The obtained BER expressions clearly present the fading-mitigation capability of collaborative communication systems that is a consequence of the collaborative communication and can be considered as a space diversity system.

The considered collaborative communication systems perform binary data communication, using BPSK. The derived expressions show that the system BER is a function of the number of collaborative nodes, with parameters related to the distribution of phase error and frequency error. The derived BER expressions are verified by simulations using MATLAB®. Numerical results confirm that collaborative communication systems sufficiently mitigate the flat Rayleigh fading, in comparison to a single user system.

The system bit error performance is degraded in the presence of phase error and frequency error; however, when the number of collaborative nodes is considerably increased, the degradation of bit error performance caused by phase and frequency error is substantially reduced.

With the derived BER expressions of collaborative communication systems and the effectiveness of collaborative communication on reducing the flat Rayleigh fading can be quantified. From the BER curves, it is evident that the fade margin needed to achieve a given BER value is significantly reduced when collaborative communication is exploited.

This significant reduction of fade margin suggests substantial transmitted power savings in wireless communication by using collaborative communication. As the number of collaborative nodes increases, the circuit power consumption of nodes becomes considerable and reduces the overall power efficiency of the network. Because of that in the next chapter, energy consumption and energy efficiency models are also proposed and investigated to find out the trade-offs between the required node circuit power and achieved power gain using collaborative communication.

References

[1] A. K. Sadek, W. Su, and K.J. Liu, "Multinode cooperative communications in wireless networks," IEEE Trans. Signal Process. vol. 55, no.1, Jan. 2007, pp. 341-355.

[2] A. S. Ibrahim, H. Zhu, and K.J. Liu, "Distributed energy-efficient cooperative routing in wireless networks," IEEE Trans. on Wireless Commun., vol.7, no.10, Oct 2008, pp. 3930-3941.

[3] L. Simic, S.M. Berber, and K.W. Sowerby, "Partner choice and power allocation for energy efficient cooperation in wireless sensor networks," in Proc. IEEE ICC'09, May 2008, pp. 4255-4260.

[4] R. Mudumbai, G. Barriac, and U. Madhow, "On the feasibility of distributed beamforming in wireless networks," IEEE Trans. Wireless Commun., vol. 6, no. 5, May 2007, pp. 1754-1763.

[5] H. Ochiai, P. Mitran, H. Poor, and V. Tarokh, "Collaborative beamforming for distributed wireless ad hoc sensor networks," IEEE Trans. Signal Process., vol. 53, no. 1053-587X, Nov. 2005, pp. 4110–4124.

[6] L. Xiao and M. Xiao, "A new energy-efficient MIMO-sensor network architecture M-SENMA," in Proc. VTC'04, vol. 4, Sept. 2004, pp. 2941- 2945.

[7] G. J. Miao, "Multiple-input multiple-output wireless sensor networks communications," US Patent 7091854, August 15, 2006.

[8] S. Cui, A. J. Goldsmith, and A. Bahai, "Energy-efficiency of MIMO and cooperative MIMO techniques in sensor networks," IEEE J. Sel. Areas Commun., vol.22, no.6, 2004, pp.1089-1098.

[9] S. Tachikawa, "An effect on chip interleaving and hard limiter against burst noise in direct sequence spread spectrum communication systems," IEICE Trans. on Fundamentals of Electronics, Communi. and Computer Science, vol.E78-A, no.2, Feb. 1995, pp. 272-277.

[10] X. Zhan, and S.M. Berber, "Development of a reverse chaos based CDMA link and fading mitigation," in Proc. IEEE ISITA'08, 2008.

[11] Y. Kimura, K. Shibata, and T. Sakai, "Precoder for chip-interleaved CDMA using space-time block-coding," IEICE Trans. Fundam. Electron. Commun. Comput. Sci., vol.E91-A, no.10, 2008, pp.2885-2888.

[12] Y. Lin and D. W. Lin, "Multicode chip-interleaved DS-CDMA to effect synchronous correlation of spreading codes in quasi-synchronous transmission over multipath channels," IEEE Transactions on Wireless Commun, vol. 5, no.10, 2006, pp. 2638-2642.

[13] Y. Na, M. Saquib, and Moe Z. Win, "Pilot-aided chip-interleaved DS-CDMA transmission over time-varying channels," IEEE J. Sel. Areas Commun., vol. 24, no.1, 2006, pp. 151-160.

[14] CC2420, Texas Instruments Chipcon Products, http://focus.ti.com/analog/docs/enggresdetail.tsp?familyId=367&genContentId=3573.

[15] AT86RF212, ATMEL Products, http://www.atmel.com/dyn/products/product_card.asp? PN=AT86RF212.

[16] P. Duangkird, S. Kraisingsomnuek, C. Kotchasarn, "BER of Alamouti STC with Multiple Relays Using Amplify and Forward Cooperative Diversity over Rayleigh Fading Channel," Second International Conference on Intelligent Systems, Modelling and Simulation (ISMS), 2011, pp. 324 – 328.

[17] W. Su, A. K. Sadek, and R. J. K. Liu, "SER performance analysis and optimum power allocation for decode-and-forward cooperation protocol in wireless networks," IEEE Wireless Computer Network and Communications, vol. 2, March 2005, pp. 984-989.

[18] A. K. Sadek, W. Su, and R. J. K. Liu, "Performance analysis for multimode decode-and-forward relaying in cooperative wireless networks," IEEE ICASSP, vol. 3, March 2005, pp. 521-524.

[19] S. Atapattu and N. Rajatheva, “Exact SER of Alamouti code transmission through amplify-and-forward cooperative relay over Nakagami-m fading channels,” IEEE ISCIT, October 2007, pp. 1429- 1433.
[20] Y. Lee and M. Tsai, “Performance of decode-and-forward cooperative communications over Nakagami-m fading channels,” IEEE Trans. Vehicular Technology, vol. 58, no. 3, March 2009, pp. 1218-1228.
[21] M.R. Islam and Jinsang Kim, “Capacity and BER analysis for Nakagami-n channel in LDPC coded wireless sensor network,” International Conference on Intelligent Sensors, Sensor Networks and Information Processing (ISSNIP 2008), 2008, pp. 167 – 172.
[22] U. Datta, C. Kundu, S. Kundu, “BER and energy level performance of layered CDMA wireless sensor network in presence of correlated interferers,” Fifth IEEE Conference on Wireless Communication and Sensor Networks (WCSN), 2009, pp. 1-6.
[23] U. Datta, P.K. Sahu, S. Kundu, “Performance of layered CDMA wireless sensor networks with space diversity in presence of correlated interferers,” IEEE 4th International Symposium on Advanced Networks and Telecommunication Systems (ANTS), 2010, pp. 91-93.
[24] S. Fang; S.M. Berber, A.K. Swain, “Closed-form average BER expression for chip-interleaved DS-CDMA system conducting M-ary communication and noncoherent demodulation in flat Rayleigh fading channel,” 15th Asia-Pacific Conference on Communications, 2009, pp. 144 – 147.
[25] C. M. Lo and W. H. Lam, "Error probability of binary phase shift keying in Nakagami-m fading channel with phase noise," Electronics Letters, vol. 36, no.21, 2000, 1773-1774.
[26] I. Al Falujah and V.K. Prabhu, "Performance anaylsis of PSK systems in the presence of slow fading, imperfect carrier phase recovery, and AWGN," IEE Proc. Commun. vol.152, no.6, 2005, pp.903-911.
[27] A. Goldsmith, Wireless communications, Cambridge University Press, 2005, pp. 31-42.
[28] D.E. Blumenfeld, Operations Research Calculations; Crc Press, N.W. Corporate Blvd., Boca Raton, Florida, 2000.

Chapter 6 The Energy Efficiency of the Collaborative Communication System

6.1 Introduction

The study in Chapter 5 has shown that collaborative communication significantly brings down the signal-to-noise ratio for a given value of the bit error rate (BER) in the flat Rayleigh fading channel. This promises a large reduction in transmitted power in sensor networks. As the number of collaborative nodes increases, the circuit power consumption of nodes becomes considerable and reduces the overall power efficiency of the network. Therefore, there is one question that was left unanswered in Chapter 5 and that is: How much power can be saved by utilizing collaborative communication at the expense of circuit power? This chapter hereby investigates the energy savings of Wireless Sensor Networks (WSNs) that employ collaborative communication as an alternative physical layer algorithm for sensor nodes to transmit data in the fading channel. To the author's best knowledge, this is the first study to investigate energy savings by using collaborative communication for the energy conservation of WSNs.

In this chapter, energy consumption models are developed for a single input single output (SISO) system and a collaborative communication system, as a function of the total received power, required circuit power and transmission distance. The comparison between an SISO system and a collaborative communication system is used to calculate the energy efficiency in wireless sensor network, as a function of the number of collaborative nodes, total received power, required circuit power and transmission distance. When the energy consumption of SISO system is equal to the energy consumption of collaborative communication system at certain distance, the energy saving is 0% and this distance is called the *break-even distance*. The *break-even distance* for a variety of collaborative communication systems is also calculated for the transceivers which are in compliance with IEEE 802.15.4 [1], which has a strong industrial background.

Of particular interest to this study is the achievement of the following:

- The development of closed form expressions for the energy consumption models for SISO and collaborative communication systems;

- The development of an energy efficiency model for a collaborative communication system in comparison with SISO systems.
- An investigation of the effect of phase and frequency errors on energy efficiency for collaborative communication systems in wireless sensor networks;
- The establishment of a WSN simulator to confirm the theoretical model and assess energy efficiency of collaborative communication with imperfect phase and frequency synchronization in presence of AWGN and Rayleigh fading using the parameters of off-the-shelf products i.e. CC2420 [2] and AT86RF212 [3];

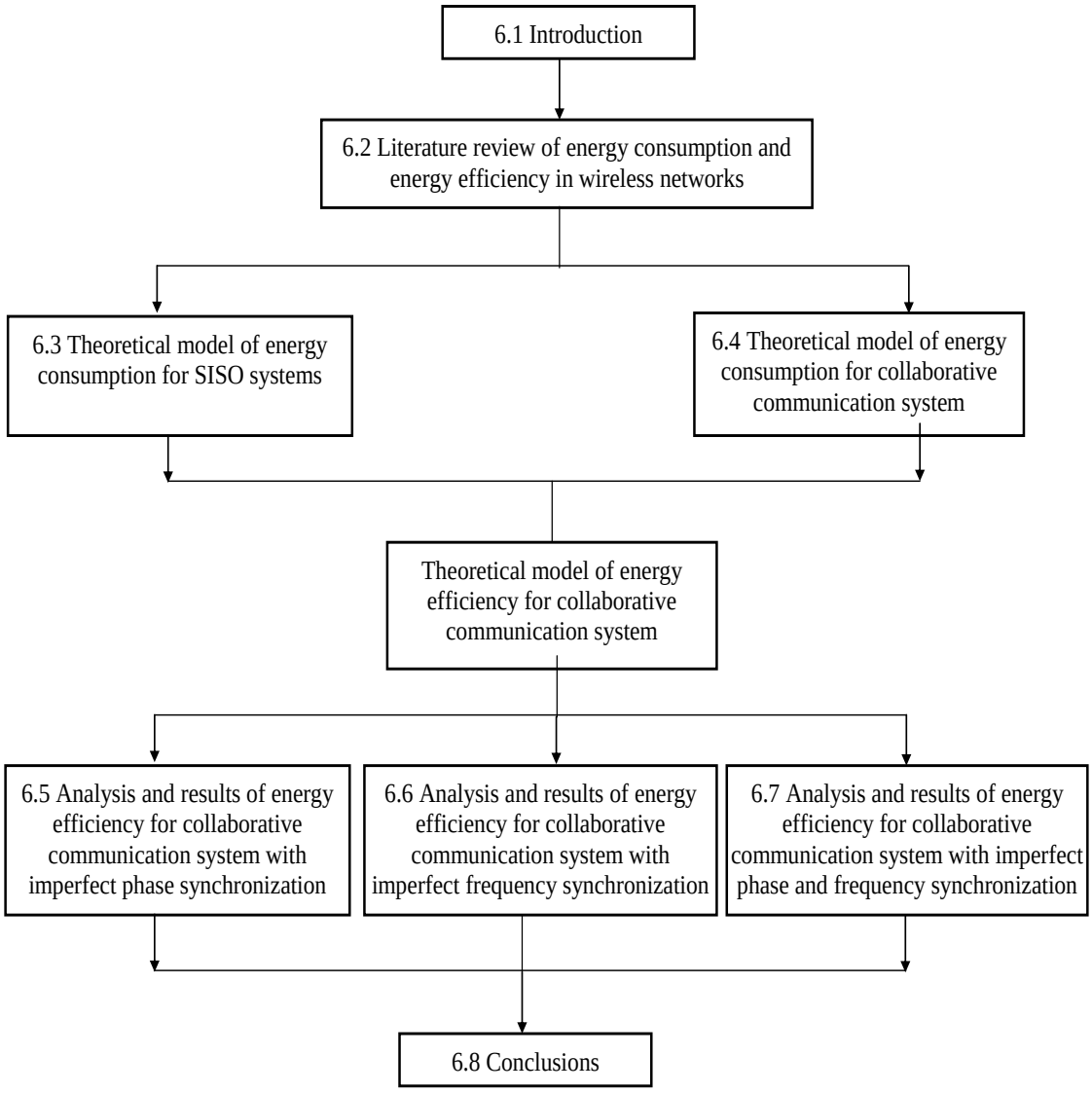

Figure 6.1 Route map of study in Chapter 6

Figure 6.1 demonstrates the route map of this chapter. The study in this chapter unfolds in the following sequence. In Section 6.2, an extensive literature review of energy

consumption models for communication systems is presented. Section 6.3 presents the development of an energy consumption model for an SISO system. A closed form expression of SISO energy consumption is derived. The power required for data transmission in a Rayleigh fading channel is calculated by a simplified path loss model (log-Distance path loss) [4]. In section 6.4, an energy consumption model of a collaborative communication system is developed; this relates to the fade margin obtained in Chapter 5 in order to compute the node transmit power. A closed form expression of collaborative communication energy consumption is derived. With this model, the energy saving is calculated for nodes that use collaborative communication rather than SISO transceivers to conduct the node-to-node communication in the Rayleigh fading channel. Sections 6.5, 6.6 and 6.7 presents the numerical results of the energy savings of the SISO system and the different collaborative communication systems presented in Chapters 4 and 5. To obtain these results, the parameters take values from off-the-shelf transceivers which are compliant with IEEE 802.15.4.

Via simulation, collaborative communication systems for wireless sensor networks are formed: this is based on the collaborative communication method explained in Chapter 4. The numerical results confirm that the collaborative communication technique can significantly reduce the energy consumption of a node, although the value of the energy saving is dependent on a few parameters; including transmission distance, the path loss exponent, and the transceiver circuit power. Section 6.5 presents the numerical results of the energy savings of the SISO system and the collaborative communication system with imperfect phase synchronization and with the assumption of perfect frequency synchronization that includes the influence of noise and Rayleigh fading. The *break-even distance* for a collaborative communication system with imperfect phase synchronization is calculated for different number of collaborative nodes. Section 6.6 presents the numerical results of the energy saving of the SISO system and the collaborative communication system with imperfect frequency synchronization and with the assumption of perfect phase synchronization that includes the influence of noise and Rayleigh fading. The *break-even distance* for a collaborative communication system with imperfect frequency synchronization is calculated for different number of collaborative nodes. Section 6.7 presents the numerical results of the energy savings of the SISO system and the collaborative communication system with imperfect phase and frequency synchronization that includes the influence of noise and Rayleigh fading. The *break-even distance* for the collaborative communication system with imperfect phase and frequency

synchronization is calculated for different number of collaborative nodes. In Section 6.8 the findings of this chapter are concluded.

In summary, the contribution of this chapter is three-fold:

7. The development of closed form expressions of energy consumption models for SISO systems and collaborative communication models and expressed as a function of the total received power, required circuit power and transmission distance;
8. The development of closed form expressions of energy efficiency of collaborative communication and expressed as a function of number of collaborative nodes, the total received power, required circuit power and transmission distance;
9. Simulation-based investigations to confirm that the proposed collaborative communication system produce a high power gain and significantly save a node's energy expenditure with imperfect phase and frequency synchronization in the presence of AWGN and Fading.

6.2 Literature Review

IEEE 802.15.4 standardizes the physical (PHY) layer and Medium Access Control (MAC) layer to interconnect low-power short-range radio frequency data communication devices [1]. The PHY layer specification stipulates a range of transmitting techniques. In [5]-[9] different energy efficient techniques for the single input single output (SISO) systems are proposed to investigate the optimized system parameters. High power gain can be achieved using multi input and multi output (MIMO) systems, however, due to complex circuit in MIMO more operational (circuit) power is required. In [10] the energy consumption model for MIMO system is presented and compared with the SISO system by consideration of the same system parameters. It is shown in [10] that, for a short range system, the SISO system is more efficient than the MIMO system. But for large range system, the MIMO system is more energy efficient. The energy efficiency of major cooperative diversity techniques, such as, the Virtual multi input single output (MISO) and decode-and-forward, is investigated in [11]. It is shown in [11] that the decode-and-forward technique is more energy efficient than the virtual MISO. The selection of optimal partner choice and power allocation for energy efficient cooperative communication in wireless sensor networks is presented and analyzed in [12]. The method presented in [12] is further extended in [13] to find efficient partner choice

heuristics in a distributed manner for sensor nodes based on either, global, or local knowledge of the average path loss values in a network for cooperative communication. In [14-16] WSNs are developed based on DS-CDMA (Direct Sequence Code Division Multiple Access) techniques which permit multiple sensor nodes to transmit concurrently at the expense of multiple access interference (MAI). To overcome MAI, several methods are reported in [17-19] for CDMA-based WSNs by setting time-division or frequency-division multiple accesses upon CDMA-based channel access. Studies reported in [4-19] neither consider the Rayleigh fading channel, nor investigate the node energy consumption in the fading channel.

6.3 Energy Consumption Model for SISO Systems

For the SISO communication the total power consumption is the sum of total power consumed by transmitter (P_{tx}) and receiver (P_{rx}). Energy consumed by single bit is given by

$$E_{SISO} = (P_{tx} + P_{rx}) / R_s . \tag{6.1}$$

where *Rs* is the data rate.

In [20] it is shown that for Rayleigh fading channel the power required for data transmission can be calculated by simplified path loss model (log-Distance path loss) [11]. This path loss model has a concise format and captures the essence of signal propagation [11]. By considering the transmitter G_t and receiver G_r antenna gains are equal to 1, P_{tx} is give by [11]

$$P_{tx} = P_{cir} + \frac{(4\pi)^2 P_r d^{\alpha}}{d_r{}^{\alpha-2} \lambda^2}, \tag{6.2}$$

where P_{cir} is the power consumed by transmitter circuit, P_r is the received signal power, α is the path loss exponent, $\lambda=2\pi\ c/w_0$, c is speed of light, w_0 is the carrier frequency, d is the distance between transmitter and receiver and d_r is the reference distance for far-field region.

Minimum received power required to achieve desired BER P_r is given by

$$P_r = P_s \times r_{eber} , \tag{6.3}$$

where P_s is the receiver sensitivity (in Watt) required to achieve desired BER for the system with AWGN only and r_{eber} is the E_b/N_o to achieve the required BER for the system with Raleigh fading and AWGN. The r_{eber} can be calculated as [10]

$$r_{eber} = \frac{\left((1-2P_e)^2\right)/\left(1-(1-2P_e)^2\right)}{\left(erfc^{-1}(2P_e)\right)^2}. \tag{6.4}$$

where $erfc^{-1}$ is the inverse function of the complimentary error function $erfc(x) = \frac{2}{\sqrt{\pi}} \int_x^{+\infty} e^{-t^2} dt$.

Using equations (6.1), (6.2) and (6.3), the total energy consumed by SISO can be written as

$$E_{SISO} = \left(P_{cir} + \frac{(4\pi)^2 P_s r_{eber} d^{\alpha}}{dr^{\alpha-2} \lambda^2} + P_{rx} \right) / R_s. \tag{6.5}$$

6.4 Collaborative Communication Energy Consumption Model

For the collaborative models presented in chapters 4 and 5, the total energy consumption is the sum of energy consumed by sensor network for local communication E_{local} and energy consumed for transmission with base station E_{long} and is given by

$$E_{COLAB} = E_{local} + E_{long}, \tag{6.6}$$

The channels within sensor network for local communication and between network and base station are considered to be Rayleigh Fading channels. The energy consumed for local communication within the sensor network is given by

$$E_{local} = \left(P_{tx\_local} + NP_{rx\_local}\right) / R_s, \tag{6.7}$$

where N is number of collaborative nodes in the sensor network and P_{tx_local} can be calculated as using equation (6.2).

The energy consumed for communication between the sensor network and base station is given by

$$E_{long} = \left(P_{tx\_long} + P_{rx}\right) / R_s, \tag{6.8}$$

where P_{tx_long} is the total energy used by all (N) collaborative nodes and is given by

$$P_{tx\_long} = NP_{cir} + \frac{(4\pi)^2 P_{r\_long} d^{\alpha}}{N d_r^{\alpha-2} \lambda^2}. \quad (6.9)$$

Minimum received power required to achieve desired BER P_{r_long} is given by

$$P_{r\_long} = P_s \times r_{col\_ber}, \quad (6.10)$$

where r_{col_ber} is the ratio between E_b/N_o for the system with phase error, Raleigh fading and AWGN and E_b/N_o for the system with AWGN only to achieve the required BER.

The r_{col_ber} can be calculated as [10]

$$r_{col\_ber} = \frac{BER^{-1}(P_e, N)}{\left(erfc^{-1}(2P_e)\right)^2}, \quad (6.11)$$

The $BER^{-1}(.)$ given in equation (6.11) is the inverse function of BER for collaborative communication systems presented in Chapter 5.

Using equations (6.6), (6.7), (6.8), (6.9) and (6.10) the total energy consumed by collaborative communication can be written as

$$Ecolab = \left(P_{cir} + \frac{(4\pi)^2 P_s r_{eber\_local} d\_local^{\alpha}}{d\_local_0^{\alpha-2} \lambda^2} + NP_{rx} + NP_{cir} + \frac{(4\pi)^2 P_{r\_long} d^{\alpha}}{N d_r^{\alpha-2} \lambda^2} + P_{rx} \right) / R_s. \quad (6.12)$$

The energy saving using collaborative communication system with respect to the SISO system is defined by

$$E_{saving}(\%) = 100 \times \frac{E_{SISO} - E_{colab}}{E_{SISO}} \%. \quad (6.13)$$

When the transmission distance is small the circuit energy is dominant over energy saved using collaborative communication. When E_{SISO} is equal to the E_{colab}, the energy saving is 0% and this distance is called *break-even distance*. For analysis and results, circuit parameters are considered from off-the-shelf RF products i.e., CC2420 and AT86RF21. Product data and the parameters used for the calculation of energy efficiency for different collaborative communication systems are shown in Table 6.1.

Table 6.1 Product data and parameters [2-3]

Symbol	Description	AT86RF212 [3]	CC2420 [2]
-	modulation	BPSK	BPSK
w_0	operating frequency	915 MHz	2.45 GHz
Δw	Maximum Frequency error	55 KHz	200 KHz
R_s	transmission data rate (BPSK)	40Kbps	250Kbps
U	operating voltage (typical)	3 V	3 V
I_{rx}	current for receiving states	9 mA	17.4 mA
P_{rx}	Receiving power, $P_{rx}= UI_{rx}$	27 mW	52.2 mW
I_{idle}	currency for idle states	0.4 mA	0.4 mA
P_{cir}	electronic circuitry power, $P_{cir} =UI_{idle}$	1.2 mW	1.2 mW
$Psen$	receiver sensitivity	- 110 dBm	- 95 dBm

6.5 Collaborative Communication with imperfect phase synchronization

In sections 4.5 and 5.4, a collaborative communication model with imperfect phase synchronization and with the assumption of perfect frequency synchronization that includes the influence of noise and Rayleigh fading has been proposed, modelled, theoretically analyzed, and simulated. The probability of error or BER for the collaborative communication model with imperfect phase synchronization is derived and given in equation (5.18), i.e.,

$$P_e = 0.5 erfc\left(\frac{\sqrt{\pi}\sin(\varphi)}{2\varphi} \sqrt{\frac{(E_b/N_0)}{\left(\frac{2b^2}{N}\left[1-\frac{\pi}{2}\left(\frac{\sin(\varphi)}{\varphi} \right)^2 + \frac{\sin(2\varphi)}{2\varphi} \right](E_b/N_0)+1 \right)}} \right)$$

Using inverse value of above equation i.e., equation (5.18), in equations (6.12) and (6.13), the energy efficiency of collaborative communication model with imperfect phase synchronization is numerically analyzed.

6.5.1 Analysis and Results

In this section the numerical results of the energy savings in the scenarios of SISO communication and collaborative communication with imperfect phase synchronization are presented. In the numerical evaluations, the parameters related to the transceivers take their values from the off-the-shelf transceiver products that are compliant with IEEE 802.15.4, i.e., CC2420 and AT86RF21. The maximum local distance between collaborative nodes is considered as 1 meter and the required BER is 10^{-5}. The value of the path loss exponent α is 4.0 ~ 6.0 [10]. The analytical and simulated results of the energy saving for the collaborative communication system with imperfect phase synchronization in the presence of AWGN and Rayleigh fading are obtained using MATLAB®. Energy saving and break-even distance for product AT86RF212, for phase errors distributed over {-0.1π to 0.1π}, {-0.2π to 0.2π}, {-0.3π to 0.3π} and {-0.4π to 0.4π} and for different number of collaborative nodes is shown in Figures 6.2, 6.3, 6.4 and 6.5 respectively.

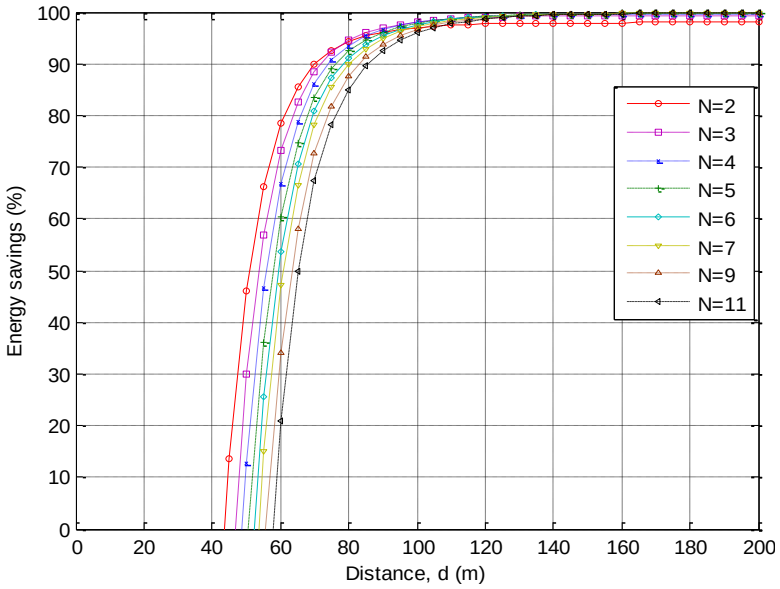

Figure 6.2 Energy saving and break-even distance with phase error {-0.1π to 0.1π} for different *N* for product AT86RF212

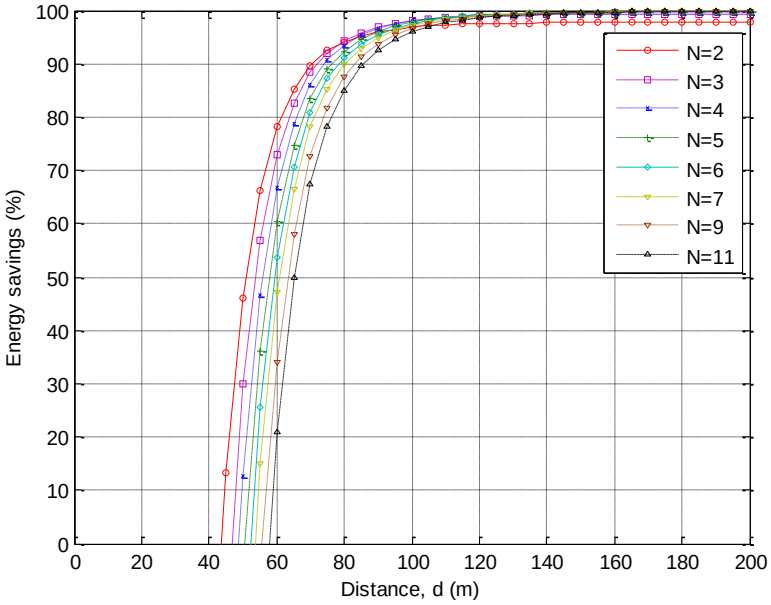

Figure 6.3 Energy saving and break-even distance with phase error {-0.2π to 0.2π} for different *N* for product AT86RF212

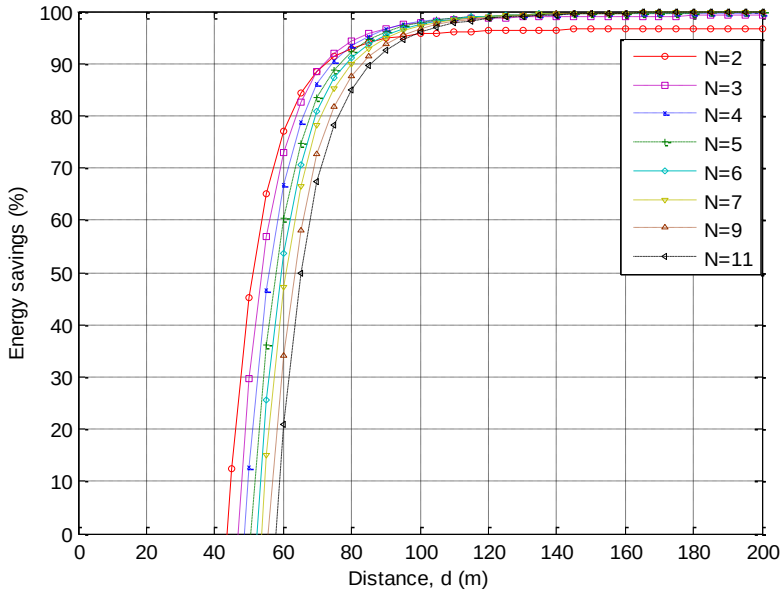

Figure 6.4 Energy saving and break-even distance with phase error {-0.3π to 0.3π} for different *N* for product AT86RF212

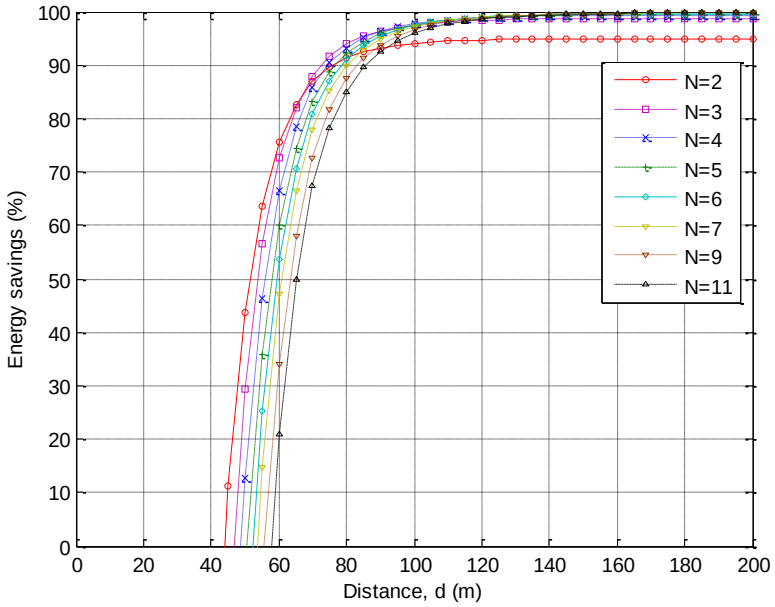

Figure 6.5 Energy saving and break-even distance with phase error {-0.4π to 0.4π} for different *N* for product AT86RF212

The energy saving and break-even distance for product CC2420, for phase errors distributed over {-0.1π to 0.1π}, {-0.2π to 0.2π}, {-0.3π to 0.3π} and {-0.4π to 0.4π} and for different number of collaborative nodes are shown in Figures 6.6, 6.7, 6.8 and 6.9, respectively. It is observed that the break-even distance increases as the number of collaborative nodes increases. AT86RF212 has a larger break-even distance than CC2420. But the energy saving in AT86RF212 is greater than CC2420 at the distances of 100m and 200m. From Figures 6.2, 6.3, 6.4, 6.5, 6.6, 6.7, 6.8 and 6.9, it is observed that energy saving is growing faster for AT86RF212 than for CC2420 as the distance increases first, then the break-even distance. AT86RF212 achieves a steady state earlier than the CC2420. AT86RF212 achieves a steady state when the distance is nearly 120m and the CC2420 achieves a steady state when the distance is approximately equal to 150m.

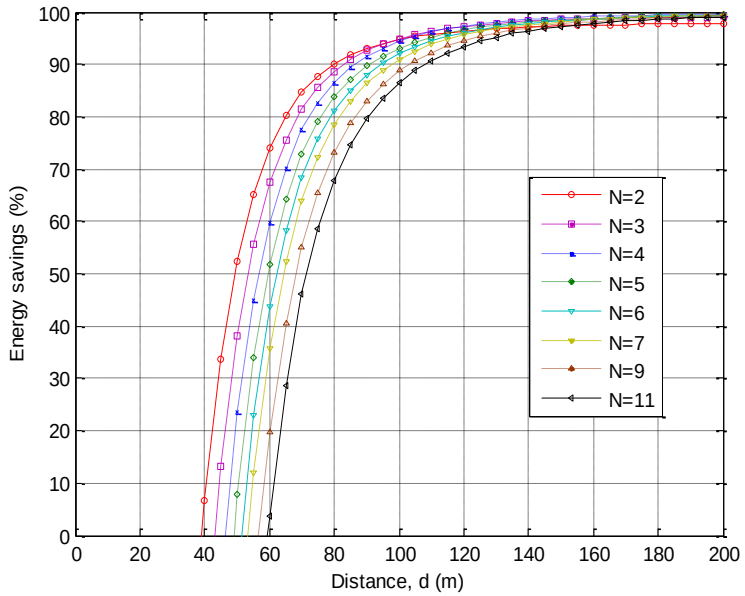

Figure 6.6 Energy saving and break-even distance with phase error {-0.1π to 0.1π} for different *N* for product CC2420

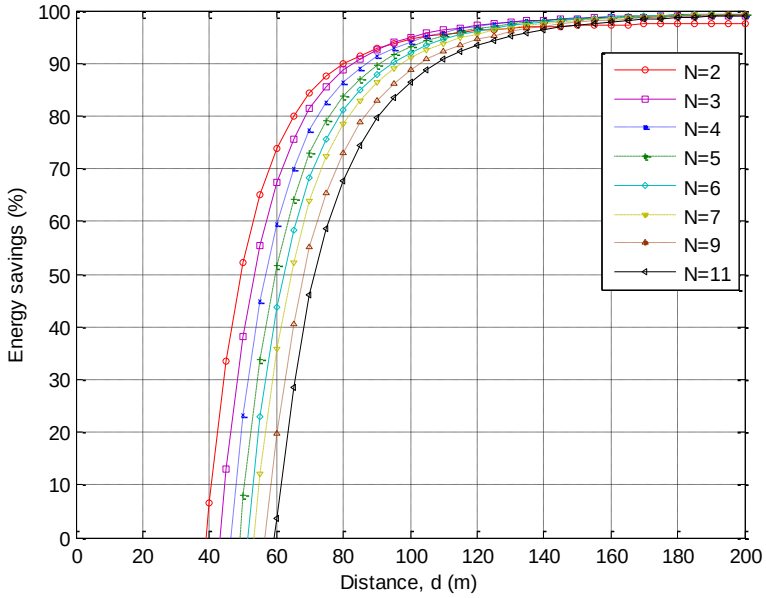

Figure 6.7 Energy saving and break-even distance with phase error {-0.2π to 0.2π} for different *N* for product CC2420

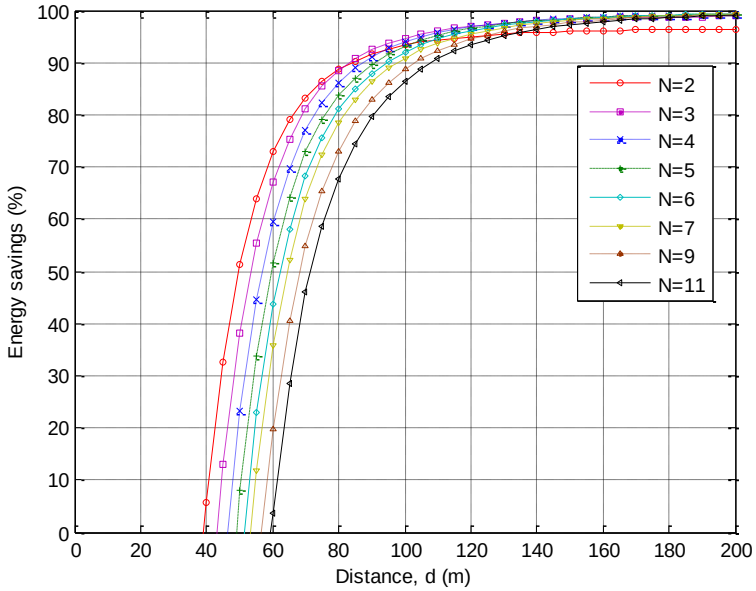

Figure 6.8 Energy saving and break-even distance with phase error {-0.3π to 0.3π} for different *N* for product CC2420

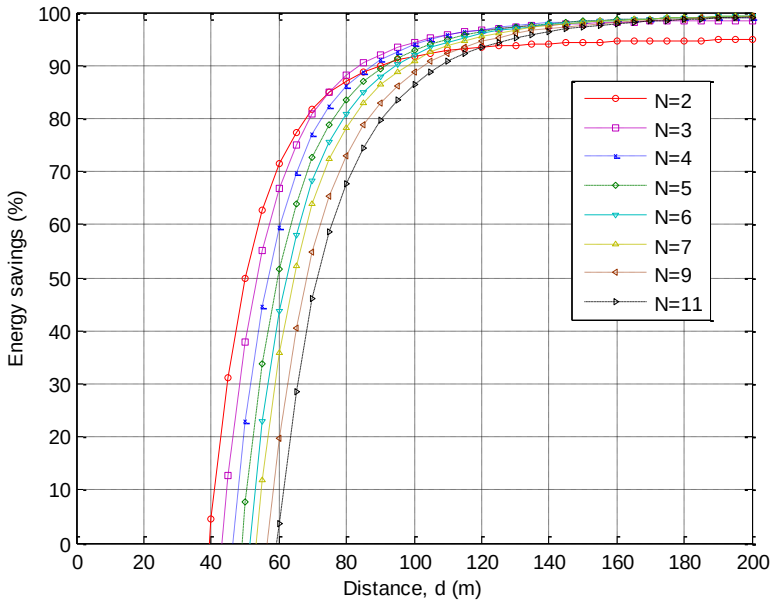

Figure 6.9 Energy saving and break-even distance with phase error {-0.4π to 0.4π} for different *N* for product CC2420

The break-even distances for CC2420 and AT86RF212 are summarized in Table 6.2. It is observed that, as the distance increases, energy saving using collaborative communication also increases and that, after a certain distance, it becomes constantly steady. The summary of the energy saving for the various phase errors at a distance of 100m and 200m for CC2420 and AT86RF212 is shown in Tables 6.3 and 6.4.

Table 6.2 Break-even distance for CC2420 and AT86RF212

N	**Break-even Distance CC2420**	**Break-even Distance AT86RF212**
2	39m	43.5m
3	43m	46.5m
4	46.2m	49m
5	49m	51m
6	51m	52.5m
7	53.5m	53.5m
9	57m	56m
11	59.7m	58m

Table 6.3 Energy Saving (%) for CC2420

N	**Phase Error 0.1π**		**Phase Error 0.2π**		**Phase Error 0.3π**		**Phase Error 0.4π**	
	200m	100m	200m	100m	200m	100m	200m	100m
2	97.7	95	97.5	94.5	96.5	93.8	94.5	91.5
3	99.1	95.5	99	95	98.8	95	98.5	94.2
4	99.6	94.5	99.4	94	99.2	94	99	94
5	99.4	93	99.5	93	99.3	93	99.1	93
6	99.3	92	99.2	92	99.3	92	99.1	92
7	99.2	91	99.1	91	99.2	91	99	91
9	99.1	89	99	89	99	90	99	89
11	98.9	86.5	98.5	86	98.1	89	98	86.5

Table 6.4 Energy Saving (%) for AT86RF212

N	**Phase Error 0.1π**		**Phase Error 0.2π**		**Phase Error 0.3π**		**Phase Error 0.4π**	
	200m	**100m**	**200m**	**100m**	**200m**	**100m**	**200m**	**100m**
2	98	97	97.7	96.7	96.5	95.6	95	94
3	99.4	98	99.2	98	99.1	97.8	98.8	97.5
4	99.7	98	99.7	98.2	99.6	98	99.4	97.7
5	99.8	97.6	99.7	97.5	99.7	97.6	99.6	97.5
6	99.8	97.4	99.8	97.3	99.7	97.5	99.7	97.3
7	99.8	97.2	99.8	97.2	99.8	97.2	99.8	94
9	99.8	96.5	99.9	96.5	99.8	96.5	99.8	96.5
11	99.9	96	99.9	96	99.8	96	99.8	96

6.6 Collaborative Communication with imperfect frequency synchronization

In sections 4.6 and 5.5 we have proposed, modelled, theoretically analyzed and simulated a collaborative communication model with imperfect frequency synchronization and with the assumption of perfect phase synchronization that includes the influence of noise and Rayleigh fading. The probability of error, or BER, for the collaborative communication model with imperfect frequency synchronization is derived and given in equation (5.27), i.e.,

$$P_e = 0.5erfc\left(b\sqrt{\frac{\pi}{2}}\left[1-\frac{(w_e T)^2}{18}\right]\sqrt{\frac{E_b/N_0}{\left(\frac{2b^2u(E_b/N_0)}{N}+1\right)}}\right)$$

Using the inverse value of the above equation i.e., equation (5.27), in equations (6.12) and (6.13), we have numerically analyzed the energy efficiency of the collaborative communication model with imperfect frequency synchronization.

6.6.1 Analysis and Results

In this section, the numerical results of the energy savings in the scenarios of SISO communication and collaborative communication with imperfect frequency synchronization are presented. In the numerical evaluations, the parameters related to the transceivers take values from the off-the-shelf transceiver products that are compliant with IEEE 802.15.4, i.e., CC2420 and AT86RF21. The maximum local distance between collaborative nodes is considered as 1 meter and the required BER is 10^{-5}. The value of the path loss exponent α is 4.0 ~ 6.0 [10]. The analytical and simulated results of the energy saving for the collaborative communication system with imperfect frequency synchronization in the presence of AWGN and Rayleigh fading are obtained using MATLAB®.

Figures 6.10, 6.11, 6.12 and 6.13 show the energy saving for different number of the collaborative nodes and break-even distance. From the results, it is observed that the break-even distance increases as the number of collaborative nodes increases. AT86RF212 has more break-even distance and less energy savings than CC2420.

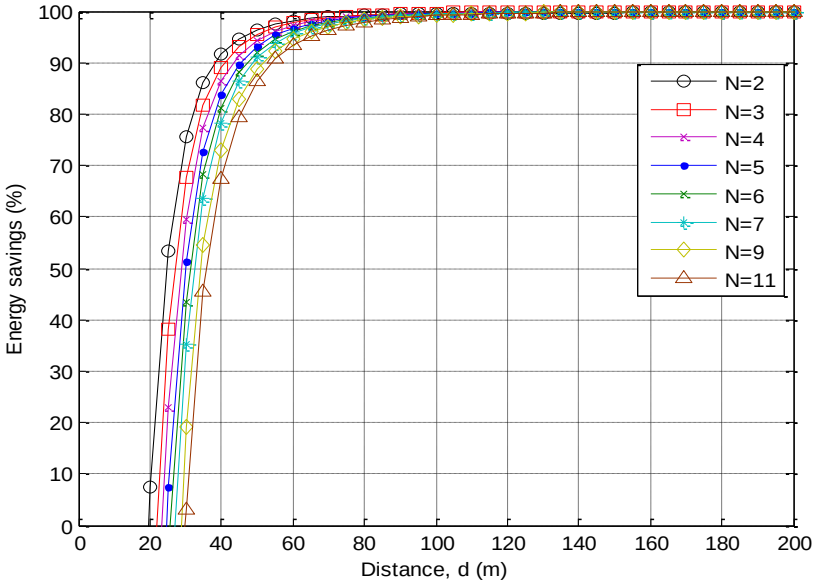

Figure 6.10 Energy saving and break-even distance with frequency error distributed over {-200 KHz ~ 200 KHz} and data rate 250 Kbps for different *N* for product CC2420

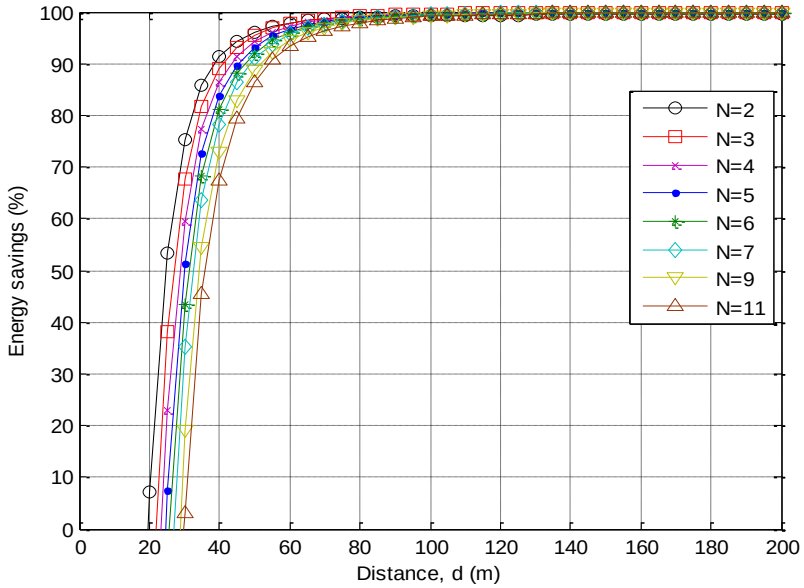

Figure 6.11 Energy saving and break-even distance with frequency error distributed over {-200 KHz ~ 200 KHz} and data rate 350 Kbps for different *N* for product CC2420

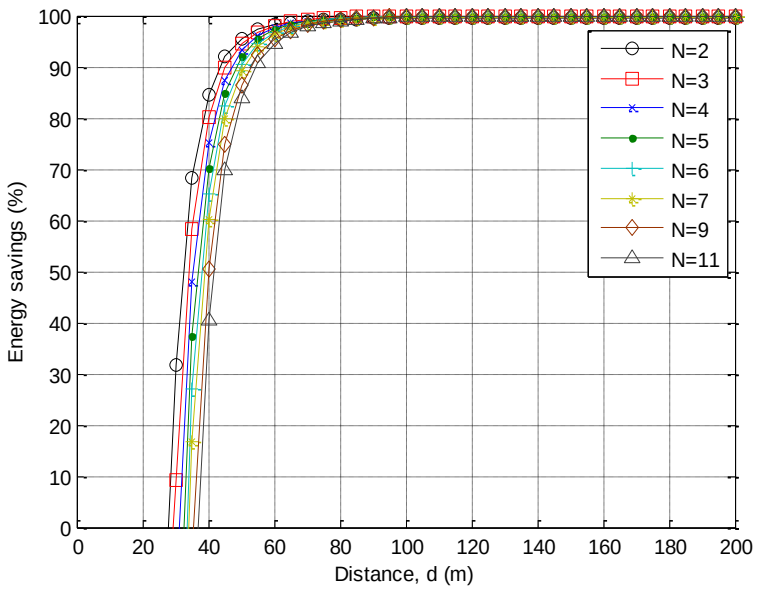

Figure 6.12 Energy saving and break-even distance with frequency error distributed over {-55 KHz ~ 55 KHz} and data rate 40 Kbps for different *N* for product AT86RF212

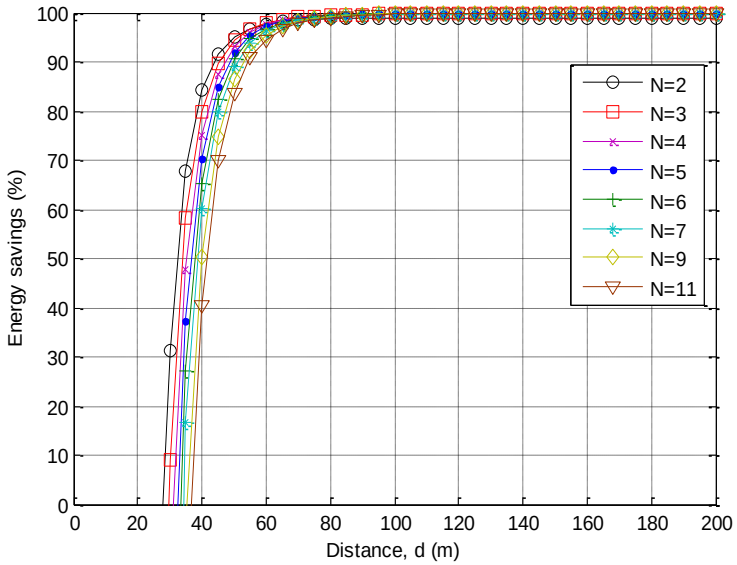

Figure 6.13 Energy saving and break-even distance with frequency error distributed over {-70 KHz ~ 70 KHz} and data rate 40 Kbps for different *N* for product AT86RF212

The break-even distance for products CC2420 and AT86RF212 is summarized in Table 6.5 for different number of collaborative nodes. It is realized that energy saving using collaborative communication increases as the distance increases. But after a certain distance it achieves its steady state. The energy savings for the various frequency errors at distances of 60m and 100m for products CC2420 and AT86RF212 are summarized in Tables 6.6. From tables 6.5 and 6.6 it is also found, that for products CC2420 and

AT86RF212, the 5 collaborative nodes produce significant energy saving using collaborative communication.

Table 6.5 Break-even distance for CC2420 and AT86RF212

N	**Break-even Distance CC2420**	**Break-even Distance AT86RF212**
2	19m	27.5m
3	22m	29.5m
4	24m	31m
5	25m	32.5m
6	26m	33.5m
7	27m	34m
9	29m	35.5m
11	30m	37m

Table 6.6 Energy Saving (%) for CC2420

N	**CC2420**		**AT86RF212**	
	100m	**60m**	**100m**	**60m**
2	99.73	99	99.45	98
3	99.9	98.7	99.83	98
4	99.94	98.6	99.86	97.5
5	99.96	98.3	99.85	97
6	99.96	98.1	99.84	99.5
7	99.96	97.5	99.8	96
9	99.5	96.5	99.75	95
11	99.4	96	98.7	94

6.7 Collaborative Communication with imperfect phase and frequency synchronization

In sections 4.7 and 5.6 we have proposed, modelled, theoretically analyzed and simulated collaborative communication model with imperfect phase and frequency synchronization that includes the influence of noise and Rayleigh fading. The probability of error or BER for collaborative communication model with imperfect phase and frequency synchronization is derived and given in equation (5.39), i.e.,

$$P_e = 0.5erfc\left(b\sqrt{\frac{\pi}{2}}\left[1-\frac{(w_eT)^2}{18}\right]\left[\frac{\sin(\psi)}{\psi}\right]\sqrt{\frac{N^2(E_b/N_0)}{2Nb^2\left\{\left(2-\frac{\pi}{2}\right)\left(1-\frac{(w_eT)^2}{18}\right)\left(\frac{\sin(\psi)}{\psi}\right)+2X\right\}(E_b/N_0)+1}}\right)$$

Using the inverse value of above equation i.e., equation (5.39), in equations (6.12) and (6.13), we have numerically analyzed the energy efficiency of the collaborative communication model with imperfect phase and frequency synchronization.

6.7.1 Analysis and Results

In this section, the numerical results of the energy savings in the scenarios of SISO communication and collaborative communication with imperfect phase and frequency synchronization are presented. In the numerical evaluations, the parameters related to the transceivers take values from the off-the-shelf transceiver products that are compliant with IEEE 802.15.4, i.e., CC2420 and AT86RF21. The local distance between collaborative nodes is considered as 1 meter and the required BER is 10^{-5}. The value of the path loss exponent α is 4.0 ~ 6.0 [10]. The analytical and simulated results of the energy saving for the collaborative communication system with imperfect frequency synchronization in the presence of AWGN and Rayleigh fading are obtained using MATLAB®.

To analyze the energy efficiency of our collaborative communication system we start our analysis by calculating the break-even distance for different number of collaborative nodes for different frequency and phase errors. Energy saving and break-even distance for product AT86RF212 i.e., frequency error distributed over {-55 KHz ~ 55 KHz} and for phase errors distributed over {-0.1π to 0.1π}, {-0.2π to 0.2π}, {-0.3π to 0.3π} and {-0.4π to 0.4π} and for different number of collaborative nodes is shown in Figures 6.14, 6.15, 6.16 and 6.17 respectively. Energy saving and break-even distance for product CC2420 i.e., {-200 KHz ~ 200 KHz} and for phase errors distributed over {-0.1π to 0.1π}, {-0.2π to 0.2π}, {-0.3π to 0.3π} and {-0.4π to 0.4π} and for different number of collaborative nodes is shown in Figures 6.18, 6.19, 6.20 and 6.21, respectively. It is observed that the break-even distance increases as the number of collaborative nodes increases. Using collaborative communication with imperfect phase and frequency synchronization, product AT86RF212 has more break-even distance and less energy savings than CC2420.

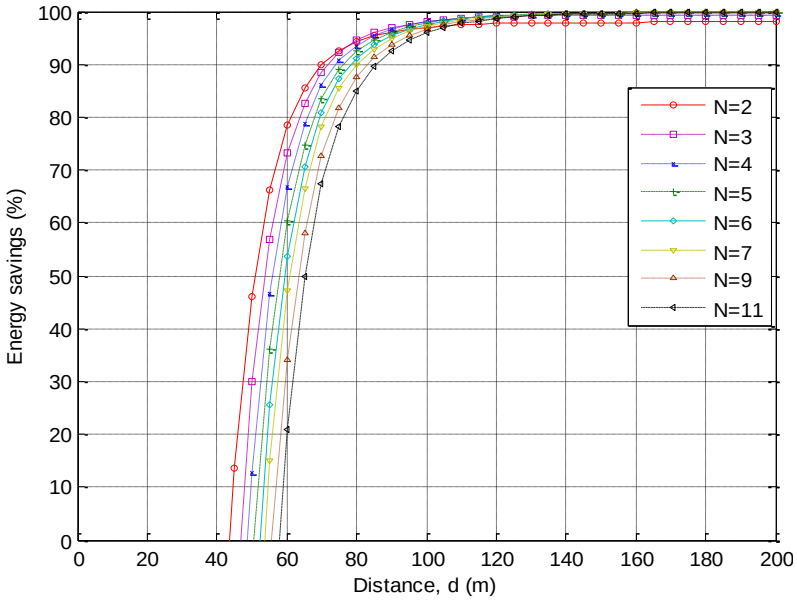

Figure 6.14 Energy saving and break-even distance, for parameters of AT86RF21 i.e., frequency error distributed over {-55 KHz ~ 55 KHz} and data rate 40 Kbps with phase error distributed over {-0.1π to 0.1π} for different *N*

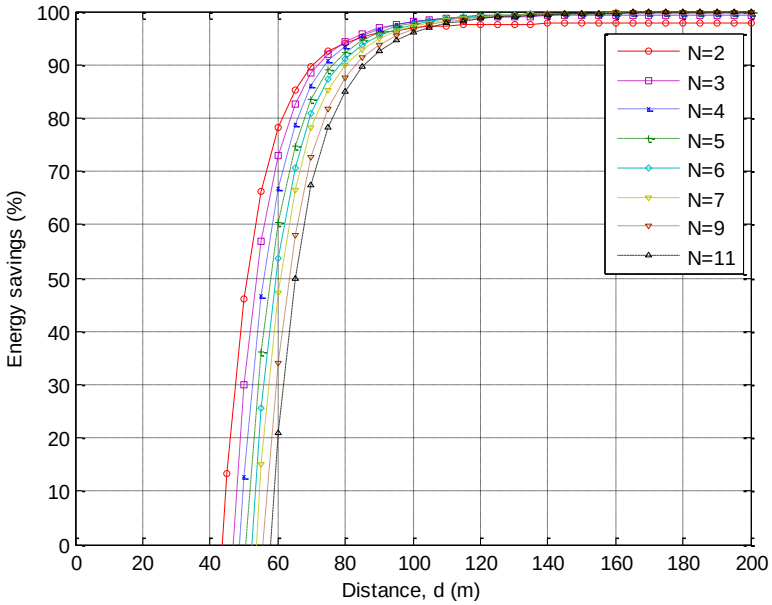

Figure 6.15 Energy saving and break-even distance, for parameters of AT86RF21 i.e., frequency error distributed over {-55 KHz ~ 55 KHz} and data rate 40 Kbps with phase error distributed over {-0.2π to 0.2π} for different *N*

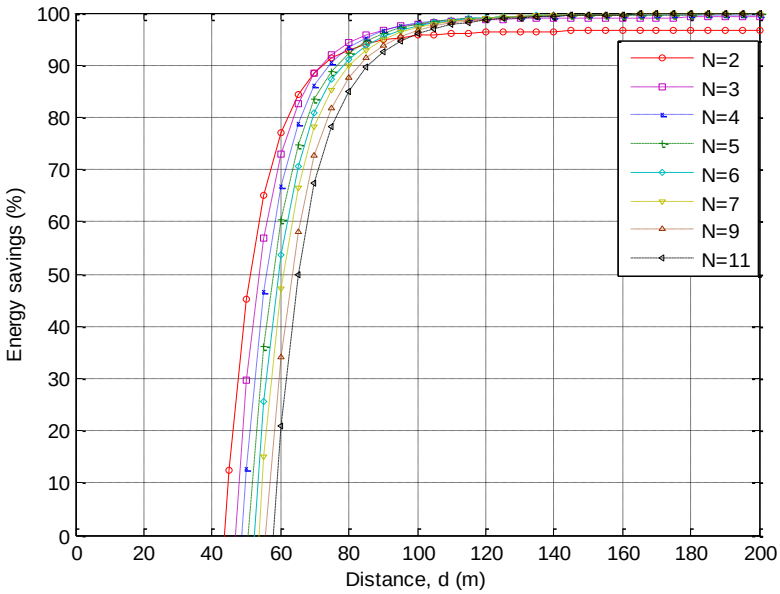

Figure 6.16 Energy saving and break-even distance, for parameters of AT86RF21 i.e., frequency error distributed over {-55 KHz ~ 55 KHz} and data rate 40 Kbps with phase error distributed over {-0.3π to 0.3π} for different *N*

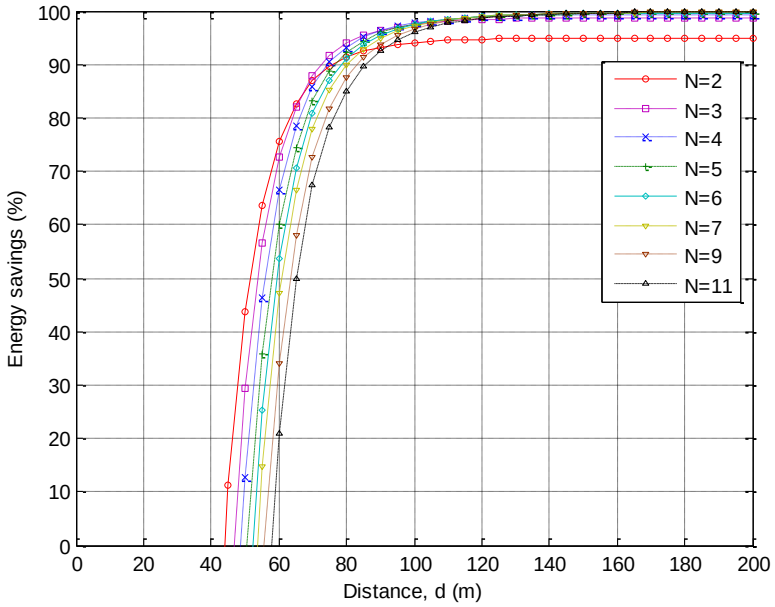

Figure 6.17 Energy saving and break-even distance, for parameters of AT86RF21 i.e., frequency error distributed over {-55 KHz ~ 55 KHz} and data rate 40 Kbps with phase error distributed over {-0.4π to 0.4π} for different *N*

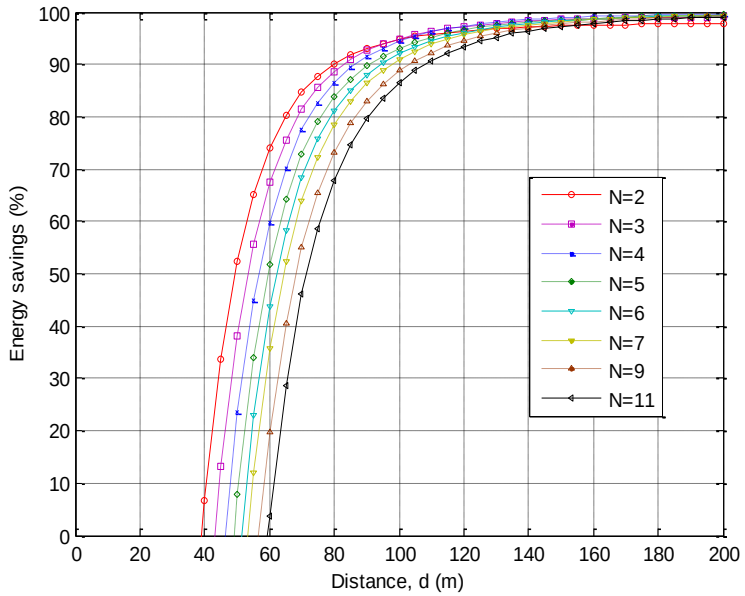

Figure 6.18 Energy saving and break-even distance, for parameters of CC2420 i.e., frequency error distributed over {-200 KHz ~ 200 KHz} and data rate 250 Kbps with phase error distributed over {-0.1π to 0.1π} for different *N*

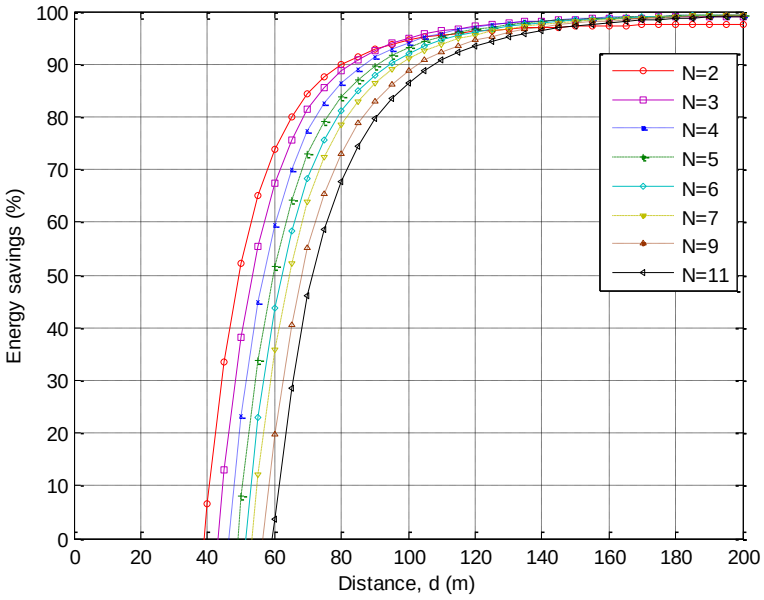

Figure 6.19 Energy saving and break-even distance, for parameters of CC2420 i.e., frequency error distributed over {-200 KHz ~ 200 KHz} and data rate 250 Kbps with phase error distributed over {-0.2π to 0.2π} for different *N*

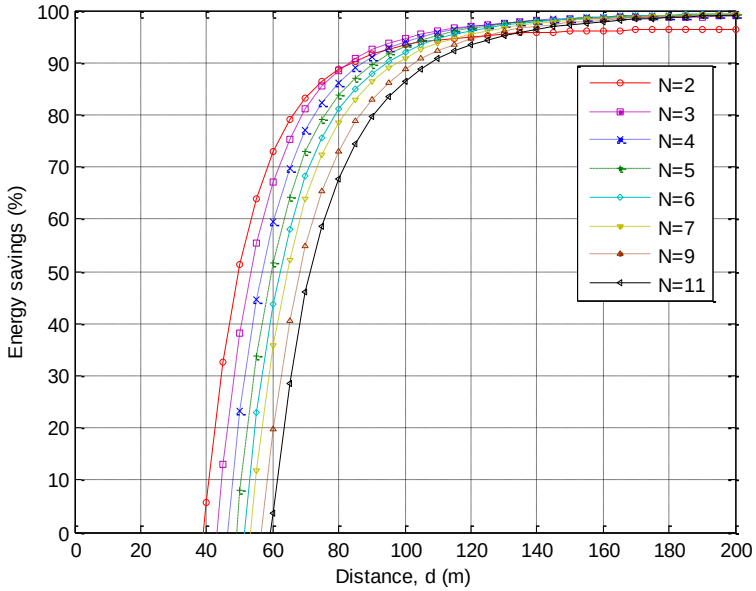

Figure 6.20 Energy saving and break-even distance, for parameters of CC2420 i.e., frequency error distributed over {-200 KHz ~ 200 KHz} and data rate 250 Kbps with phase error distributed over {-0.3π to 0.3π} for different *N*

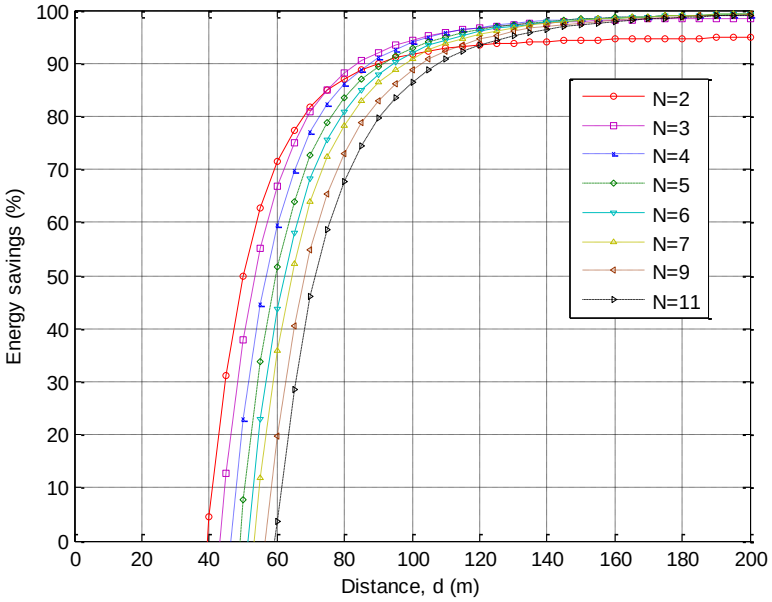

Figure 6.21 Energy saving and break-even distance, for parameters of CC2420 i.e., frequency error distributed over {-200 KHz ~ 200 KHz} and data rate 250 Kbps with phase error distributed over {-0.4π to 0.4π} for different *N*

The break-even distance and energy saving for CC2420 and AT86RF212 are summarized in Tables 6.7, 6.8 and 6.9 for different number of collaborative nodes. Results show that that the proposed collaborative communication system outperforms the SISO system in terms of energy efficiency at a transmission distance greater than the break-even distance. It is also observed, that as the distance increases, the energy saving using collaborative communication also increases and that after a certain distance, it becomes steady.

Table 6.7 Break-even distance for CC2420 and AT86RF212

N	**Break-even Distance CC2420**	**Break-even Distance AT86RF212**
2	40m	44.3m
3	43.6m	47.1m
4	47m	49.5m
5	49.8m	51.7m
6	52m	53m
7	54.4m	54.1m
9	57.8m	56.2m
11	60.2m	58.5m

Table 6.8 Energy Saving (%) for CC2420

N	**Phase Error 0.1π**		**Phase Error 0.2π**		**Phase Error 0.3π**		**Phase Error 0.4π**	
	200m	100m	200m	100m	200m	100m	200m	100m
2	98	95.2	97.5	94	96.5	93.8	94.5	91.5
3	99.2	95.6	99.2	94.6	98.8	95	98.5	94.2
4	99.7	94.5	99.3	94	99.2	94	99	94
5	99.5	93.2	99.1	92.8	99.3	93	99.1	93
6	99.3	92.7	99	91	99.3	92	99.1	92
7	99.1	91.6	99	90	99.2	91	99	91
9	99	90	99	89.7	99	90	99	89
11	98.5	88	98.5	86	98.1	89	98	86.5

Table 6.9 Energy Saving (%) for AT86RF212

N	**Phase Error 0.1π**		**Phase Error 0.2π**		**Phase Error 0.3π**		**Phase Error 0.4π**	
	200m	**100m**	**200m**	**100m**	**200m**	**100m**	**200m**	**100m**
2	98	97	97.7	96.7	96.5	95.6	95	94
3	99.4	98	99.2	98	99.1	97.8	98.8	97.5
4	99.7	98	99.7	98.2	99.6	98	99.4	97.7
5	99.8	97.6	99.7	97.5	99.7	97.6	99.6	97.5
6	99.8	97.4	99.8	97.3	99.7	97.5	99.7	97.3
7	99.8	97.2	99.8	97.2	99.8	97.2	99.8	94
9	99.8	96.5	99.9	96.5	99.8	96.5	99.8	96.5
11	99.9	96	99.9	96	99.8	96	99.8	96

6.8 Chapter Conclusions

In this chapter collaborative communication is employed as an alternative physical layer algorithm to improve the energy efficiency of wireless sensor networks. From the theoretical perspective, this chapter investigates the energy savings of wireless sensor networks which consist of sensor nodes using a collaborative communication system rather than an SISO system to transmit data in flat Rayleigh fading channel.

The Collaborative communication transceivers that are specified by IEEE 802.15.4 are studied. A node power consumption model is developed and related to the fade margin to quantify the energy savings of nodes which use collaborative communication transceivers rather than SISO transceivers to transmit data in the fading channel. Exploiting this model, the energy savings are analyzed for the scenarios of SISO communication and collaborative communication.

The *break-even distance* for the various collaborative communication models is also calculated. From the theoretical analyses and simulation-based investigations, significant energy savings are confirmed by the use of collaborative communication. The value of energy saving is heavily dependent on the values of the path loss exponent and the transmission distance. When the path loss exponent or the transmission distance becomes large, network energy efficiency can be significantly increased due to the use of collaborative communication.

From the simulated results of the collaborative communication in this chapter and in Chapter 4, we may conclude that network energy efficiency can be significantly improved by using the collaborative communication.

References

[1] IEEE 802.15.4 version 2006, IEEE Standards Association. [Online]. Available: http://standards.ieee.org/getieee802/download/802.15.4-2003.pdf.

[2] CC2420, Texas Instruments, [Online]. Available: http://focus.ti.com/analog/docs/enggresdetail.tsp?familyId=367&genContentId=3573. [Access: Jan 5, 2009].

[3] AT86RF212, ATMEL Products, [Online]. http://www.atmel.com/dyn/products/product_card.asp? PN=AT86RF212. [Access: Jan 5, 2009].

[4] A. Goldsmith, Wireless communications, Cambridge University Press, 2005, pp. 31-42, 5-6.

[5] C. Schurgers, O. Aberthorne, and M. B. Srivastava, "Modulation scaling for energy aware communication systems," in Proc. Int. Symp. Low Power Electronics Design, Aug. 2001, pp. 96–99.

[6] R. Min and A. Chandrakasan, "A framework for energy-scalable communication in high-density wireless networks," in Proc. Int. Symp. Low Power Electronics Design, Aug. 2002, pp. 36–41.

[7] S. Cui, A. J. Goldsmith, and A. Bahai, "Modulation optimization under energy constraints," in Proc. ICC'03, AK, May 2003, pp. 2805–2811.

[8] G. J. Miao, Multiple-input multiple-output wireless sensor networks communications, US Patent no. 7091854, 9 April, 2004.

[9] L. Xiao and M. Xiao, "A new energy-efficient MIMO-sensor network architecture M-SENMA," in Proc. VTC'04, vol. 4, 2004, pp. 2941- 2945.

[10] S. Cui, A. J. Goldsmith, and A. Bahai, "Energy-Efficiency of MIMO and Cooperative MIMO Techniques in Sensor Networks," in IEEE Journal on Selected Areas In Communications, vol. 22, NO. 6, August 2004, pp. 1089-1098.

[11] L. Simić, S. Berber and K. W. Sowerby, "Energy-Efficiency of Cooperative Diversity Techniques in Wireless Sensor Networks," in the 18th Annual IEEE International Symposium on Personal, Indoor and Mobile Radio Communications .

[12] L. Simic, Stevan M. Berber, and K. W. Sowerby, "Partner Choice and Power Allocation for Energy Efficient Cooperation in Wireless Sensor Networks," in Proc. IEEE ICC'08, pp. 4255-4260.

[13] L. Simic, Stevan M. Berber, K. W. Sowerby, "Distributed Partner Choice for Energy Efficient Cooperation in a Wireless Sensor Network," in Proc. IEEE GLOBECOM'08, pp. 4799-4804.

[14] S. De, C. Qiao, D. A. Pados, M. Chatterjee, and S. J. Philip, "An integrated cross-layer study of wireless CDMA sensor networks," IEEE J. Sel. Areas Commun., vol. 22, no. 7, 2004, pp. 1271-1285.

[15] T. Shu, M. Krunz, and S.Vrudhula, "Joint Optimization of Transmit Power-Time and Bit Energy Efficiency in CDMA Wireless Sensor Networks," IEEE Trans. on Wireless Commun., vol. 5, no. 11, 2006, pp. 3109-3118.

[16] H. Kang, H. Hong, S. Sung, and K. Kim, "Interference and sink capacity of wireless CDMA sensor networks with layered architecture," ETRI Journal, vol.30, no.1, 2008, pp.13-20.

[17] C.-H. Liu and H. H. Asada, "A source coding and modulation method for power saving and interference reduction in DS-CDMA sensor network systems," in Proc. American Control Conf., Anchorage, 2002, pp. 3003–3008.

[18] O. Dousse, F. Baccelli, and P. Thiran, "Impact of interference on connectivity in ad hoc networks," in Proc. IEEE INFOCOM, 2003, pp. 1724–1733.

[19] A. Muqattash and M. Krunz, "CDMA-based MAC protocol for wireless ad hoc networks," in Proc. ACM MobiHoc, 2003, pp. 153–164.

[20] B. Sklar, "Rayleigh fading channels in mobile digital communication systems Part I. Characterization," in IEEE Communications Magazine, Vol. 35, Issue 7, July 1997, pp. 90 – 100.

Chapter 7 Capacity of the Collaborative Communication System

7.1 Introduction

From the collaborative communication models presented in Chapter 4, it is revealed that high power gain can be achieved without perfect frequency and phase synchronization in the presence of AWGN and Fading. The study in Chapter 5 has shown that collaborative communication significantly brings down the signal-to-noise ratio for a given value of bit error rate (BER) in the flat Rayleigh fading channel. This promises a large reduction in transmitted power in sensor networks. From the results shown in Chapter 6, it is observed that significant energy savings can be achieved using collaborative communication. Therefore, collaborative communication may be employed as an alternative physical layer algorithm to transmit data in the fading channels in Wireless Sensor Networks (WSNs). One question left unanswered in Chapters 4 and 6 relates to how much capacity is required by a collaborative communication system with imperfect phase and frequency synchronization in presence of AWGN and Fading. This chapter hereby investigates one of the basic design requirements in wireless sensor networks, i.e., to determine the required capacity of a collaborative communication system in presence of AWGN and fading, that can be tested on devices that comply with the requirements of IEEE 802.15.4 [1]. To the author's best knowledge, this is the first study investigating the capacity of collaborative communication systems.

The aim of this chapter is to analyze the capacity of the collaborative communication system and to estimate the capability of collaborative communication to increase the capacity of a communication system and to endeavour to solve the technique's limitations. In this research, a procedure for the capacity calculation for different collaborative communication systems in an Additive White Gaussian Noise (AWGN) channel with Rayleigh fading is studied. Collaborative communications systems have:

- Perfect time, frequency and phase synchronization among the collaborative nodes and a base station.
- Imperfect phase synchronization and an assumption of perfect time and frequency synchronization between the collaborative nodes and the base station.

- Imperfect frequency synchronization and an assumption of perfect time and phase synchronization between the collaborative nodes and the base station.

In cases where the sensor nodes are randomly distributed, it is very difficult to achieve perfect phase and frequency synchronization between the collaborative nodes and the base station in a real time environment. Therefore, a capacity calculation for the collaborative communication model with imperfect phase and frequency synchronization between the collaborative nodes and the base station is proposed, modelled, theoretically analyzed and simulated.

Of particular interest to this study is the following:

- The development of a closed form expression for the channel capacity of collaborative communication systems;
- An investigation of the effect of phase and frequency errors on the capacity of the collaborative communication systems in wireless sensor networks;
- The establishment of a WSN simulator to calculate the capacity of a collaborative communication system with imperfect phase and frequency synchronization in the presence of AWGN and Rayleigh fading, using the parameters of off-the-shelf products i.e. CC2420 [2] and AT86RF212 [3];

Figure 7.1 demonstrates the route map of this chapter. The study in this chapter unfolds in the following sequence:

In Section 7.2, an extensive literature review of Capacity and collaborative communication is presented. Section 7.3 presents the development of a closed form expression of capacity for an ideal collaborative communication system i.e., by assuming perfect phase, frequency and time synchronization. The system model, which is a mathematical model for the capacity calculation of an ideal collaborative communication system, is developed. Theoretical and simulation results reveal that significant capacity gain can be achieved by using collaborative communication.

In section 7.4 a closed form expression of capacity for collaborative a communication system with imperfect phase synchronization and with the assumption of perfect frequency synchronization that includes the influence of noise and Rayleigh fading, is presented. The theoretical model of the system is presented; the theoretical analysis and Monte Carlo simulation are conducted in order to validate the performance of the collaborative communication algorithm in terms of its capacity for different phase errors.

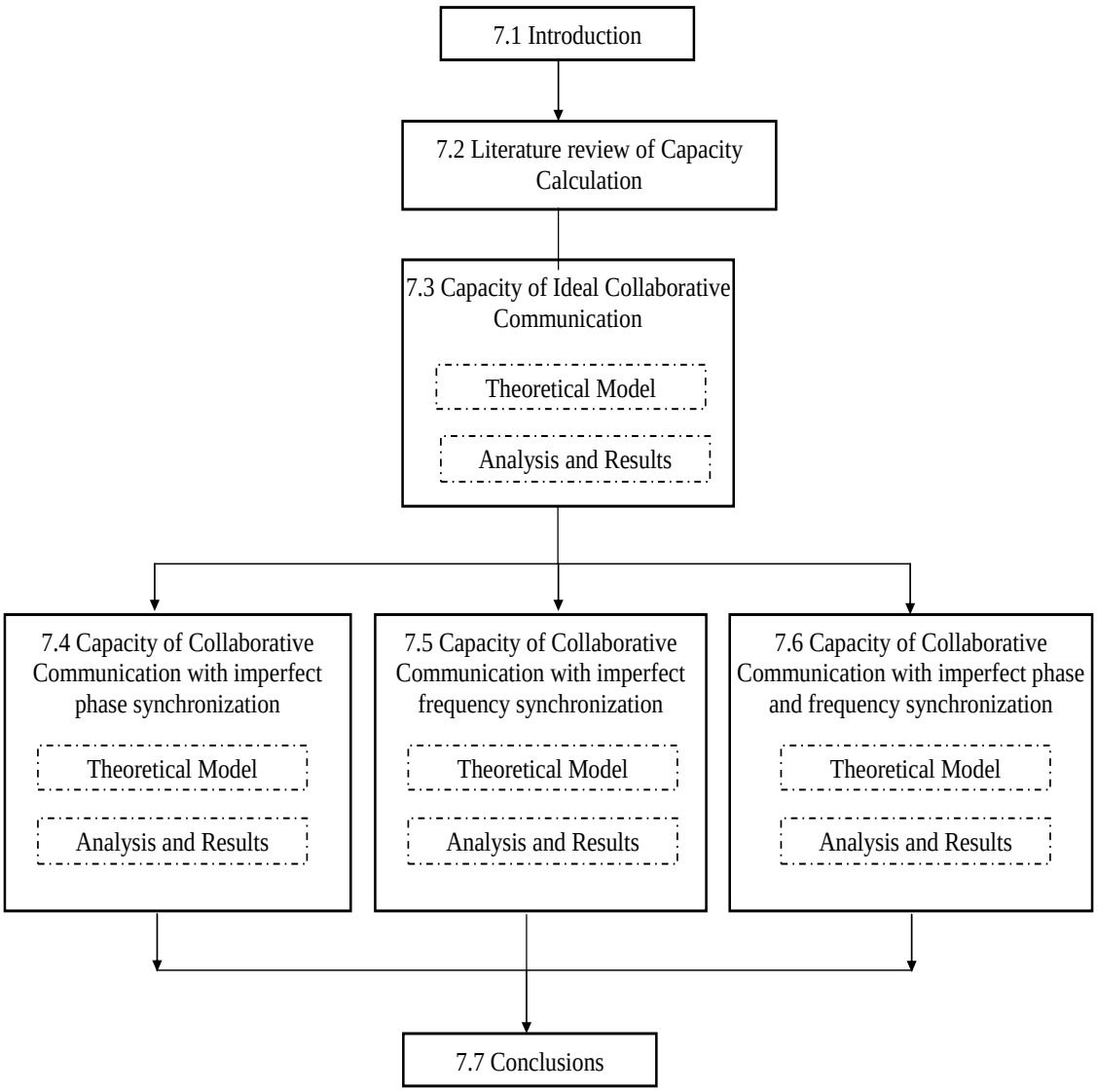

Figure 7.1 Route map of study in Chapter 7

In Section 7.5 the closed form expression of capacity for a collaborative communication system with imperfect frequency synchronization with the assumption of perfect phase synchronization that includes the influence of noise and Rayleigh fading, is modelled, theoretically analyzed, and simulated using using the parameters of off-the-shelf products i.e. CC2420 [2] and AT86RF212 [3]. In Section 7.6 a closed form expression of capacity for a more realistic collaborative communication system with imperfect phase and frequency synchronization that includes the influence of noise and Rayleigh fading, is modelled, theoretically analyzed, and simulated.

In summary, the contribution of this chapter is three-fold:

10. Closed form expressions of capacity are derived and expressed as a function of signal to noise ratio and the number of collaborative nodes as parameter, for a collaborative communication system that includes the influence of the phase error, frequency error, AWGN and Rayleigh fading in the channel;
11. It has been proved that capacity can be significantly increased using collaborative communication, which is a consequence of the fact that collaborative communication can be considered as a space diversity system;
12. Investigations based on the simulation confirmed that the proposed collaborative communication system can produce significant capacity gain with imperfect phase and frequency synchronization in the presence of AWGN and fading;

7.2 Literature Review

One of the basic design requirements in wireless sensor networks is to determine their required capacity. If the sensor network is of a star configuration, where a base station or destination communicates with the surrounding sensor nodes that are sources of information, capacity can be found in a way that is similar to the way in which it is done for wireless cellular networks. However, when the network uses multiple relays to achieve diversity in signal transmission, the problem that arises is how to determine the network capacity; this has been the subject of extensive research work. A good survey of multi-way channels was developed in 1976; this included relay channels, and is presented in [4]. The capacity theorems for the Gaussian degraded, reversely degraded and feedback relay channels are presented in [5]. The capacity of a general wireless network with N nodes randomly located in a region of area 1 m^2 is investigated and presented in [6].

In [7], the analyses of cooperative strategies are conducted and the capacity theorems proved for relay networks that are based on either, compress-and-forward, or decode-and-forward relay strategies. It was assumed that the Gaussian noise and Rayleigh fading are present in the channels. The upper and lower capacity boundaries for cooperative diversity are derived in [8]. In particular, the decode and forward relay networks are analyzed in [9-12] and the exact expressions for the probability of error and channel capacity are derived over independent and non-identical Rayleigh fading channels [11] and the Nakagami channel [12]. Channel models and their impact on error distribution are analyzed in [13] and [14]. The capacity of noise channel and the cooperative channels are presented and analyzed in [15] and [16]. The capacity limits of data collection in random

wireless sensor networks have been studied in the literature, which is presented in [17-22]. In [17-18] the many-to-one transport capacity of dense and random sensor networks under a protocol interference model is presented and analyzed. In [19-20] the capacity for data collection with the complex physical layer techniques, such as antenna sharing, channel coding and cooperative beam forming, is presented and analyzed. The capacity of a general some-to-some communication paradigm under a protocol interference model in random networks with multiple randomly selected sources and destinations is presented and analyzed in [21]. The capacity for data collection under a protocol interference model with multiple sinks is analyzed in [22]. The capacity calculation analyzed in [17-22] has the assumption of a large number of sensor nodes, and nodes are either located on a grid structure, or randomly and uniformly distributed on a plane. The theoretical limits of data collection in a TDMA-based sensor network in terms of possible and achievable maximum capacity are presented and analyzed in [23]. The capacity calculation of cooperative communications systems is presented and analyzed in [24]. It is shown in [24] that, by using cooperative communication in a fading channel, a larger amount of information can be transmitted through the channel with less transmission time and power.

However, the procedure for developing closed-form expressions for the channel capacity of collaborative communication systems with imperfect phase and frequency synchronization remains an open issue. Moreover, such expressions are absent in the existing literature.

7.3 The Capacity of the Ideal Collaborative Communication Model

In this section, the capacity of an ideal collaborative communication model with the assumption that there is perfect time, frequency and phase synchronization, among the collaborative nodes and the base station is presented. A collaborative node has to transfer the data to the base station and this data is sent to the N collaborative nodes. The collaborative communication network shown in Figure 4.3 can be presented by a scheme shown in Figure 7.2. It is composed of N collaborative node transmitters represented as Source (Node). Each collaborative node has a transceiver to receive signals from other collaborative nodes within the network and to transmit signals to the base station. Each collaborative node also has a phase lock loop (PLL) for offset correction and a modulator to modulate the signal. The channel is considered as an AWGN channel. On the receiver

side, denoted as the base station, there is a demodulator to demodulate a received signal. The demodulator multiplies the received signal with a cosine signal; passes it through a low pass filter (LPF) and then integrates it. Then the power of the demodulated signal and channel capacity is calculated.

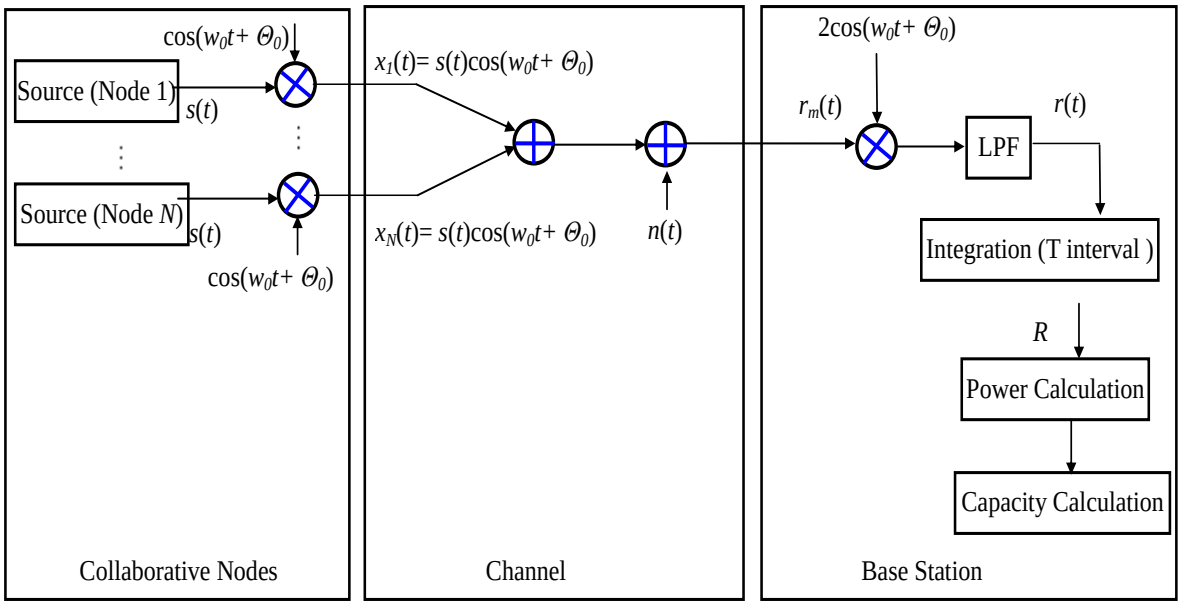

Figure 7.2 System Model

7.3.1 Theoretical Model of the Capacity of an ideal collaborative communication model

In section 4.3, the received power of an ideal collaborative communication model is proposed, modelled, theoretically analyzed, and simulated. The power of the received signal is presented in equation (4.4) and expressed as

$$P_R = \left[\sum_{i=1}^{N} S + n \right]^2 . \tag{7.1}$$

As n are the independent random variables and n is zero-mean, we have to calculate the mean value of received power as

$$E[P_R] = E\left[\left[\sum_{i=1}^{N} S \right]^2 \right] + \sigma_n^2 , \tag{7.2}$$

where σ^2_n is the variance of noise. Equation (7.2) can also be developed as follows

$$E[P_R] = N^2 S^2 + \frac{N_0}{2}. \tag{7.3}$$

The power of the received signal is the sum of the signal and noise parts. Thus the capacity of the ideal collaborative communication system can be found as

$$C = \frac{1}{2}\log_2\left(1 + \frac{S_P}{N_P}\right), \tag{7.4}$$

where S_P is signal power N_P and is noise power.

Using the values of signal power and noise power from equation (7.3) into equation (7.4), we may have

$$C = \frac{1}{2}\log_2\left(1 + \frac{N^2 S_P}{N_0/2}\right), \tag{7.5}$$

where, N is number of collaborative nodes.

Special Case:

If the transmitted power of each relay node is reduced by N times, the equation (7.5) may be written as,

$$C = \frac{1}{2}\log_2\left(1 + \frac{N S_P}{N_0/2}\right), \tag{7.6}$$

This is the case when the power of each collaborative node is reduced by factor N, i.e., the total transmitted is P. This reduction will be used to investigate the capacity of each collaborative node with reduced power consumption. This case can be used to investigate the effect of total transmitted power on capacity.

7.3.2 Analysis and Results

In this section the analytical and simulated results for the capacity of an ideal collaborative communication system are presented. A Monte Carlo simulation to analyze the capacity of ideal collaborative communication system is performed using MATLAB®. The wireless communication environment used in the simulation is established using SIMULINK's AWGN and Rayleigh channel blocks.

Results show that the analytical results match very well with the simulated results. Figure 7.3 presents the analytical and simulated results for the capacity of an ideal collaborative communication model by considering that the power of each collaborative node is P, thus, the total transmitted power of the network is equal to NP. Figure 7.4 present the analytical and simulated results for the capacity of an ideal collaborative communication model by considering the power of each collaborative is P/N, thus, the total transmitted power of the network is P.

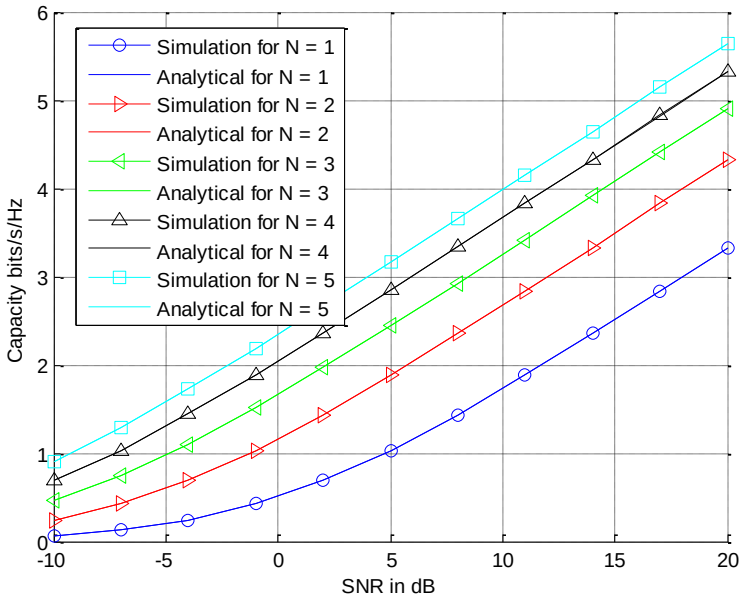

Figure 7.3 Capacity for an ideal collaborative communication system with each node transmitting power P, so that the total of power transmitted by the network is NP

From the results shown in Figures 7.3 and 7.4, it is confirmed that the capacity of the system increases as number of collaborative nodes increases. It is also found that if the total transmitted power of the network is decreased by factor N, where N is number of collaborative nodes, substantial capacity gain can still be achieved. From equations (7.5) and (7.6) and the results shown in Figures 7.3 and 7.4, it is also observed that if the total transmitted power is decreased by factor N, the capacity will approximately decrease by only factor $0.5\log_2(N)$.

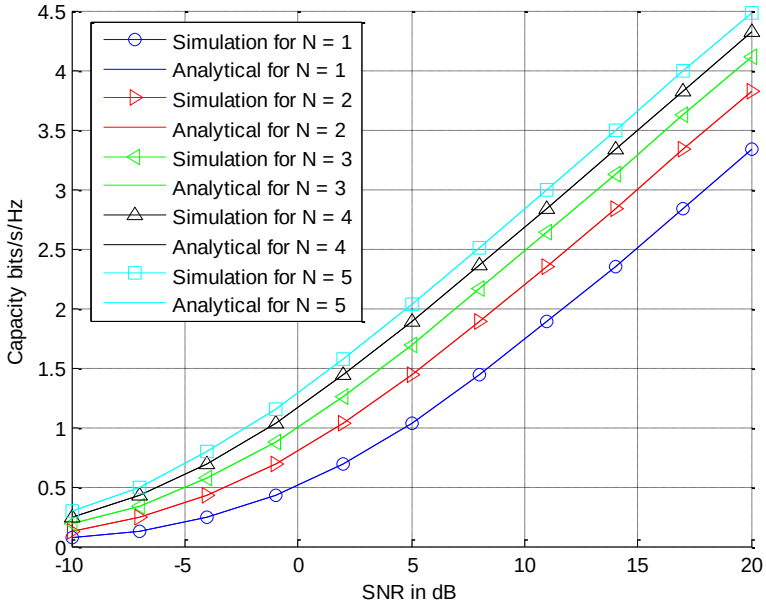

Figure 7.4 Capacity for an ideal collaborative communication system with each node transmitting power P/N, so that the total power transmitted by the network is P

7.4 Capacity of a Collaborative Communication Model with imperfect phase synchronization

In this section, we present the capacity of a collaborative communication model with imperfect phase synchronization and with the assumption that there is perfect time and frequency synchronization between the collaborative nodes and the base station in the presence of AWGN and Rayleigh fading. The system model for the collaborative communication system with imperfect phase synchronization in the presence of AWGN and Rayleigh fading is shown in Figure 7.5. It is composed of N collaborative node transmitters, represented as Source (Node). Each collaborative node has a transceiver to receive signals from other collaborative nodes within the network and transmits signals to the base station. Each collaborative node also has a phase lock loop (PLL) for offset correction and a modulator to modulate the signal. The channel is considered as an AWGN and Rayleigh fading channel. The Rayleigh fading channel for each transmitted signal has an independent effect. On the receiver side, denoted as the base station, there is a demodulator to demodulate the received signal. The demodulator multiplies the received signal with a cosine signal; passes it through a low pass filter (LPF) and then integrates it. Then the power of demodulated signal and channel capacity is calculated.

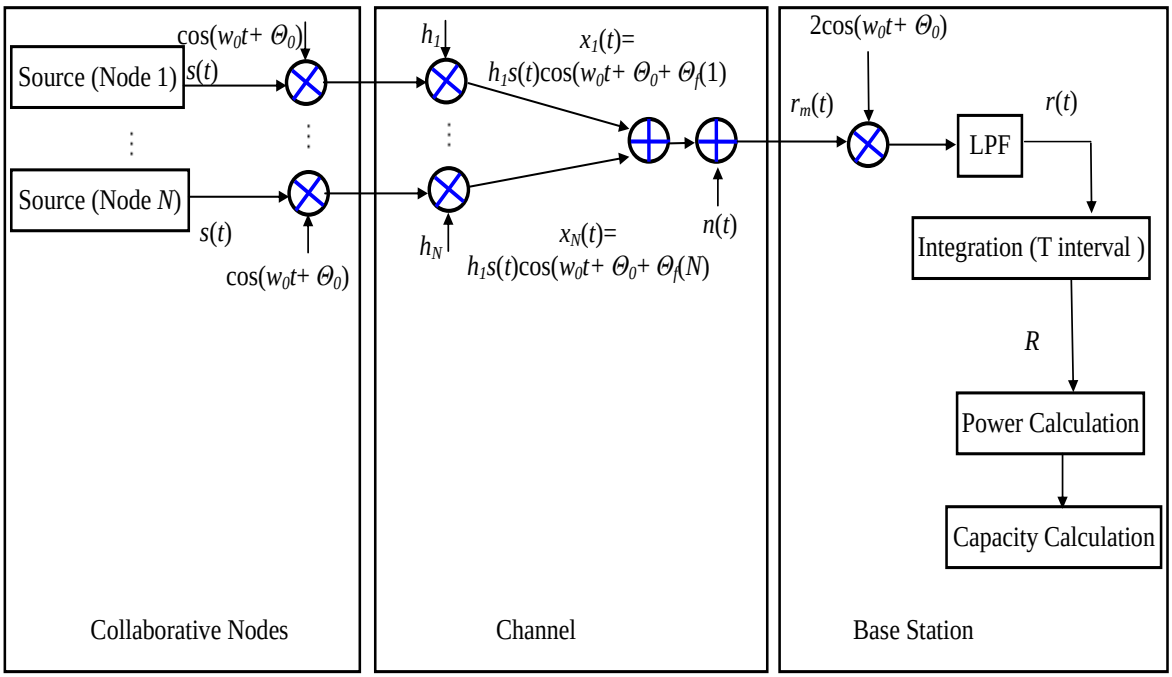

Figure 7.5 System Model

7.4.1 Theoretical Model for collaborative communication with imperfect phase synchronization

In section 4.5, we have proposed, modelled, theoretically analyzed, and simulated the received power of a collaborative communication model with imperfect phase synchronization and with the assumption that there is perfect time and frequency synchronization between the collaborative nodes and the base station in the presence of AWGN and Rayleigh fading. The power of the received signal is presented in equation (4.12) and expressed as

$$P_R = \left[\sum_{i=1}^{N} h_i S \cos(\Theta_f(i)) + n \right]^2 . \qquad (7.7)$$

As $\Theta_f(i)$, h_i and n are the independent random variables and n is the zero-mean, we have to calculate the mean value of received power as

$$E[P_R] = E\left[\left[\sum_{i=1}^{N} h_i S \cos(\Theta_f(i)) \right]^2 \right] + \sigma_n^2 , \qquad (7.8)$$

where σ^2_n is the variance of noise. Equation (7.8) can also be developed as follows

$$E[P_R] = NS^2\left[\frac{1}{2} + \frac{\sin(2\varphi)}{4\varphi}\right] + \frac{N(N-1)b^2S^2\pi}{2}\left[\frac{\sin(\varphi)}{\varphi}\right]^2 + \frac{N_0}{2}, \qquad (7.9)$$

where φ is distribution limit of phase error and b is the mode of Rayleigh random variable h.

The power of the received signal is the sum of the signal and noise parts. Thus the capacity for the ideal collaborative communication system can be found as

$$C = \frac{1}{2}\log_2\left(1 + \frac{S_P}{N_P}\right), \qquad (7.10)$$

Where S_P is signal power N_P and is noise power.

Using the values of signal power and noise power from equation (7.9) into equation (7.10), we may have

$$C = \frac{1}{2}\log_2\left(1 + \frac{NS^2\left[1 + \frac{\sin(2\varphi)}{2\varphi}\right] + N(N-1)b^2S^2\pi\left[\frac{\sin(\varphi)}{\varphi}\right]^2}{N_0}\right), \qquad (7.11)$$

Special Case:

If the transmitted power of each relay node is decreased by N, the equation (7.11) may be written as,

$$C = \frac{1}{2}\log_2\left(1 + \frac{S^2\left[1 + \frac{\sin(2\varphi)}{2\varphi}\right] + (N-1)b^2S^2\pi\left[\frac{\sin(\varphi)}{\varphi}\right]^2}{N_0}\right). \qquad (7.12)$$

This is the case when the power of each collaborative node is reduced by factor N, i.e., the total transmitted is P. This reduction is used to investigate the capacity with reduced power consumption for each collaborative node. This case can be used to investigate the effect on capacity of the total of the power transmitted.

7.4.2 Analysis and Results

In this section, the analytical and simulation results of the capacity of the collaborative communication system in the presence of phase error are presented. A Monte Carlo simulation is performed to analyze the capacity of a collaborative communication system in the presence of phase error using MATLAB®. The wireless communication environment used in the simulation is established using SIMULINK's AWGN and Rayleigh channel blocks.

Results show that the analytical results match very well with the simulated results. Figures 7.6 and 7.7 present the analytical and simulated results of capacity for the collaborative communication system in the presence of phase error and Rayleigh fading in cases where the phase error is distributed over $\{-0.1\pi \sim 0.1\pi\}$ and $\{-0.4\pi \sim 0.4\pi\}$ respectively, and assuming that the power of each collaborative node is P, the total transmitted power of the network is equal to NP. Figures 7.8 and 7.9 present the analytical and simulated results for phase error distributed over $\{-0.1\pi \sim 0.1\pi\}$ and $\{-0.4\pi \sim 0.4\pi\}$, respectively, for cases when the transmitted power of each collaborative node is P/N, thus, the total transmitted power of the network is P.

From the results shown in Figures 7.6, 7.7, 7.8 and 7.9, it is confirmed that the capacity of the system increases as number of collaborative nodes increases. It is also shown that the capacity decreases as the phase error increases. From Figures 7.6, 7.7, 7.8 and 7.9, it is obvious that capacity decreases by approximately 0.3 bits/sec/Hz, when the phase error distribution increases from $\{-0.1\pi \sim 0.1\pi\}$ to $\{-0.4\pi \sim 0.4\pi\}$.

From Figures 7.8 and 7.9, it is observed that if the total transmitted power of the network is decreased by factor N, where N is the number of collaborative nodes, a substantial capacity gain can still be achieved. From equations (7.11), (712) and the results shown in Figures 7.6, 7.7, 7.8 and 7.9, it is also observed that if the total transmitted power is decreased by factor N, capacity will approximately decrease by only factor $0.5\log_2[(N\text{-}1)(\sin(\varphi)/\varphi)^2]$, where φ is the phase error, in the presence of AWGN, fading and phase errors.

The proposed collaborative communication system modelling and capacity calculation can be a very useful tool in practice, because the required capacity of the network can be maintained with the reduced energy consumption in the network. Thus, by using collaborative communication inside the complex networks can be used as a method for reducing overall power consumption in the network.

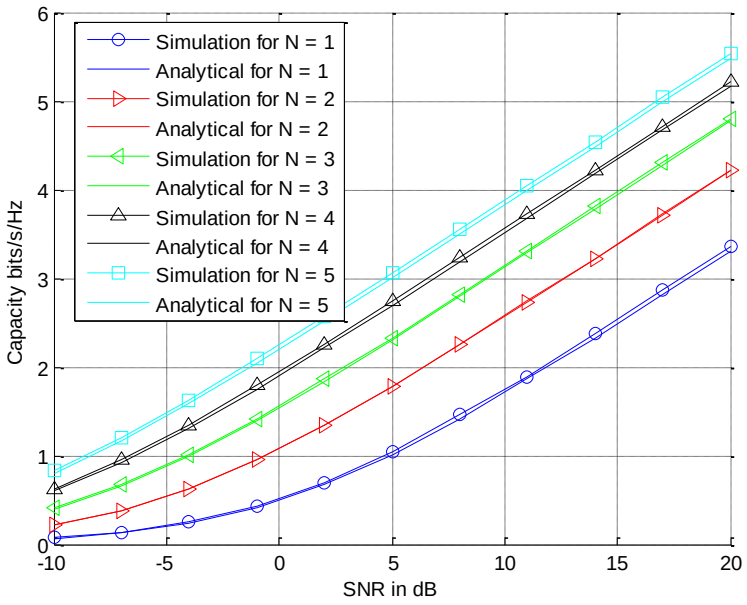

Figure 7.6 Capacity for phase error distributed over $\{-0.1\pi \sim 0.1\pi\}$ and each node transmits power P, so total transmitted power by the network is NP

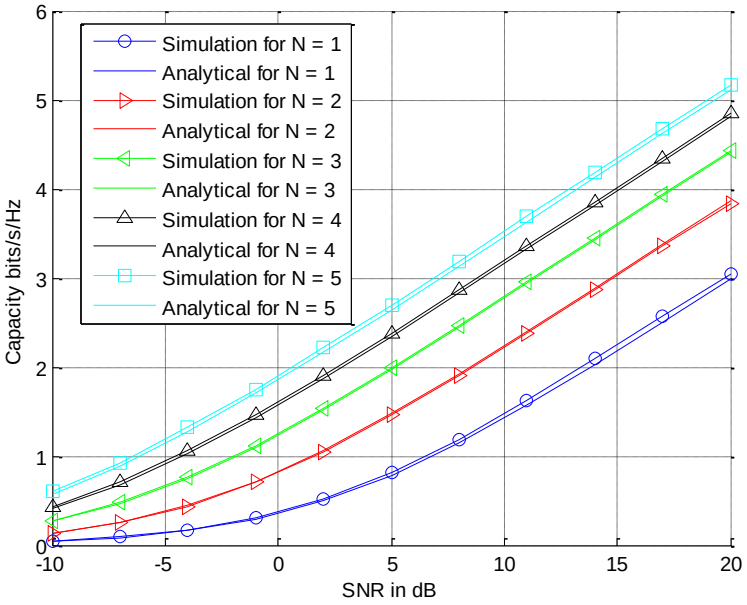

Figure 7.7 Capacity for phase error distributed over $\{-0.4\pi \sim 0.4\pi\}$ and each node transmits power P, so total transmitted power by the network is NP

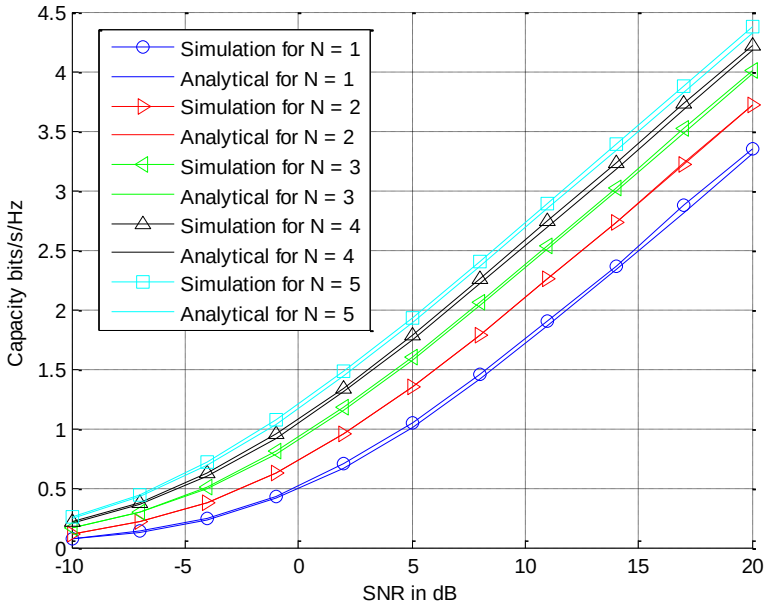

Figure 7.8 Capacity for phase error distributed over {-0.1π~0.1π} and each node transmits power *P/N*, so total transmitted power by the network is *P*

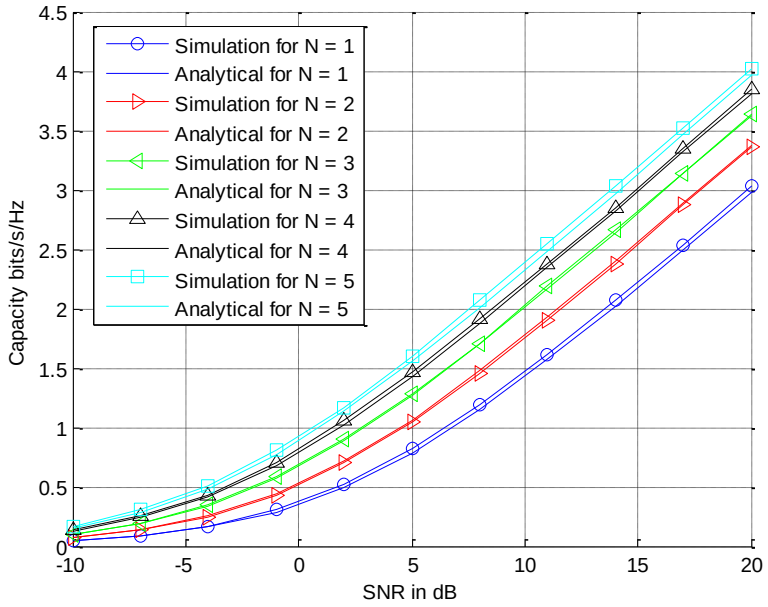

Figure 7.9 Capacity for phase error distributed over {-0.4π~0.4π} and each node transmits power *P/N*, so total transmitted power by the network is *P*

7.5 Capacity of Collaborative Communication Model with imperfect frequency synchronization

In this section, the capacity of collaborative communication model with imperfect frequency synchronization and with the assumption that there is perfect time and phase

synchronization between the collaborative nodes and the base station in the presence of AWGN and Rayleigh fading is presented. Let *N* collaborative nodes make a network to transfer the information to the base station. As each collaborative node has its own oscillator, there may be frequency mismatch between the collaborative nodes and the base station. The system model for the collaborative communication model with imperfect frequency synchronization in the presence of AWGN and Rayleigh fading is shown in Figure 7.10. It is composed of *N* collaborative node transmitters represented as Source (Node). Each collaborative node has a transceiver to receive a signal from other collaborative nodes within the network and transmit the signal to the base station. Each collaborative node also has a phase lock loop (PLL) for offset correction and a modulator to modulate the signal. The channel is considered as an AWGN and a Rayleigh fading channel. For each transmitted signal, the Rayleigh fading channel has an independent effect. On the receiver side, denoted as the base station, there is a demodulator to demodulate the received signal. The demodulator multiplies the received signal with a cosine signal; passes it through a low pass filter (LPF) and then integrates it. Then the power of demodulated signal and channel capacity is calculated.

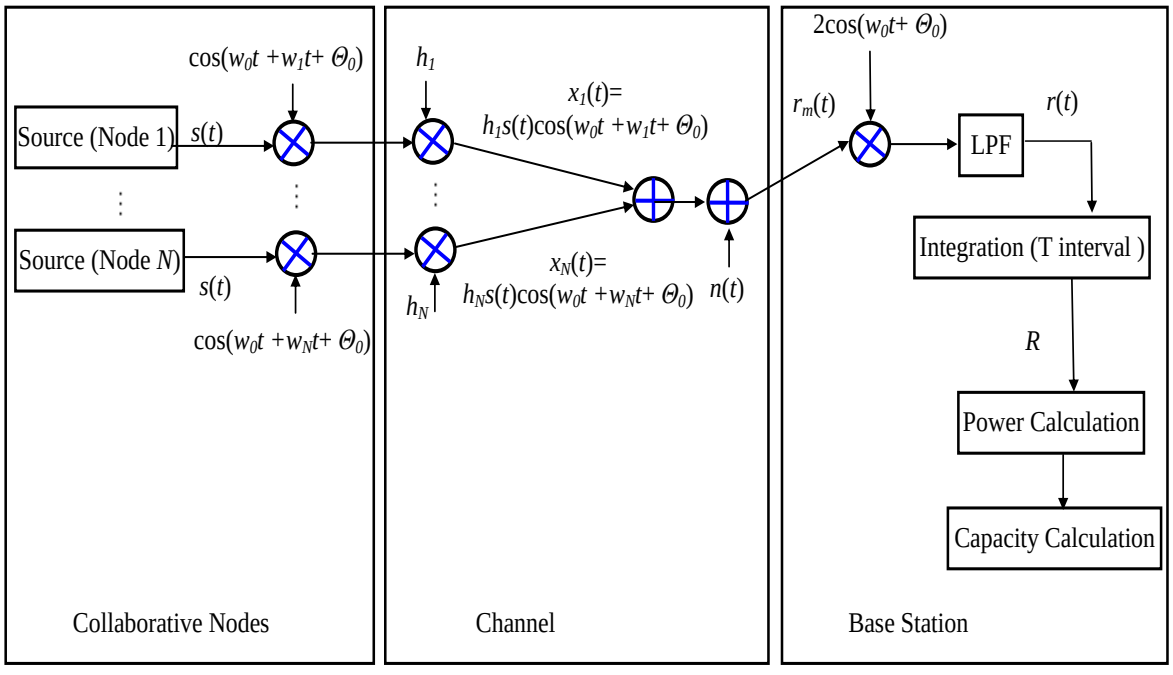

Figure 7.10 System Model

7.5.1 Theoretical Model of Collaborative Communication with imperfect frequency synchronization

In section 4.6, a collaborative communication model with imperfect frequency synchronization and on the assumption that there is perfect time and phase synchronization between the collaborative nodes and the base station in the presence of AWGN and Rayleigh fading is modelled, theoretically analyzed, and simulated. The power of the received signal is presented in equation (4.21) and is expressed as

$$P_R = \left| \sum_{i=1}^{N} h_i S \frac{\sin(\Delta w_i T)}{\Delta w_i T} + n \right|^2 . \tag{7.13}$$

As h_i, Δw_i and n are the random variables, so we have to calculate the mean value of received power.

$$E[P_R] = E\left[\left| \sum_{i=1}^{N} h_i S \frac{\sin(\Delta w_i T)}{\Delta w_i T} + n \right|^2 \right]. \tag{7.14}$$

As h_i, Δw_i and n are the independent random variables and n is zero-mean random variable, the above equation can be written as

$$E[P_R] = NS^2 \left[1 + \frac{(w_e T)^4}{180} - \frac{(w_e T)^2}{9} \right] + \frac{N(N-1)\pi b^2 S^2}{2} \left[1 - \frac{(w_e T)^2}{18} \right]^2 + \frac{N_0}{2}. \tag{7.15}$$

where w_e is distribution limit of frequency error and b is the mode of Rayleigh random variable h. The power of the received signal is the sum of the signal part and noise part. Thus the capacity of the ideal collaborative communication system can be found as

$$C = \frac{1}{2} \log_2 \left(1 + \frac{S_P}{N_P} \right), \tag{7.16}$$

Where S_P is signal power N_P and is noise power.

Using the values of signal power and noise power from equation (7.15) into equation (7.16), we may have

$$C = \frac{1}{2}\log_2\left(1+\frac{NS^2\left[1+\frac{(w_eT)^4}{180}-\frac{(w_eT)^2}{9}\right]+\frac{N(N-1)\pi b^2S^2}{2}\left[1-\frac{(w_eT)^2}{18}\right]^2}{\frac{N_0}{2}}\right) . \quad (7.17)$$

Special Case:

If the transmitted power of each relay node is reduced by N times, equation (7.17) may be written as

$$C = \frac{1}{2}\log_2\left(1+\frac{S^2\left[1+\frac{(w_eT)^4}{180}-\frac{(w_eT)^2}{9}\right]+\frac{(N-1)\pi b^2S^2}{2}\left[1-\frac{(w_eT)^2}{18}\right]^2}{\frac{N_0}{2}}\right) . \quad (7.18)$$

This is the case when the power of each relay node by factor N, i.e., the total transmitted is P is reduced. This reduction will be used to investigate the capacity of each relay node with reduced power consumption. This case can be used to investigate the effect of total transmitted power on capacity.

7.5.2 Analysis and Results

In this section the analytical and simulated results of the capacity of a collaborative communication system in the presence of frequency error are presented. A Monte Carlo simulation is performed to analyze the capacity of collaborative communication system in the presence of frequency error using MATLAB®. The wireless communication environment used in simulation is established using SIMULINK's AWGN and Rayleigh channel blocks.

From Figures 7.11, 7.12, 7.13 and 7.14 it is found that if the total transmitted power of the network is decreased by factor N, where N is number of collaborative nodes, we can still achieve substantial capacity gain. From equations (7.17), (7.18) and results shown in Figures 7.11, 7.12, 7.13 and 7.14, it is also observed, that if the total transmitted power is decreased by factor N, capacity will decreased by only factor $0.5\log_2[(N\text{-}1)(1\text{-}(w_eT)^2/18)^2]$ approximately, where w_e is the frequency error, in the presence of AWGN, Rayleigh fading and frequency errors.

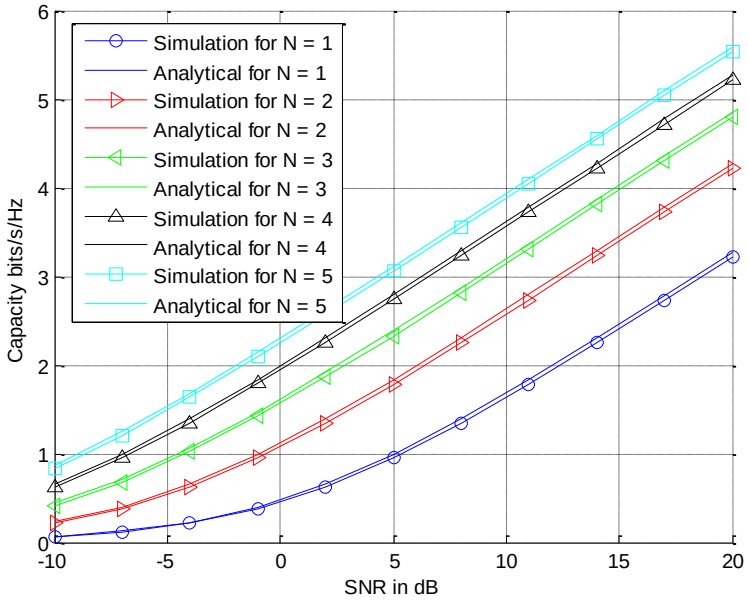

Figure 7.11 Capacity by considering the parameters of CC2420 i.e., frequency error distributed over {-200 KHz ~200 KHz} and data rate 250 Kbps and each node transmits power *P*, so total transmitted power by the network is *NP*

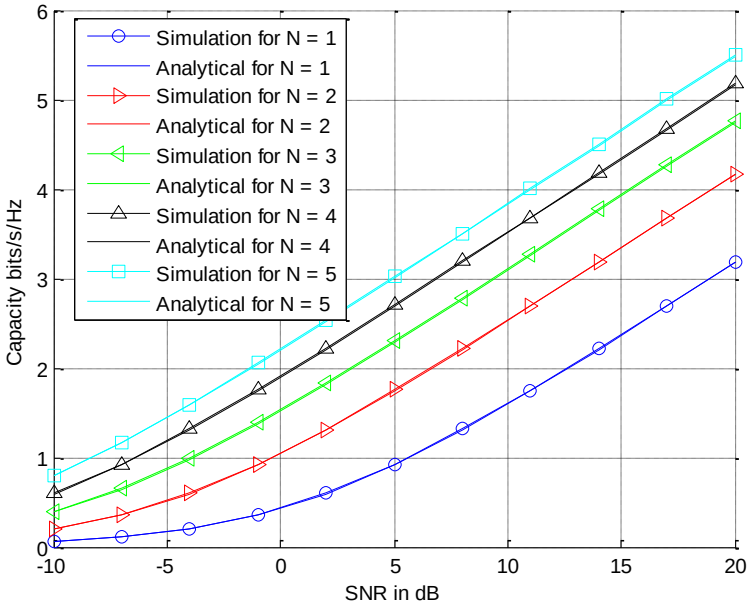

Figure 7.12 Capacity by considering the parameters of AT86RF21 i.e., frequency error distributed over {-55KHz ~55KHz} and data rate 40 Kbps and each node transmits power *P*, so total transmitted power by the network is *NP*

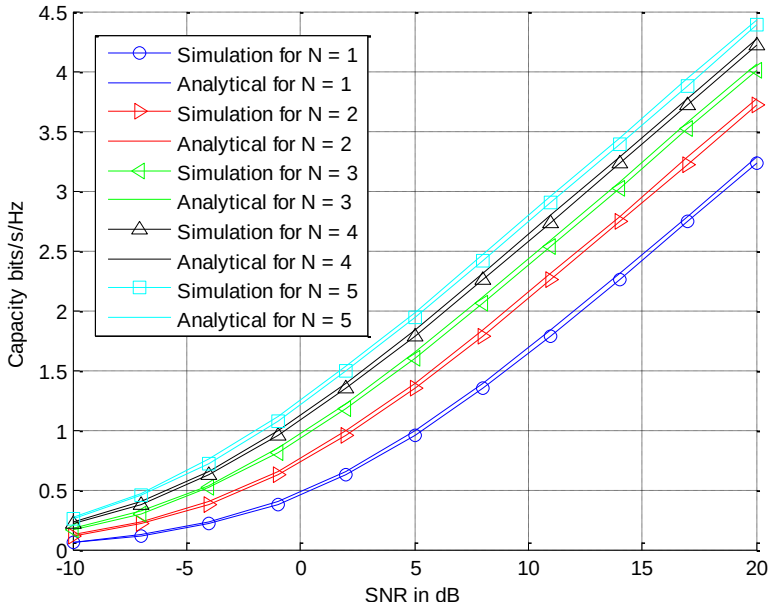

Figure 7.13 Capacity by considering the parameters of CC2420 i.e., frequency error distributed over {-200 KHz ~200 KHz} and data rate 250 Kbps and each node transmits power *P/N*, so total transmitted power by the network is *P*

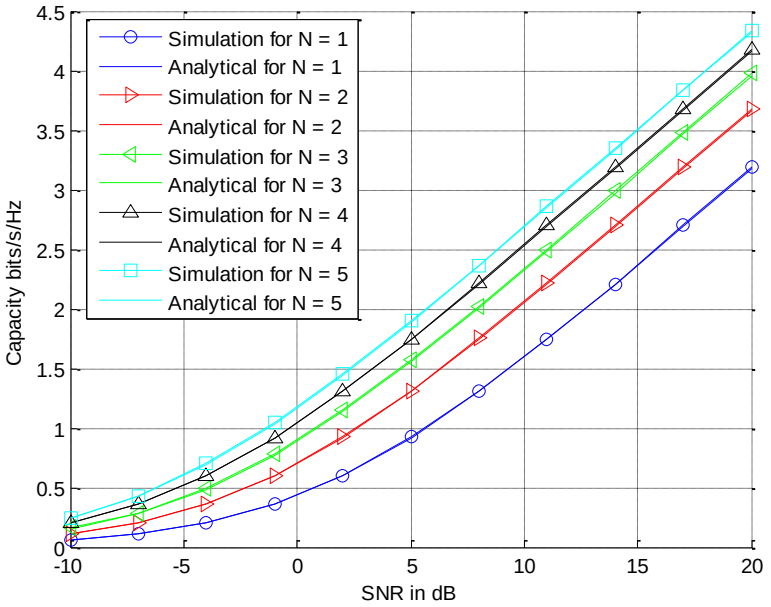

Figure 7.14 Capacity by considering the parameters of AT86RF21 i.e., frequency error distributed over {-55KHz ~55KHz} and data rate 40Kbps and each node transmits power *P/N*, so total transmitted power by the network is *P*

7.6 Capacity of Collaborative Communication Model with imperfect phase and frequency synchronization

In this section, the capacity of collaborative communication model with imperfect phase and frequency synchronization among the collaborative nodes and the base station in the presence of AWGN and Rayleigh fading is presented. Let *N* collaborative nodes make a network to transfer the information to the base station. The system model of a collaborative communication model with imperfect phase and frequency synchronization in the presence of AWGN and Rayleigh fading is shown in Figure 7.15. It is composed of *N* collaborative nodes transmitters represented as Source (Node). Each collaborative node has a transceiver to receive signals from other collaborative nodes within the network and to transmit signals to the base station. Each collaborative node also has a phase lock loop (PLL) for offset correction and a modulator to modulate the signal. The channel is considered as an AWGN and a Rayleigh fading channel. The Rayleigh fading channel for each transmitted signal has an independent effect. On the receiver side, denoted as the base station, there is a demodulator to demodulate the received signal. The demodulator multiplies the received signal with a cosine signal; passes it through low pass filter (LPF) and then integrates it. Then the power of demodulated signal and channel capacity is calculated.

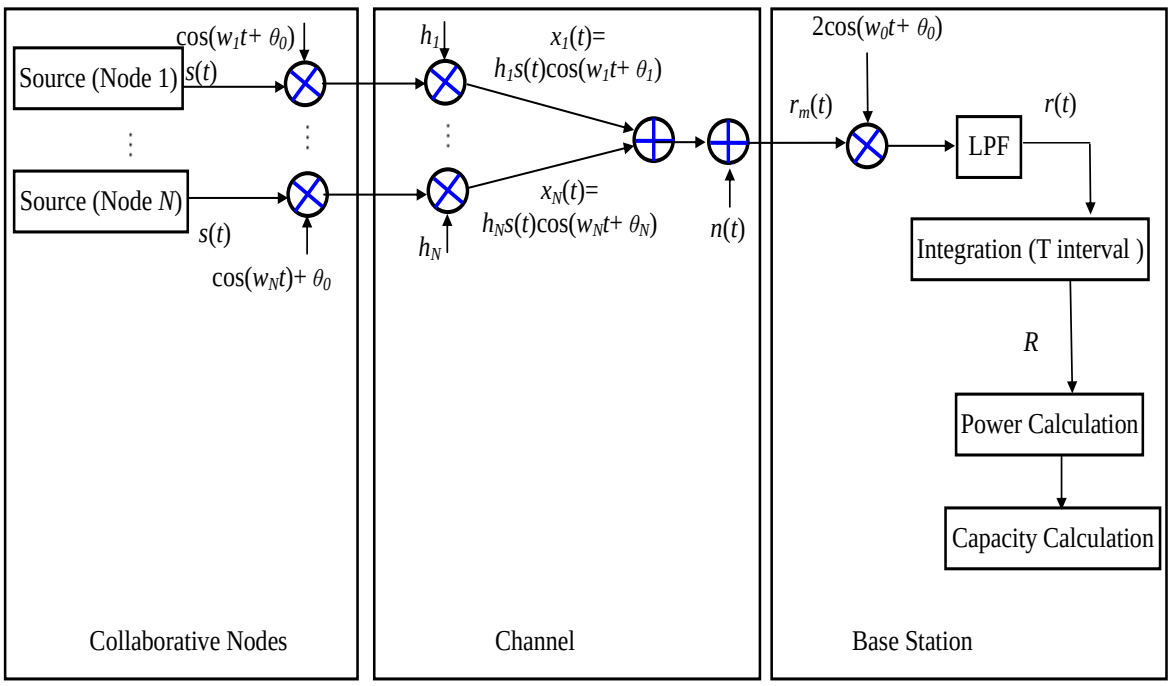

Figure 7.15 System Model

7.6.1 Theoretical Model of Collaborative Communication with imperfect phase and frequency synchronization

In section 4.7, a collaborative communication model with imperfect frequency synchronization and with the assumption that there is perfect time and phase synchronization between the collaborative nodes and the base station in the presence of AWGN and Rayleigh fading is proposed, modelled, theoretically analyzed, and simulated. The power of the received signal is presented in equation (4.29) and expressed as

$$P_R = \left[\sum_{i=1}^{N} h_i S \left(\frac{\sin(\Delta w_i T + \Delta\theta_i)}{\Delta w_i T} - \frac{\sin(\Delta\theta_i)}{\Delta w_i T} \right) + n \right]^2 . \tag{7.19}$$

As Δw_i, $\Delta\theta_i$, h_i and n are the random variables, so we have to calculate the mean value of received power as

$$E[P_R] = E\left[\sum_{i=1}^{N} h_i S \left(\frac{\sin(\Delta w_i T + \Delta\theta_i)}{\Delta w_i T} - \frac{\sin(\Delta\theta_i)}{\Delta w_i T} \right) + n \right]^2 . \tag{7.20}$$

As Δw_i, $\Delta\theta_i$, h_i and n are the independent random variables and n is zero-mean random variable, the above equation can be written as

$$\begin{aligned} E[P_R] &= NS^2 \left[1 + \frac{(w_e T)^4}{180} - \frac{(w_e T)^2}{9} \right] \left[\frac{1}{2} + \frac{\sin(2\psi)}{4\psi} \right] + \\ &\frac{N(N-1)S^2 b^2 \pi}{2} \left[\left(1 - \frac{(w_e T)^2}{18} \right) \left(\frac{\sin(\psi)}{\psi} \right) \right]^2 + \frac{N_0}{2} \end{aligned} \tag{7.21}$$

where ψ is distribution limit of phase error, w_e is distribution limit of frequency error and b is the mode of Rayleigh random variable h.

The power of the received signal is the sum of the signal part and noise part. Thus the capacity of the ideal collaborative communication system can be found as

$$C = \frac{1}{2} \log_2 \left(1 + \frac{S_P}{N_P} \right), \tag{7.22}$$

Where S_P is signal power N_P and is noise power. Using the values of signal power and noise power from equation (7.21) into equation (7.22), we may have

$$C = \frac{1}{2}\log_2\left(1 + \frac{NS^2\left[1 + \frac{(w_eT)^4}{180} - \frac{(w_eT)^2}{9}\right]\left[\frac{1}{2} + \frac{\sin(2\psi)}{4\psi}\right] + \frac{N(N-1)S^2b^2\pi}{2}\left[\left(1 - \frac{(w_eT)^2}{18}\right)\left(\frac{\sin(\psi)}{\psi}\right)\right]^2}{\frac{N_0}{2}}\right) \tag{7.23}$$

Special Case:

If the transmitted power of each relay node is decreased by *N*, equation (7.23) may be written as,

$$C = \frac{1}{2}\log_2\left(1 + \frac{S^2\left[1 + \frac{(w_eT)^4}{180} - \frac{(w_eT)^2}{9}\right]\left[\frac{1}{2} + \frac{\sin(2\psi)}{4\psi}\right] + \frac{(N-1)S^2b^2\pi}{2}\left[\left(1 - \frac{(w_eT)^2}{18}\right)\left(\frac{\sin(\psi)}{\psi}\right)\right]^2}{\frac{N_0}{2}}\right) \tag{7.24}$$

This is the case in which the power of each relay node is reduced by factor *N*, i.e., the total transmitted is *P*. This reduction will be used to investigate the capacity with reduced power consumption of each relay node. This case can be used to investigate the effect of total transmitted power on capacity.

7.6.2 Analysis and Results

In this section the analytical and simulated results of the capacity of a collaborative communication system with imperfect phase and frequency synchronization are presented. A Monte Carlo simulation is performed to analyze the capacity of collaborative communication with imperfect phase and frequency synchronization using MATLAB®. The wireless communication environment used in the simulation is established using SIMULINK's AWGN and Rayleigh channel blocks.

Results show that the analytical results match very well with the simulated results. Figures 7.16 and 7.17 present the analytical and simulated results of the model in the presence of Rayleigh fading for product CC2420 i.e., frequency error distributed over {-200 KHz ~ 200 KHz} and phase error distributed over {-0.1π~0.1π} and {-0.4π~0.4π} respectively, and assuming that the power of each collaborative node is *P*, so the total

transmitted power of the network is equal to *NP*. Figures 7.18 and 7.19 present the analytical and simulated results of our model in the presence of Rayleigh fading for product AT86RF212 i.e., frequency error distributed over {-55 KHz ~ 55 KHz} and phase error distributed over {-0.1π~0.1π} and {-0.4π~0.4π} respectively, and assuming that the power of each collaborative node is *P*, thus, the total transmitted power of the network is equal to *NP*.

Figures 7.20 and 7.21 present the analytical and simulated results of the model in the presence of Rayleigh fading for product CC2420 i.e., frequency error distributed over {-200 KHz ~ 200 KHz} and phase error distributed over {-0.1π~0.1π} and {-0.4π~0.4π} respectively, for instances where the transmitted power of each collaborative node is *P*/*N*, so the total transmitted power of the network, is *P*. Figures 7.22 and 7.23 present the analytical and simulated results of the model in the presence of Rayleigh fading for product AT86RF212 i.e., frequency error distributed over {-55 KHz ~ 55 KHz} and phase error distributed over {-0.1π~0.1π} and {-0.4π~0.4π} respectively, for the instances where the transmitted power of each collaborative node is *P*/*N*, so the total transmitted power of the network is *P*.

From results shown in Figure 7.16 to Figure 7.23, it is confirmed that the capacity of the system increases as number of collaborative nodes increases. It is also shown that capacity decreases as the phase error increases. From Figures 7.16 to Figure 7.23, it is obvious that capacity decreases by approx. 0.3 bits/sec/Hz, when the phase error distribution increases from {-0.1π~0.1π} to {-0.4π~0.4π}.

From Figure 7.16 to Figure 7.23 it is observed that, if the total transmitted power of the network is decreased by factor *N*, where *N* is number of collaborative nodes, substantial capacity gain can still be achieved. From equations (7.23), (7.24) and the results shown in Figure 7.16 to Figure 7.23, it is also analyzed that, if the total transmitted power is decreased by factor *N*, capacity will decreased by only factor $0.5\log_2[(N-1)\{(\sin(\varphi)/\varphi)(1-(w_eT)^2/18)\}^2]$ approximately, where φ is the phase error and w_e is the frequency error, in the presence of AWGN.

In practice, the proposed collaborative communication system modelling and capacity calculation is a very useful tool, because the required capacity of the network can be maintained with the reduced energy consumption in the network. Thus, the use of collaborative communication inside complex networks can be employed as a method for reducing overall power consumption in the network.

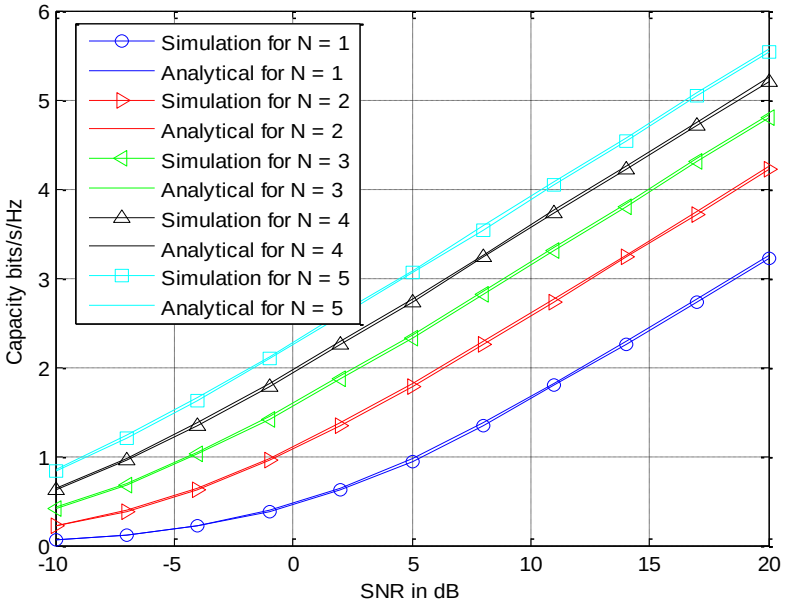

Figure 7.16 Capacity by considering the parameters of CC2420 i.e., frequency error distributed over {-200 KHz ~200 KHz} and data rate 250 Kbps, with phase error distributed over $\{-0.1\pi \sim 0.1\pi\}$ and each node transmits power P, so total transmitted power by the network is NP

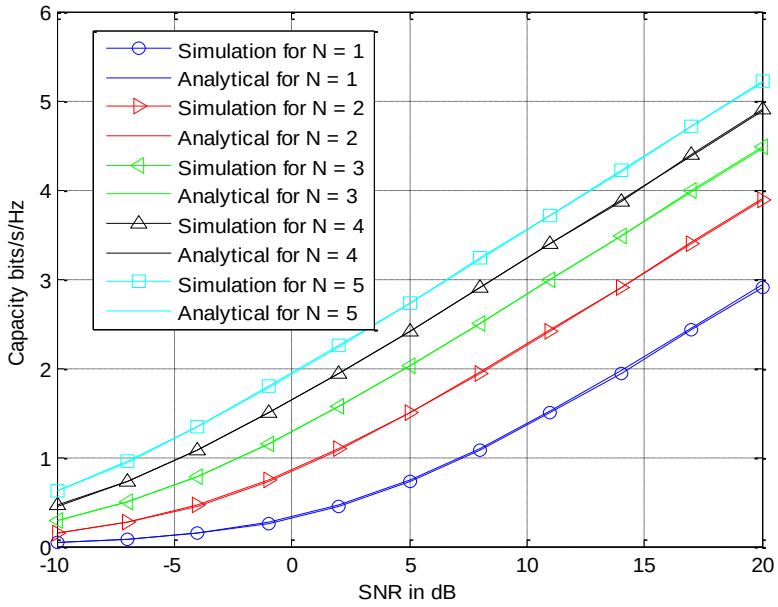

Figure 7.17 Capacity by considering the parameters of CC2420 i.e., frequency error distributed over {-200 KHz ~200 KHz} and data rate 250 Kbps, with phase error distributed over $\{-0.4\pi \sim 0.4\pi\}$ and each node transmits power P, so total transmitted power by the network is NP

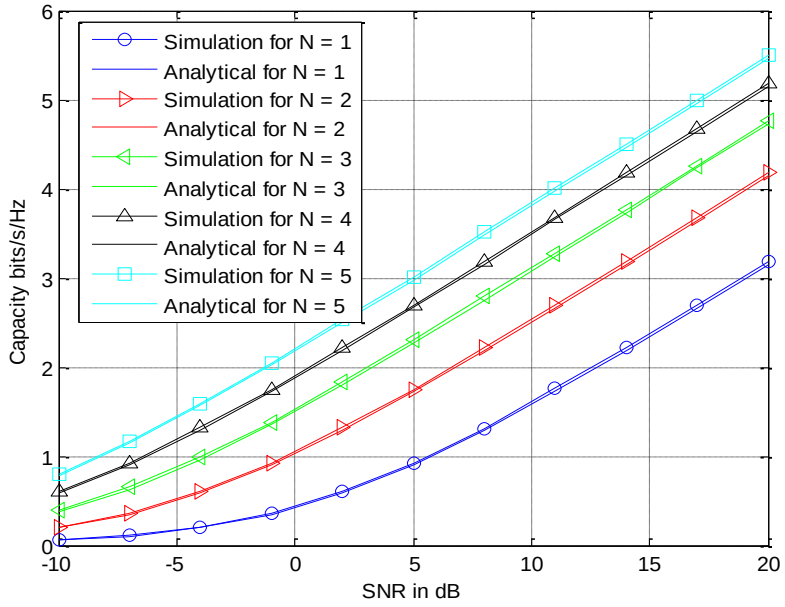

Figure 7.18 Capacity by considering the parameters of AT86RF21 i.e., frequency error distributed over {-55 KHz ~55 KHz} and data rate 40 Kbps, with phase error distributed over $\{-0.1\pi \sim 0.1\pi\}$ and each node transmits power P, so total transmitted power by the network is NP

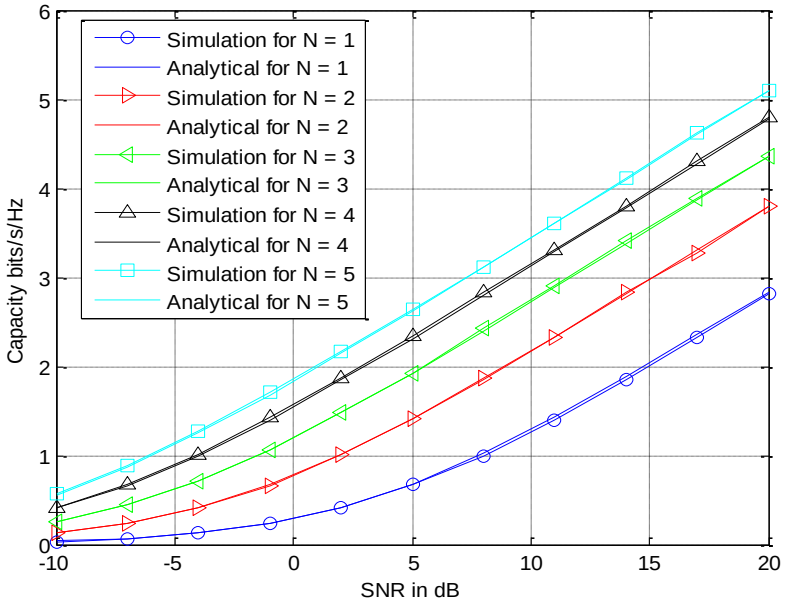

Figure 7.19 Capacity by considering the parameters of AT86RF21 i.e., frequency error distributed over {-55 KHz ~55 KHz} and data rate 40 Kbps, with phase error distributed over $\{-0.4\pi \sim 0.4\pi\}$ and each node transmits power P, so total transmitted power by the network is NP

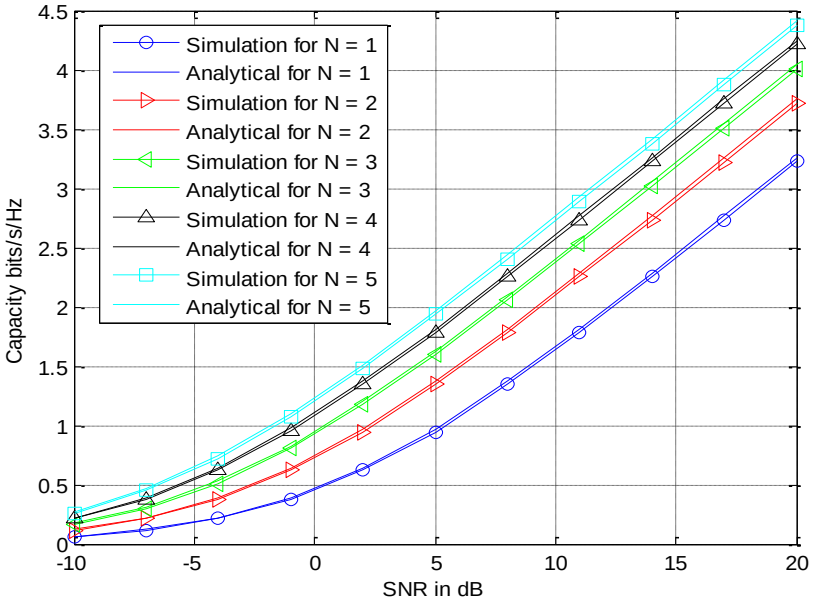

Figure 7.20 Capacity by considering the parameters of CC2420 i.e., frequency error distributed over {-200 KHz ~200 KHz} and data rate 250 Kbps, with phase error distributed over $\{-0.1\pi \sim 0.1\pi\}$ and each node transmits power P/N, so total transmitted power by the network is P

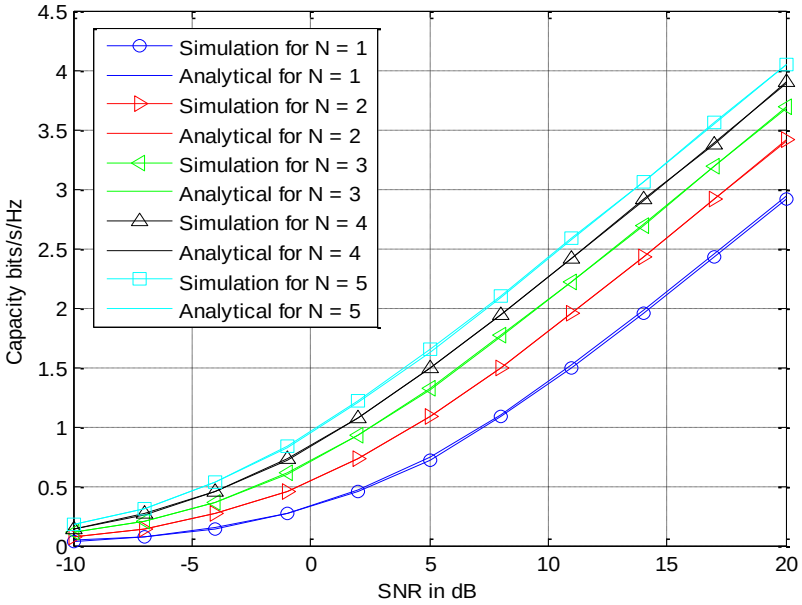

Figure 7.21 Capacity by considering the parameters of CC2420 i.e., frequency error distributed over {-200 KHz ~200 KHz} and data rate 250 Kbps, with phase error distributed over $\{-0.4\pi \sim 0.4\pi\}$ and each node transmits power P/N, so total transmitted power by the network is P

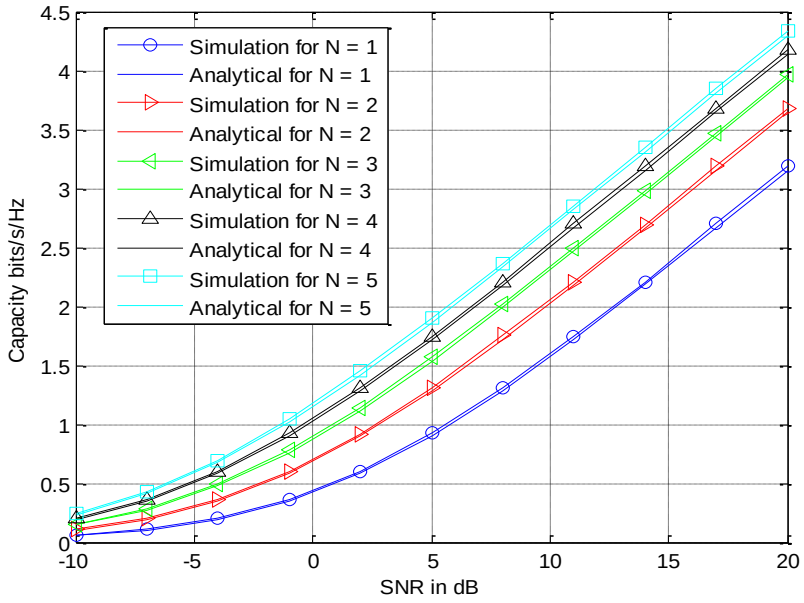

Figure 7.22 Capacity by considering the parameters of AT86RF21 i.e., frequency error distributed over {-55 KHz ~55 KHz} and data rate 40 Kbps, with phase error distributed over {-0.1π~0.1π} and each node transmits power *P/N*, so total transmitted power by the network is *P*

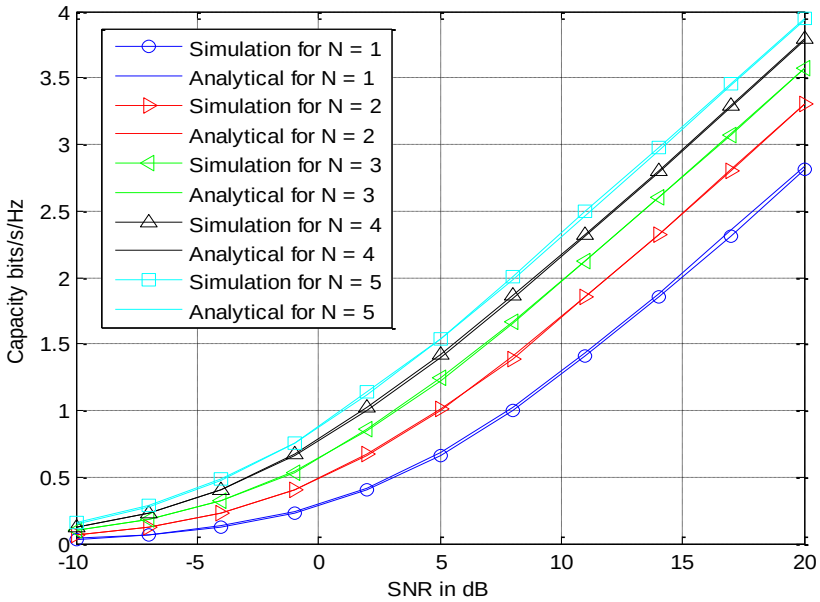

Figure 7.23 Capacity by considering the parameters of AT86RF21 i.e., frequency error distributed over {-55 KHz ~55 KHz} and data rate 40 Kbps, with phase error distributed over {-0.4π~0.4π} and each node transmits power *P/N*, so total transmitted power by the network is *P*

7.7 Chapter Conclusions

In this chapter the capacity of four collaborative communication systems is investigated i.e., the ideal collaborative communication model, collaborative communication with imperfect phase synchronization only, collaborative communication with imperfect frequency synchronization only, and collaborative communication with imperfect phase and frequency synchronization, in the presence of flat Rayleigh fading and AWGN. This research contributes to the development of average capacity expressions for these four systems, expressed as a function of signal to noise ratio, with the number of collaborative nodes as a parameter. The obtained capacity expressions clearly present the capacity gain capability of collaborative communication systems that is the consequence of the collaborative communication that can be considered as a space diversity system. The derived expressions show that the channel capacity is a function of the number of collaborative nodes, the parameters relate to the distribution phase error and frequency error.

A MATLAB®-based WSN simulator is developed to confirm the results of these algorithms. For analysis, the parameters of two off-the-shelf products i.e. CC2420 and AT86RF212 are considered. It is concluded that a significant capacity gain can be achieved by increasing the number of collaborative nodes, without increasing the total transmitted power. This is the consequence of the collaborative communication that can be considered as a space diversity system. It is observed, that that capacity gain significantly increases as the number of collaborative nodes increases, and capacity gain significantly decreases as phase error and frequency error increases.

In particular, the author analysed the case in which the power of the transmitted signal is reduced by N times where N is the number of collaborative nodes. It is concluded that capacity will decreased only by factor of $0.5\log2(N)$ in an ideal case, by factor of $0.5\log_2[(N\text{-}1)(\sin(\varphi)/\varphi)^2]$ in presence of phase error, by factor of $0.5\log_2[(N\text{-}1)(1\text{-}(w_eT)^2/18)^2]$ in presence of frequency error and by factor of $0.5\log_2[(N\text{-}1)\{(\sin(\varphi)/\varphi)(1\text{-}(w_eT)^2/18)\}^2]$ in the presence of phase and frequency error, if the total transmitted power is decreased by N times. It is shown that the capacity can be maintained at high, in this case, which leads to substantial power saving in the system.

References

[1] IEEE 802.15.4 version 2006, IEEE Standards Association. [Online]. Available: http://standards.ieee.org/getieee802/download/802.15.4-2003.pdf. [Access: Aug 5, 2009].

[2] AT86RF212, ATMEL Products, [Online]. http://www.atmel.com/dyn/products/product_card.asp?PN=AT86RF212. [Access: Jan 5, 2009].

[3] CC2420, Texas Instruments, [Online]. Available: http://focus.ti.com/analog/docs/enggresdetail.tsp?familyId=367&genContentId=3573. [Access: Jan 5, 2009].

[4] E.C.van der Meulen, "A survey of multiway channels in information theory: 1961-1976", IEEE Trans. on Inf. Theory, Vol. IT-23, No. 1, Jan. 1977, pp. 1 – 37.

[5] T.M. Cover, "Capacity theorems for the relay channel", IEEE Trans. on Inf. Theory, Vol. IT-25, No. 5, Sep. 1979, pp. 572 – 584.

[6] P. Gupta, P.R. Kumar, "The capacity of wireless network", IEEE Trans. on Inf. Theory, Vol. 46, No. 2, Mar. 2000, pp. 388 – 404.

[7] G. Kramer, M. Gaspar, P. Gupta, "Cooperative strategies and capacity theorems for relay networks", IEEE Trans. on Inf. Theory, Vol. 51, No. 9, Sep. 2005, pp. 3037 – 3063.

[8] Host-Madsen, "Capacity bounds for cooperative diversity", IEEE Trans. on Inf. Theory, Vol. 52, No. 4, Apr. 2006, pp. 1522 – 1544.

[9] S.S. Ikki, M.H. Ahmed, "Performance analysis of adaptive decode-and-forward cooperative diversity networks with best relay selection", IEEE Trans. on Communications, Vol. 53, No. 1, January 2010, pp. 68 - 72.

[10] T. Wang, A. Cano, G. B. Giannakis and J.N. Laneman, "High-performance cooperative demodulation with decode-and-forward relays", IEEE Trans. on Communications, Vol. 55, No. 7, July 2007, pp. 1427 – 1438.

[11] S.S. Ikki, M.H. Ahmed, "Exact error probability and channel capacity of the best-relay cooperative-diversity networks", IEEE Signal Processing Letter, Vol. 16, No. 12, Dec. 2009, pp. 1051 - 1054.

[12] S.S. Ikki, M.H. Ahmed, "Performance analysis of multi-branch decode-and-forward cooperative diversity networks over Nakagami-m fading channel", IEEE Conf. on Communications, ICC 2009, Vol. 53, No. 1, January 2009, pp. 1-6.

[13] N.L Kanal, A.R.K. Sastry, "Models for channels with memory and their application to error control", Proceedings of IEEE, Vol. 66, No. 7, July 1978, pp.724-744.

[14] S. Berkovits, E.L. Cohen and N. Zierler, "A model for error digital distribution", 1st IEEE Annual Communication Conference, June 1965, pp. 103-111.

[15] E.N. Gilbert, "Capacity of a burst noise channel", B.S.T.J., Vol. 39, September 1960, pp.1253-1265.

[16] G.N. Karystinos and A.P. Liavas "Outage capacity of a cooperative scheme with binary input and a simple relay", IEEE International Conference on Acoustics, Speech and Signal Processing (ICASSP), March 2008, pp. 3221 - 3224.

[17] E.J. Duarte-Melo and M. Liu, "Data-Gathering Wireless Sensor Networks: Organization and Capacity," Computer Networks, vol. 43, 2003, pp. 519-537.

[18] D. Marco, E.J. Duarte-Melo, M. Liu, and D.L. Neuhoff, "On the Many-to-One Transport Capacity of a Dense Wireless Sensor Network and the Compressibility of Its Data," Proc. Int'l Workshop Information Processing in Sensor Networks, 2003.

[19] H. El Gamal, "On the Scaling Laws of Dense Wireless Sensor Networks: The Data Gathering Channel," IEEE Trans. Information Theory, vol. 51, no. 3, Mar. 2005, pp. 1229-1234.

[20] R. Zheng and R.J. Barton, "Toward Optimal Data Aggregation in Random Wireless Sensor Networks," Proc. IEEE INFOCOM, 2007.

[21] B. Liu, D. Towsley, and A. Swami, "Data Gathering Capacity of Large Scale Multihop Wireless Networks," Proc. IEEE Fifth Int'l Mobile Ad Hoc and Sensor Systems (MASS), 2008.

[22] S. Chen, Y. Wang, X.-Y. Li, and X. Shi, "Capacity of Data Collection in Randomly-Deployed Wireless Sensor Networks," Wireless Networks, vol. 17, no. 2, Feb. 2011, pp. 305-318.

[23] S. Chen, M. Huang, S. Tangand Y. Wang, “Capacity of Data Collection in Arbitrary Wireless Sensor Networks”, IEEE Transactions on Parallel and Distributed Systems, Vo. 23, Issue 1, 2012, pp. 52 – 60.
[24] Q. Tao, S. Berber and Y.Cheng, “Capacity calculation and control in wireless sensor network with cooperative decode and forward communications”, 7th International Wireless Communications and Mobile Computing Conference (IWCMC), 2011, 1624 – 1629.
[25] S. Chen, M. Huang, S. Tangand Y. Wang, “Capacity of Data Collection in Arbitrary Wireless Sensor Networks”, IEEE Transactions on Parallel and Distributed Systems, Vo. 23, Issue 1, 2012, pp. 52 – 60.

Chapter 8 Conclusions and Future Work

This thesis tackles several problems that are related to reducing the energy consumption of sensor nodes in carrying out wireless communication. The ultimate target is to maximize the lifetime of wireless sensor network (WSN) in providing a satisfactory service for data sensing and transmission. The studies are dedicated to developing energy-efficient communication systems for wireless sensor networks in the presence of AWGN and Rayleigh fading by exploiting the theory of virtual array of independent transmitters. The key requirements of a virtual array for sensor networks are identified and considered in the development of a collaborative communication system. The key factors that degrade the performance of collaborative communication are also identified.

The developed collaborative communication system is an energy efficient algorithm for wireless sensor networks in the presence of AWGN and Rayleigh fading, due to the following advantages:

- Produces substantial power gain at the receiver.
- Considerably mitigates fading effects.
- Produces significant channel capacity gain.
- Collaborative communication outperforms SISO systems for medium and long range communication systems.

This chapter summarizes the important findings in the development of these algorithms, the performance evaluation of the algorithms and the performance evaluation of the networks based on these algorithms. Also, suggestions for future work are presented in the reminder of this chapter.

8.1 Summary of Important Findings

The first step of this research was to understand the feasibility of collaborative communication i.e., virtual array of independent transmitters for sensor networks to achieve the benefits of centralized antenna array. It is found that in a sensor network, the accurate position of the sensor nodes is generally not known and that each transmitter has its own local oscillator; the theory of centralized antenna array cannot be applied directly. Specifically, the two related assumptions in regard to frequency synchronization and phase synchronization among the transmitters are much more challenging for a

distributed wireless sensor network than for a centralized antenna array. Hence, the key requirements for the development of collaborative communication for wireless sensor networks i.e., phase, frequency and time synchronization among the collaborative nodes and base station, are identified. The synchronization process is developed to achieve time, frequency and phase synchronization between the collaborative nodes and the base station.

From the study of several synchronization algorithms for wireless communication, it is observed that 100% synchronization among the transmitters is very difficult to achieve. Therefore, we have proposed, modelled, theoretically analyzed and simulated several collaborative communication systems for sensor networks in the presence of AWGN and Rayleigh fading.

The developed systems for wireless sensor networks are:

4. Collaborative communication algorithm with imperfect phase synchronization and assuming perfect time and frequency synchronization.
5. Collaborative communication algorithm with imperfect frequency synchronization and assuming perfect time and phase synchronization.
6. Collaborative communication algorithm with imperfect phase and frequency synchronization.

To evaluate the performance of the proposed collaborative communication systems, several figure of merits are considered i.e., received power, bit error rate (BER) and channel capacity.

From study of different wireless network algorithms, it is understood that significant fade margin is often needed to compensate for the effects of channel fading on signal power loss. The exploitation of the space diversity of collaborative communication was considered; this has been confirmed as effective in reducing the channel fading, as the energy-efficient physical layer algorithm for sensor networks. In this regard, the fading-mitigating capability of collaborative communication was investigated. Then, collaborative communication was employed for sensor nodes to save energy in conducting data transmissions in the fading channel.

To determine the fading-mitigating capability of the proposed system, the bit error rate (BER) expressions were developed for several collaborative communication systems for the AWGN and Rayleigh fading channel. Specifically, closed form expressions for the BER of a collaborative communication system with imperfect phase and frequency synchronization were derived. The derived BER expressions were verified by simulations

using parameters of off-the-shelf products i.e. CC2420 [18] and AT86RF212 [19]. Simulation results confirmed that, for a given BER value, the signal-to-noise ratio needed by collaborative communication systems was much less than that needed by corresponding SISO systems. For example, given that the bit error probability is set to be 10^{-3}, a collaborative communication system with 7 collaborative nodes, can reduce the required signal-to-noise ratio (E_b/N_o) by more than 13 dB, compared to the E_b/N_o of the corresponding single-user system. This means that the fade margin needed by the collaborative communication systems is much less than that required by the conventional SISO to compensate the channel fading.

It is observed that collaborative communication gains increases as the number of collaborative nodes increases. However, more circuit energy is required for data transmission. Therefore, we investigated how much power could be saved by utilizing collaborative communication at the expense of circuit power. In this regard, energy consumption and energy efficiency models are developed for collaborative communication system and SISO systems.

The collaborative nodes were compliant with the IEEE 802.15.4 standard. The energy efficiency for different collaborative communication systems was simulated using parameters of off-the-shelf products i.e. CC2420 [18] and AT86RF212 [19]. It was found that significant energy savings were attained by using the collaborative communication systems. However, for given values of fade margins, the values of energy savings were dependent on the path loss exponent and the transmission distance. According to the theoretical analysis and simulations, when the values of path loss exponent and transmission distance were increased, it was found that, in some cases, the lifetime of the sensor network could be extended several times.

To explore the channel capacity of a collaborative communication system, closed form expressions of channels capacity of several collaborative communication systems for wireless sensor networks were developed. Specifically closed form expressions for channel capacity of collaborative communication system with imperfect phase and frequency synchronization were derived. Simulation-based investigations using the parameters of off-the-shelf products i.e. CC2420 [18] and AT86RF212 [19], were carried out to verify the derived channel capacity expressions of several collaborative communication systems. It was found that significant capacity gain can be achieved using collaborative communication.

This allows us to conclude that the network energy efficiency can be improved by using collaborative communication.

8.2 Suggestions for Future Work

Large scale wireless sensor networks will carry on rising in popularity, offering many opportunities for diverse military and civilization applications. In regard to the emerging applications and related requirements of the communication between sensor nodes, there is always room for possible extensions that would extend the results of this thesis. A few suggestions are made to push the research forward in several directions as follows.

Firstly, more precise synchronization algorithms can be developed for sensor networks using precise distance estimation techniques.

Secondly, the investigation of collaborative communication systems may be extended to channels of a more complicated nature, such as the frequency selective fading channel and the fast fading channel [3-5]. In addition, the acquisition of channel status and time synchronization for collaborative communication systems, needs to be studied.

Thirdly, investigations of channel capacity for complex channels and other senor network techniques, such as; cooperative communications [6-8], chip interleaving technique [9-11], Multi-Input-Multi-Output (MIMO) signal processing [12-14] and CDMA-based systems [15- 17] can be carried out.

Last but not least, the harvesting of the understanding of node energy savings from cooperative communications [18, 19], chip-interleaving signal processing and multi-hop relay [20], a systematic study may be conducted, aimed at maximizing network energy efficiency by using these techniques in an optimal manner.

References

[1] CC2420, Texas Instruments Chipcon Products, http://focus.ti.com/analog/docs/ enggresdetail .tsp? familyId=367&genContentId=3573.

[2] AT86RF212, ATMEL Products, http://www.atmel.com/dyn/products/product_ card .asp? PN =AT86RF212.

[3] Y. Lin and D. Lin, "Multiple access over fading multipath channels employing chip-interleaving code division direct-sequence spread spectrum," IEICE Trans. on Commun., vol.E86-B(1), 2003, pp. 114-121.

[4] S. Zhou, G.B. Giannakis, and C. Le Martret, "Chip-interleaved block-spread code division multiple access, " IEEE Trans. on Commun, vol. 50, no.2, 2002, pp. 235-248.

[5] Y. Lin and D. W. Lin, "Multicode chip-interleaved DS-CDMA to effect synchronous correlation of spreading codes in quasi-synchronous transmission over multipath channels," IEEE Trans. on Wireless Commun, vol. 5, no.10, 2006, pp. 2638-2642.

[6] Z. Zhou, S. Zhou, S.Cui, and J. Cui , "Energy-efficient cooperative communication in a clustered wireless sensor network," IEEE Trans. Veh. Technol., vol.57, no.6, 2008, pp. 3618-3628.

[7] S. Cui and A. J. Goldsmith, "Cross-layer design in energy-constrained networks using cooperative MIMO Techniques," EURASIP Signal Processing Journal, vol. 86, no. 8, 2006, pp. 1804-1814.

[8] L. Simic, S. M. Berber, K. W. Sowerby, “Partner choice and power allocation for energy efficient cooperation in wireless sensor networks. in Proc. IEEE ICC’08, 2008, pp. 4255-4260.

[9] Y. Kimura, K. Shibata, and T. Sakai, "Precoder for chip-interleaved CDMA using space-time block-coding," IEICE Trans. Fundam. Electron. Commun. Comput. Sci., vol.E91-A, no.10, 2008, pp.2885-2888.

[10] Y. Lin and D. W. Lin, "Multicode chip-interleaved DS-CDMA to effect synchronous correlation of spreading codes in quasi-synchronous transmission over multipath channels," IEEE Transactions on Wireless Commun, vol. 5, no.10, 2006, pp. 2638-2642.

[11] S. Fang; S.M. Berber, A.K.Swain, “Closed-form average BER expression for chip-interleaved DS-CDMA system conducting M-ary communication and noncoherent demodulation in flat Rayleigh fading channel,” 15th Asia-Pacific Conference on Communications, 2009, pp. 144 – 147.

[12] L. Xiao and M. Xiao, "A new energy-efficient MIMO-sensor network architecture M-SENMA," in Proc. VTC’04, vol. 4, Sept. 2004, pp. 2941- 2945.

[13] G. J. Miao, "Multiple-input multiple-output wireless sensor networks communications," US Patent, No. US7091854, August 15, 2006.

[14] S. Cui, A. J. Goldsmith, and A. Bahai, "Energy-efficiency of MIMO and cooperative MIMO techniques in sensor networks," IEEE J. Sel. Areas Commun., vol.22, no.6, 2004, pp.1089-1098.

[15] H. Kang, H. Hong, S. Sung, and K. Kim, "Interference and sink capacity of wireless CDMA sensor networks with layered architecture," ETRI Journal, vol.30, no.1, 2008, pp.13-20.

[16] T. Shu and M. Krunz, "Energy-efficient power/rate control and scheduling in hybrid TDMA/CDMA wireless sensor networks," Computer Networks, vol. 53, no. 9, 2009, pp. 1395-1408.

[17] B.H. Liu, B.P. Otis, S. Challa, P. Axon, C. T. Chou, and S. K. Jha, "The impact of fading and shadowing on the network performance of wireless sensor networks," International Journal of Sensor Networks, vol. 3, no.4, 2008, pp. 211 – 223.

[18] L. Simic, Stevan M. Berber, and K. W. Sowerby, "Partner Choice and Power Allocation for Energy Efficient Cooperation in Wireless Sensor Networks," in Proc. IEEE ICC'08, pp. 4255-4260.

[19] L. Simic, Stevan M. Berber, K. W. Sowerby, "Distributed Partner Choice for Energy Efficient Cooperation in a Wireless Sensor Network," in Proc. IEEE GLOBECOM'08, pp. 4799-4804.

[20] S.Guo, J. Zheng, Y. Qu, B. Zhao, and Q. Pan, "Clustering and multi-hop routing with power control in wireless sensor networks," The Journal of China Universities of Posts and Telecommunications, vol. 14, no.1, 2007, pp. 49-57.

Appendix

Let Θ_f be having uniform distribution from {$-\varphi$ to φ}.

Appendix A.1

$$E\left[\cos(\Theta_f)\right] = \int_{-\infty}^{\infty} \cos(\Theta_f)\, p(\Theta_f)\, d\Theta_f = \int_{-\varphi}^{\varphi} \cos(\Theta_f)\, \frac{1}{2\varphi}\, d\Theta_f$$

$$E\left[\cos(\Theta_f)\right] = \frac{\sin(\varphi)}{\varphi}. \tag{A.1}$$

Appendix A.2

$$E\left[\cos^2(\Theta_f)\right] = \int_{-\infty}^{\infty} \cos^2(\Theta_f)\, p(\Theta_f)\, d\Theta_f = \int_{-\varphi}^{\varphi} \cos^2(\Theta_f)\, \frac{1}{2\varphi}\, d\Theta_f$$

$$E\left[\cos^2(\Theta_f)\right] = \frac{1}{2} + \frac{\sin(2\varphi)}{4\varphi}. \tag{A.2}$$

Appendix A.3

$$Var(\cos(\Theta_f)) = E\left[\cos^2(\Theta_f)\right] - \left(E\left[\cos(\Theta_f)\right]\right)^2$$

Using equation (A.1) and equation (A.2) above equation becomes

$$Var(\cos(\Theta_f)) = \frac{1}{2} + \frac{\sin(2\varphi)}{4\varphi} - \left(\frac{\sin(\varphi)}{\varphi}\right)^2. \tag{A.3}$$

Appendix A.4

The variance of the multiplication of two independent random variables can be calculated as

$$Var\left[\mathrm{Sh}\cos(\Theta_f)\right] = S^2\left[Var[h]\left(E\left[\cos(\Theta_f)\right]\right)^2 + \left(E[h]\right)^2 Var\left[\cos(\Theta_f)\right] + Var[h]\,Var\left[\cos(\Theta_f)\right]\right] \tag{A.4}$$

Using the values, $Var(h) = \sigma_h{}^2 = \left(2 - \frac{\pi}{2}\right)b^2$, $E[h] = \mu_h = \left(\sqrt{\frac{\pi}{2}}\right)b$, equations (A.1) and (A.3) in equation (A.4)

$$Var\left[Sh\cos(\Theta_f)\right] = b^2S^2\left[1-\frac{\pi}{2}\left(\frac{\sin(\varphi)}{\varphi}\right)^2+\frac{\sin(2\varphi)}{2\varphi}\right]. \quad (A.5)$$

Let Δw_i be uniformly distributed over $\{-w_e \sim w_e\}$. From the parameters of off-the-shelf products like CC2420 and AT86RF212, the product of Δw_i and T is small.

Appendix A.5

$$E\left[\frac{\sin(\Delta wT)}{\Delta wT}\right] = \int_{-w_e}^{w_e}\frac{1}{\Delta wT}\left(\Delta wT-\frac{(\Delta wT)^3}{3!}+\frac{(\Delta wT)^5}{5!}-\frac{(\Delta wT)^7}{7!}+....\right)\frac{1}{2w_e}d\Delta w$$

As the $\Delta w_i T$ is small, we can ignore higher order terms.

$$=1-\frac{(w_eT)^2}{18}. \quad (A.6)$$

Appendix A.6

$$E\left[\left(\frac{\sin(\Delta wT)}{\Delta wT}\right)^2\right] = \int_{-w_e}^{w_e}\left\{\frac{1}{\Delta wT}\left(\Delta wT-\frac{(\Delta wT)^3}{3!}+\frac{(\Delta wT)^5}{5!}-\frac{(\Delta wT)^7}{7!}+....\right)\right\}^2\frac{1}{2w_e}d\Delta w$$

As the Δw_iT is small, we can ignore higher order terms.

$$E\left[\left(\frac{\sin(\Delta wT)}{\Delta wT}\right)^2\right] = 1-\frac{(w_eT)^2}{9}+\frac{(w_eT)^4}{180}. \quad (A.7)$$

Appendix A.7

$$Var\left(\frac{\sin(\Delta wT)}{\Delta wT}\right) = E\left[\left(\frac{\sin(\Delta wT)}{\Delta wT}\right)^2\right]-\left(E\left[\frac{\sin(\Delta wT)}{\Delta wT}\right]\right)^2$$

Using equation (A.1) and equation (A.2) the above equation becomes

$$=\left[1-\frac{(w_eT)^2}{9}+\frac{(w_eT)^4}{180}\right]-\left(1-\frac{(w_eT)^2}{18}\right)^2=\frac{(w_eT)^4}{405}. \quad (A.8)$$

Appendix A.8

The variance of the multiplication of two independent random variables can be calculated as

$$Var\left[h\frac{\sin(\Delta wT)}{\Delta wT}\right]=\begin{bmatrix} Var[h]\left(E\left[\frac{\sin(\Delta wT)}{\Delta wT}\right]\right)^2+(E[h])^2 Var\left[\frac{\sin(\Delta wT)}{\Delta wT}\right]+ \\ Var[h]Var\left[\frac{\sin(\Delta wT)}{\Delta wT}\right] \end{bmatrix}. \quad (A.9)$$

Using the values $Var(h)=\sigma_h^2=\left(2-\frac{\pi}{2}\right)b^2$, $E[h]=\mu_h=\left(\sqrt{\frac{\pi}{2}}\right)b$, equations (A.7) and (A.8) in Equation (A.9)

$$Var\left[h\frac{\sin(\Delta wT)}{\Delta wT}\right]=b^2\left[0.429-.048(w_eT)^2+0.0063(w_eT)^4\right]. \quad (A.10)$$

Let $\Delta\theta$ is uniformly distributed over $\{-\psi$ to $\psi\}$ and Δw is uniformly distributed over $\{-w_e \sim w_e\}$. From the parameters of off-the-shelf products like CC2420 and AT86RF212, the product of Δw and T is small.

Appendix A.9

$$E\left[\frac{\sin(\Delta wT+\Delta\theta)}{\Delta wT}-\frac{\sin(\Delta\theta)}{\Delta wT}\right]=\int_{-\infty}^{\infty}\int_{-\infty}^{\infty}\left[\frac{\sin(\Delta wT+\Delta\theta)}{\Delta wT}-\frac{\sin(\Delta\theta)}{\Delta wT}\right]p(\Delta w)\,p(\Delta\theta)d\Delta w d\Delta\theta$$

$$=\frac{1}{4\psi w_e}\begin{bmatrix} \int_{-w_e}^{w_e}\frac{\sin(\Delta wT)}{\Delta wT}\int_{-\psi}^{\psi}\cos(\Delta\theta)d\Delta\theta d\Delta w+\int_{-w_e}^{w_e}\frac{\cos(\Delta wT)}{\Delta wT}\int_{-\psi}^{\psi}\sin(\Delta\theta)d\Delta\theta d\Delta w- \\ \int_{-w_e}^{w_e}\frac{1}{\Delta wT}\int_{-\psi}^{\psi}\sin(\Delta\theta)d\Delta\theta d\Delta w \end{bmatrix}$$

As the ΔwT is small, ignoring its higher order terms we can simplify the above equation as.

$$=\left(1-\frac{(w_eT)^2}{18}\right)\left(\frac{\sin(\psi)}{\psi}\right). \quad (A.11)$$

Appendix A.10

$$E\left[\left(\frac{\sin(\Delta wT+\Delta\theta)}{\Delta wT}-\frac{\sin(\Delta\theta)}{\Delta wT}\right)^2\right]$$

$$=\int_{-\infty}^{\infty}\int_{-\infty}^{\infty}\left(\frac{\sin(\Delta wT+\Delta\theta)}{\Delta wT}-\frac{\sin(\Delta\theta)}{\Delta wT}\right)^2 p(\Delta w)\,p(\Delta\theta)d\Delta w d\Delta\theta$$

$$= \frac{1}{4\psi w_e}\left[\begin{array}{l} \int_{-w_e}^{w_e} \frac{\sin^2(\Delta wT)}{(\Delta wT)^2} d\Delta w \int_{-\psi}^{\psi} \cos^2(\Delta\theta) d\Delta\theta + \int_{-w_e}^{w_e} \frac{\cos^2(\Delta wT)}{(\Delta wT)^2} d\Delta w \int_{-\psi}^{\psi} \sin^2(\Delta\theta) d\Delta\theta + \\ \int_{-w_e}^{w_e} \frac{1}{(\Delta wT)^2} d\Delta w \int_{-\psi}^{\psi} \sin^2(\Delta\theta) d\Delta\theta + 2\int_{-w_e}^{w_e} \frac{\sin(\Delta wT)\cos(\Delta wT)}{(\Delta wT)^2} d\Delta w \int_{-\psi}^{\psi} \sin(\Delta\theta)\cos(\Delta\theta) d\Delta\theta - \\ 2\int_{-w_e}^{w_e} \frac{\sin(\Delta wT)}{\Delta wT} d\Delta w \int_{-\psi}^{\psi} \sin(\Delta\theta)\cos(\Delta\theta) d\Delta\theta - 2\int_{-w_e}^{w_e} \frac{\cos(\Delta wT)}{(\Delta wT)^2} d\Delta w \int_{-\psi}^{\psi} \sin^2(\Delta\theta) d\Delta\theta \end{array}\right]$$

The terms given in above equation have the solutions as given below:

$$\int_{-\psi}^{\psi} \sin^2(\Delta\theta) d\Delta\theta = \frac{1}{2}\int_{-\psi}^{\psi} \left(1 - \cos(2\Delta\theta)\right) d\Delta\theta = \frac{1}{2} - \frac{\sin 2\psi}{4\psi}. \qquad \text{(A.12.1)}$$

$$\int_{-\psi}^{\psi} \cos^2(\Delta\theta) d\Delta\theta = \frac{1}{2}\int_{-\psi}^{\psi} \left(1 + \cos(2\Delta\theta)\right) d\Delta\theta = \frac{1}{2} + \frac{\sin 2\psi}{4\psi}. \qquad \text{(A.12.2)}$$

$$\int_{-\psi}^{\psi} \sin(\Delta\theta)\cos(\Delta\theta) d\Delta\theta = 0. \qquad \text{(A.12.3)}$$

$$\int_{-w_e}^{w_e} \frac{1}{(\Delta wT)^2} d\Delta w = \frac{-2}{3T^2 w^3{}_e}. \qquad \text{(A.12.4)}$$

$$\int_{-w_e}^{w_e} \frac{\cos(\Delta wT)}{(\Delta wT)^2} d\Delta w = \int_{-w_e}^{w_e} \left[\frac{1}{(\Delta wT)^2} - \frac{1}{2} + \frac{(\Delta wT)^2}{4!} - \ldots.\right] d\Delta w$$

$$= \frac{-2}{3T^2 w^3{}_e} - w_e + \frac{2T^2 w^3{}_e}{4!} + \ldots. \qquad \text{(A.12.5)}$$

$$\int_{-w_e}^{w_e} \frac{\cos^2(\Delta wT)}{(\Delta wT)^2} d\Delta w = \int_{-w_e}^{w_e} \left[1 - \frac{(\Delta wT)^2}{2!} + \frac{(\Delta wT)^4}{4!} \ldots.\right]^2 d\Delta w$$

$$= \frac{-2}{3T^2 w^3{}_e} - w_e + \frac{2T^2 w^3{}_e}{4!} + \ldots. \qquad \text{(A.12.6)}$$

Using Equations (A.6.1) to (A.6.6) and as the ΔwT is small, we can ignore higher order terms. We may have:

$$E\left[\left(\frac{\sin(\Delta wT + \Delta\theta)}{\Delta wT} - \frac{\sin(\Delta\theta)}{\Delta wT}\right)^2\right] = \left[1 - \frac{(w_e T)^2}{9} + \frac{(w_e T)^4}{180}\right]\left[\frac{1}{2} + \frac{\sin(2\psi)}{4\psi}\right]. \qquad \text{(A.12)}$$

Appendix A.11

$$Var\left[h\left(\frac{\sin(\Delta wT+\Delta\theta)}{\Delta wT}-\frac{\sin(\Delta\theta)}{\Delta wT}\right)\right]=$$
$$E\left[\left(\frac{\sin(\Delta wT+\Delta\theta)}{\Delta wT}-\frac{\sin(\Delta\theta)}{\Delta wT}\right)^2\right]-\left(E\left[\frac{\sin(\Delta wT+\Delta\theta)}{\Delta wT}-\frac{\sin(\Delta\theta)}{\Delta wT}\right]\right)^2$$

Using equation (A.11) and equation (A.12) the above equation becomes

$$=\left[\begin{array}{l}\frac{1}{2}-\frac{(w_eT)^2}{18}+\frac{(w_eT)^4}{180}+\frac{\sin(2\psi)}{4\psi}-\frac{(w_eT)^2\sin(2\psi)}{36\psi}+\frac{(w_eT)^4\sin(2\psi)}{720\psi}-\frac{\sin^2(\psi)}{\psi^2}-\\ \frac{(w_eT)^4\sin^2(\psi)}{324\psi^2}+\frac{(w_eT)^2\sin^2(\psi)}{9\psi^2}\end{array}\right] \quad \text{(A.13)}$$

Appendix A.12

The variance of multiplication of two independent random variables can be calculated as

$$Var\left[h\left(\frac{\sin(\Delta wT+\Delta\theta)}{\Delta wT}-\frac{\sin(\Delta\theta)}{\Delta wT}\right)\right]=Var[h]\left[E\left(\frac{\sin(\Delta wT+\Delta\theta)}{\Delta wT}-\frac{\sin(\Delta\theta)}{\Delta wT}\right)\right]^2+$$
$$(E[h])^2 Var\left[\frac{\sin(\Delta wT+\Delta\theta)}{\Delta wT}-\frac{\sin(\Delta\theta)}{\Delta wT}\right]+Var[h]Var\left[\frac{\sin(\Delta wT+\Delta\theta)}{\Delta wT}-\frac{\sin(\Delta\theta)}{\Delta wT}\right] \quad \text{(A.14)}$$

Using the values, $Var(h)=\sigma_h{}^2=\left(2-\frac{\pi}{2}\right)b^2$, $E[h]=\mu_h=\left(\sqrt{\frac{\pi}{2}}\right)b$, equations (A.11) and (A.13) in equation (A.14)

$$Var\left[h\left(\frac{\sin(\Delta wT+\Delta\theta)}{\Delta wT}-\frac{\sin(\Delta\theta)}{\Delta wT}\right)\right]=b^2\left\{\left(2-\frac{\pi}{2}\right)\left(1-\frac{(w_eT)^2}{18}\right)\left(\frac{\sin(\psi)}{\psi}\right)+2X\right\}. \quad \text{(A.15)}$$

where $X=\left[\begin{array}{l}\frac{1}{2}-\frac{(w_eT)^2}{18}+\frac{(w_eT)^4}{180}+\frac{\sin(2\psi)}{4\psi}-\frac{(w_eT)^2\sin(2\psi)}{36\psi}+\frac{(w_eT)^4\sin(2\psi)}{720\psi}-\\ \frac{\sin^2(\psi)}{\psi^2}-\frac{(w_eT)^4\sin^2(\psi)}{324\psi^2}+\frac{(w_eT)^2\sin^2(\psi)}{9\psi^2}\end{array}\right]$